Anatomical changes in brown and beige fat development in response to changes in diet and ambient temperature in virgin and pregnant rats

By

Layla Ahmad Mohammad Albustanji

Division of Child Health, Obstetrics and Gynaecology

School of Medicine

Faculty of Medicine and Health Sciences

University of Nottingham

Thesis submitted to the University of Nottingham for the degree of

Doctor of Philosophy

April 2019

Abstract

Brown adipose tissue (BAT) can rapidly generate heat following the activation of its unique mitochondrial uncoupling protein (UCP) 1 which may therefore have a role in regulating energy balance. The main anatomical location of BAT in rodents is the interscapular region, although thermogenic adipocytes termed beige can develop within white adipose tissue (WAT). As cold exposure is the main factor promoting BAT activity and browning in WAT, my thesis investigated the influence of housing at a mild cold temperature of 20°C on the interscapular BAT activity and the browning capacity of omental and inguinal WAT. This study also examined the potential effect of pregnancy on these depots and whether inguinal adipocytes transform to mammary cells (by a process termed pinking) through gestation. Excess adiposity is also associated with low-grade inflammation characterised by adipocyte hypertrophy and hyperplasia and referred to as meta-inflammation. I, therefore, studied the effect of housing temperature on biomarkers of inflammation in omental fat in response to an obesogenic diet and whether this was further affected by pregnancy. The extent to which mild cold exposure would modulate any adaptations were also examined. The overall aim of my thesis was to identify the consequences of housing temperature on UCP1 and gene markers of brown adipocyte development in order to determine how it can modulate dietary-induced obesity.

Female Sprague Dawley rats were fed either a standard (18% of energy from fat; 24% from protein; 58% from carbohydrates, of which 7% are mono- and disaccharides; energy density of 3.1 kcal/g), or an obesogenic diet that was high in fat and sucrose (39% of energy from fat; 23% from protein; 39% from carbohydrate, of which 44% are mono- and disaccharides; energy density of 4.6 kcal/g) and housed at either a cool i.e. 20°C, or thermoneutral i.e. 27°C temperature. Body weight was recorded three times a week and food intake was measured, but only prior to pregnancy. Animals were tissue sampled, either before pregnancy or at 10 and 19 days of gestation which corresponds to 50% and 90% of the term; respectively. Expression of genes associated with thermogenesis, browning, pinking, inflammation and fatty acids metabolism were measured using qPCR while histological appearance was determined in H & E stained sections.

The obesogenic diet resulted in more fat accumulation. UCP1 protein in iBAT was more abundant in virgin animals fed the high energy diet at mild cold than at thermoneutrality. This response was modulated with pregnancy whereby UCP1 protein expression was similar between all groups. UCP1 gene expression was similar between groups but there was a decline in mRNA abundance for UCP1 with gestation that was more pronounced at 20°C. UCP1 mRNA was not detected in inguinal or omental adipose tissue in any group. Inguinal adipocytes transformed to alveolar epithelial cells with gestation as determined by changes at the gross, histological and molecular levels. Histologically, inguinal adipocytes looked more compact as gestation proceeded and alveoli formation was apparent. Gene expression for mammary cell markers ELF5 and WAP, increased with gestation, which are indicative of alveologenesis and the capacity to synthesise milk. There was no effect of diet or temperature on gene expression for pro-inflammatory markers NFkB and TNFα or anti-inflammatory genes e.g. IL10 biomarkers in response to housing temperature or diet but pro-inflammatory markers declined as pregnancy progressed.

In conclusion, housing at a standard temperature enhanced brown characteristics in iBAT. Mild cold exposure could therefore be an effective strategy to reduce fat deposition and thus obesity through enhanced thermogenesis. Exposure of dams to such conditions may subsequently influence the extent to which their offspring develop obesity in later life and reduce the negative effects on the mother.

Dedication

TO MY FATHER, AHMAD ALBUSTANJI

TO MY MOTHER, WADHA ALBUSTANJI

Acknowledgements

Foremost, I thank GOD Almighty for giving me the strength, patience, knowledge and opportunity to work through all these years so that today I stand proudly with my head held high.

Firstly, I acknowledge the people who mean the most to me, my family. My parents, Ahmad Albustanji and Wadha Albustanji, for showing faith in me, for your selfless love, care, and pain, and for the sacrifices you made to shape my life. I can never pay back the love and affection you showed upon me. I also express my thanks to my siblings, Mohammad, Haneen, Ibrahim, Hashim, Osama, Hayat and Maha for their support, valuable prayers and for taking care of my daughter during my study. And from the bottom of my heart, thanks to a very special person, my husband, Ismail Albostanji for his continued and unfailing love, support and understanding during my pursuit of the PhD and for making the completion of this thesis possible. I greatly value your contribution and deeply appreciate your belief in me. I appreciate my wonderful children, my son; Abed Alhameed for bearing with me during my lab work and thesis writing, and my daughter; Raghad, Thank you for loving me and giving me joy and a fulfilling life, even though I spent long times away from you. To Aunt Hanan; thanks for being always there. Words can never say how grateful I am to all of you.

Special mention goes to my principal supervisor, Michael Symonds. I thank him wholeheartedly, not only for his tremendous academic support, but also for positive appreciation and his guidance through each stage of my PhD.

I would like to express my gratitude to Dr Mohammad Abu Lubbad and Mrs Alia Almajali, your support will not be forgotten.

I am extremely thankful to Dr Neele Dellschaft for her help and assistance especially during the lab training, thanks also go to my second supervisor Professor Helen Budge for her support, Mrs Vicky Wilson and Mr Mark Pope for providing me with the technical support.

To my great friends, Dr Reham Alagal, Dr Widad Nasuf and Dr Enas AlHarethi, your help and encouragement was worth more than I can express on papers.

Last but not the least, I would like to thank all the friends (too many to list here but you know who you are!) in the UK and Jordan for supporting me spiritually throughout writing this thesis and my life in general.

Declaration

The work in this thesis was performed within the Academic Division of Child Health, Obstetrics and Gynaecology at Nottingham University Hospital, Queens Medical Centre, Nottingham, between July 2015 and April 2019.

Unless otherwise stated, this thesis illustrates my own work completed under the supervision of Professor Michael Symonds, Professor Helen Budge and Dr Neele Dellschaft of the University of Nottingham.

This thesis is an accurate representation of the work performed and no other study reproducing this work, to my knowledge, has been carried out within the University of Nottingham.

Layla Ahmad Mohammad Albustanji

April 2019

Publications

Albustanji, L.; Perez, G.; Alharethi, E.; Aldiss, P.; Bloor, I.; Barreto-Medeiros, J.;Budge, H.; Symonds, M. E. & Dellschaft, N. 2019. Housing temperature modulates the impact of diet-induced rise in fat mass on adipose tissue before and during pregnancy in rats. Frontiers in Physiology, 10**,** 209.

Dellschaft, N; Perez, G; **Albustanji, L**; Budge, H; Symonds, M. White and Brown Adipose Tissue Characteristics Influenced by High Fat, High Sucrose Diet and Thermoneutral Temperature in Non-Pregnant Females and During Pregnancy. Conference of "The Power of Programming-Developmental Origins of Adiposity and Long-term Health", 13-15 October 2016. Munich, Germany.

Budge, H.; Dellschaft, N.; **Albustanji, L.**; Alharethi, E.; Perez, G.; Aldiss, P. & Symonds, M. Impact of housing temperature on the adaptation of brown adipose tissue to pregnancy in lean and obese rats. FASEB Journal, 2018. Federation Amer Soc Exp Biol 9650 Rockville Pike, Bethesda, MD 20814-3998 USA.

Dellschaft, N.; Perez, G.; Aldiss, P.; **Albustanji, L.**; Budge, H. & Symonds, M. 2017. Brown and Paracardial Adipose Tissue Characteristics Influenced by High Fat, High Sucrose Diet and Thermoneutral Temperature in Pregnancy. *The FASEB Journal,* 31**,** 966.21-966.21.

Presentations

Albustanji, L.; Dellschaft, N.; Budge, H. and Symonds, M. Anatomical changes in brown fat development and early life programming (poster and oral). M & HS Faculty Postgraduate Research Forum, School of Medicine, University of Nottingham. June 2016.

Albustanji, L.; Dellschaft, N.; Budge, H. and Symonds, M. Temperature study. Division of Child Health, Obstetrics and Gynaecology, School of Medicine, University of Nottingham. February 2016.

Albustanji, L.; Dellschaft, N.; Budge, H. and Symonds, M**.** Temperature study. Division of Child Health, Obstetrics and Gynaecology, School of Medicine, University of Nottingham. November 2016.

Albustanji, L.; Dellschaft, N.; Budge, H. and Symonds, M. Browning biomarkers. Division of Child Health, Obstetrics and Gynaecology, School of Medicine, University of Nottingham. August 2017.

Albustanji, L.; Dellschaft, N.; Budge, H. and Symonds, M. Effect of ambient temperature and pregnancy on brown adipose tissue characteristics in rats fed a high energy diet. Sue Watson Postgraduate Presentation Prize, School of Medicine, University of Nottingham. October 2017.

Albustanji, L.; Dellschaft, N.; Budge, H. and Symonds, M. Effect of ambient temperature and high energy diet on brown adipose tissue weight in rats during pregnancy. Division of Child Health, Obstetrics and Gynaecology, School of Medicine, University of Nottingham. December 2017.

Albustanji, L.; Dellschaft, N.; Budge, H. and Symonds, M. Effect of ambient temperature and pregnancy on mesenteric adipose tissue characteristics in rats fed a high energy diet. Division of Child Health, Obstetrics and Gynaecology, School of Medicine, University of Nottingham. January 2018.

Albustanji, L.; Dellschaft, N.; Budge, H. and Symonds, M. Effect of ambient temperature and pregnancy on mesenteric adipose tissue characteristics in rats fed a high energy diet. Division of Child Health, Obstetrics and Gynaecology, School of Medicine, University of Nottingham. April 2018.

Albustanji, L.; Dellschaft, N.; Budge, H. and Symonds, M. Effect of ambient temperature and pregnancy on brown adipose tissue characteristics in rats fed a high energy diet. Division of Child Health, Obstetrics and Gynaecology, School of Medicine, University of Nottingham. June 2018.

Table of contents

Abstract I

Dedication III

Acknowledgements IV

Declaration VI

Publications VII

Presentations VII

Table of contents IX

List of figures XIV

List of tables XVIII

List of appendices XIX

List of abbreviations XX

Chapter 1. Introduction 1

1.1 Obesity 1

1.1.1 Definition and prevalence 1

1.1.2 Causes of Obesity 2

1.2 Adipose tissue 3

1.2.1 White adipose tissue (WAT) 3

1.2.2 Brown adipose tissue 11

1.2.3 Beige adipose tissue 17

1.3 Browning process 18

1.3.1 Browning factors 19

1.4 Obesity studies: rat as a model 21

1.4.1 Advantages 21

1.4.2 Limitations 22

1.5 Maternal metabolism and obesity 23

1.5.1 Maternal metabolism 23

1.5.2 Maternal obesity 24

1.5.3 Programming of obesity 24

Chapter 2. Materials and Methods 32

2.1 Procedural & legislative declaration 32

2.2 Power of the study 32

2.3 Study design 32

2.3.1 Animals and housing conditions 33

2.3.2 Interventions 34

2.3.3 Animals Mating 35

2.3.4 Dissection and tissues sampling 35

2.4 Laboratory procedures 36

2.4.1 Plasma Separation 36

2.4.2 Histology 36

2.4.3 Haematoxylin and Eosin (H & E) tissue staining 38

2.4.4 Immunohistochemical staining 40

2.4.5 Gene expression analysis 41

2.5 Statistical Analysis 61

Chapter 3. The response of interscapular adipose tissue to diet, housing temperature and pregnancy 62

3.1 Introduction 62

3.2 Hypothesis 63
3.3 Aims 63
3.4 Methods 64
3.5 Results 64
3.5.1 Body weight 64
3.5.2 Interscapular BAT mass 65
3.5.3 Expression of genes and protein in iBAT 67
3.5.4 Metabolic and endocrine profiles 80
3.6 Summary of main findings 80
3.7 Discussion 80
3.8 Conclusion 84
Chapter 4. The response of inguinal adipose tissue to diet, housing temperature and pregnancy 86
4.1 Introduction 86
4.2 Hypothesis 87
4.3 Aims 88
4.4 Methods 88
4.5 Results 89
4.5.1 Gross anatomy of the inguinal adipose tissue 89
4.5.2 Inguinal adipose tissue H & E stained histological sections 90
4.5.3 Inguinal adipose tissue mass 91
4.5.4 Expression of genes in the inguinal adipose tissue 91
4.6 Summary of main findings 98
4.7 Discussion 98

4.8 Conclusion....103

Chapter 5. The response of omental adipose tissue to diet, housing temperature and pregnancy 104

5.1 Introduction 104

5.2 Hypothesis 105

5.3 Aims....105

5.4 Methods....106

5.5 Results 107

5.5.1 Histology of the omental adipose tissue 107

5.5.2 Omental fat mass....108

5.5.3 Expression of genes in the omental adipose tissue 108

5.6 Summary of main findings....117

Discussion 118

5.7 Conclusion....122

Chapter 6. Conclusion 123

6.1 Hypothesis 123

6.2 Methods....123

6.3 Summary of main findings....124

6.3.1 Mild cold ambient temperature enhances a thermogenic activity of BAT that is modulated with pregnancy 124

6.3.2 No browning was detected in the inguinal adipose tissue....124

6.3.3 Inguinal adipocytes differentiate to mammary cells with pregnancy 125

6.3.4 Absence of browning and inflammatory biomarkers downregulation in the omental fat in response to mild cold exposure 125

6.3.5 Inflammation process in omental fat is suppressed with gestation. 126

6.4 Limitations 126
6.4.1 Small amount of iBAT in rats 126
6.4.2 Technical limitations 126
6.5 Future work 127
6.5.1 Maternal obesity programming effect on offspring postnatally 127
6.5.2 Postnatal effects of maternal diet in relation to the sex of offspring 127
6.5.3 BAT and WAT plasticity in lactation and beyond. 128
6.5.4 Browning and inflammation in male adipose tissues. 128
6.5.5 Standard housing temperature precautions 128
6.5.6 Staining virgin inguinal fat with mammary cells biomarker 128
6.5.7 Measuring deiodinase 2 (MDI 2) expression in iBAT 128
6.6 Summary of the thesis 129
References 130
Appendices 150

List of figures

Figure 1.1 The worldwide prevalence of obesity among males (A) and females (B) 1

Figure 1.2 Major white adipose tissue (WAT) depots in (A) Humans and (B) rodents 4

Figure 1.3 Histological image of subcutaneous adipose tissue from 17 days pregnant mouse 8

Figure 1.4 Schematic diagram of adipocytes types 11

Figure 1.5 Brown fat main depots in (A) Human adult, (B) Human infant and (C) Rodents 12

Figure 1.6 Mechanism of action of uncoupling protein 1 (UCP1) 13

Figure 2.1 Schematic overview of the experimental design and numbers of animals involved in each group of the housing temperature study 33

Figure 2.2 Immunohistochemistry Principle of action 40

Figure 2.3 Reverse transcription-polymerase chain reaction (RT-PCR) process 45

Figure 2.4 Illustration of PCR reaction steps for a target DNA sequence amplification. 50

Figure 2.5 PCR products in agarose gel 53

Figure 2.6 Representative amplification plot 57

Figure 2.7 Representative Melt curve 58

Figure 2.8 Representative standards curve 59

Figure 3.1 Effect of housing temperature, diet and pregnancy on body weight 65

Figure 3.2 Effect of housing temperature, diet and pregnancy on interscapular BAT absolute mass 66

Figure 3.3 Effect of housing temperature, diet and pregnancy on relative interscapular BAT iBAT mass 66

Figure 3.4 Uncoupling Protein 1 (UCP1) gene expression in the interscapular BAT 67

Figure 3.5 Uncoupling Protein 1 (UCP1) protein abundance in the interscapular BAT 68

Figure 3.6 Representative anti-UCP1 immunohistochemistry images 68

Figure 3.7 Beta-3 adrenergic receptor (β3AR) gene expression in the interscapular BAT ... 69

Figure 3.8 Transient receptor potential cation channel subfamily V member 1 (TRPV1) gene expression in the interscapular BAT 70

Figure 3.9 Sarcoplasmic/endoplasmic reticulum Ca2+ transporting 2 B (SERCA2B) gene expression in the interscapular BAT 70

Figure 3.10 11β-Hydroxysteroid dehydrogenase (11βHSD) gene expression in the interscapular BAT 71
Figure 3.11 Peroxisome proliferator activated receptor gamma (PPARɣ) gene expression in the interscapular BAT..... 72
Figure 3.12 Leptin gene expression in the interscapular BAT 73
Figure 3.13 Peroxisome proliferator-activated receptor gamma coactivator 1-alpha (PGC-1α) gene expression in the interscapular BAT 73
Figure 3.14 Transcription factor 7-like 2 (TCF7L2) gene expression in the interscapular BAT 74
Figure 3.15 Mammalian target of rapamycin (mTOR) gene expression in the interscapular BAT 75
Figure 3.16 Insulin receptor substrate (IRS1) gene expression in the interscapular BAT ... 76
Figure 3.17 Insulin receptor substrate (IRS2) gene expression in the interscapular BAT ... 76
Figure 3.18 Fatty acid translocase (CD36) gene expression in the interscapular BAT 77
Figure 3.19 Adipose triglyceride lipase (ATGL) gene expression in the interscapular BAT .. 78
Figure 3.20 Lipoprotein lipase (LPL) gene expression in the interscapular BAT..... 79
Figure 3.21 Fatty acid transport protein 4 (FATP4) gene expression in the interscapular BAT 79
Figure 3.22 Illustration of changes in interscapular brown adipose tissue (iBAT)..... 85
Figure 4.1 Representative images for inguinal fat of both Virgin (A) and Pregnant (B) rats during the tissues sampling process..... 89
Figure 4.2 Representative microscopic slides of the inguinal adipose tissue..... 90
Figure 4.3 Effect of housing temperature, diet and pregnancy on inguinal fat mass..... 91
Figure 4.4 Beta-3 adrenergic receptor (β3AR) gene expression in the inguinal adipose tissue 92
Figure 4.5 Peroxisome proliferator-activated receptor gamma (PPARɣ) gene expression in the inguinal adipose tissue..... 92
Figure 4.6 Leptin gene expression in the inguinal adipose tissue..... 93
Figure 4.7 Insulin receptor substrate 2 (IRS2) gene expression in the inguinal adipose tissue 94

Figure 4.8 Fatty acid binding protein 4 (FABP4) gene expression in the inguinal adipose tissue 95
Figure 4.9 E74-Like ETS Transcription Factor 5 (ELF5) gene expression in the inguinal adipose tissue 95
Figure 4.10 Whey Acidic Protein (WAP) gene expression in the inguinal adipose tissue 96
Figure 4.11 Signal transducer and activator of transcription 5A (STAT5A) gene expression in the inguinal adipose tissue 97
Figure 4.12 Oxytocin receptor (OXTR) gene expression in the inguinal adipose tissue 97
Figure 4.13 Summary diagram of inguinal adipose tissue analysis findings. 103
Figure 5.1 Representative Haematoxylin and Eosin stained-microscopic slides of the omental adipose tissue 107
Figure 5.2 Effect of housing temperature, diet and pregnancy on omental adipose tissue mass.....108
Figure 5.3 Beta-3 adrenergic receptor (β3AR) gene expression in the omental adipose tissue 109
Figure 5.4 Leptin gene expression in the omental fat 109
Figure 5.5 Sarcoplasmic/endoplasmic reticulum Ca2+ transporting 2 B (SERCA2B) gene expression in the omental adipose tissue 110
Figure 5.6 Ryanodine receptor 2 (RYR2) gene expression in the omental adipose tissue ..110
Figure 5.7 Vascular endothelium growth factor A (VEGFA) gene expression in the omental adipose tissue 111
Figure 5.8 Insulin receptor substrate 1 (IRS1) gene expression in the omental adipose tissue.....112
Figure 5.9 Insulin receptor substrate (IRS2) gene expression in the omental adipose tissue 112
Figure 5.10 Fatty acid binding protein 4 (FABP4) gene expression in the omental adipose tissue.....113
Figure 5.11 Fatty acid transport protein 4 (FATP4) gene expression in the omental adipose tissue.....114
Figure 5.12 Interleukin 10 (IL10) gene expression in the omental adipose tissue.....114

Figure 5.13 Interleukin 6 (IL6) gene expression in the omental adipose tissue 115
Figure 5.14 Nuclear factor kappa B subunit (NF-kB) gene expression in the omental adipose tissue.....116
Figure 5.15 Monocyte chemoattractant protein1 (MCP1) gene expression in the omental adipose tissue 116
Figure 5.16 Tumour necrosis factor alpha (TNFα) gene expression in the omental adipose tissue.....117
Figure 5.17 Summary diagram of omental adipose tissue analysis findings. 122
Figure 6.1 Summary diagram of study design, methods and main findings 129

List of tables

Table 1.1 Summary of studies on maternal programming of offspring adiposity 30

Table 2.1 Macronutrient composition of diets 34

Table 2.2 Tissue Processing programme of small samples (BAT, soleus, 10d gestation foetuses) 37

Table 2.3 Tissue processing programme of the temperature study big samples (WAT, gastrocnemius, liver and heart) 37

Table 2.4 Haematoxylin and eosin (H & E) staining protocol 39

Table 2.5 Details of the 'RT RNA 2 cDNA ' programme cycles for the polymerase chain reaction 46

Table 2.6 primers, forward and reverse sequences 48

Table 2.7 Contents of the PCR master mix for "standards" programme 51

Table 2.8 "Standards" programme details in the PCR run 51

Table 2.9 Details of the quantities used to prepare the qPCR dye-based (syber green) master mix 55

Table 2.10 Details of the quantities used to prepare the qPCR probe-based (TaqMan) master mix (amounts are for reaction per well) 56

Table 2.11 Dye-labelled (syber green) qPCR programme 56

Table 2.12 Probe-based (Taqman) qPCR programme 56

Table 4.1 List of studies in rodents' inguinal adipose tissue where UCP1 was detected or induced. 99

Table 5.1 List of published studies where UCP1 was detected or induced in the omental adipose tissue 119

Table 5.2 List of studies about meta-inflammation in omental adipose tissue 121

List of appendices

Appendix 1 Probes and primers sequences 150

Appendix 2 Interscapular brown adipose tissue mass, UCP1 protein and gene expression measurements 152

Appendix 3 Plasma metabolites and hormones 156

Appendix 4 Inguinal adipose tissue mass and gene expression measurements 157

Appendix 5 Omental adipose tissue mass and gene expression measurements 159

Appendix 6 List of Suppliers 163

List of abbreviations

Abbreviation	Definition
ANOVA	Analysis of variance
ATGL	Adipose triglyceride lipase
ATP	Adenosine triphosphate
BAT	Brown adipose tissue
BLAST	Basic Local Alignment Search Tool
BMI	Body mass index
BMP	Bone morphogenetic protein
Brite	Brown in white
β3AR	Beta-3 adrenergic receptor
°C	Celsius degree
CCAAT/EBP α	CCAAT/Enhancer binding protein alpha
CCAAT/EBP β	CCAAT/Enhancer binding protein beta
CD36	Fatty acid translocase
cDNA	Complementary deoxyribonucleic acid
CNS	Central nervous system
COSHH	Control of substances hazardous to health
Cq	Quantification cycle
CT	Computerised tomography
Ct	Cycle threshold
DAB	3,3 diaminobenzidine
db/db	Diabetic strain
DIT	Diet-induced thermogenesis
DIO	Diet-induced obesity
DNA	Deoxyribonucleic acid
dNTP	Deoxyribonucleotide
EDTA	Ethylenediaminetetraacetic acid
ELF5	E74 Like ETS Transcription Factor 5
EMR1	EGF-Like Module-Containing Mucin-Like Hormone Receptor-Like 1
FABP	Fatty acid binding protein
FATP	Fatty acid transport protein
FA	Fatty acids
FFAs	Free fatty acids
FTO	Fat mass and obesity associated gene
GDM	Gestational diabetes mellitus
H diet	High fat and sucrose diet
H_2O_2	Hydrogen peroxide
H&E	Haematoxylin and eosin
HFD	High fat diet
HFHS	High fat and sucrose
HPA	Hypothalamic pituitary adrenal axis
HSL	Hormone sensitive lipase
IHC	Immunohistochemistry
iBAT	Interscapular brown adipose tissue
IL	Interleukin
IL6	Interleukin 6
IL10	Interleukin 10
IRS1	Insulin receptor substrate 1
IRS2	Insulin receptor substrate 2
KDa	Kilo Dalton

LPL	Lipoprotein lipase
LSD	Low significant difference
MCP1	Monocyte chemoattractant protein 1
MC4R	Melanocortin-4 receptor gene
MDI	Monodeiodinases
MG	Monoacylglycerol
µL	Microlitre
mRNA	Messenger ribonucleic acid
mTOR	Mammalian target or rapamycin
$MYF5^{-}$	Myogenic factor 5 - progenitors
$MYF5^{+}$	Myogenic factor 5 + progenitors
NCBI	National centre for biotechnology information
NEFAs	Non esterified fatty acids
NF_KB	Nuclear Factor Kappa B Subunit
NRTC	No-reverse transcriptase control
NST	Nonshivering thermogenesis
NTC	No-template control
Ob/ob	Leptin-deficient
OXTR	Oxytocin receptor
PCR	Polymerase chain reaction
PGC-1α	Peroxisome proliferator-activated receptor gamma coactivator 1-alpha
PPARα	Peroxisome proliferator activated receptor alpha
PPARδ	Peroxisome proliferator activated receptor delta
PPARɣ	Peroxisome proliferator activated receptor gamma
PRDM16	PRD1-BF1-RIZ1 homologous domain containing 16
PRLR	Prolactin receptor
PUFA	Polyunsaturated fatty acids
qPCR	Quantitative polymerase chain reaction
RB	Retinoblastoma protein
RIP140	Receptor-interacting protein 140
RPLP0	Ribosomal Protein Lateral Stalk Subunit P0
RPM	Revolutions per minute
RT-PCR	Reverse transcriptase-polymerase chain reaction
RYR2	Ryanodine receptor 2
Rn	Normalised reporter
RNA	Ribonucleic acid
S diet	Standard diet
SDHA	Succinate Dehydrogenase Complex Flavoprotein Subunit A
SEM	Standard error of the mean
SERCA2B	ATPase sarcoplasmic/endoplasmic reticulum Ca+2 transporting 2 B
SNPs	Single nucleotide polymorphisms
SNS	Sympathetic nervous system
SR	Sarcoplasmic reticulum
STAT5A	Signal transducer and activator of transcription 5A
TBP	TATA-Box Binding Protein
TCF7L2	Transcription factor 7-like 2
TG	Triglyceride
Tm	Melting Temperature
TNFα	Tumour necrosis factor alpha
tRNA	Transfer ribonucleic acid
TRPs	Transient receptor potential channels
TRPV1	Transient receptor potential vanilloid 1
T3	Triiodothyronine
UCP1	Uncoupling protein 1

VEGFA	Vascular endothelial growth factor A
WAP	Whey acidic protein
WAT	White adipose tissue
WBCs	White blood cells
WHO	World health organisation
YWHAZ	Tyrosine 3-Monooxygenase/Tryptophan 5-Monooxygenase Activation Protein Zeta
10 d/g	10 days of gestation
19 d/g	19 days of gestation
11βHSD	11β-Hydroxysteroid dehydrogenase
≈	Almost equal to

Chapter 1. Introduction

1.1 Obesity

1.1.1 Definition and prevalence

As the rate of obesity has increased dramatically over the last decade (Figure 1.1), it has become a major health issue that requires further investigation into the causes, consequences and possible ways of prevention (Ohkuma et al., 2015). Overweight and obesity are defined by the World Health Organization (WHO) as an abnormal or excessive fat accumulation that presents a risk to health. It is grossly indicated by body mass index (BMI) which is calculated by dividing the body mass (in kilograms) by the square of body height (in meters) (WHO, 2018). An individual who has a BMI higher than 30 is considered obese. The average BMI has increased across the world indicating that an obesity epidemic is occurring (Renehan et al., 2015, WHO, 2014).

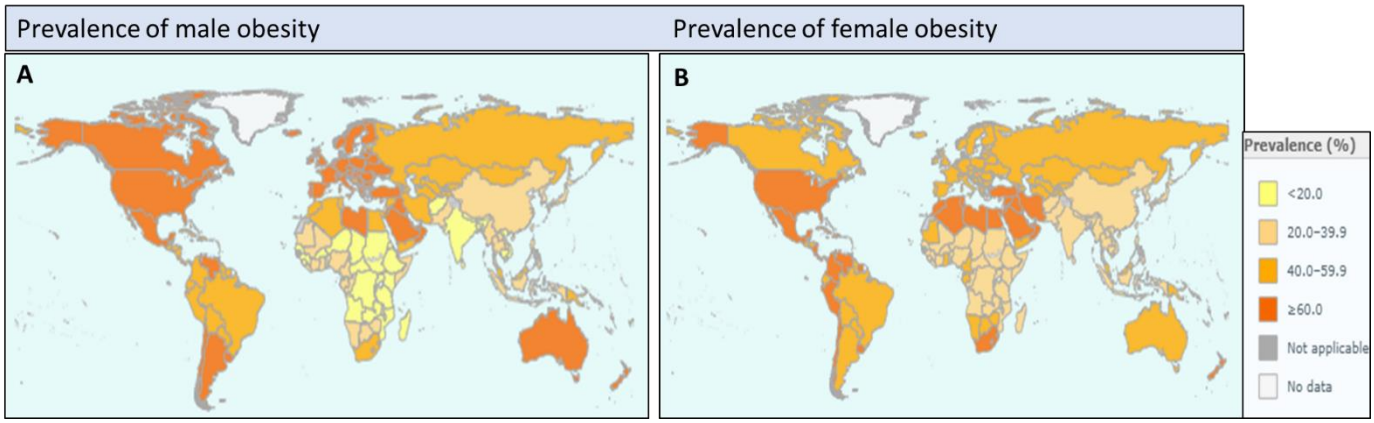


Figure 1.1 The worldwide prevalence of obesity among males (A) and females (B)

These maps illustrate the prevalence of overweight among adults around the world in 2016 by gender. Data from World Health Organization (WHO) (WHO, 2019b).

1.1.2 Causes of Obesity

Obesity is the accumulation of excess adipose tissue (WHO, 2018) which may be a cause or a consequence of changes in the control of energy homeostasis, i.e. more energy is stored than expended (Richard, 2015). Interactions between behavioural, genetic and environmental factors also contribute to obesity (Symonds et al., 2011). Behavioural factors include a poor diet, i.e. diet with a high amount of saturated fat, sugar and industrially manufactured food and low amount of fruits, vegetables and dairy products (Landsberg et al., 2013). Modern life style in which there is a greater dependence on automated systems and less physical activity also appears to be a major factor contributing to excess fat accumulation and thus energy imbalance (Richard, 2015, Symonds et al., 2011, Landsberg et al., 2013). Eating habits may also play a role as a recent study suggests a positive correlation between the speed by which an individual eats and their body weight (Ohkuma et al., 2015). Individuals who eat rapidly would potentially consume more food before a satiety signal is received and recognised by the brain which normally sends a feedback signal to stop eating (Chaudhri et al., 2008). A delay in satiety signal recognition would mean that rapid eating is associated with more energy intake leading to a delayed release of appetite regulatory factors from the hypothalamus (Ohkuma et al., 2015).

Genetics contributes to obesity with a range of studies on different populations (Europeans, Asians, South Africans) showing a significant association between BMI and genetic variants (Pillay et al., 2015). The examination of several single nucleotide polymorphisms (SNPs) which represent a source of genetic variation has shown an association with BMI in adults. A high proportion of these loci (i.e. 9 out of 13 loci) which determine BMI in adults also represent determinants for BMI in childhood (Zhao et al., 2009). Genetic variants of fat mass and obesity associated gene (FTO) and melanocortin-4 receptor gene (MC4R) found to be positively associated with BMI, but this effect was sex-specific and was modulated with diet (Marcadenti et al., 2013).

Susceptibility to obesity is also determined by gender, as in the WHO obesity statistics separated by region, women were more likely to develop obesity than men; in 2016, 11% of men and 15% of women of the world adults population were obese (WHO, 2019a). The cause of this may be a difference in their lifestyles and dietary habits or genetic differences (Fiala and Brázdová, 2000).

1.2 Adipose tissue

Adipose tissue is an independent tissue with its specific characteristics, histological appearance, plus biochemical and molecular features for its three sub-types, i.e. white, brown and beige (Frühbeck et al., 2009, Wood, 2006). It had been widely thought that adipose tissue serves only as a place for excess fat deposition, but it has been discovered that it is involved in many critical functions. Adipose tissue is divided into three types, white, brown and beige (Wu et al., 2012b) which differ in cell composition, histological appearance, mode of action, embryonic origin and anatomical location (Wood, 2006).

1.2.1 White adipose tissue (WAT)

White adipose tissue (WAT) is a loose connective tissue (Trayhurn and Beattie, 2001) composed of unilocular cells characterised by a single large fat vacuole and a peripheral nucleus (Figure 1.4 A) (Frühbeck et al., 2009).

1.2.1.1 WAT anatomical locations

WAT is distributed throughout the human body. According to its anatomical location, it is divided into visceral and subcutaneous fat which represent the largest white fat depots in mammals. Visceral WAT encloses the major internal organs (e.g. liver, intestine, kidney and heart) whilst subcutaneous WAT is located in the upper and lower body (around the buttocks, extremities and face (Wood, 2006, Wu et al., 2012b, Kwok et al., 2016) (Figure 1.2). Subcutaneous WAT is more abundant in women than men and is not as

metabolically active as visceral WAT (Mcmanus and Mitchell, 2014). Health comorbidities due to excess subcutaneous fat are lower than for visceral fat (Lara-Castro et al., 2002).

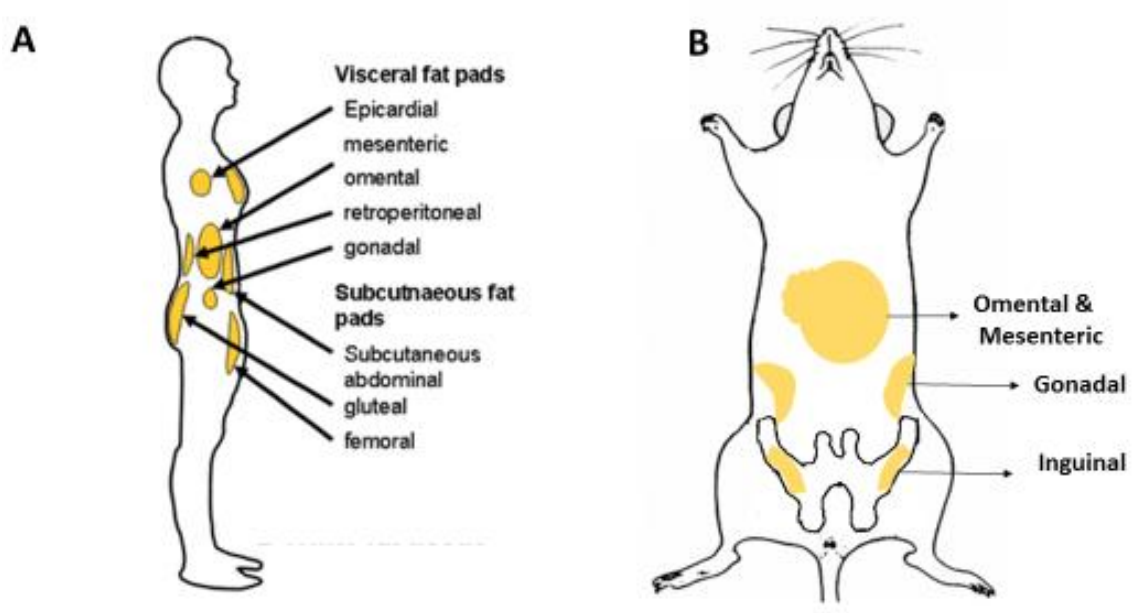


Figure 1.2 Major white adipose tissue (WAT) depots in (A) Humans and (B) rodents

Black arrows indicate major WAT locations in A: Human; main WAT depots are visceral and subcutaneous, B: Rodents; visceral WAT includes mainly omental, mesenteric and gonadal, subcutaneous WAT represented mainly by the inguinal fat. Diagrams Adapted from (Awada et al., 2013).

1.2.1.2 White adipocytes origin

Different factors, such as time of development and difference in functions between BAT and WAT suggested a distinct embryological origin for them. Differences between white fat depots in the morphology, functions and anatomical distribution in humans and mice have been recorded and indicate a different developmental origin (Billon and Dani, 2012). For example, the visceral and subcutaneous WAT showed difference in the metabolic activity which may be caused by the difference in their expression of specific factors known as determinants for their conversion to the brown phenotype of adipose tissue (Zuriaga et al., 2017). In addition, the omental and mesenteric WAT depots are located close to each other and are both considered to be visceral fat, but they have

different gene expression profiles, replication and differentiation capacities (Billon and Dani, 2012).

WAT originates from the mesoderm in mid-pregnancy in the human foetus and soon after birth in rodents arises from cells with a lineage not expressing Myf5 factor unlike the brown adipocytes (i.e. Myf5 negative cells) (Gesta et al., 2007) (Kajimura et al., 2010)

1.2.1.3 WAT functions

The main functions of WAT can be placed in one of three categories, i.e. lipid metabolism, glucose metabolism and endocrine function. BAT shares with WAT some of these functions.

1.2.1.3.1 Lipid metabolism

WAT stores energy as lipids that can be mobilised in response to metabolic signals. Fatty acids from food are stored as triglycerides (TGs) in the adipose tissue representing an energy store that is used in times of food shortage (Lieberman and Marks, 2009). When needed, TGs are hydrolysed into free fatty acids (FFA) and released into the circulation as fuel for tissues through its oxidation and adenosine triphosphate (ATP) formation, which represents the energy source of the body (Lieberman and Marks, 2009, Avram et al., 2005). The quantity of FFA oxidised is determined by the amount of energy needed, and lipid metabolism in adipocytes is regulated by FFA uptake, lipogenesis and lipolysis. (Avram et al., 2005).

1.2.1.3.2 Glucose metabolism

WAT participates in glucose metabolism (Rosen and Spiegelman, 2006). It expresses genes of proteins that regulate glucose transport between cells and circulation and influences glucose metabolism in other tissues (Avram et al., 2005). The action of insulin on carbohydrate and lipid metabolism is mediated by members of the insulin receptor substrate (IRS) family (Previs et al., 2000). Cold exposure has a major positive effect on

glucose clearance and insulin sensitivity that is achieved by triggering the insulin signalling pathway evident by the upregulation of insulin receptors family members (IRS1&IRS2) in BAT (Wang and Wahl, 2014) and WAT (Gasparetti et al., 2003), for example, disruption of IRS1 and IRS2 in mice was linked to impaired glucose transport and insulin signalling, respectively (Rondinone et al., 1997, Withers et al., 1998). The regulation of the insulin signalling pathways is tissue specific (Gasparetti et al., 2003), IRS1 functions mainly in muscles while in addition to muscle, IRS2 affects the liver and adipose tissue (Previs et al., 2000).

1.2.1.3.3 Endocrine function

WAT acts as an endocrine organ by secreting many hormones that affect different organs and processes. In addition to the autocrine and paracrine action of factors released by adipocytes, they exhibit an endocrine function by producing bioactive products that are carried by the circulation (Avram et al., 2005, Wozniak et al., 2009). Proteins produced by WAT play a role in inflammation and lipid metabolism (Trayhurn and Beattie, 2001). Leptin represents one of them; it is a hormone released from WAT and signals the brain to control appetite (Halford and Blundell, 2000, Avram et al., 2005). Receptors in the brain, specifically in the hypothalamus, respond to leptin by binding to it, which informs the brain about the body's energy status (Schwartz et al., 1996). A mouse study revealed the relatively high expression of leptin in WAT compared to BAT in lean mice while it has been detected in the BAT of obese mice (Cinti et al., 1997). Obese mice given leptin can reduce body weight and increase UCP1 gene expression in BAT and WAT which means that leptin triggers energy utilisation (Commins et al., 1999). In rats, treatment of adipose tissue with leptin enhances glucose utilisation (Siegrist-Kaiser et al., 1997). It also contributes to low-grade chronic inflammation in adipose tissue (Ye, 2011).

Adiponectin represents another important adipokine that is expressed specifically in the adipose tissue. It has been known for its antidiabetic properties where is a reduction in

its circulatory concentration is associated with the development of metabolic syndrome and diabetes. Plasma concentration of adiponectin is affected by different factors like the dietary factors and gender. Adiponectin increases energy consumption and decreases TG in the liver which may explain its role in improving insulin sensitivity (Kadowaki et al., 2006)

1.2.1.3.4 High plasticity

In addition to browning which is a reversible trans-differentiation of adipocytes located in WAT to beige adipocytes (Sections 1.2.3 & 1.3), subcutaneous adipocytes (inguinal) show a high plasticity in rats and mice as they are capable of differentiating into mammary glands during pregnancy and lactation in a process referred to as "Pinking" (Figure 1.3). It occurs in the female inguinal adipose tissue, and the mammary cells colour becomes pink at the gross level (Giordano et al., 2014). Mammary gland alveoli development occurs in two stages. In the first stage of pregnancy, alveoli are composed of epithelial cells that are devoid of lipid droplets while in the second stage of pregnancy, they are constituted of epithelial cells that are filled with lipid droplets. The second stage is accompanied by the shrinking of subcutaneous adipocytes (Giordano et al., 2014). This process is regulated by many factors, of which ELF5 is the most important and is considered to be the master regulator of alveologenesis (Choi et al., 2009). ELF5 is a member of the ETS transcription factor family (Zhou et al., 1998) that is expressed during embryogenesis in many depots including mammary cells and remains high during lactation (Lee and Ormandy, 2012, Zhou et al., 2005). ELF5 expression in virgin rats results in alveolar genesis (Lee and Ormandy, 2012). The whey acidic protein (WAP) which is specific to mammary cells and upregulated extensively during pregnancy (Burdon et al., 1991) has been detected in the inguinal fat in mice during gestation (Giordano et al., 2014).

Adipocytes appear to be able to programme their genome according to the physiological stimuli to maintain homeostasis of the organism (Cinti, 2017). In a recent study on

mice, UCP1 positive multilocular cells were detected in subcutaneous fat after lactation, suggesting that trans-differentiation of milk-producing mammary cells to brown adipocytes occurs in the post-lactation period (Giordano et al., 2017).

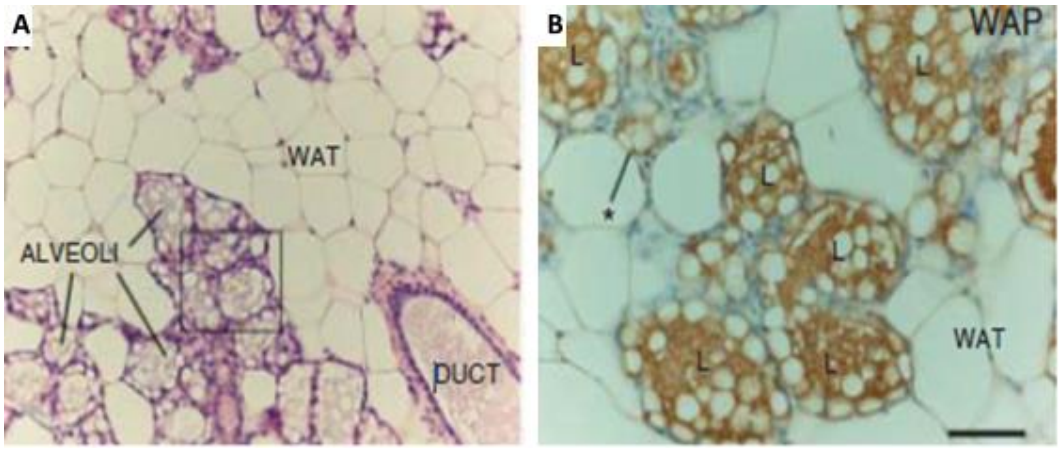


Figure 1.3 Histological image of subcutaneous adipose tissue from 17 days pregnant mouse
(A) Haematoxylin and eosin stained microscopic histological section. (B) WAP immunoreactive microscopic histological section. Adapted from (Giordano et al., 2014)

1.2.1.3.5 Immunity

The immune system is composed of the innate and the adaptive responses; it functions in protecting the host organism from infections, and its ability to distinguish foreign agents from the host cells is crucial in defence (Aderem and Ulevitch, 2000). If this fails, autoimmune disease may develop (Karopka et al., 2006). Once a pathogen enters the body across the external skin barrier, for example, it will be attacked by different types of white blood cells (WBC) where it will be ingested and digested. These can then act further to develop protective immunity by presenting the degraded particles of the pathogen on their cell surface to enable immune cells to be swiftly identified in future infections, thus activating the adaptive immune system (Aderem and Ulevitch, 2000). The immune cells communicate between each other and respond to stress by secreting factors (chemokines, cytokines or proteins) that trigger inflammation in the infected area (Baron and Albrecht, 1996).

The development of obesity induces a type of chronic low-grade metabolic inflammation called meta-inflammation in which immune cells infiltrate the adipose tissue (Hotamisligil, 2006). If this infiltration continues, it may lead to insulin resistance, glucose intolerance and adipose tissue dysfunction (Hotamisligil, 2006, Hotamisligil, 2017, Lee et al., 2014). Adipose tissue represents the main, but not, the only tissue where this process takes place (Hotamisligil, 2017).

WAT responds to metabolic stress by increasing cell size and recruiting new adipocytes by hypertrophy and hyperplasia, respectively; therefore, it increases the body's ability to store lipids (Hausman et al., 2001). In visceral WAT, reduced vascularisation occurs and can lower oxygen availability leading to hypoxia (Pasarica et al., 2009, Lee et al., 2014) that will cause the influx and activation of inflammatory cells into the tissue (Caputo et al., 2017), that has beneficial effects by acting as a signal to trigger angiogenesis and promotes capillary density to meet adipose tissue growth demand (Ye, 2011). It occurs through proangiogenic factors produced from adipocytes, such as vascular endothelial growth factor (VEGF) which induces endothelial cell proliferation (Ye, 2011).

Much evidence supports the presence of a cross-talk between obesity, insulin resistance and low-grade chronic inflammation (Bastard et al., 2006). Pro-inflammatory markers are positively correlated with excess fat mass deposition which indicates that obesity is strongly linked to meta-inflammation (Hotamisligil, 2006). Among the most important pro- and anti-inflammatory factors that participate in the inflammation process are:

- Pro-inflammatory factors
    - Nuclear factor kappa-light-chain-enhancer of activated B cells (NFKB): controls the expression of inflammation genes (Lawrence, 2009). Its activation is triggered in all cell types causes upregulation of inflammatory mediators (Vitseva et al., 2008).
    - Tumour necrosis factor (TNFα): it is highly expressed in obese rodents and humans (Kern, 1997). It functions in immune signalling, promoting insulin

resistance by inhibiting insulin receptor signalling pathways (Hotmansgili et al., 1993, Hotamisligil, 2003), regulates the production of other inflammatory factors (Trayhurn and Wood, 2004) and acts as a proangiogenic factor (Ye, 2011).

- Interleukin 6 (IL6): secreted by adipose tissue (adipocytes and macrophages) (Trayhurn and Wood, 2004). As with other inflammatory mediators, IL6 expression is high in obese subjects (Maachi et al., 2004, Trayhurn and Wood, 2004).
- EGF-like module-containing mucin-like hormone receptor-like 1 (EMR1): a macrophages biomarker in rodents that mediates the inflammatory process in adipose tissue and participates in insulin resistance (Lumeng et al., 2007b). These resident macrophages constitute a high percent of WAT (more than 10%), and their numbers correlate with adipocytes size and body mass index (Weisberg et al., 2003).
- Monocyte chemoattractant protein (MCP1): upregulated in obese subjects and contributes to adipose tissue infiltration by macrophages and the development of insulin resistance (Kanda et al., 2006).

- Anti-inflammatory biomarkers.
  - Interleukin 10 (IL10): an interleukin expressed primarily in adipocytes (Lumeng et al., 2007a). Its plasma concentration is negatively correlated with glucose tolerance (Blüher et al., 2005) as it protects the body from insulin resistance (Lumeng et al., 2007a) and can suppress the inflammatory response (Baker et al., 2011).

1.2.1.3.6 Insulation and protection

WAT has many other functions. Subcutaneous WAT provides insulation by preventing heat loss in order to maintain body temperature (Sidossis et al., 2015), protects the body by acting against mechanical stress and forms a barrier that prevents infectious agents from entering the body through the skin (Kwok et al., 2016).

1.2.2 Brown adipose tissue

Brown adipocytes are highly vascularised multilocular cells that contain many lipid droplets with a centrally located nucleus, characterised by containing a large number of mitochondria (Ovalle and Nahirney, 2013) (Figure 1.4 C). The thermogenic tissue, BAT, was thought to disappear after the neonatal period in humans in which it is present in the newborn as a "kite shape" in their back to provide heat (Heaton, 1972). In 2009, significant amounts of functional BAT were detected in adults (Figure 1.5 A) (Virtanen et al., 2009). Its role in energy homeostasis was the main reason for the upsurge in academic interest in its function. BAT activation could, therefore, be a potential anti-obesity target with ≈ 50g of functional BAT being estimated to have the potential to increase systemic energy expenditure by 5-10% (van der Lans et al., 2013).

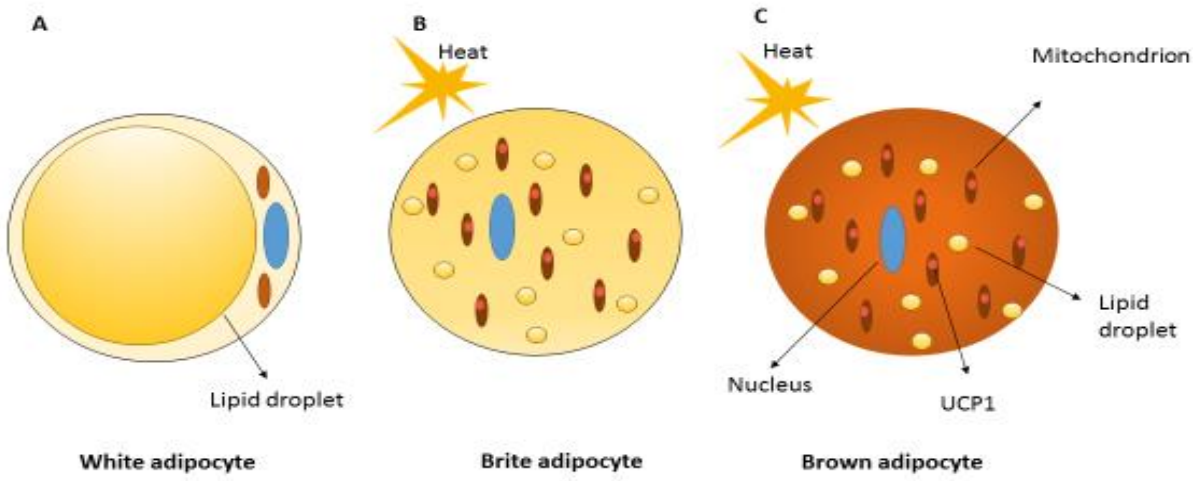


Figure 1.4 Schematic diagram of adipocytes types

White adipocyte (A) has one large lipid droplet with the nucleus squeesed to the periphery, Brite (B) and brown (C) adipocytes have many lipid droplets and mitochondria. Brite adipocytes are morphologically similar to brown, dispersed through the WAT and have a different embryological origin from both.

BAT is characterised by possessing a unique protein, uncoupling protein (UCP1), located in the inner mitochondrial membrane and has a molecular weight of 32 Kilodalton (Heaton et al., 1978). It has the ability to uncouple the movement of protons down their electrochemical gradient from ATP synthesis in order to generate heat (Heaton et al.,

1978) (Figure 1.6). The activity of BAT is primarily regulated by the sympathetic nervous system (SNS) and the endocrine system (Nakamura et al., 2007). The major BAT depots in humans and rodents are supraclavicular and interscapular (Figure 1.5), respectively, that are highly innervated by the SNS (Wirsen, 1965, Bartness et al., 2010). Other small depots of BAT like the mediastinum and the epicardial are also innervated by the parasympathetic nervous system (Giordano et al., 2004, Schäfer et al., 1998).

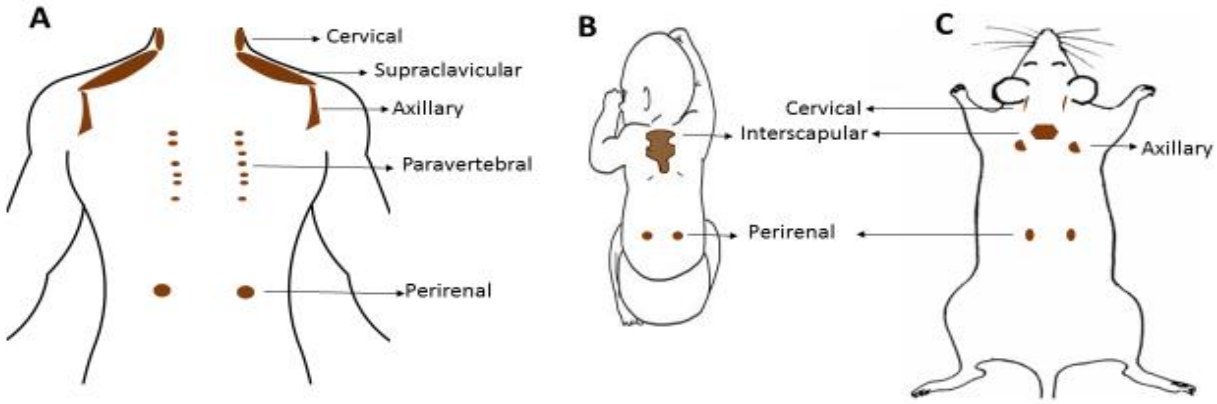


Figure 1.5 Brown fat main depots in (A) Human adult, (B) Human infant and (C) Rodents

Black arrows indicate BAT depots in the two species. Main location in human adult (A) is in the supraclavicular area, the interscapular area in human infant appears as a kite shape (B) and in the interscapular region in the rodents (C).

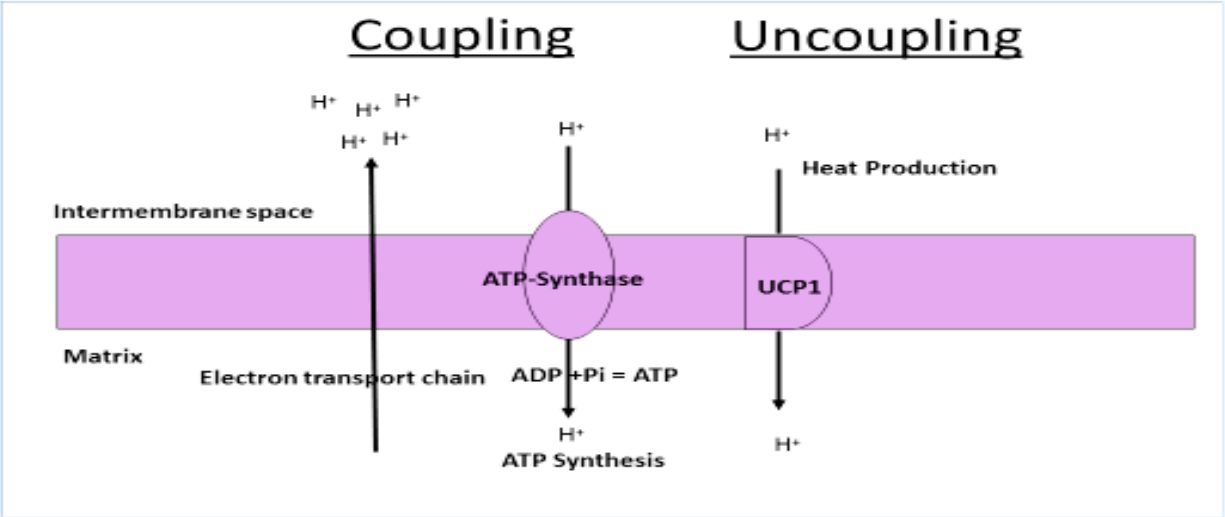


Figure 1.6 Mechanism of action of uncoupling protein 1 (UCP1)

During respiration, proton pumping through the electron transport chain generates a proton gradient, the energy of which is used by ATP-synthase to synthesise ATP. In the uncoupling, UCP1 uncouples the movements of protons down their electrochemical gradient from ATP synthesis and dissipating this energy as heat.

1.2.2.1 Brown adipocytes origin

Lineage tracing analysis and gene fate mapping, have revealed that brown adipocytes are of mesenchymal origin (Farmer, 2008). Interscapular brown adipocytes exhibited a myogenic signature (Gesta et al., 2007), and appear to be developmentally close to skeletal muscles, i.e. both arise from progenitor cells in the mesoderm from a myogenic transcription factor 5 ($Myf5^{+}$)-expressing cell lineage (Kajimura et al., 2010).

1.2.2.2 Brown adipose tissue functions

As a thermogenic tissue, the primary function of brown fat is heat production "thermogenesis" (van der Lans et al., 2013). BAT was identified in animals during their arousal from hibernation, and showed a role in adaptation to cold after birth (Himms-Hagen, 1990). In mammals, thermogenesis is mainly mediated by shivering and nonshivering. Shivering thermogenesis is triggered by cold exposure and takes place in

the skeletal muscles (Martineau and Jacobs, 1988) where energy from ATP is converted to mechanical energy (kinetic) resulting in heat release. Nonshivering and diet-induced thermogenesis are both potential functions of BAT (Cannon and Nedergaard, 2004). Except in brown fat which has its unique mechanism for energy dissipation, the metabolic rate in all other tissues is determined by ATP mobilisation that is reflected by the mitochondrial proton electrochemical gradient dissipation rate (Himms-Hagen, 1990).

Lipids are carried in the circulation in the form of triglyceride-rich lipoproteins where they are hydrolysed by lipoprotein lipase resulting in FFA release (Bartelt et al., 2011). FFAs are translocated by fatty acid translocase (CD36) (Bartelt et al., 2011) and fatty acid transport proteins (FATPs) (Hagberg et al., 2010) in the cytoplasm, where they are transported by FABPs (Calderon-Dominguez et al., 2016). The triglycerides, which had been synthesised in the cytosol are hydrolysed in lipid droplets by three main lipases, adipose triglyceride lipase ATGL, hormone-sensitive lipase (HSL) and monoacylglycerol lipase (MGL) (Zechner et al., 2009). The enzyme ATGL catalyses the hydrolysis of TG to FFAs and diacylglycerol (Zimmermann et al., 2004) which is then hydrolysed by HSL into monoacylglycerol (MG) and FFA and finally monoacylglycerol lipase converts MG to glycerol and FFAs (Zechner et al., 2009) which drive the thermogenesis (Calderon-Dominguez et al., 2016, Bartelt et al., 2011).

In addition to thermogenesis, BAT is able to improve glucose tolerance and insulin sensitivity (Chondronikola et al., 2014), e.g. BAT transplantation in both high fat (HF), and chow diet-fed male mice improved their glucose tolerance; transplantations also attenuated the increased body weight caused by HFD feeding (Stanford et al., 2012).

1.2.2.2.1 Non-shivering thermogenesis

Members from the Transient Receptor Potential family TRP (mostly TRPM8) are expressed in the sensory neurons that innervate the skin, those mediate the sensation of temperature change by providing temperature information to the thermoregulatory

centre in the hypothalamus (arcuate nucleus) in the central nervous system (Wang and Siemens, 2015). When SNS is activated in response to cold, it releases norepinephrine which induces thermogenesis in BAT (van Marken Lichtenbelt et al., 2009). Norepinephrine acts on the beta-3 adrenergic receptor (β3AR), which are predominant in BAT (Krief et al., 1993, Cypess et al., 2015), starts a cascade where lipolysis is stimulated (Wang et al., 2001) resulting in FFAS as products (Hondares et al., 2011) that will induce UCP1 gene expression and promote protein activity (González-Barroso et al., 1998, Matthias et al., 2000). A recent study showed that short exposure (10 days) of humans to a standardised low ambient temperature regime causes an increase in BAT activity, energy dissipation and thermogenesis (van der Lans et al., 2013).

1.2.2.2.2 Diet-induced thermogenesis (DIT)

Diet can also enhance BAT activity (Rothwell and Stock, 1979). High dietary intake will be sensed by the hypothalamus which will activate the SNS. The SNS will send a signal to the thermogenic tissue (BAT) received by β3AR which will stimulate lipolysis and FFA production and transport that activates BAT (Lowell and Bachman, 2003, Labbé et al., 2015). Many factors contribute to the variability in the thermogenic effect of different diets have been studied in humans. These include feeding frequency (Tai et al., 1991), energy content (Westerterp et al., 1999) and diet composition (Westerterp et al., 1999, Scott and Devore, 2005). Other factors like the energy cost of digestion and transport contribute to the variance of the food thermic effect but is relatively very low when compared to meal composition and energy content (de Jonee and Bray, 1997). A study in human females volunteers showed that thermic response (measured using a respiration champer) would be higher if the diet is rich in protein and carbohydrate compared with fat (Westerterp et al., 1999). In rats that were fed either a cafeteria-style or a control diet, the former showed 76% more oxygen consumption in BAT (Rothwell and Stock, 1981b). DIT is reduced in obese women due to a low thermogenic response (Schutz et al., 1984).

1.2.2.3 Brown adipocytes differentiation-transcriptional control

The overall mechanism of brown adipocyte development is not well elucidated, but many factors have been studied and documented to have a role, including the following:

- PRD1-BF1-RIZ1 homologous domain containing 16 (PRDM16): a transcriptional regulator that activates brown adipocytes differentiation (Seale et al., 2007). Its absence causes the disappearance of specific morphological characteristics of brown adipocytes and a reduction in the thermogenic genes (Seale et al., 2008).
- Peroxisome proliferator-activated receptor gamma (PPARɣ): a significant transcription factor contributes to adipocyte differentiation regulation (Spiegelman, 1998). PPARɣ-ablated cells cannot undergo differentiation (Rosen, 2005) while mice adipocytes devoid of PPARɣ do not survive (Imai et al., 2004). In addition, two other isoforms of PPAR; PPARα and PPARδ may have a role in adipogenesis, PPARɣ regulates adipocyte differentiation with a possible contribution of PPARα, while PPARδ showed no effect (Brun et al., 1996).
- PPARɣ coactivator-1 alpha (PGC-1α): a transcriptional coactivator upregulated in BAT upon cold exposure in mice and enhanced PPARɣ transcriptional activity, its ectopic expression in white fat caused increased *UCP1* expression (Puigserver et al., 1998). Lack of PGC-1α downregulates thermogenic genes expression and reduces mitochondrial biogenesis (Uldry et al., 2006).
- Retinoblastoma protein (RB): has an inhibitory role in brown adipocyte differentiation, with downregulation promoting adipocytes differentiation to a brown phenotype (Hansen et al., 2004). Members of this family regulate the PGC-1α expression by binding to and inhibiting its promotor which will control trans-differentiation between white and brown adipocytes (Scimè et al., 2005).
- Bone morphogenetic protein family (BMP): members of this family have variable effects on adipogenesis, and the differentiation of white, beige and brown adipocytes. BMP2, if used in vitro with PPARɣ, will stimulate adipocyte differentiation of mesenchymal cells (Sottile and Seuwen, 2000). BMP7 can

induce the development of brown adipocytes even in the absence of other primary factors or hormones, and if the gene is deleted in the embryo, there is a reduction in BAT mass with complete loss of UCP1 (Tseng et al., 2008). BMP4 stimulates PPARɣ expression and enhances adipocytes differentiation to BAT (Gustafson et al., 2015).

- CCAAT/Enhancer binding protein (CCAAT/EBPα&β): mouse fibroblasts lacking C/EBPα can undergo adipogenesis but only in the presence of PPARɣ (Rosen, 2005). Its expression triggers the insulin-sensitive glucose uptake cascade (El-Jack et al., 1999). C/EBPβ forms a transcriptional complex with PRDM16 which regulates preadipocytes differentiation to mature brown adipocytes (Kajimura et al., 2009). Fibroblasts expressing PRDM16 and EBPβ transplanted in mice exhibited a full conversion to BAT as determined by their morphological and biochemical characteristics (Kajimura et al., 2009).

1.2.3 Beige adipose tissue

In 1992, Cousins and Cinti either exposed rats to cold or treated them with beta-adrenergic receptor agonists. Both interventions showed a significant increase in mitochondrial UCP1 expression of cells located in white fat (Cousin et al., 1992, Giralt and Villarroya, 2013); this represents the third type of adipose tissue, which is found within white fat depots and is known to develop by a process called "browning" (Bonet et al., 2013, Lean et al., 1986). Browning occurs in response to signal induction which could be due to a physiological stimulus such as cold or administration of pharmaceuticals like PPARγ agonists that promotes UCP1 gene expression and mitochondrial biogenesis (Petrovic et al., 2010). These cells are known as being inducible, beige or brite (brown in white) adipocytes and are morphologically similar to BAT and express UCP1 but in much lower amounts (Figure 1.4B). However, they have some differences from BAT, including 1) a distinct gene expression pattern (Okamatsu-

Ogura et al., 2013) 2) are different in regulation as they are inducible and 3) have a different embryonic origin (Harms and Seale, 2013).

1.2.3.1 Beige adipocytes origin

Although beige adipocytes express UCP1, they are not always derived from the $Myf5^{+}$ lineage as BAT (Wu et al., 2012a). Beige adipocytes are therefore considered to originate from smooth-muscle-like cells or share white adipocytes in their origin (Himms-Hagen, 1990) but their exact origin still unknown (Long et al., 2014).

1.2.3.2 Beige adipocytes function

Beige adipocytes can function in UCP1-dependent thermogenesis (Giralt and Villarroya, 2013) but recently, a UCP1-independent thermogenesis mechanism has been suggested whereby thermogenic calcium cycling is triggered in response to norepinephrine activation in the absence of UCP1 (Ikeda et al., 2017).

In a mice study, lacking UCP1 and housing at cold (4°C) was accompanied by increased oxygen consumption (Ukropec et al., 2006). The mechanism by which animals adapt to cold without UCP1 was explored later. It suggested that after activation by catecholamines, the SNS will trigger calcium mobilisation where it is released from the sarcoplasmic reticulum (SR) through the ryanodine receptor 2 (RYR2) and taken back by the SERCA2B pump in an ATP-dependent manner (Ikeda et al., 2017, Mottillo et al., 2018). Heat will then be dissipated which will contribute to the total body energy expenditure (Mottillo et al., 2018).

1.3 Browning process

Defined as any significant increase in UCP1 gene expression in brite/beige adipocytes (Nedergaard and Cannon, 2014), numerous factors have been shown to induce browning, that are either natural factors or synthetic drugs. These include nutrients, drugs, gene deletion, living conditions or surrounding environment (Nedergaard and

Cannon, 2014, Kalinovich et al., 2017). Browning is thought to have beneficial effects on adiposity, insulin resistance and general metabolic health problems (Bartelt and Heeren, 2014).

1.3.1 Browning factors

Many substances induce browning through activation of the SNS; this includes the stimulation of lipolysis and lipid oxidation and upregulation of thermogenic genes (Bonet et al., 2013).

1.3.1.1 Pharmacological agents

- β3AR agonists: UCP1 was elevated in the inguinal adipose tissue and iBAT after chronic injection of β3AR in mice (Pico et al., 1998). Rats given a β3AR agonist showed raised UCP1 expression in WAT that was similar to iBAT and higher in lean than in obese animals (Cousin et al., 1992). Cold exposure of β3AR knocked out mice revealed a decrease in UCP1 expression and a reduction in the density of multilocular cells in white depots while UCP1 expression in BAT was not affected (Jimenez et al., 2003).
- PPARɣ ligands: caused browning in white fat depots (Ohno et al., 2012). Prolonged treatment with PPARɣ agonists increased UCP1 expression, mitochondrial biogenesis and expression of WAT browning-related genes such as PGC-1α (Petrovic et al., 2010).

1.3.1.2 Thyroid hormones

Triiodothyronine (T3) acts as a mediator for mitochondrial biogenesis and treatment with T3 upregulates UCP1 expression in WAT in vitro (Lee et al., 2011). T4 is converted to T3 in a process called deiodination that mediates thyroid hormonal metabolism (Norris and Carr, 2013, Bollepalli and Rose, 2012), this is achieved by the action of three different 5' monodeiodinases (MDI), i.e. types I, II, and III. Type 2 MDI which is present in BAT (Bollepalli and Rose, 2012) performs deiodination of T4 to produce the active thyroid

hormone T3 (Bianco and Kim, 2006). Cold-induced thermogenesis in BAT can be dependent on local T3 production catalysed by type 2 MDI which induces thermogenic genes expression like UCP1 (Bianco and Kim, 2006).

1.3.1.3 Dietary factors

Capsinoids activate transient receptor potential (TRP) channels, which are functioning as receptors for capsaicin (GeneCardsDatabase) and trigger browning in WAT depots by enhancing thermogenic marker expression (UCP1, PPARɣ, PGC-1α) (Thyagarajan and Baskaran, 2017, Baskaran et al., 2016). The transient receptor potential vanilloid 1 (TRPV1) responds by promoting UCP1 expression of BAT (Iwasaki et al., 2011) and inhibiting adipogenesis (Randhawa et al., 2009); this was shown in a study on mice where treatment with red pepper increased fat oxidation and UCP1 protein and gene expression in BAT (Birerdinc et al., 2013, Baskaran et al., 2017). Capsinoid ingestion raises energy expenditure and reduced fat accumulation in humans if chronically administered (Saito and Yoneshiro, 2013).

High-fat diet (HFD) upregulates UCP1 expression in iBAT but has different outcomes regarding the onset of browning in WAT between species, i.e. HFD feeding reduced mitochondrial biogenesis in mice WAT but increased UCP1 mRNA in abdominal WAT of rats (Bonet et al., 2013). The fat composition of the HFD appears to affect the degree to which thermogenesis is stimulated in mice (Mercer and Trayhurn, 1987). Feeding a large amount of polyunsaturated fatty acids (PUFA) stimulated UCP1 expression and thermogenesis in mice. The HFD that is rich in fish oil increased expression of thermogenic markers in iBAT in rats and attenuated their weight gain while induced browning in WAT (Okla et al., 2017, Fromme and Klingenspor, 2010). Consumption of a diet that is high in sucrose also upregulated UCP1 gene expression in the BAT and WAT of mice (Maekawa et al., 2017).

1.3.1.4 Environment

Exposure to a cold temperature triggers browning of WAT in vivo, and such stimulation is necessary to maintain stable body temperature and protect from hypothermia (Shore et al., 2013). Changes in morphology and UCP1 expression in inguinal adipocytes were noticed after cold exposure in mice (Paschos et al., 2018). A reduction in incubator temperature from 37°C to 32°C triggered browning in vitro (Velickovic et al., 2018). Several factors, like the magnitude and duration of cold exposure, sex, age, body composition and the exposure medium affect the extent to which cold will induce browning and subsequently thermogenesis (Brychta and Chen, 2017).

1.4 Obesity studies: rat as a model

Rats have been considered as a superior component of the scientific research, especially in biomedical fields (Sengupta, 2013). While rodents represent about 80% of experimental animals, rats are the most frequently used among them (Fagundes and Taha, 2004). The average life span of laboratory rats is three years (Andreollo et al., 2012), they wean at three weeks of age (Sengupta, 2013) and reach sexual maturity at six weeks of age (Andreollo et al., 2012).

1.4.1 Advantages

Rats are widely used as an experimental model for examining the effects of dietary manipulation during pregnancy for several reasons. Their short gestational period and short life span enable scientists to study different generations in a relatively short time. Also, the production of large litter size is desirable in some studies, e.g. some studies tend to study interventions on offspring from the same mother to remove any confounding factor, i.e. genetic or pregnancy conditions (Symonds and Budge, 2009).

From a physiological point of view, a large amount of data has been collected from rats that have been extensively studied over the years. Consequently, a lot is known about

their responses, pathways, mechanisms and genome; therefore, this would facilitate research and enhance comparisons. For instance, substantial metabolic studies have been performed on Sprague Dawley and Wistar rats as they showed susceptibility to diet-induced obesity and insulin resistance (Buettner et al., 2007).

1.4.2 Limitations

Rats in their natural environment are adapted to live off a high variation in the available food supply; this reflects their ability to adapt easily to any food provided in an experimental setting which may include a resistance to becoming obese (Symonds et al., 2009). This adaptation might be critical in studies on obesity because the rat's response to obesogenic diets can be different from expected as they can adapt, thereby minimising or even preventing obesity induction (Symonds et al., 2009).

The hypothalamic-pituitary-adrenal (HPA) axis in rats which is responsible for appetite control matures postnatally after a short gestation (Dussault and Labrie, 1975). This pattern of development is different from large mammals such as humans in which the HPA-axis matures in the last trimester (Mühlhäusler et al., 2004, Symonds et al., 2006). The arcuate nucleus, the part of the hypothalamus involved in the appetite regulation mechanism, develops postnatally in rodents (Arai and Matsumoto, 1978, Minokoshi et al., 2004). The browning capacity in WAT can be different between humans and murine, a recent study has shown that expression of browning genes was higher in visceral compared to subcutaneous WAT in humans while the opposite case was in mice (Zuriaga et al., 2017).

1.5 Maternal metabolism and obesity

1.5.1 Maternal metabolism

1.5.1.1 Lipids metabolism in pregnancy

Fat metabolism changes during pregnancy to accommodate the increased metabolic needs of the foetus (Lain and Catalano, 2007). Pregnancy is characterised by hyperlipidaemia (Warth et al., 1975). In the first 14 weeks of pregnancy in humans, the circulating lipid, especially triglycerides, concentrations decline (Butte, 2000, Herrera, 2002b) and then rise up to term (FÅhraeus et al., 1985). Cholesterol follows the same pattern except that its rise is less than that of triglycerides (FÅhraeus et al., 1985). Lipids are important for placental function, and membrane formation and their concentration through pregnancy adapts primarily to changes in adipose tissue metabolism, endocrine adaptations and carbohydrate metabolism (Butte, 2000).

The degree of lipid transport through the placenta depends mainly on gestational age (Robertson and Sprecher, 1968). Lipids do not readily cross the placenta, but concentrations of NEFA and TAG were found to be correlated between the mother and foetus. Impaired transfer of long-chain polyunsaturated fatty acids by the placenta can cause a reduction in birth weight which supports a hypothesis of maternal lipid metabolism involvement in fetal adiposity (Herrera and Ortega-Senovilla, 2014).

1.5.1.2 Carbohydrates metabolism in pregnancy

Glucose homeostasis is influenced by insulin secretion and sensitivity while both glucose and insulin concentrations are affected by protein and lipid metabolism (Nelson et al., 2009). In early pregnancy, plasma glucose concentration declines, to reflect maternal adaptations rather than changes in fetal utilisation (Mills et al., 1998) and is accompanied by a slightly improved or normal glucose tolerance (Catalano et al., 1991, Catalano et al., 1992, Catalano et al., 1993). Changes in glucose concentration in late

pregnancy showed differences between studies. Some studies revealed no change in its concentration while others exhibited a further decrease (Mills et al., 1998).

The development of insulin resistance with pregnancy is a normal physiological process (Ryan et al., 1985). Progressive insulin resistance with pregnancy, maternal adiposity and placental hormones can all contribute to the development of a metabolic disorder called gestational diabetes mellitus (GDM) (Buchanan and Xiang, 2005). The definition of GDM is the onset of glucose intolerance first detected in pregnancy (Obstetrics, 1995, Butte, 2000). Heavier women are of higher risk of GDM (Chu et al., 2007); this may lead to insulin resistance in some obese women when non-pregnant (Butte, 2000, Lain and Catalano, 2007).

1.5.2 Maternal obesity

Obesity among pregnant women is becoming more prevalent, and it has the potential to contribute to complications during pregnancy and in the long term health of the offspring (Drake and Reynolds, 2010). Maternal weight gain during gestation is expected and occurs to support fetal development (Nelson et al., 2009). Many observational studies support the presence of a link between maternal obesity and a greater risk of obesity for their offspring in later life (Whitaker, 2004, Koupil and Toivanen, 2008, Tequeanes et al., 2009, Li et al., 2005, Stuebe et al., 2009). It can cause more fat accumulation in neonates (Hull et al., 2008, Sewell et al., 2006, Catalano et al., 2009) and children (Burdette et al., 2006, Blair et al., 2007, Gale et al., 2007).

The extent to which maternal obesity influences fetal weight and body composition depends on many factors. These include exposure time, i.e. early, mid or late pregnancy or lactation, diet composition and energy content (Nelson et al., 2009).

1.5.3 Programming of obesity

Clinical and epidemiological studies indicate a strong association between maternal dietary intake and composition and the risk of adult obesity in the offspring (Ravelli et

al., 1998, Ravelli et al., 1999). Maternal obesity as reflected by an imbalance in whole-body energy homeostasis can affect fetal adipose tissue differentiation and contributes to the impairment in the offspring's adipose tissue function in later life (Lukaszewski et al., 2013). The effects may include changes in cell size (enlargement as a result of triglyceride deposition, hypertrophy) or an increase in number as a result of white adipocyte differentiation (hyperplasia) (Lukaszewski et al., 2013).

1.5.3.1 Studies on animals

In a study conducted in 2007 (Bayol et al., 2007), rats were exposed to either control with junk diet during gestation and/or lactation and/or postnatally or to control diet throughout. This study aimed to investigate whether maternal exposure to junk food can promote the development of obesity by influencing the feeding behaviour in offspring. Obese dams ate more food during gestation with most of this energy derived from junk food as they preferred eating fat, salt and carbohydrate-rich food. They were heavier by late gestation due to higher energy intake and reduced activity, but their body mass at the end of lactation was comparable to those fed control diet (Bayol et al., 2007); this may be because they invest more energy in milk production (Bayol et al., 2007). Milk composition was not measured in Bayol study; however, it was analysed in a previous study (Rolls et al., 1986) that found the milk was richer in fat and energy in mothers which have been fed a variety of palatable food (cafeteria diet) (Rolls et al., 1986). Although the control group consumed less energy through gestation and lactation, their offspring were heavier at birth and at weaning compared to cafeteria diet fed-dam pups. This can be explained possibly in terms of maternal protein intake, dams fed the cafeteria diet reduced their protein intake during gestation and lactation relatively while they increased their energy intake from fat and carbohydrates. In other studies, the use of protein-restricted diets in pregnancy had caused a reduction in birth weight (Langley-Evans and Nwagwu, 1998, Bieswal et al., 2006).

Furthermore, it was found in another study that the increase in fat percentage in the milk of cafeteria-diet fed rats was accompanied with a reduction in protein deposition and with slower growth of pups (Rolls et al., 1986). For the offspring weaned on junk food, those who were exposed to junk food during gestation and lactation showed higher energy intake (mainly from junk food) compared to rats fed only control diet during gestation and lactation or fed junk during gestation and control diet during lactation. This suggests that the offspring's preference for junk food (rich in fat, sugar and salt) is promoted with their exposure to it during gestation and lactation or during gestation alone, a response that would partly explain the differences in their poor ability to control intake of junk food (Bayol et al., 2007) (Table 1.1).

At weaning, rats that were switched to junk food exhibited hyperphagia compared to those switched to chow diet while rats exposed to junk food during gestation and lactation and switched to chow food exhibited a reduction in food intake. Junk food was the main source of energy in rats fed the cafeteria diet after weaning; this can be attributed to the palatability that may play an important role in appetite regulation and energy intake both in dams and offspring as these rats preferred the food rich in fat and sugar. Body mass of rats exposed to control diet during lactation period only was similar to those fed control diet through the study; they also exhibited less energy intake than rats exposed to junk food through the whole period. This indicates the role of lactation in the regulation of appetite. It was concluded that a well-balanced diet (i.e. moderate energy content) during pregnancy and lactation could prevent adverse programming of the offspring eating behaviour and prevent later obesity (Bayol et al., 2007) (Table 1.1).

In a study by Shankar (Shankar et al., 2008) aimed to investigate whether the exposure of the offspring to maternal obesity during gestation alone would promote their ability to develop obesity later. Dams fed an obesogenic diet became heavier with 98% more fat than dams fed a control diet. No effect was observed on the offspring birth weight or caloric intake; this suggests the presence of a subtle mechanism of programming that is not dependent on energy intake. For those pups fed a control diet postnatally, no effect

of maternal obesity was seen on their body weight. However, postnatal high fat diet feeding reinforced the effect of in-utero exposure to HFD on weight gain, indicating a contribution of postnatal feeding in modifying the programming effect of maternal obesity. Serum insulin was higher in offspring of obese dams, and this response was reinforced when fed HFD postnatally. Programming of obesity during gestation thus appeared to occur without inducing changes in birth weight and may be linked to metabolic and endocrine changes that are not depending on caloric intake (Shankar et al., 2008) (Table 1.1).

Also in 2008 (Chen et al., 2008), dams fed an HFD had heavier body weights compared to dams fed chow diet that increased with pregnancy. They also showed higher serum insulin and TG compared to lean dams. No effect of maternal obesity on birth weight was observed which is consistent with the previous study findings (Shankar et al., 2008) and suggests a specific programming pathway. After weaning, pups of HFD-fed dams gained more body weight, and serum TG was higher in pups overfed postnatally (Chen et al., 2008). In Chen study, the pups were exposed to HFD during gestation and lactation; therefore, it was difficult to differentiate which HFD diet exacerbated the long-term effects on the offspring. However, according to previous studies (Bayol et al., 2007, Shankar et al., 2008, Chen et al., 2008) the maternal programming effect might be more likely was generated during the lactation period (Table 1.1).

In a study by Kirk in 2009 (Kirk et al., 2009), dams fed an obesogenic diet, which is high in fat and sugar, exhibited heavier weights during pregnancy. Offspring of obese dams were heavier than those born to controls at weaning, possibly due to the critical programming role of maternal diet during gestation and lactation period on obesity development by offspring. No difference was observed in their weight after 30 days on a control diet, switching offspring of obese dams from a diet rich in sugar and fat to a chow diet can reduce their energy intake as happened in the Bayol study (Bayol et al., 2007). At 90 days of age, pups of obese dams were heavier, deposited more fat and developed hyperphagia. These effects can be attributed to their exposure to a high

energy diet in gestation and lactation (Kirk et al., 2009). In the neonatal period, the chronic release of leptin that may be amplified in the offspring of obese dams could impair leptin signalling which caused a reduction in leptin due to the downregulation of its receptors (Kirk et al., 2009).

In a study by Nivoit (Nivoit et al., 2009), obesity was induced in females over a long time (from weaning) using a diet high in both fat and sugar. They were then fed obesogenic diet through gestation and lactation but transferred to a control diet postnatally. At mating and through gestation, dams on the obesogenic diet gained more weight that was accompanied by higher daily energy intake compared to lean rats. This may be caused by the presence of fat and sugar which makes the diet highly palatable. Plasma glucose, insulin and leptin were higher in obese dams at days 10 and 11 of gestation while lipids were not affected by the diet. Offspring of obese dams had a lower birth weight than pups of control dams; this is consistent with the same observation by Bayol et al. (Bayol et al., 2007) and Rolls et al. (Rolls et al., 1986) and can be explained by the high consumption of fat and sugars at the expense of protein (Bayol et al., 2007, Rolls et al., 1986). (Nivoit et al., 2009) (Table 1.1).

One week after weaning, offspring of control and obese rats had similar body weights, possibly, switching pups to a control diet from a highly palatable diet reduced their food intake. As the animals matured, offspring of obese dams exhibited higher weight gain, food intake, fat mass and non-esterified fatty acids (NEFA) concentration, this suggests a programming effect of maternal exposure to a high energy diet before and during pregnancy and lactation on the susceptibility of offspring to develop obesity. Insulin resistance as a phenotype of metabolic syndrome was observed in different degrees between males and females of obese dams compared to controls; this response can be due to sex-related differences in weight gain and food intake which can be an effect of maternal programming of metabolic syndrome features in offspring (Nivoit et al., 2009) (Table 1.1).

This difference in weight gain pattern between males and females was clear in a study by Desai (Desai et al., 2014). In this study, offspring were exposed to either a high fat or control diet in gestation and/or lactation; all groups were then fed a standard diet until 30 weeks of age. The dam's exposure to HFD during gestation did not increase fat mass or energy intake compared to controls. HFD fed dams increased their caloric intake in lactation and showed higher cholesterol regardless of the lactation diet. However, dams weight and caloric intake appeared to be influenced by weight gain of the offspring during lactation, e.g. except the HFD dams nursing control pups which show a reduction in weight gain that was accompanied with a reduction in the serum insulin and leptin through lactation, the other three groups showed weight loss only by the end of lactation (Desai et al., 2014).

In agreement with some previous studies (Chen et al., 2008, Shankar et al., 2008), no effect of maternal diet was seen on birth weight but offspring exposed to HFD during gestation and lactation or in lactation alone exhibited rapid weight gain which continues postnatally in different ways (rapid, intermediate, same) depending on sex (Desai et al., 2014).

At 24 weeks of age, offspring exposed to HF diet during lactation alone gained more weight, an effect further enhanced in males only if exposed to a maternal HFD during pregnancy (Desai et al., 2014). The exposure of HFD at lactation or both periods caused elevated glucose and insulin concentrations which resulted in impaired glucose tolerance and subsequently insulin resistance. These changes in the body weight and plasma profile indicate a programming effect of diet in gestation and lactation on the offspring susceptibility to obesity. HFD exposure through both gestation and lactation or lactation alone appeared to have an important programming effect on offspring weight gain compared to exposure in pregnancy alone. A sex-dependent response was recorded only in offspring exposed to HFD during lactation where males had elevated cholesterol; the reason was unclear although other studies revealed different effects of early overfeeding on males and females (Desai et al., 2014). (Table 1.1).

Table 1.1 Summary of studies on maternal programming of offspring adiposity

First author	Temperature	Fat % of energy	High sugar?	Weeks exposure	+% body weight	Birth weight
(Chen et al., 2008)	20±2°C	34	No	5	23.4	Same
(Desai et al., 2014)	Constant temperature	60	No	8	20	Same
(Kirk et al., 2009)	21C±2°C	Unclear (mix of diet with condensed milk)	Yes	6	20	
(Shankar et al., 2008)	Not mentioned	45	High carbohydrate	3	21	Same
(Nivoit et al., 2009)	20±2°C	Unclear (mix of diet with condensed milk)	High in simple sugar	~9	~17	Obese< control
Bayol	20±2°C	Chow with junk (cafeteria)	Junk food	-	13	Obese<contrl ol
<Ours>	20°C 27°C	39	yes	6	4 11	At day 19 of gestation same

A crucial effect of maternal diet composition during gestation and lactation on the offspring metabolism and caloric intake later was detected (Bayol et al., 2007, Nivoit et al., 2009). Consumption of a highly palatable diet that is rich in fat and sugars during gestation and lactation induced hyperphagia in mothers and offspring, an effect that was reduced with the transition to a chow diet where they reduced their food intake (Bayol et al., 2007). Fatty acids composition also plays a role, offspring of dams fed a saturated FA-rich diet exhibited less insulin sensitivity compared to those fed a diet rich in unsaturated fatty acids at 12 months of age (Siemelink et al., 2002).

The main negative outcome of maternal obesity in women is the increase in birth weight. In contrast, studies on rodents showed no effect of maternal obesity on birth weight (Chen et al., 2008, Desai et al., 2014, Shankar et al., 2008) or even showed lower pups

weight compared to controls (Bayol et al., 2007, Nivoit et al., 2009). Studies, where offspring of obese dams had lower birth weight compared to control, may be attributed to restricted protein intake, diet exposure time or other experimental conditions. The comparable birth weight of offspring between obese and controls is suggested to be caused by the housing temperature which represents a state of a mild cold. As cold is the most potent factor established to induce BAT activity, it could be the reason for the reduced impact of maternal obesity on birth weights. Consequently, birth weight and other pregnancy outcomes may be programmed through changes in maternal housing temperature.

In conclusion, adiposity in offspring can be programmed during several developmental windows (Shankar et al., 2008). A positive effect of maternal obesity in the development of metabolic syndrome features by the offspring was clear (Nivoit et al., 2009, Chen et al., 2008, Shankar et al., 2008). Maternal diet during gestation and lactation influences the offspring appetite in the long-term (Bayol et al., 2007), an effect that is exaggerated further by the postnatal consumption of obesogenic food (Chen et al., 2008, Shankar et al., 2008). The consumption of a well-balanced diet during gestation and lactation will protect the mothers and offspring from developing features of metabolic syndrome, e.g. obesity and insulin resistance. Furthermore, exposing mothers during gestation and/or lactation to mild cold may be able to activate BAT and protect them from insulin resistance and excess weight gain. It would also protect their offspring from obesity later through maternal programming of their metabolism. However, obesity studies on pregnant rodents have yet to be conducted at thermoneutrality to ensure the elimination of the ambient temperature as a confounding factor that reduces diet-induced obesity in dams and its programming effect in offspring.

Chapter 2. Materials and Methods

2.1 Procedural & legislative declaration

All animal procedures were performed according to the UK Home Office Act of 1986 with the necessary approval from the local ethics committee of the University of Nottingham.

The animal study was carried out in the bio support unit at the medical school of Nottingham University. All laboratory procedures were performed at laboratories of Academic Department of Child Health, School of Medicine, University of Nottingham with ethical approval from the University of Nottingham. All laboratory-based work was performed according to the UK Health and Safety Executive's Control of Substance Hazardous to Health (COSHH, SI NO 1657, 1988) and Risk Assessment guidelines.

2.2 Power of the study

Power of the study was calculated by Dr Neele Dellschaft based on published research on this area using Minitab v16 statistical software (Minitab Ltd, Coventry, Warwickshire, UK). With six animals in each group, the power to detect any significant biological increase of the primary outcome measures i.e. UCP1 in response to both interventions was 85%.

2.3 Study design

The study was a 2×2 factorial design. Four groups were produced by subjecting four weeks old rats to two interventions. Animals were dissected at three time points: unmated animals at 10 weeks of age, and after mating at day 10 or 19 of gestation, 50% and 90% of pregnancy, respectively (Figure 2.1).

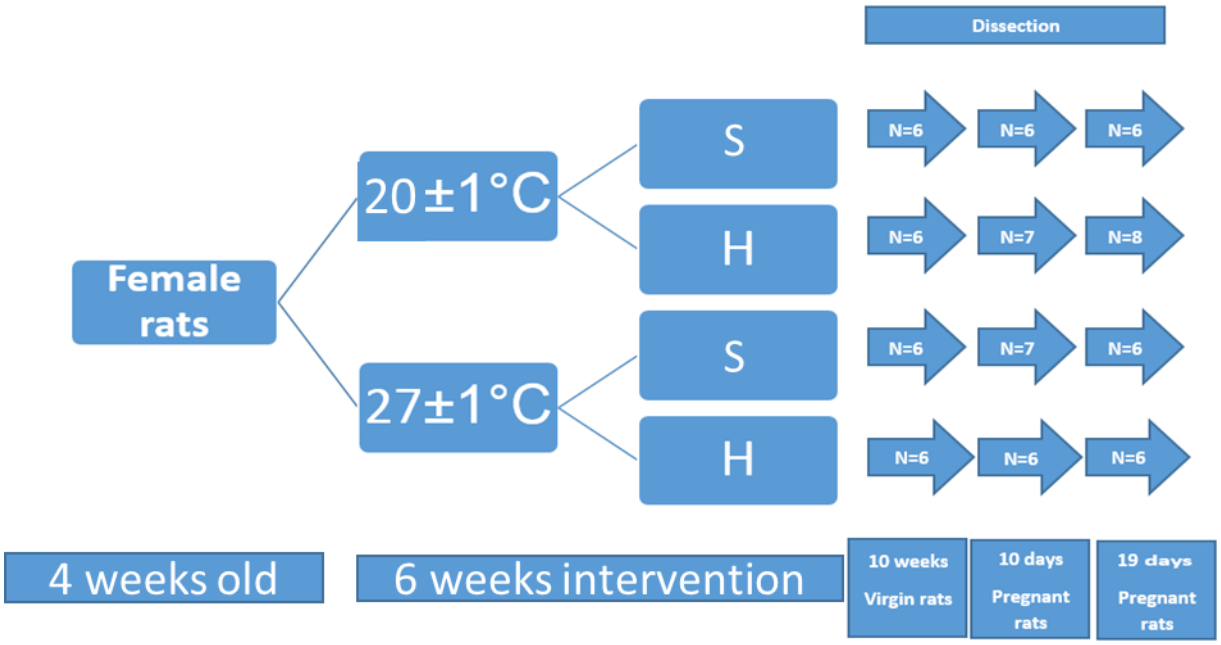


Figure 2.1 Schematic overview of the experimental design and numbers of animals involved in each group of the housing temperature study

Female and male Sprague Dawley rats were kept at either a standard housing temperature or at thermoneutrality and on either a standard (S) diet or a high fat and sucrose (H) diet. Females were sacrificed at 10 weeks of age (n=6), and after mating at 10 days (n=6-7) or 19 days of gestation (n=6-8). Females which failed to mate or lost pregnancy were not included in the numbers (N) shown.

2.3.1 Animals and housing conditions

Eighty-eight 4-weeks old female and sixteen males of Sprague-Dawley rats aged 4 weeks for mating purposes were delivered to the bio-support unit from Charles River Laboratories. Three females were housed in one cage and maintained under controlled conditions; 12:12 light-dark cycle with lights on at 07:00 am and humidity of 40% to 50%. Animals were identified in the cage for monitoring and weight measurement purposes by ear notching (right, left or no notching). All animals had ad libitum access to food and water. Food intake was measured once every three days before mating occurs, water consumption and animals' weights were recorded three times a week for both virgin and pregnant rats.

All measurement were entered in Microsoft Excel software and weight gain was calculated. Food and water intake were calculated for each animal by dividing the whole cage consumption on the number of animals in the cage.

2.3.2 Interventions

Half of both males and females rats were immediately randomised to be housed either at:

- 20±1°C, the standard husbandry temperature.
- 27±1°C, their thermoneutral temperature.

They were then randomised to receive either:

- Standard diet (S) contained 18.2% fat, 24.2% protein, and 57.6% carbohydrates (of which 7% are mono- and disaccharides); 3.1 kcal/g, (Teklad Global 18% Protein Rodent Diet; Harlan Laboratories).
- High fat and sucrose (H) diet contained 38.8% fat, 22.6% protein and 38.6% carbohydrates (of which 44 % are mono- and disaccharides), 4.6 kcal/g (Abbot Nutrition).

Table 2.1 summarises the Macronutrients composition of the diets.

Table 2.1 Macronutrient composition of diets

	Standard diet (S)	High fat and sucrose diet (H)
% of weight		
Protein	18.6	26.2
Fat	6.2	20
Carbohydrate	44.2	44.7
Mono-, disaccharides	3	19.5
Energy density (kcal g-1)	3.1	4.6
% of energy		
Protein	24.2	22.6
Fat	18.2	38.8
Carbohydrate	57.6	38.6
Mono-, disaccharides	3.9	16.8

2.3.3 Animals Mating

Every female assigned to be pregnant was housed with one male from the same intervention (diet and temperature) group and monitored daily. Females were assumed to be pregnant (day 1) on the day that a copulation plug was found. After that, they were returned to their original cages and their weight was recorded three times a week until dissection.

2.3.4 Dissection and tissues sampling

Scale boats weighted, tubes for deep freezing and cassette for tissue blocking were labelled in advance for each animal tissue to ensure rapid freezing necessary for keeping nucleic acid intact.

Animals had not fasted before dissection which had started at 9:00 am to avoid effects on the brown fat. They were killed by CO_2 inhalation and subsequent cervical dislocation. Blood was collected by cardiac puncture in anticoagulant Ethylenediaminetetraacetic acid (EDTA) tubes. The animal then was sprayed with 70% ethanol. The animal then was laid in its front to dissect the interscapular BAT. The fat depots (inguinal, omental, perirenal), major organs (liver, kidneys, heart, brain, hypothalamus (gastrocnemius and soleus) and foetuses were excised and weighted. The head was cut, and by using dissection scissors, the skull was opened and brain removed, hypothalamus excised and stored in a tube in the liquid nitrogen. Aliquots were stored in formalin (10% in saline) for histological preparation or flash-frozen in liquid nitrogen and then stored at -80°C freezer for molecular analysis purposes. The only exception to this was the hypothalamus, which was only frozen due to its tiny size.

2.4 Laboratory procedures

2.4.1 Plasma Separation

Blood samples were kept in anticoagulant blood collection tubes, were placed in dry ice during the process of dissection and then centrifuged in a previously cooled centrifuge (4°C) at 3000g for 10 minutes. Then, the plasma which forms the upper layer was aspirated to another sterile tube and kept at -80 °C for further analysis. Concentrations of plasma metabolites and hormones were measured with commercial assays (Glucose (GO) Assay, Sigma Aldrich GAGO-20, LabAssay WAKO Triglyceride (GPO DAOS method)) by Miss Gabriella Perez, Dr Enas AlHarethi and Mr Peter Aldiss.

2.4.2 Histology

2.4.2.1 Principle of the Technique

Histology is the anatomical study of tissues by using a microscope. Cellular components need to be preserved once removed from the organism to keep the structure of the cell intact for further analysis. Chemical preservative solutions are used to achieve this by cross-linking the proteins irreversibly, the most common preservative of which is formalin (Werner et al., 2000). Water is removed from tissues through transferring in baths of increasing concentrations of ethanol, followed by xylene to clear alcohol. For tissue to be cut in thin sections, embedding of tissue with paraffin (for light microscopic visualisation) is performed so that it infiltrates the tissue and the tissue will solidify.

Microtomes are then used to make thin sections of tissue that can be transferred in a slide. The ability to visualise the fine structures of the tissues is enhanced by staining of the tissues as it gives contrast to the tissue and exposes specific features of interest (Werner et al., 2000, Spitalnik, 2016).

2.4.2.2 Tissue Histological preparation and Tissue processing

Tissues were fixed in 10% formalin for 5 to 6 days and then separated in the Shandon Excelsior processor (Thermo Fisher Scientific, USA). Smaller tissues (BAT, soleus and foetuses at 10 days of gestation) were run for five hours in the processor (Table 2.2) to avoid drying out of the tissues. The other tissues were run for thirteen hours in the processor (Table 2.3) which immersed them for a longer time in each bath of the three solutions. The processed tissues were then blocked in paraffin and kept for further histological analysis and immunohistochemical staining.

Table 2.2 Tissue Processing programme of small samples (BAT, soleus, 10d gestation foetuses)

Solution	Number of baths	Temperature	Time(minute)/bath
Alcohol	6	15°C	30
Xylene	3	15°C	20
Wax	3	60°C	20

Table 2.3 Tissue processing programme of the temperature study big samples (WAT, gastrocnemius, liver and heart)

Solution	Number of baths	Temperature	Time(minute)/bath
Alcohol	6	15°C	60
Xylene	3	15°C	60
Wax	3	62°C	20

2.4.2.3 Tissue sectioning

I cut the paraffin-blocked tissue samples stored in room temperature into sections of 5 µm of thickness using a sledge microtome (AS200; Anglia Scientific, Cambridge, UK) then float it in 70% ethanol to unfold folded parts. After that, it was transferred to water bath (40°C) after which it was removed with a Superfrost™ Plus glass microscope slides (Menzel-Gläser; Gerhard Menzel, Braunschweig, Germany) and put on a heating plate at 50 °C for two hours before being put in the oven overnight.

2.4.3 Haematoxylin and Eosin (H & E) tissue staining

2.4.3.1 Principle of technique

In histological staining, the contrast seen under the microscope results from the ionic bond formed between ions in the tissue and ions in the stain. H & E is the most common staining procedure in histology. It is a combination of two components, the haematoxylin which needs a mordant (e.g. aluminium) to bind it to the tissue that both act as a basic dye to stain the nuclear components blue and the eosin which is an acidic dye that stains the proteins in the cytoplasm non-specifically with different degrees of pink colour (Fischer et al., 2008, Spitalnik, 2016).

2.4.3.2 H & E staining procedures

Tissue sections were deparaffinised by immersion in a plastic rack containing xylene (2 periods of 3 minutes) and then rehydrated by immersion through decreasing concentration of ethanol baths starting with absolute ethanol (2×3 minutes) and ending with 70% ethanol followed by distilled water immersion for 3 minutes. The nuclei were stained in Harris' Haematoxylin for three minutes and a half before being washed for five minutes with running tap water to remove the excess stain. Differentiation was performed by immersion in an acid-alcohol (1% concentrated hydrochloric acid in 70% ethanol) solution for 3 seconds and by bluing in alkaline Scott's tap water (a 0.2% sodium bicarbonate and 20% magnesium sulphate distilled water solution). Running tap water was used to wash them for two minutes. A 1% concentrated Eosin solution was used to stain the tissues for 3 minutes before being rinsed in running tap water for 2 minutes to decrease the staining intensity. Dehydration was then performed by passing the slides rack through containers with absolute ethanol (2×2 minutes). Tissues were then cleared by two baths of xylene lasts for 2 and 3 minutes. Finally, sections were mounted with the proper size of coverslip using DPX mounting medium (Fisher Scientific). Prepared sections were left overnight to dry (Table 2.4).

Table 2.4 Haematoxylin and eosin (H & E) staining protocol

Step	Chemical	Time
1	Xylene	3 min
2	Xylene	3 min
3	Absolute Alcohol	3 min
4	Absolute Alcohol	3 min
5	70% IMS	3 min
6	Distilled water	3 min
7	Harris' haematoxylin	3:30 min
8	Tap water	5 min
9	HCl in 70% alcohol	3 sec
10	Scott's tap water	2 min
11	Tap water	5 min
12	1% Eosin	3 min
13	Tap water	2 min
14	Absolute Alcohol	2 min
15	Absolute Alcohol	2 min
16	Xylene	2 min
17	Xylene	3 min

HCL: hydrochloric acid; IMS: Industrial methylated spirit

2.4.3.3 H & E stained sections imaging

Images for H & E stained slides were seen using a Nikon Eclipse 90i microscope (Nikon UK Limited, Surrey, UK) and imaged by Volocity© v5.2.0 image software (Perkin Elmer, Massachusetts, USA) at 4, 10 and 20X magnification to reveal fine structures for specific studying of tissue.

2.4.4 Immunohistochemical staining

2.4.4.1 Principle of Technique

Defined as the use of a directed antibody to localise specific antigen in tissue to reveal the tissue expression of an antigen. The immunoreaction cannot be visualised without having a label which can be fluorescent. Target antigens which are primary or secondary can be detected directly or indirectly. In the direct method, the labelled antibody binds directly to the antigen. This method of detection is rapid but less specific (Ramos-Vara, 2005) (Figure 2.2 A). In the indirect method, a primary antibody (not labelled) bind to the target antigen in the section and a secondary (labelled) antibody binds to the primary one (Figure 2.2 B), this method is known to be more specific (Coons et al., 1955) and it is the one used here to stain the tissue.

In the UCP1-positive slides, the first antibody conjugates with the antigen which is a UCP1 epitope; this antibody then binds to the fluorescent-labelled secondary antibody that was added later.

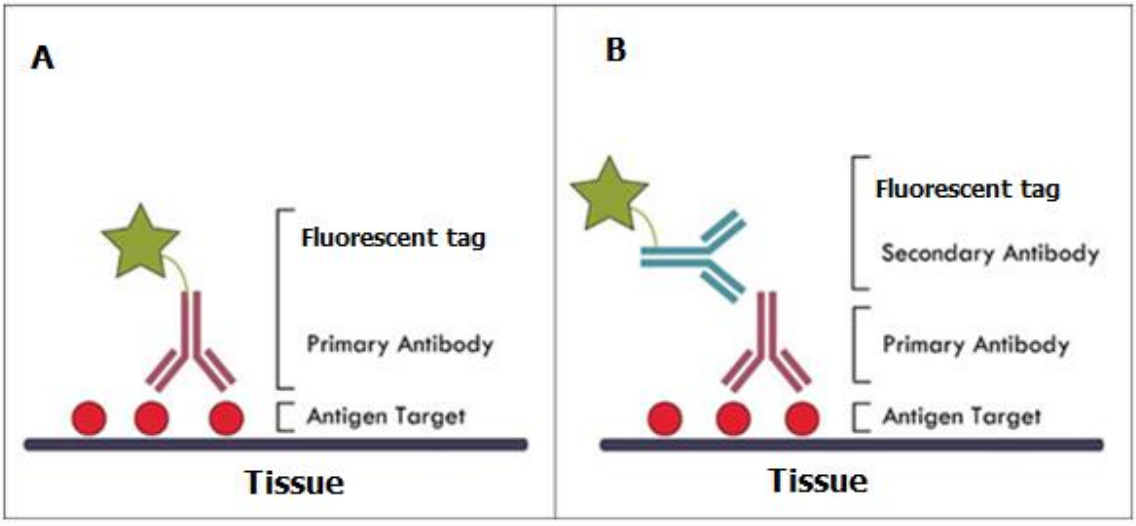


Figure 2.2 Immunohistochemistry Principle of action

A: direct immunoassay in which a primary antibody binds to the target.
B: indirect immunoassay: a secondary antibody binds to the bounded primary antibody to form a complex. Fluorescent tag: for quantification of the target expression.

2.4.4.2 IHC staining procedures

Immunohistochemical staining was done for sections from interscapular BAT of rats by Dr Enas AlHarethi to study the difference in abundance of UCP1 protein expression between the different interventional groups at the three observations.

UCP1 primary antibody (ab10983, Abcam, Cambridge, UK) was diluted 3000 times with antibody diluent. Four positive and one negative control slides for animals were chosen randomly and placed into Lecia BondMax™ IHC slide processor (Leica Microsystems) where an automated software programme has been run (Vision Biosystems Bond version 3.4A) using bond Polymer Refine Detection reagent (Leica, Newcastle, UK).

In the run, after being washed with xylene and ethanol and incubated with citrate buffer, sections were treated with peroxide block to block endogenous peroxidases and reduce the background signal. Except for the negative control, slides were exposed to the UCP1 primary antibody. Slides were washed with Bond wash solution and distilled water before being exposed to HRP conjugated secondary antibody and rewashed. The slides were exposed to 3, 3'-DAB followed with Harris' Haematoxylin nuclear staining.

The slides were removed from the run, dehydrated by ethanol and cleared by xylene. Finally, they were mounted with glass coverslips using DPX mounting medium (Fisher Scientific, Loughborough, Leicestershire, UK) and left overnight to dry. Slides were viewed and photographed at 10X magnification (Nikon Eclipse 90i, Nikon, Tokyo, Japan; with Hamamatsu ORCA-ER camera, Hamamatsu, Hamamatsu City, Japan). Minimum of five images per sample were analysed with Fiji, using trainable Weka segmentation.

2.4.5 Gene expression analysis

Gene expression is the process by which the genetic code of a gene is used to direct product (nucleic acid or protein) synthesis and produce the structures of the cell. It involves two main stages; transcription and translation. Transcription is mRNA production by the enzyme RNA polymerase using DNA strand as a template, while the

use of this mRNA as a code to direct protein synthesis by the ribosomes and subsequent protein processing is called the translation. The ability of the cells to control the number of mRNA copies in response to environmental or pathological conditions is critical for its survival (Weaver, 2012). Total cell mRNA is extracted from the tissue, reversed transcribed to DNA and quantified using Quantitative polymerase chain reaction (qPCR)

2.4.5.1 Ribonucleic acid extraction

Benches and instruments were cleaned with RNAse Zap® (Ambion, California, USA). Sterile nuclease-free water (Ambion, Inc, UK) was used for all dilutions and reagent preparations. All work was performed on dry or wet ice to preserve the integrity of nucleic acids.

2.4.5.1.1 Chopping

Tubes containing tissues were transferred from -80°C storage and kept in dry ice during the procedure. Tissue was removed from the tube using forceps and the desired amount of the tissue was cut on a chopping board using a steel knife, weighted and placed in a labelled dispomix tube. The remained tissues were returned immediately to -80°C.

2.4.5.1.2 RNA extraction

RNA extraction was performed using the RNeasy plus kit (Qiagen, Crawley, UK). Tissues were homogenized with 500 µl of Trizol ((Sigma Aldrich, Gillingham, UK) which effectively dissolves DNA, RNA and protein using Dispomix homogeniser "programme 9" (Wilten, Etten-Leur, the Netherlands) at 3000 rpm for 40 seconds. Samples were then left at room temperature for 10 minutes to allow the breakdown of lipid content. Homogenates were then vortexed five times over 30 seconds and centrifuged at 3220g for one minute at 4 °C which produced a precipitate that was pipetted in a 1.5 sterile labelled Eppendorf tube. 100 µl of chloroform was added to each sample, mixed by vortex and incubated for 10 minutes at room temperature to allow layers separation.

Centrifugation of the sample was performed at 12,000 g for 15 minutes in 4 °C. The mixture separates into 3 phases with the upper clear aqueous phase containing the RNA is transferred carefully to a genomic deoxyribonucleic acid (gDNA) eliminator column which was then centrifuged at 8000g for 1 minute to remove any remaining DNA. The solution passed through the column was mixed with an amount between 170-300 µl of 70% diluted ethanol by vortexing. After that, 700 µl of each sample was transferred to a labelled RNeasy spin column and centrifuged at 8000g for 15 seconds in room temperature. The flow-through was re-pipetted again in the column to increase the concentration as the RNA is now trapped in the column.

700 µl of buffer RW1 was then added to each column and mixed for 15 seconds, the flow-through discarded and 500 µl of RPE centrifuged with the sample at 8000g for 15 seconds. Another 500 µl from the RPE buffer was added but centrifugation this time was at 8000g for 2 minutes. The RNeasy column was moved to a sterile 2 ml collection tubes and centrifugation performed at 8000g for 1 minute to remove all remaining buffer RPE. Next, the RNeasy spin column was transferred to a new labelled sterile 1.5 ml Eppendorf tubes where 30 µl of RNAase free water added and centrifuged at 8000g for 1 minute. The product of this was re-pipetted back through the column and centrifugation repeated at 8000 for 1 minute to increase the mRNA concentration.

2.4.5.1.3 RNA quality

The quality of the extracted mRNA, and its concentration and purity was evaluated by using the a Nanodrop® spectrophotometer (Thermo Scientific, DE, USA) where RNA with a 260:280 nm ratio of 2 and a 260:230 nm ratio of 1.8–2.2 was considered intact and usable for quantitative PCR (qPCR) and other follow-up experiments. The samples were returned immediately to the -80 °C after measurement to save the RNA integrity.

2.4.5.2 Reverse Transcription and polymerase chain reaction (RT-PCR)

RT-PCR is a technique by which RNA molecules are converted into their complementary DNA (cDNA) sequences by reverse transcriptase enzyme, followed by the amplification of the newly synthesised cDNA by classical PCR procedures (section 2.3.5.3.2.2); this is critical in understanding actively expressed genes and their functions at a specific time point as the RNA is single-stranded and unstable making it difficult to work within the normal laboratory conditions.

2.4.5.2.1 Principle of technique

The first step is the reverse transcription (RT) which is the transfer of genetic information from RNA sequences to DNA sequences using reverse transcriptase enzyme; it is responsible for the synthesis of the first cDNA strand. It starts with the binding of a primer to the mRNA single strand. Then, the reverse transcriptase enzyme will elongate the sequence to produce complementary DNA (cDNA), which is then converted to double-stranded cDNA by the action of DNA polymerase. Classical PCR amplifies these double-stranded DNA molecules (Figure 2.3 & 2.4).

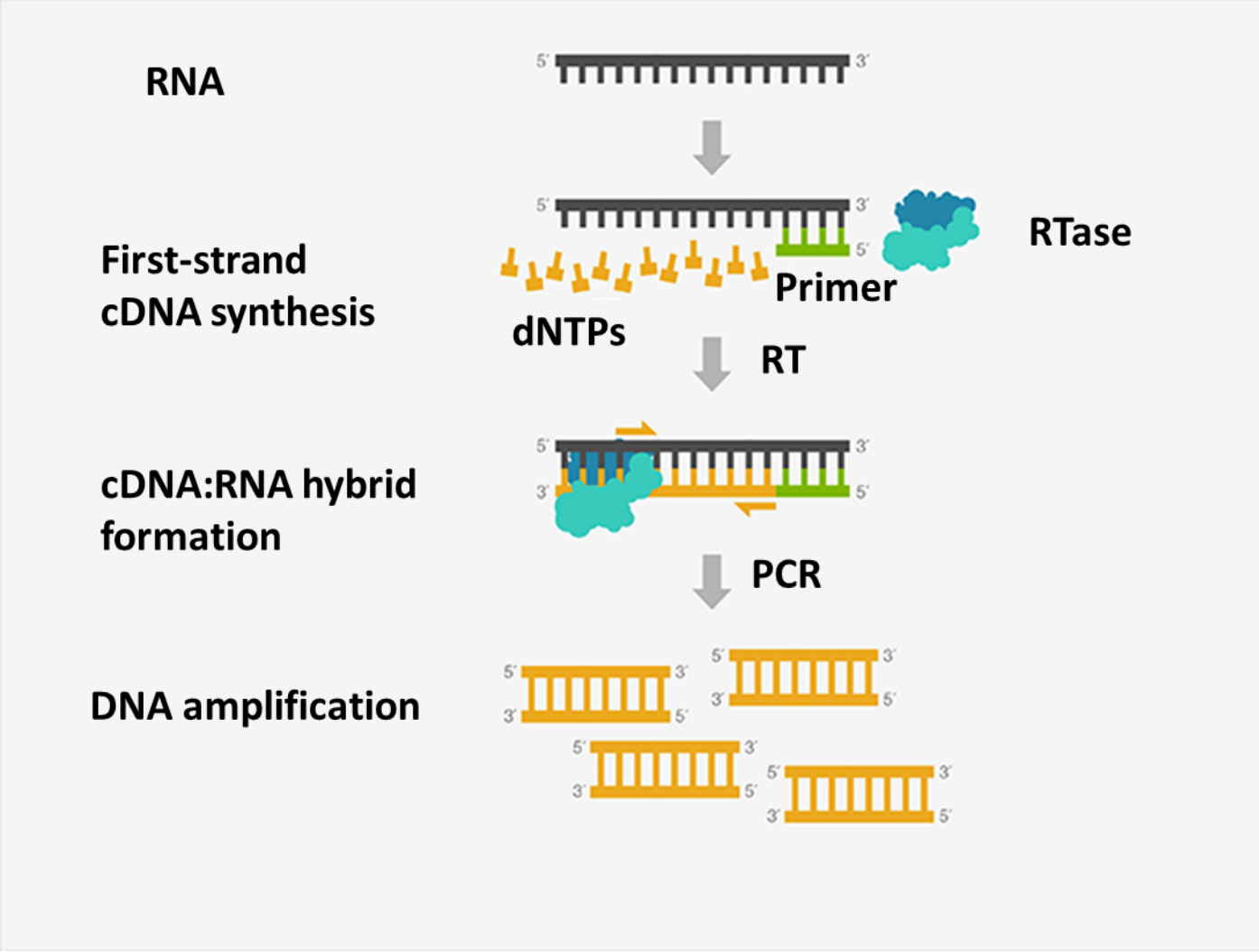


Figure 2.3 Reverse transcription-polymerase chain reaction (RT-PCR) process

RT process starts with primer binding to the RNA strand. The reverse transcriptase enzyme (RTase) binds to the RNA and initiates cDNA strand synthesis. The double-stranded cDNA is created by the action of DNA polymerase. RTase: reverse transcriptase; dNTPs: deoxyribonucleotide triphosphate. Adapted from (ThermoFisherScientific, 2019)

2.4.5.2.2 RT-PCR procedure

Calculations made in excel spreadsheet to determine the proper dilution of samples. For samples with a high mRNA concentration, two steps of dilution were performed to ensure accurate concentration will go in the reaction tube. High Capacity RNA-to-cDNA kit (Applied Biosystems, Warrington, UK) was used. A 200 µl sterile Eppendorf tube was labelled for each sample and both controls. The reverse transcriptase enzyme and buffer

were thawed in wet ice, and RNA samples were thawed later to prevent degradation. An RT master mix was made from the reverse transcriptase enzyme and the buffer to reduce the number of pipetting steps, and loaded in each sample-labelled tube except in the negative control of the RT reaction tube.

The calculated amount of each mRNA sample was diluted with nuclease-free water to an amount of 9 µl, and 11 µl of the master mix was added to each sample tube (but not to the negative control tube). Two negative controls were prepared, one without the RT enzyme and the other without an RNA template, to ensure the reproducibility of the reaction. All samples centrifuged for one minute at 4000g, then were transferred to the thermal cycler (Techne Incorporate, New Jersey, USA) where the ”RT RNA 2 cDNA programme” was run (Table 2.5). Finally, samples were diluted 1:10 with RNase-free water and both diluted and undiluted samples were kept in -20 °C for qPCR analysis.

Table 2.5 Details of the 'RT RNA 2 cDNA ' programme cycles for the polymerase chain reaction

Temperature (°C)	Time (minutes)
37	60
95	5
8	Hold ∞

2.4.5.3 Quantitative Polymerase Chain Reaction (qPCR)

2.4.5.3.1 Principle of technique

Quantitative PCR (qPCR) is helpful in the characterisation and quantification of nucleic acids for numerous applications like measuring the expression of the genes of interest. DNA undergoes three repetitive phases of denaturation, primer annealing and elongation, such cycles repetition is enough to produce a large amount of specific DNA copies in a relatively short time. cDNA is amplified using a solution contains DNA polymerase, nucleotide and primers complementary to the target DNA sequence. The

double-stranded DNA denatures and separates into two strands when heated, and the primers anneal to the target sequence in the single DNA strands when cooled. The DNA polymerase then forms a new strand by extending the primers with nucleotides, creating a complimentary copy of the target DNA sequence. This repetitive cycle of denaturing, annealing, and extending increases exponentially the number of target DNA sequences (Figure 2.4). Ideally, no amplification occurs if the target DNA sequence is not present. The qPCR could be either dye-labelled or probe. In dye-labelled, the fluorescence dye binds to the double-stranded DNA by intercalating between the DNA bases. As more syber green dye (commonly used fluorescence labelling dye) binds to the double-stranded DNA, the fluorescence intensity increases which can be measured at the end of each amplification cycle to determine how much DNA has been amplified (Arya et al., 2005). In probe-based qPCR, the probe binds to its specific signal, and no fluorescence is detected while the probe is intact. During the amplification and extension of the probe-bound sequence, the probe is hydrolysed and amplification-dependent fluorescence emission is produced. Probe-based qPCR is more specific than dye-based (Heid et al., 1996).

2.4.5.3.2 Primers validation

Primer is a short sequence of oligonucleotides that starts the amplification of nucleic acid; they are used in qPCR to determine the piece of DNA to be amplified and quantified. Specific amplification of the target DNA template requires that primers do not have matches to other targets in certain criteria that cause undesired amplification (Ye et al., 2012). Primers were designed by myself or previously optimised by the staff of the academic department of child health laboratory, Queen's Medical Centre, Nottingham.

If gene primer sequence was not in the primer database of the Academic Child Health department or not in published papers, I designed them by myself using a web-based database and online designing tools. I searched for the gene sequence in the National

Centre for Biotechnology Information (NCBI) online database. Once found, the whole original gene sequence was specified to get primers by using the Assay Design Centre in the ”life science Roche” website where the Rattus Norvegicus species specified and the whole sequence pasted. The designing tool produced one possible primer pair. The selected primers were specified to have a PCR product between 100bp-200bp and a length of 20 nucleotides. The guanine cytosine (GC) content was between 50%-60%. All designed primers were checked against for gene and species specificity in the NCBI database to ensure proper sequence amplification. Some primers were designed by copying the whole sequence in the NCBI primer blast which gave many primers pairs, but only the first two pairs were picked (Table 2.6) Appendix 1.

Table 2.6 primers, forward and reverse sequences

Gene	Abbreviation	Forward Primer	Reverse Primer
Tyrosine 3 monooxygenase tryptophan	YWHAZ	GATGAAGCCATTGCTGAACTTG-	GTCTCCTTGGGTATCCGATGTC
TATA box binding protein	TBP	TGGGATTGTACCACAGCTCCA	CTCATGATGACTGCAGCAAACC
Succinate dehydrogenase complex transferase	SDHA	TCCTTCCCACTGTGCATTACAA-	CGTACAGACCAGGCACAATCTG-
Ribosomal protein large P0	RPLP0 (36B4)	TGCTGGACATCACAGAGCAG	TCCACAGACAAAGCCAGGAC
Insulin receptor substrate 1	IRS-1	GAAGTTCCTTCCGCAGTGTC	GTTGCCACCCCTAGACAAAA
Insulin receptor substrate 2	IRS-2	CTACCCACTGAGCCCAAGAG	CCAGGGATGAAGCAGGACTA
Fatty acid binding protein 4	FABP-4	AACTGGGCGTGGAATTCGAT	CCAGCTTGTCACCATCTCGT
Fatty acid transport protein 4	FATP-4	GACTTCTCCAGCCGTTTCCA	CACCTGGCTGTCAAAGTTGC
Mammalian target of rapamycin	mTOR	TGGAGGGAGAGCGTCTGAGA	TGATGTGCCGAGGCTTTGT
Transcription factor 7 like 2	TCF7L2	GTCCACCCACTCACACCTCT	TTCCTGTTTTGGGGTCTACG
Interleukin 6	IL-6	ATGGATGCTTCCAAACTGGAT	TGAATGACTCTGGCTTTGTCT
Tumour necrosis factor alpha	TNF-α	ACGTCGTAGCAAACCACCAA	GCAGCCTTGTCCCTTGAAGA

Uncoupling protein 1	UCP1	GCCTAGCAGACATCATCACCT	GTTTCGGCAATCCTTCTGTC
Peroxisome proliferator activated receptor gamma	PPARɣ	CCCAATGGTTGCTGATTACA	GGACGCAGGCTCTACTTTGA
Beta-3 Adrenergic receptor	β3AR	TAGCAAGGAGCCTGACTTCTG	TTCTGGAGAGTTGCGGTTCC
Sarcoplasmic reticulum calcium ATPase	SERCA2B	TCATGGACGAGACGCTCAAG	TTCCCCAAGCTCAGTCATGC
Monocyte chemoattractant protein 1	MCP1	AGCATCCACGTGCTGTCTC	GATCATCTTGCCAGTGAATGAG
Vascular endothelial growth factor A	VEGFA	TGAGTTAAACGAACGTACTTGCAG	TCTAGTTCCCGAAACCCTGA
Interleukin 10	IL10	CAGATTCCTTACTGCAGGACTTTA	CAAATGCTCCTTGATTTCTGG
EGF-like module-containing mucin-like hormone receptor-like 1	EMR1(F4/80)	AATTTCACAGACCAAGAAGTGACA	GCAGTTGTAGGAACCTGGTACA
Nuclear factor kappa-light-chain-enhancer of activated B cells	NFKB	TCATCAACATGAGAAACGATCTG	CTCAGCAAGTCCTCCACCA
Lipoprotein Lipase	LPL	TGGTGGGAAATGATGTGGCC	TGCATACTCAAAGTTAGGCCCA
E74-like factor 5	ELF5	GGACCTAGCCACCACTTGTC	ACATCAGGGGGTCACAGAAG
Oxytocin receptor	OXTR	AGCGTTTGGGACGTCAAT	GTTGAGGCTGGCCAAGAG
Signal transducer and activator of transcription 5A	STAT5A	ACCTTTCTGCTGCGATTCAG	CTTCAGATTCCACAGGTTTCG

2.4.5.3.2.1 Primers processing

Primers were brought by "Sigma Aldrich" in a dry form. Tubes were centrifuged to spin the primers down. Re-suspended in RNase–free water to get 100 µmol/l stock solution. Eppendorf tube was labelled for each primer sequence and 1:40 dilution was done for all the primers with nuclease-free water before being stored in -20 °C for later processing and use in qPCR.

2.4.5.3.2.2 Classical Polymerase Chain Reaction (PCR).

Classical PCR is a technique that allows exponential amplification of DNA sequences that is primer mediated, depending on the DNA ability to produce a DNA strand complementary to the one that present. Such activity needs a primer from which the DNA polymerase can initiate the process and elongate the strand by adding more nucleotides (Saiki et al., 1988) (Figure 2.4). The PCR reaction requires essential components including a purified double-stranded DNA, a thermostable DNA polymerase, oligonucleotide primers, deoxyribonucleoside triphosphate and a buffer system to provide the proper condition for DNA denaturation and renaturation and a suitable environment for the polymerase activity.

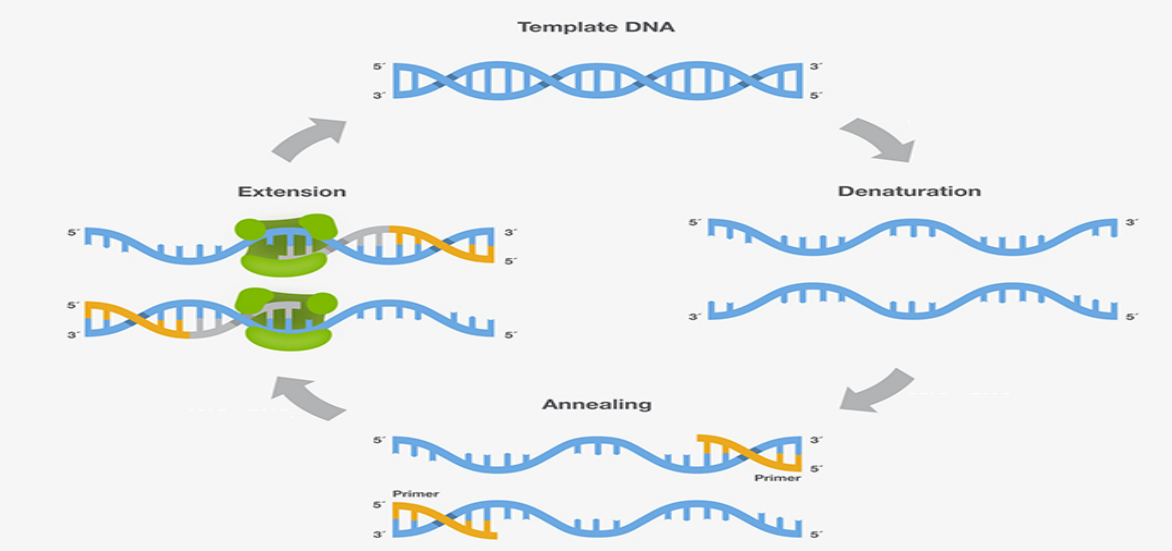


Figure 2.4 Illustration of PCR reaction steps for a target DNA sequence amplification.

The initial denaturation step separates the double-stranded template DNA into single strands. In the annealing, the reaction temperature is lowered to allow binding of the primer to the target DNA. Then, DNA polymerase extends the primer end to synthesise the new strands. Adapted from (ThermoFisherScientific, 2019).

A set of 3 tubes for each primer was prepared, 2 identical tubes contain the primers and a third tube as a negative control to ensure the integrity of the subsequent RT-PCR reaction (Table 2.7).

Table 2.7 Contents of the PCR master mix for "standards" programme

	Primer-containing tubes	Negative control
Stock Thermo-Start PCR Master Mix	10	10 µl
Forward primer (diluted1:40)	4 µl	4 µl
Reverse primer diluted1:40)	4 µl	4 µl
DNA template	2 µl	0
RNase-free water	0	2 µl
Total volume	20 µl	20 µl

All tubes were centrifuged at 4000g for 1 minute and placed in the "standards" programme (Techne Incorporate, New Jersey, USA) (Table 2.8). Samples were removed after run finished and stored in -20°C Freezer.

Table 2.8 "Standards" programme details in the PCR run

Process		Temperature (°C)	Time
Initiation and enzyme activation		94	30 seconds
40 cycles	cDNA strands Denaturing	94	30 seconds
	Primer annealing	60	30 seconds
	Primer extension	68	1 minute
Final extension		68	5 minutes
Hold		8	∞

2.4.5.3.2.3 Gel Electrophoresis

Agarose gel electrophoresis is a method used to separate nucleic acids or proteins. Nucleic acid molecules are separated by the electrical field according to their size where the negatively charged molecules migrate toward the positive pole. The migration speed is determined by the molecular weight as the molecules with lower weight will migrate faster than the larger molecules. Size-dependent DNA fractionations is an initial step for imaging with ultraviolet light and the desired band purification (Yılmaz et al., 2012).

I ran the PCR products on the gel to confirm the presence and specificity of the designed primers. One gram of agarose powder (Invitrogen Life Technologies) was mixed with 50ml TAE buffer (prepared form a stock solution of tris (hydroxyethyl) aminomethane base (Tris), glacial acetic acid (Fischer Scientific) and EDTA buffer). The solution was heated to dissolve the agarose powder. A 2.5 µl of 10mg/ml ethidium bromide was then added to the flask before being powered in the gel tray. The combs were inserted immediately after mixture pouring, and the whole mixture was left to cool and solidify at room temperature. Combs inserted to create wells for DNA was removed carefully, and the solidified gel was transferred with the holding tray to the electrophoresis tank with TAE covering the gel. Samples and ladder now removed from the freezer and put to thaw in wet ice. Ten µl of a 100bp ladder (Fisher Scientific Ltd, UK) inserted on each line in the gel to compare bands sizes with previously-known ladder bands, and the 20 µl of samples were loaded in the adjacent wells. After loading, the power switched on at 110 volts for 35 minutes. The gel was removed when the run finished and now ready to be imaged by a UV trans-illuminator CCD camera (Fujifilm luminescent image analyser LAS-3000 v1.01; Raytek; Sheffield, UK) (Figure 2.5).

Gel image determines the specificity and validity of the primer. The presence of a band in the control indicates contamination or non-specific primers, and if it is the same size as that produced by the primer positive sample, this may point to a nucleotide contaminated water. If multiple bands produced or a band appeared in an unexpected place compared to the amplicon size, the proper primers were dismissed, and in such cases, the primers were designed again for that gene. Gel bands were cut out and stored in a labelled sterile 1.5 ml Eppendorf tubes at -20°C until their DNA is extracted.

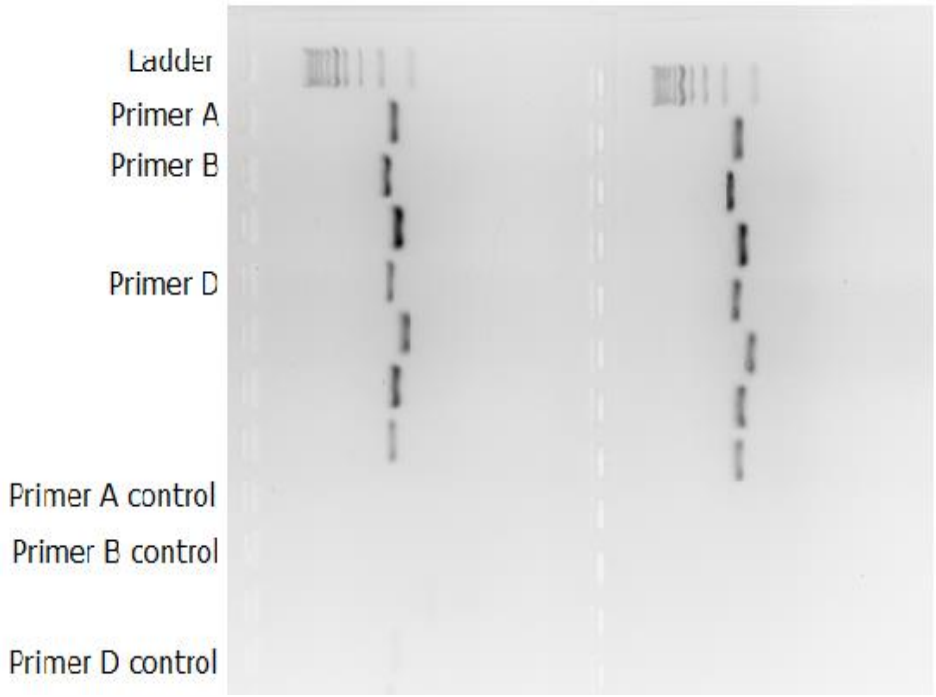


Figure 2.5 PCR products in agarose gel

PCR products for primers A&B produced one band on both gel sides and no band is shown in the control indicating a single product. Primer D produced one band but a faint band was detected in the control indicating more than one product.

2.4.5.3.2.4 DNA extraction from the gel

The DNA bands which have been cut from the gel were extracted using QIAquik gel extraction kit (Qiagen; Wset Sussex, UK). Gel bands weight was measured by calculating the difference in weight between the empty tube and gel band-containing tubes. Three volumes of the QG buffer was added to one volume of the excised band in a ratio of 3:1 to dissolve it and the mixture incubated for 10 minutes at 50°C with vortexing every 2-3 minutes. One hundred microlitre of isopropanol (Fisher Scientific) was then added per 100 µg of gel and mixed with it before applying the whole solution into a QIAquick spin column. Here, the DNA replicates are mixed, and the columns were centrifuged for 1 minute at 8000g. Flow through discarded, and 500 µl of the QG buffer was added to the columns which were then centrifuged for 1 minute at 8000g to remove residual agarose. Next, 700 µl of PE buffer (premade buffer) was used to wash by adding to the columns

and incubation for three minutes at room temperature. Centrifugation followed this for one minute at 8000g where the filtrate was discarded and another one minute of centrifugation was applied to remove all PE buffer residuals. The columns were transferred to a new, sterile and labelled 1.5 ml Eppendorf tubes and the DNA was eluted by adding 30 µl of elution buffer (Buffer EB, 10Mm Tris.Cl, PH 8.5) directly to the QIAquick membrane and incubation for one minute at room temperature before being centrifuged finally for one minute at 8000g. The eluted DNA concentration was checked using Nanodrop spectrophotometer (Nanodrop Technologies; Wilmington, USA).

2.4.5.3.2.5 DNA sequencing

For designed primers, the DNA and its forward primers were sent to the DNA sequencing laboratory in the school of biomedical science at the University of Nottingham for sequencing. When sequencing results were received, amplicon sequences were compared to the NCBI online database, and if no similarity found between the amplicon sequence and the original gene sequence, primers discarded and designed again. The purified DNA samples were diluted to 1ng/µl aliquots and stored at -20°C for standard curve production.

2.4.5.3.2.6 Standards production

Standards curve is crucial in checking the efficiency of the designed primers as well-working primers will result in a proportional dose-response curve. It is known to be a critical tool in examining the efficiency of the overall qPCR assay. I tested 8 concentrations for each primer from the 1ng/µl aliquots with a dilution factor of 1:10, I did sequential dilution using tRNA (diluted 1:000 in nuclease-free water) as a carrier and inserted a negative control to check for any contamination and to compare the amplification in the negative control with that of the standards.

2.4.5.3.3 Quantitative Polymerase Chain Reaction (qPCR) Procedure.

Clean gloves and lab coats were worn and changed when contamination suspected. Reaction tubes and containers kept closed as much as possible. Benches, micropipettes and equipment were sterilised continuously. Samples vortexed before loading and RNAase-free water was aliquoted to reduce the possibility of contamination. A 1:10 diluted cDNA samples, positive control, syber green, standards and a calibrator were transferred from the freezer to wet ice to thaw. Plates were labelled with tissue type, date, time point, and assay name. A master mix was prepared contained forward and reverse primers (diluted 1:40 in nuclease-free water) and the syber green dye. Seven µl of master mix was loaded in all wells followed by pipetting 3µl of the samples and the standards to their previously assigned wells. A negative control was inserted where nuclease-free water was added instead of a cDNA. A calibrator was also included in the plates of the same assay to correct for technical inter-runs variation (Table 2.9). As this sample should yield the same results in any qPCR run, measurements were corrected depending on the observed technical variation (D'haene and Hellemans, 2010).

Table 2.9 Details of the quantities used to prepare the qPCR dye-based (syber green) master mix

	Samples (µl)	qPCR negative control (µl)	Calibrator (µl)
DNA sample	3	0	3
Forward primer	1	1	1
Reverse primer	1	1	1
Syber green	5	5	5
RNase free water	0	3	0
Total volume	10	10	10

In Probe-based qPCR, the same procedure in terms of samples loading was carried out except the amounts and components of the master mix and the run method in the qPCR. Here in the probe-based qPCR, only no template transcriptase negative control has been used and no standards included (Table 2.10).

Table 2.10 Details of the quantities used to prepare the qPCR probe-based (TaqMan) master mix (amounts are for reaction per well)

	Samples (µl)	qPCR negative control (µl)
DNA sample	2	0
probes	0.5	1
Taqman master mix	5	5
RNase free water	2.5	3
Total volume	10	10

The prepared qPCR plate was sealed with thermal plate sealer (Abgene, Thermo Fisher Scientific Inc. UK) and put in the Stepone plus Real-Time PCR system (Applied Biosystems, Warrington, UK) (Table 2.11) and (Table 2.12).

Table 2.11 Dye-labelled (syber green) qPCR programme

Process	Temperature	Duration
1-Intial denature of cDNA standard	95°C	15 minutes
2-Denaturing cDNA standard	95°C	15 seconds
3-Primers annealed	60°C ± 2°C	30 seconds
5-Producing melt curve	65-95°C	15 minutes
6-Hold		10 minutes

Table 2.12 Probe-based (Taqman) qPCR programme

Process	Temperature	Duration
1-Initial denaturing of cDNA standard	50°C	2 minutes
2- iTaq polymerase activation	95°C	20 Seconds
3- Melt curve for analysis	95°C	1 second
4- Anneal /Extend	60°C	20 seconds

2.4.5.3.3.1 QPCR quality control

2.4.5.3.3.1.1 Amplification plot

The amplification plot is a sigmoidal shape that is used for amplification efficiency determination by detecting the change in fluorescence emission in the linear phase (Peirson et al., 2003). It represents the product accumulation over the duration of qPCR and created when the fluorescence is plotted against the cycle number. Four phases can be distinguished in the amplification curve. The first is the lag phase where no signal can be detected due to the very low amplification. The quantification is measured in the exponential phase where the fluorescence signal is detectable, and the quantification cycle (Cq values) can be determined for the different target samples. This is followed by a region of decreased amplification and a plateau phase at the end. Presence of inhibitors may affect the reaction efficiency; this can be distinguished by looking to the amplification plot which will result in a lower plateau phase levels (D'haene and Hellemans, 2010) (Figure 2.6).

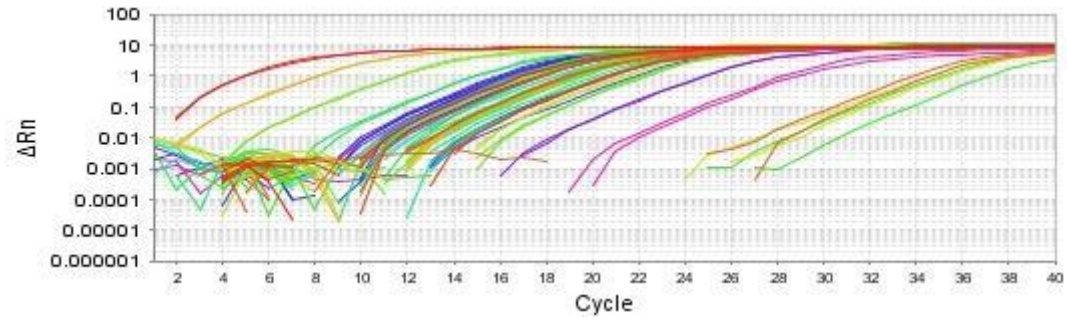


Figure 2.6 Representative amplification plot

The amplification contrasts the fluorescent signal (ΔRn) and cycle number, the fluorescent signal increases exponentially with amplification.

2.4.5.3.3.1.2 Melt curve

The melt curve is used to assess the specificity of the dye-based qPCR by measuring if it has produced a single specific product. Assessment of the specificity is an important step when an intercalating dye, not probe, is used as it binds to any dsDNA and not sequence specific (Bustin and Nolan, 2004). The resulting fluorescence is plotted as a function of temp, which is produced after the amplification cycles are completed. When the DNA is

heated gradually, it weakens and eventually breaks the bonds between the dsDNA molecules; this causes the release of the bounded dye and a reduction in the fluorescence when the DNA melting point is reached (Figure 2.7). A specific PCR reaction will result in a single sharp peak. Non-specific PCR reaction will generate extra peaks or a single but broader peak depending on different factors; such as the production of non-specific products and the melting temperature. Primer dimers formation will give rise to a more broader and flattened peak, such effect is more common in reactions with low template concentration and negative controls (NTC) (D'haene and Hellemans, 2010).

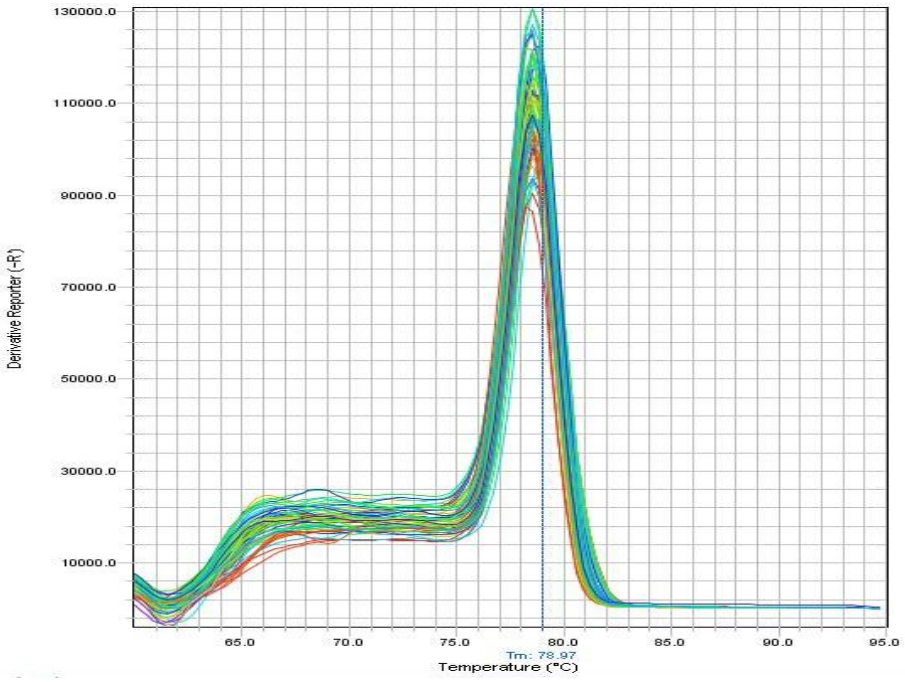


Figure 2.7 Representative Melt curve

Melt curve represents a plot of data collected during the melt curve stage. Peaks indicate the melting temperature (Tm) of the target, it can identify nonspecific PCR amplification.

2.4.5.3.3.1.3 Standards curve

Charts the log of each known concentration in the serial dilutions against the Ct value for that specific concentration (Figure 2.8). If the efficiency is greater than 120%, this may point to an excessive formation of primers dimers, the presence of inhibitors or inaccurate pipetting.

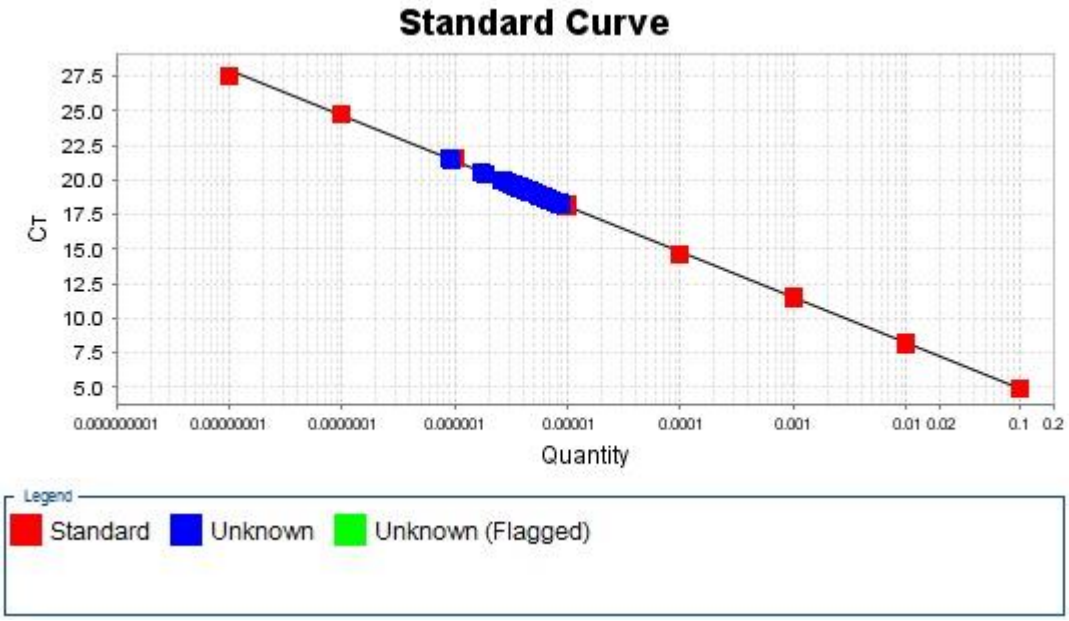


Figure 2.8 Representative standards curve

A linear graph formed by plotting the cycle number at cycle threshold against the known concentrations of DNA.

2.4.5.3.3.1.4 Controls

- No template control (NTC): this is critical for PCR contamination detection. It helps in establishing a condition for dealing with data from syber green assay. If amplification noticed, this indicates potential contamination of the reagents with the template or a formation of primers dimers.
- No reverse transcriptase control (NRTC): used to ensure the absence of contaminating gDNA. If a signal detected here, it indicates residual gDNA contamination or primers dimers formation.
- True positive control: will provide information about the efficiency of the qPCR run; especially if the gene of interest is expected not to be expressed or if its expression is expected to be very low.
- True negative control: included when the target gene is expected to be expressed (D'haene and Hellemans, 2010, Heid et al., 1996).

2.4.5.3.4 Quantification of gene expression

Reference genes are used to normalise mRNA levels between different samples for proper and accurate comparison of mRNA transcription level of target gene. They should not be influenced by the experimental procedure, so expected to show a minimal variation in expression between samples and a relatively constant high expression compared to the genes of interest. Selection of high-quality reference genes is critical for the interpretation of data generated by qPCR (Nygard et al., 2007, Silver et al., 2006). The use of a single reference gene may result in invalid or wrong results as many of them showed a high variability of expression (Silver et al., 2006).

Four genes in my study have been considered as a housekeeping gene in previous studies, they are Tyrosine 3-Monooxygenase/tryptophan 5-monooxygenase activation protein zeta polypeptide (YWHAZ), TATA box binding protein (TBP), succinate dehydrogenase complex subunit A (SDHA) (Vandesompele et al., 2002) and ribosomal proteins encoding genes (RPLP0) (Bamias et al., 2013). The most stable reference genes were determined by calculating the geometric mean for each pair of the selected reference genes. M value was then calculated for each pair where YWHAZ and TBP showed the least M value and an acceptable level of expression among all the investigated tissues (interscapular, inguinal and omental) which indicates that they are stable references to use for the normalisation in adipose tissues of rats.

For each assay, the efficiency; acceptable range falls between 95% and 105%, and the inter-run calibrator Ct values were recorded before the results were exported to Excel spreadsheet. Mean of the replicates Ct values were considered for each sample unless a high standard deviation noticed due to possible contamination where the mean was ignored. Expression of target gene was normalised to the geometric mean of the TBP and YWHAZ as their combination showed the least variation among the other reference genes combinations. This relative quantification of target gene was calculated using the 2-ΔΔCt method (Livak and Schmittgen, 2001).The reason for exclusion of any animal or

individual samples from the analysis included low RNA concentration or purity, problems during reverse transcription or RNA loading in the 96-well plates like inconsistent liquid volume loading or very rarely wells with clear trapped air bubbles.

2.5 Statistical Analysis

All statistical analyses were carried out in SPSS (Version 24, IBM, Portsmouth, UK) and GraphPad (Version 7, GraphPad Software, La Jolla, CA, USA). Data was tested for normality using a Shapiro wilk test. If normally distributed, data was analysed i) with Two-way analysis of variance (ANOVA) with Least Significant Difference (LSD) post hoc comparisons (20S vs. 20H, 27S vs. 27H, 20S vs. 27S, 20H vs. 27H) within each of the three time points (0d, 10d, 19d gestation) to test for changes due to the interventions, and ii) with one-way ANOVA with a priori comparisons (0d vs. 10d, 10d vs. 19d, 0d vs. 19d) within each interventional group to test for changes with pregnancy. If data was not normally distributed, Mann Whitney with Kruskal-Wallis tests were carried.

Chapter 3. The response of interscapular adipose tissue to diet, housing temperature and pregnancy

3.1 Introduction

Brown adipose tissue (BAT) is a thermogenic organ characterised by its ability to generate heat and regulate metabolic activity through the adrenergic receptor pathway (Cypess et al., 2015, Ursino et al., 2009). Ambient temperature and diet are known factors that affect the activity of BAT (Shore et al., 2013, Rothwell and Stock, 1981a). Pregnancy causes changes in the metabolism which involve a reduction in thermogenesis carried in the interscapular BAT (iBAT) in order to reduce energy expenditure to avoid exposing mothers and foetuses to a nutrient shortage (McIlvride et al., 2017). In this chapter, I will explore the effect of exposure to mild cold and a high energy diet on iBAT mass, histological and molecular characteristics by examining the effect on genes involved in thermogenesis regulation, insulin sensitivity and fat transport in interscapular BAT of virgin and pregnant rats at 50% and 90% of pregnancy (10 and 19 days of gestation; 10 d/g and 19 d/g) and if there is any interaction between the interventions.

Cold exposure and high caloric diet consumption will activate the sympathetic nervous system to release catecholamines like norepinephrine (NE) which binds to receptors (adrenergic receptors) and activates the thermogenic pathway in BAT by increasing the expression of uncoupling protein 1 (UCP1) which uncouples respiration from ATP synthesis resulting in heat production (Cypess et al., 2015, Bachman et al., 2002, van Marken Lichtenbelt et al., 2009, Matthias et al., 2000). This will start a cascade of events that consequently affect the utilisation and transport of energy substrate (free fatty acids and glucose) between the circulation and tissues. Examination of factors that participate in lipid transport and fatty acid uptake from the circulation e.g. ATGL, LPL, FATP4 *and* CD36 (Zimmermann et al., 2004, Su and Abumrad, 2009, Herrera, 2002a, Gimeno,

2007) and factors that affect glucose mobilisation and insulin release (*IRS1 & IRS2*) (Previs et al., 2000) will reveal changes in energy status of animals in response to the interventions.

BAT activation will trigger mitochondrial biogenesis and brown adipocytes differentiation that is regulated by many hormones e.g. leptin which participates also in appetite regulation (Halford and Blundell, 2000) and transcription factors (PGC1α, PPARɣ) (Rosen, 2005, Puigserver et al., 1998).

3.2 Hypothesis

I will test the hypothesis that housing of rats at a thermoneutral temperature will increase the susceptibility to weight gain and storage of energy as fat due to the absence of a thermogenic stimulus to promote BAT differentiation and activity. Furthermore, I also hypothesised that thermoneutral temperature is more suitable than the normal husbandry temperature of 20°C to investigate obesity as the activity of BAT is stimulated when animals are kept at a temperature lower than 27°C due to a cold stimulus (Xiao et al., 2015, Cui et al., 2016)

I also test the hypothesis that pre-conceptional induction of obesity by feeding a high energy diet in combination with living at thermoneutrality will amplify the negative outcomes on body weight and insulin sensitivity in the dams (Shankar et al., 2008).

3.3 Aims

The Main aim of this chapter is to test whether housing at standard husbandry temperature (20$\pm$1°C) will affect Uncoupling protein 1 (UCP1) gene expression and protein abundance in the interscapular brown adipose tissue iBAT, and to explore how UCP1 expression in iBAT is modulated with pregnancy.

3.4 Methods

Methods, laboratory protocols and statistical analysis used to produce the results of this chapter were detailed in chapter 2. mRNA was extracted using TRIZOl by Miss Gabriela Perez, transcribed to cDNA and diluted with nuclease-free water 1:10 then ran in a qPCR 96-well plate using primers or probes for gene expression quantification by Miss Gabriela Perez, Dr Enas AlHarethi and myself.

Representative samples from the 4 intervention groups at each of the three time points were sectioned, Immunohistochemistry for UCP1 protein quantification was performed by Dr Enas AlHarethi. All statistical analysis was performed as described in section (2.5). All animal experimentations, i.e. dissection, tissue weights, plasma analysis, histological and molecular analysis was supervised by Professor Michael Symonds, Professor Helen Budge and Dr Neele Dellschaft.

3.5 Results

3.5.1 Body weight

Prior to conception, body weight was only higher due to the H diet when animals were kept at thermoneutrality. By 10 d/g, body weight was higher with the H diet regardless of housing temperature, both intervention effects on body weight diminish at 19 d/g. body weight increased with gestation in all interventional group (Figure 3.1).

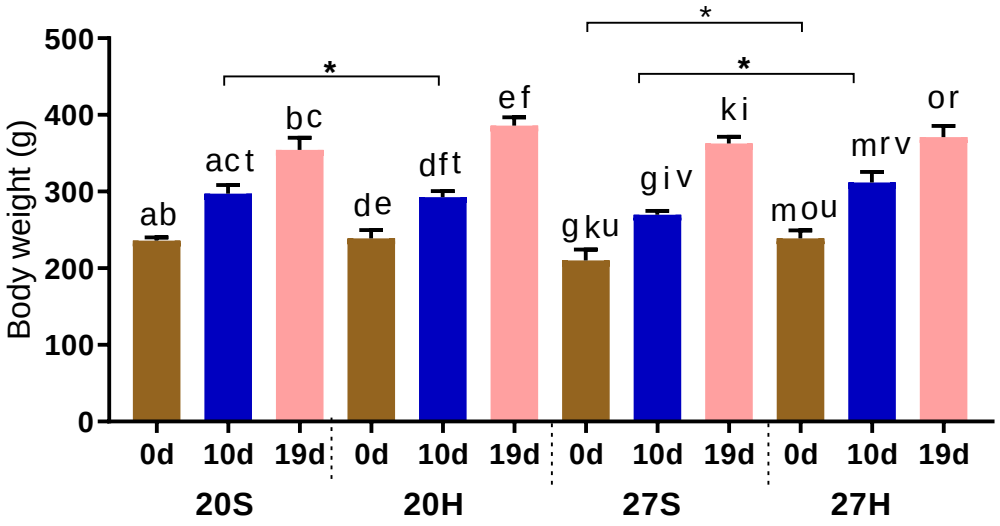


Figure 3.1 Effect of housing temperature, diet and pregnancy on body weight

Body weight of unmated (0), 10 and 19 days (d) pregnant rats housed at 20°C or 27°C and fed a standard (S) diet or high fat and sucrose (H) diet. Values are represented as mean ± SEM. Columns with the same superscripts are significantly different (P<.0.05); t, v, u: p<.05, a, c, d, m, r: p <.01, g: p<.001, b, e, f, i, o: p<.0001.

3.5.2 Interscapular BAT mass

No significant effect of either temperature or diet was detected between the unmated animals' iBAT mass groups. In 10 and 19 d/g pregnant rats, iBAT mass was significantly higher at the cool temperature compared with thermoneutrality when fed a H diet. By 19 d/g and only at a cool temperature, iBAT mass was higher for animals fed a high energy diet than those fed a standard one. At 19 d/g, iBAT mass increased compared to pre-pregnancy but only in those housed at the cool ambient temperature (Figure 3.2 & 3.3).

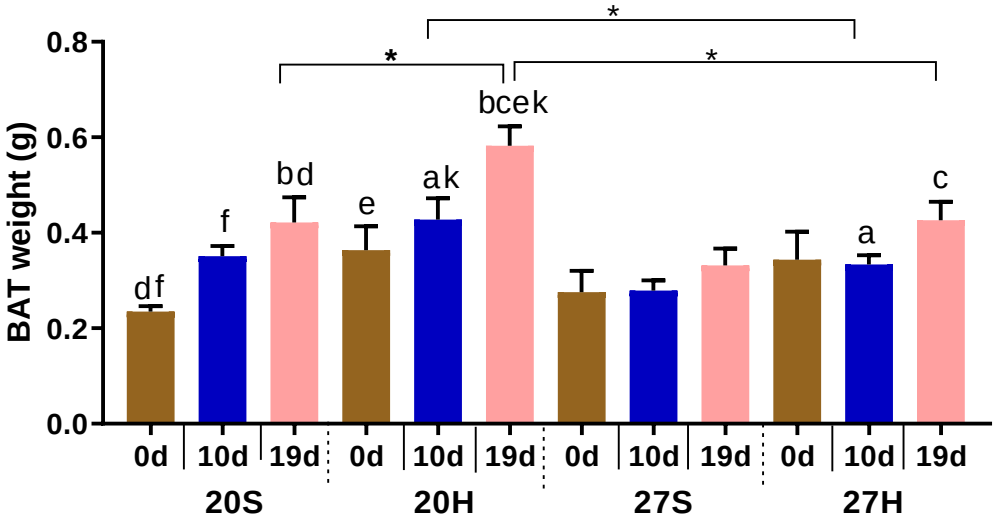


Figure 3.2 Effect of housing temperature, diet and pregnancy on interscapular BAT absolute mass

Interscapular brown adipose tissue (BAT) mass of unmated (0), 10 and 19 days (d) pregnant rats housed at 20°C or 27°C and fed a standard (S) diet or high fat and sucrose (H) diet. Values are represented as mean ± SEM. Columns with the same superscripts are significantly different (P<.0.05); a, b, c, f, k: p <.05, d, e: p<.01.

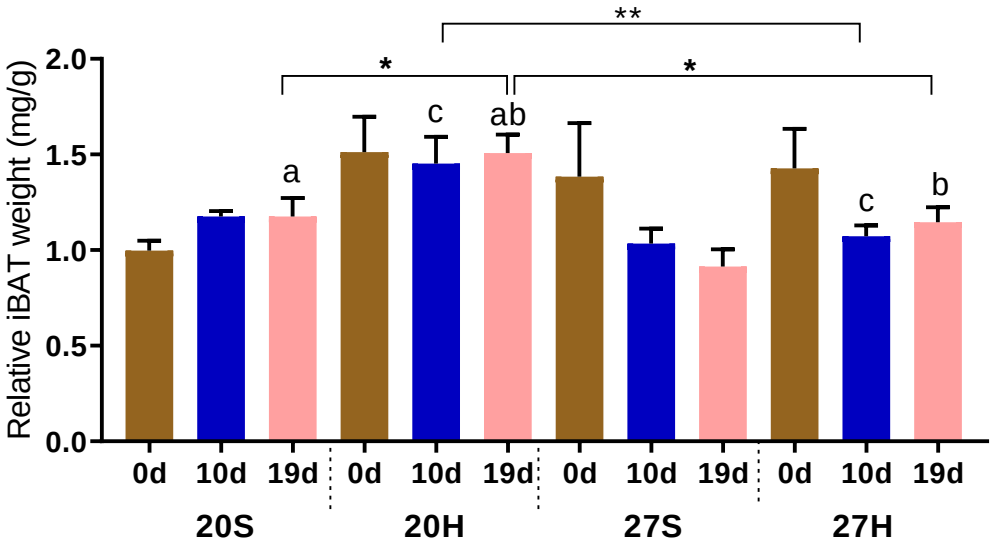


Figure 3.3 Effect of housing temperature, diet and pregnancy on relative interscapular BAT iBAT mass

Interscapular brown adipose tissue (BAT) relative mass of unmated (0), 10 and 19 days (d) pregnant rats housed at 20°C or 27°C and fed a standard (S) diet or high fat and sucrose (H) diet. Values are represented as mean ± SEM. Columns with the same superscripts are significantly different (P<.0.05); a, b: p <.05, c: p <.01.

3.5.3 Expression of genes and protein in iBAT

3.5.3.1 Expression of thermogenic genes and protein in iBAT

UCP1 gene expression was similar between groups and downregulated with gestation (Figure 3.4), In contrast, UCP1 protein was more abundant in unmated animals fed the H diet at the cooler temperature than at thermoneutrality, it declined significantly with pregnancy in the 20S group (Figure 3.5 & 3.6).

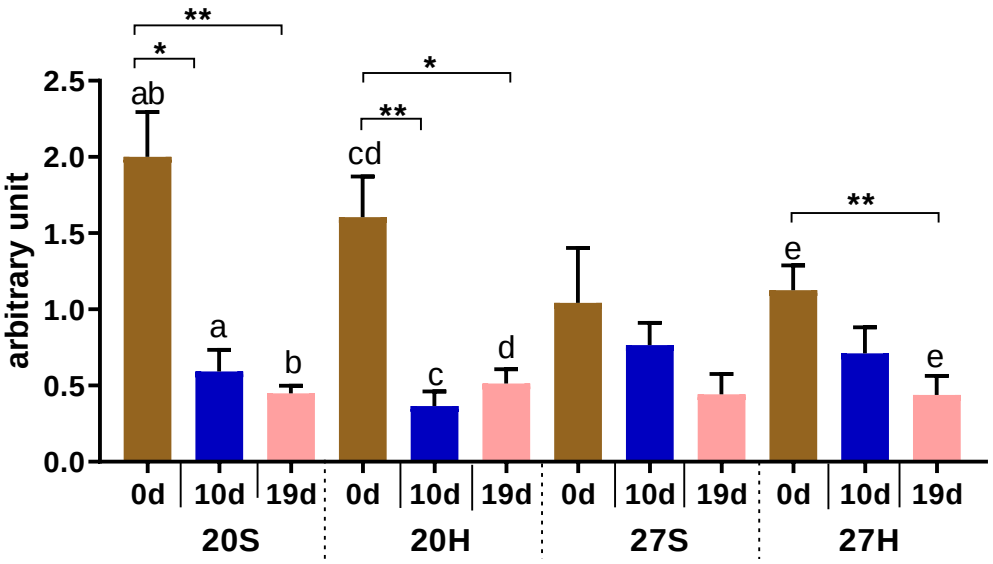


Figure 3.4 Uncoupling Protein 1 (UCP1) gene expression in the interscapular BAT

UCP1 gene expression in the interscapular brown adipose tissue (BAT) of unmated (0), 10 and 19 days (d) pregnant rats housed at 20°C or 27°C and fed a standard (S) diet or high fat and sucrose (H) diet. Values are represented as mean ± SEM. Columns with the same superscripts are significantly different (P<.0.05); a, d: p <.05, b, c, e: p<.01.

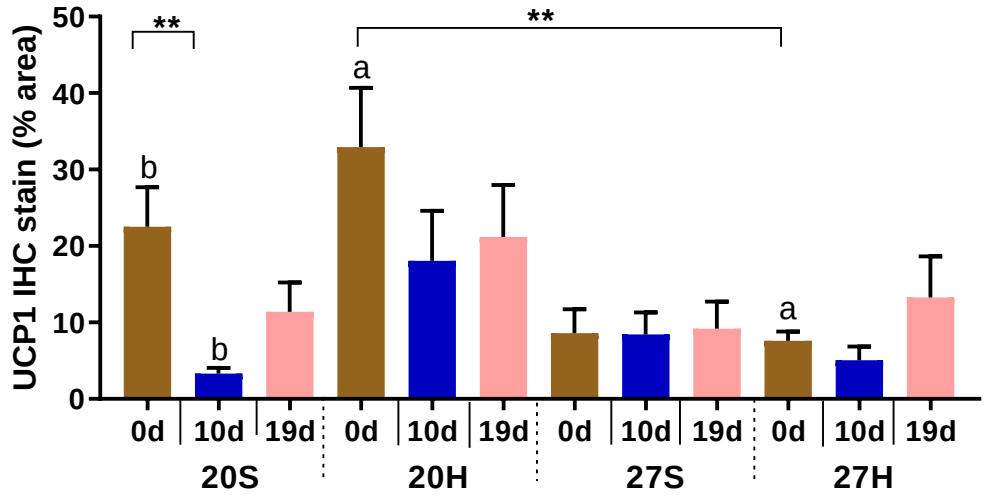


Figure 3.5 Uncoupling Protein 1 (UCP1) protein abundance in the interscapular BAT

UCP1 protein expression in the interscapular brown adipose tissue (BAT) of unmated (0), 10 and 19 days (d) pregnant rats housed at 20°C or 27°C and fed a standard (S) diet or high fat and sucrose (H) diet. Values are represented as mean ± SEM. Columns with the same superscripts are significantly different (P<.0.05); a, b: p<*0.01*.

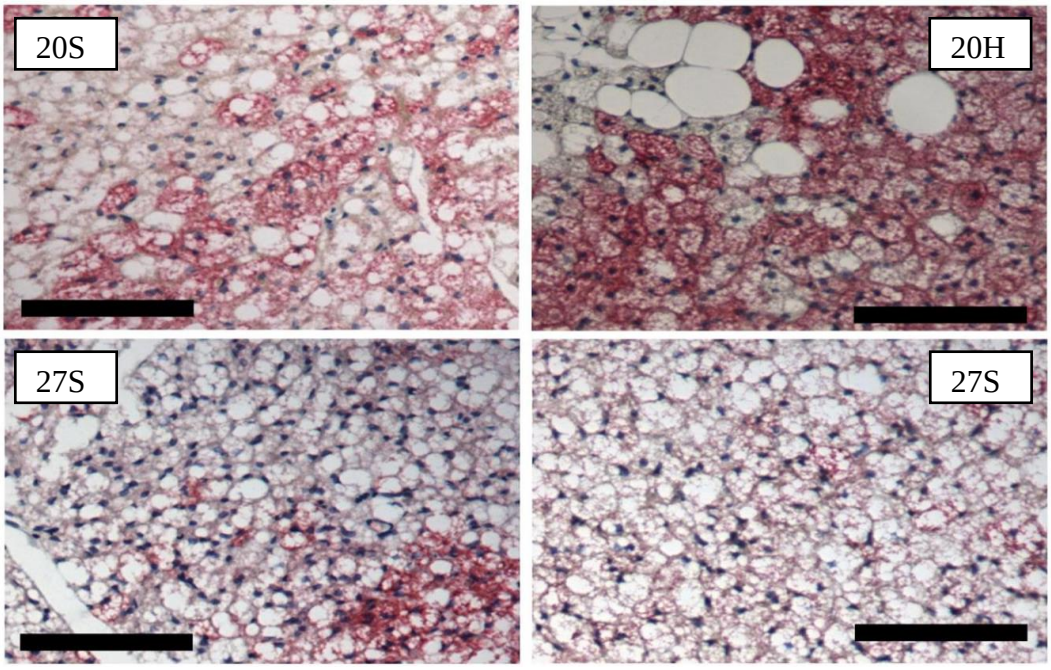


Figure 3.6 Representative anti-UCP1 immunohistochemistry images

Anti-UCP1 stained microscopic slides of interscapular brown adipose tissue from unmated females of the 20S (top left), 20H (top right), 27S (bottom left) and 27H groups (bottom right), with size bars indicating 100µm.

There was no significant change in β3AR gene expression with diet or temperature but was downregulated in iBAT with pregnancy at 10 d/g in the 20H group (Figure 3.7).

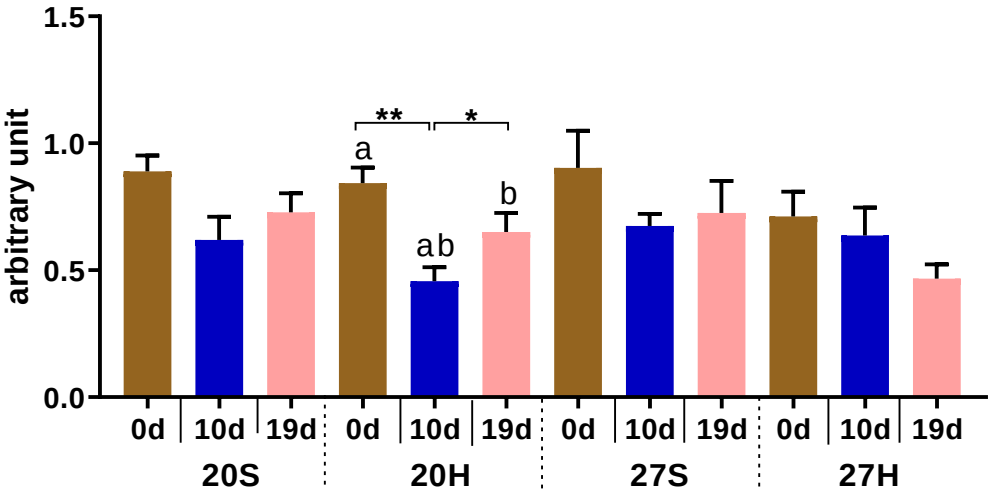


Figure 3.7 Beta-3 adrenergic receptor (β3AR) gene expression in the interscapular BAT

β3AR gene expression in the interscapular brown adipose tissue (BAT) of unmated (0), 10 and 19 days (d) pregnant rats housed at 20°C or 27°C and fed a standard (S) diet or high fat and sucrose (H) diet. Values are represented as mean ± SEM. Columns with the same superscripts are significantly different (P<.0.05); b: p<.05, a: p<.01.

TRPV1 gene expression peaked at 10 d/g in all interventional groups (Figure 3.8) while SERCA2B gene expression was not affected by any intervention at any time point except a downregulation with pregnancy at 10 d/g in the 20H group (Figure 3.9).

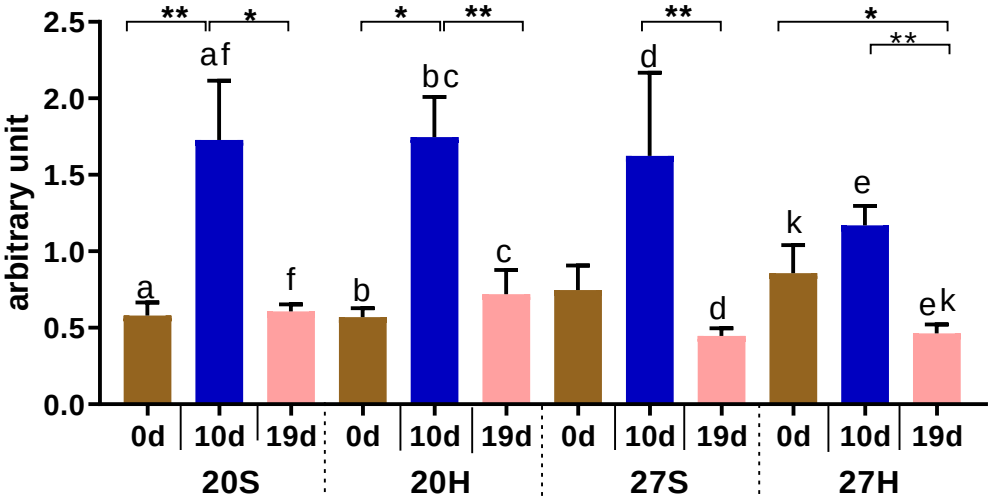


Figure 3.8 Transient receptor potential cation channel subfamily V member 1 (TRPV1) gene expression in the interscapular BAT

TRPV1 gene expression in the interscapular brown adipose tissue (BAT) of unmated (0), 10 and 19 days (d) pregnant rats housed at 20°C or 27°C and fed a standard (S) diet or high fat and sucrose (H) diet. Values are represented as mean ± SEM. Columns with the same superscripts are significantly different (P<.0.05); b, f, k: p<.05; a, c, d, e: p<.01.

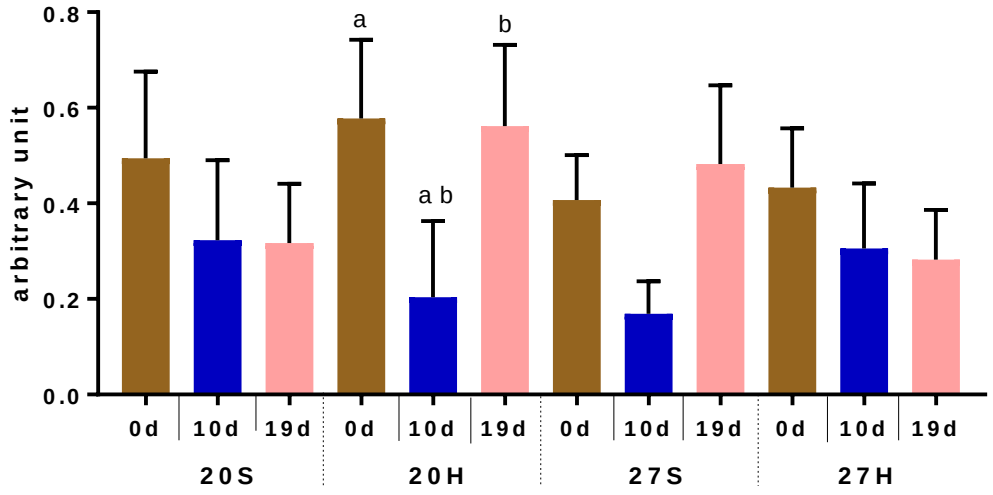


Figure 3.9 Sarcoplasmic/endoplasmic reticulum Ca2+ transporting 2 B (SERCA2B) gene expression in the interscapular BAT

SERCA2B gene expression in the interscapular brown adipose tissue (BAT) of unmated (0), 10 and 19 days (d) pregnant rats housed at 20°C or 27°C and fed a standard (S) diet or high fat and sucrose (H) diet. Values are represented as mean ± SEM. Columns with the same superscripts are significantly different (P<.0.05); a, b: p<.05**.**

Gene expression of BHSD11 was consistently higher in 27H than 20H groups and higher in 27S than 20S at 19 d/g, as it rose substantially by the end of pregnancy in those dams maintained at thermoneutrality (Figure 3.10). PPARɣ gene expression in iBAT was not affected by the diet or temperature in the unmated and pregnant rats at 10 d/g. By late gestation, its expression was higher at thermoneutrality irrespective of diet. PPARɣ exhibited a significant decline with pregnancy in animals kept at mild cold regardless of diet (Figure 3.11).

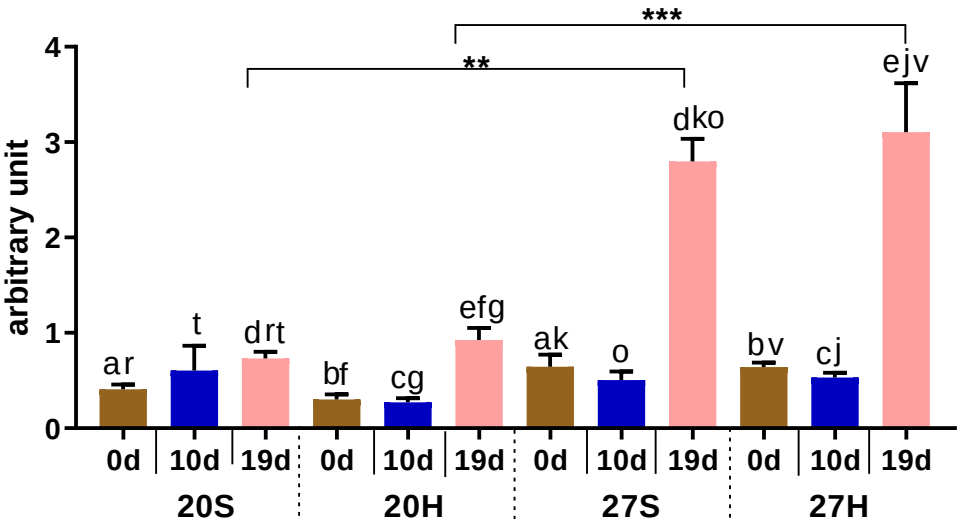


Figure 3.10 11β-Hydroxysteroid dehydrogenase (11βHSD) gene expression in the interscapular BAT

11BHSD gene expression in the interscapular brown adipose tissue (BAT) of unmated (0), 10 and 19 days (d) pregnant rats housed at 20°C or 27°C and fed a standard (S) diet or high fat and sucrose (H) diet. Values are represented as mean ± SEM. Columns with the same superscripts are significantly different (P<.0.05); a, b, r, t, v: p<.05; d, o, c, f, k: p<.01; e, j, g: p<.001.

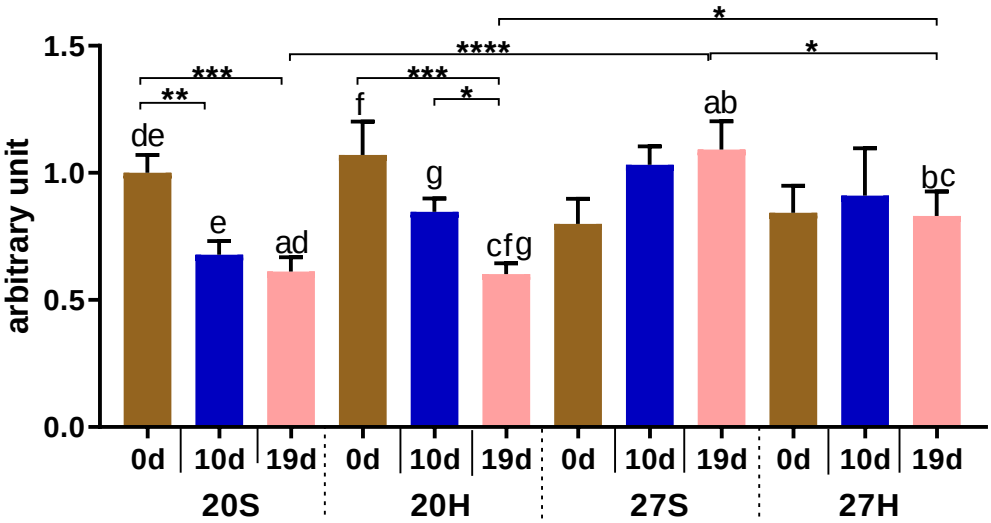


Figure 3.11 Peroxisome proliferator activated receptor gamma (PPARɣ) gene expression in the interscapular BAT

PPARɣ gene expression in the interscapular brown adipose tissue (BAT) of unmated (0), 10 and 19 days (d) pregnant rats housed at 20°C or 27°C and fed a standard (S) diet or high fat and sucrose (H) diet. Values are represented as mean ± SEM. Columns with the same superscripts are significantly different (P<.0.05); c, b, g: p<.05; e: p<.01; d, f: p<.001; a: p<.0001.

In virgin and 10 d/g rats, leptin gene expression was higher in 27H, compared with 20H group, this effect of temperature was observed at 19 d/g but for those animals fed the standard diet. Pregnancy had no effect on leptin gene expression except for the 27S group where it was higher at mid-pregnancy compared to virgin animals (Figure 3.12).

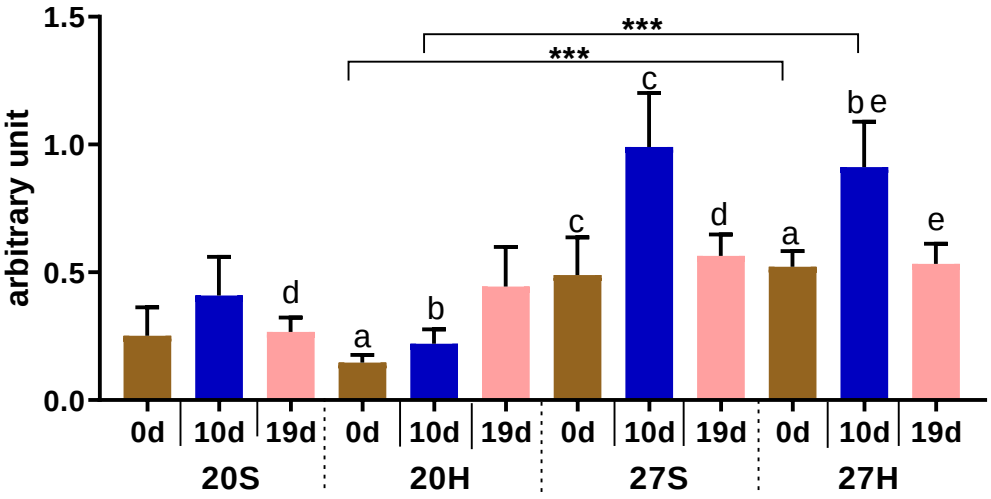


Figure 3.12 Leptin gene expression in the interscapular BAT

Leptin gene expression in the interscapular brown adipose tissue (BAT) of unmated (0), 10 and 19 days (d) pregnant rats housed at 20°C or 27°C and fed a standard (S) diet or high fat and sucrose (H) diet. Values are represented as mean ± SEM. Columns with the same superscripts are significantly different (P<.0.05); c, d, e: p<.05; a, b: p<.01**.**

There was a higher gene expression of PGC1α in 20H compared with 27H groups prior to mating and at late gestation. PGC1α gene expression was lower at the 19 d/g compared to virgin animals in all groups (Figure 3.13).

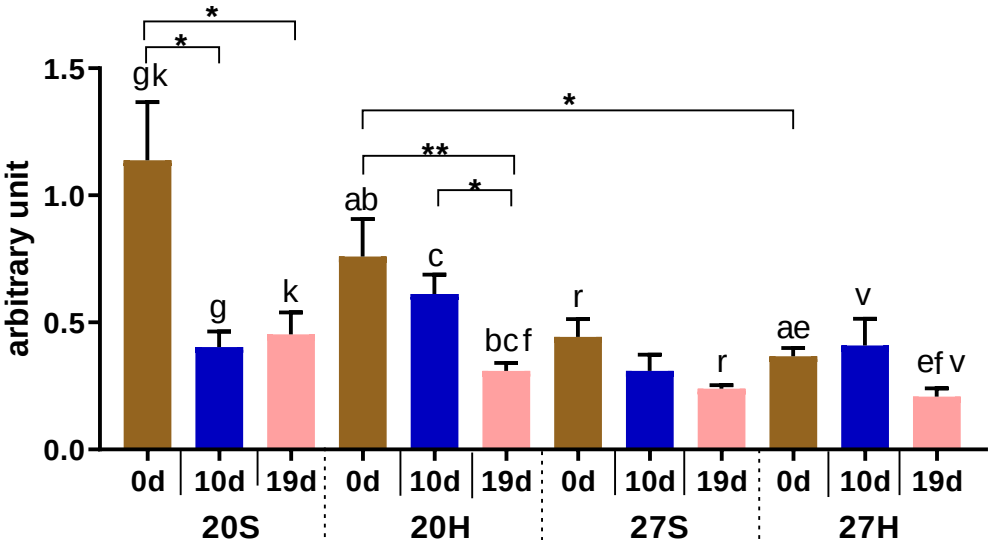


Figure 3.13 Peroxisome proliferator-activated receptor gamma coactivator 1-alpha (PGC-1α) gene expression in the interscapular BAT

PGC-1α gene expression in the interscapular brown adipose tissue (BAT) of unmated (0), 10 and 19 days (d) pregnant rats housed at 20°C or 27°C and fed a standard (S) diet or high fat and sucrose (H) diet. Values are represented as mean ± SEM. Columns with the same superscripts are significantly different (P<.0.05); a, c, e, f, g, k, v: p <.05; b, r: p<.01.

3.5.3.2 Expression of insulin sensitivity and energy sensing genes in iBAT

TCF7L2 was upregulated through pregnancy (Figure 3.14) while mTOR was upregulated in mid-pregnancy compared to prior to mating irrespective of diet and temperature (Figure 3.15).

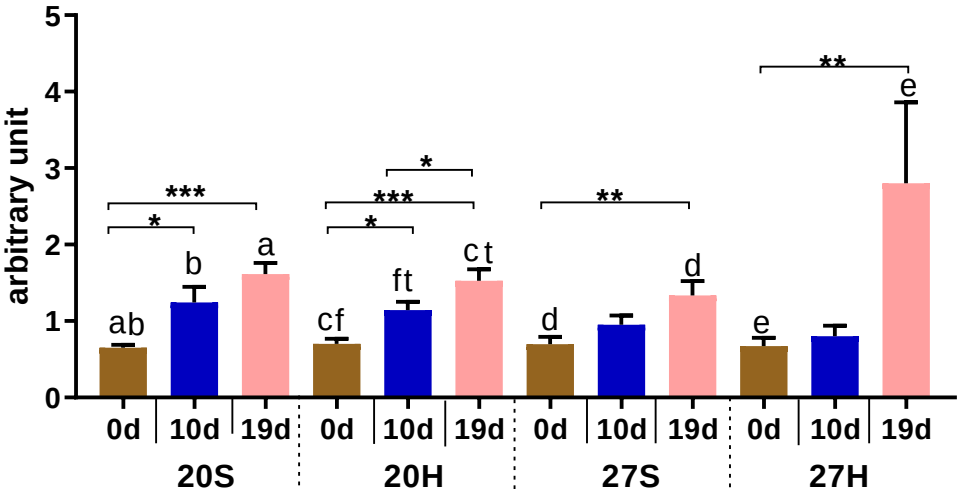


Figure 3.14 Transcription factor 7-like 2 (TCF7L2) gene expression in the interscapular BAT

TCF7L2 gene expression in the interscapular brown adipose tissue (BAT) of unmated (0), 10 and 19 days (d) pregnant rats housed at 20°C or 27°C and fed a standard (S) diet or high fat and sucrose (H) diet. Values are represented as mean ± SEM. Columns with the same superscripts are significantly different (P<.0.05); b, f, t: p<.05; d, e: p<.01; a, c: p<.001.

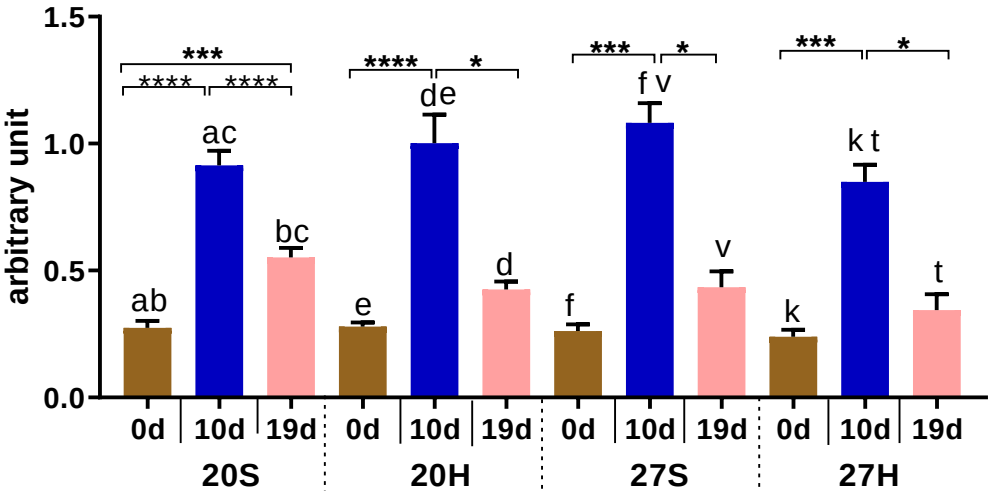


Figure 3.15 Mammalian target of rapamycin (mTOR) gene expression in the interscapular BAT

mTOR gene expression in the interscapular BAT of unmated (0), 10 and 19 days (d) pregnant rats housed at 20°C or 27°C and fed a standard (S) diet or high fat and sucrose (H) diet. Values are represented as mean ± SEM. Columns with the same superscripts are significantly different (P<.0.05); d, v, t: p<.05; b, f, k: p<.001; a, c, e: p<.0001.

IRS1 gene expression was significantly lower in 27H compared to the other three groups at 19 d/g and was downregulated with pregnancy in the 27H group (Figure 3.16), whilst IRS2 was reduced with the H diet at both temperatures prior to pregnancy but was not different between groups through pregnancy, it was upregulated in late gestation in all interventional groups (Figure 3.17).

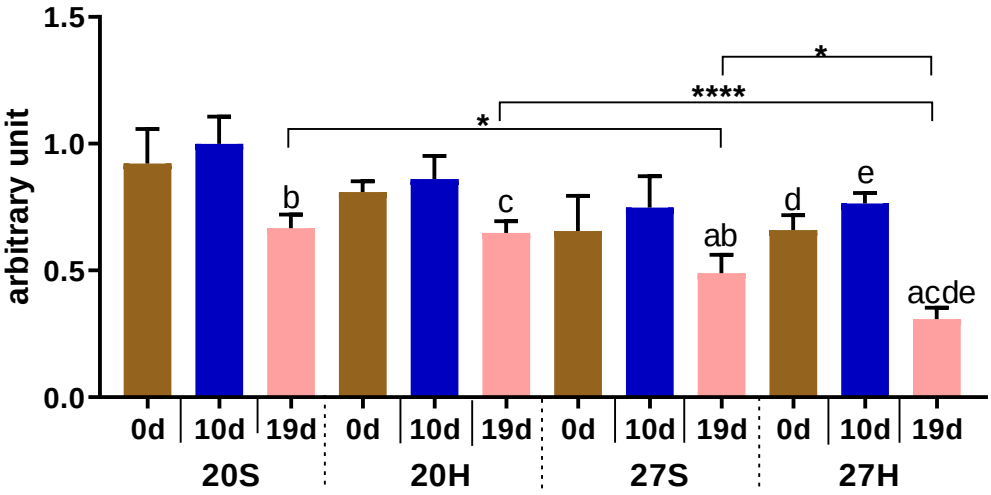


Figure 3.16 Insulin receptor substrate (IRS1) gene expression in the interscapular BAT

IRS1 gene expression in the interscapular BAT of unmated (0), 10 and 19 days (d) pregnant rats housed at 20°C or 27°C and fed a standard (S) diet or high fat and sucrose (H) diet. Values are represented as mean ± SEM. Columns with the same superscripts are significantly different (P<.0.05); a, b: p<.05; d: p<.001; c, e: p<.0001.

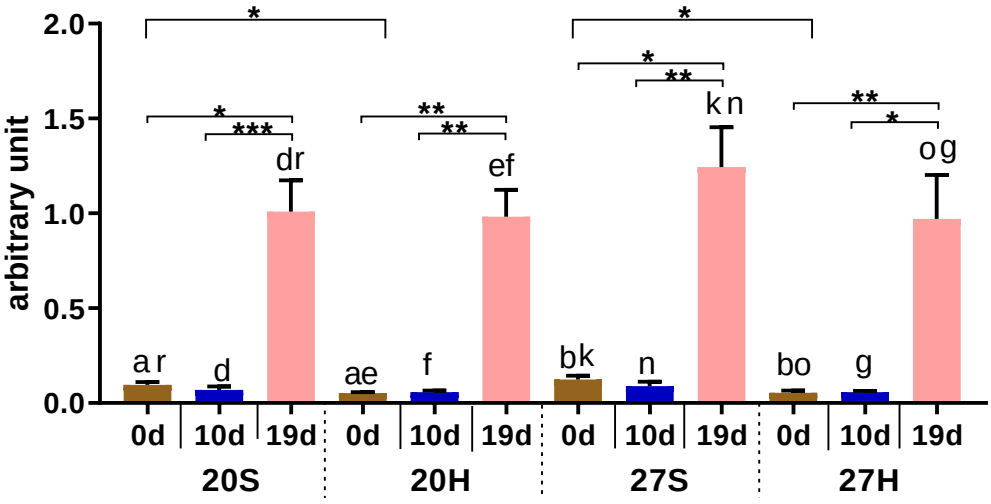


Figure 3.17 Insulin receptor substrate (IRS2) gene expression in the interscapular BAT

IRS2 gene expression in the interscapular brown adipose tissue (BAT) of unmated (0), 10 and 19 days (d) pregnant rats housed at 20°C or 27°C and fed a standard (S) diet or high fat and sucrose (H) diet. Values are represented as mean ± SEM. Columns with the same superscripts are significantly different (P<.0.05); a, b, k, g, r: p<.05; e, f, n, o: p<.01; d: p<.001.

3.5.3.3 Expression of fat transport genes in iBAT

Of the genes involved in fat transport, CD36 gene expression in late gestation was higher in animals kept at thermoneutrality irrespective of diet. It was upregulated with pregnancy but only in animals kept at thermoneutrality (Figure 3.18).

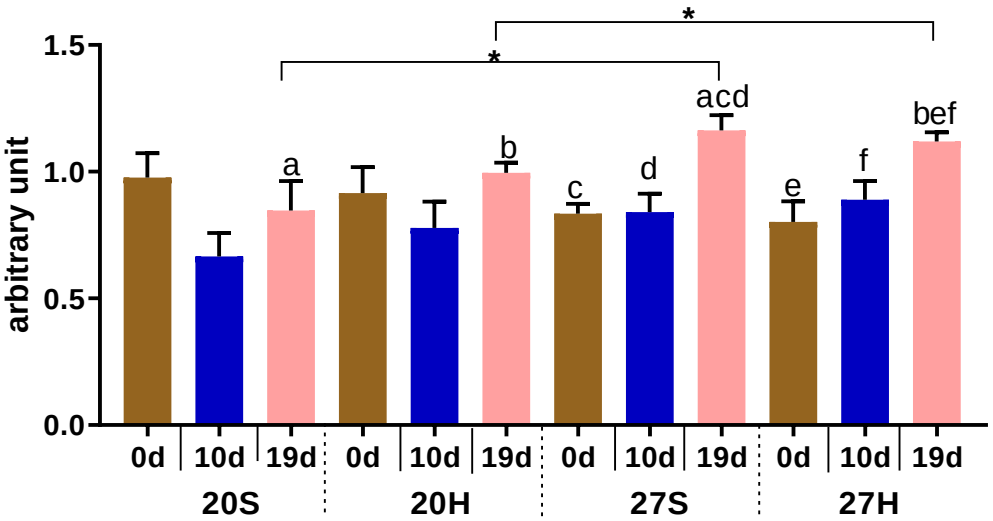


Figure 3.18 Fatty acid translocase (CD36) gene expression in the interscapular BAT

CD36 gene expression in the interscapular brown adipose tissue (BAT) of unmated (0), 10 and 19 days (d) pregnant rats housed at 20°C or 27°C and fed a standard (S) diet or high fat and sucrose (H) diet. Values are represented as mean ± SEM. Columns with the same superscripts are significantly different (P<.0.05); a, b, f: p<.05; c, d, e: p<.01.

ATGL gene expression was higher in 27S than 27H in virgin and 19 d/g rats, it was downregulated with pregnancy in the 20S group (Figure 3.19).

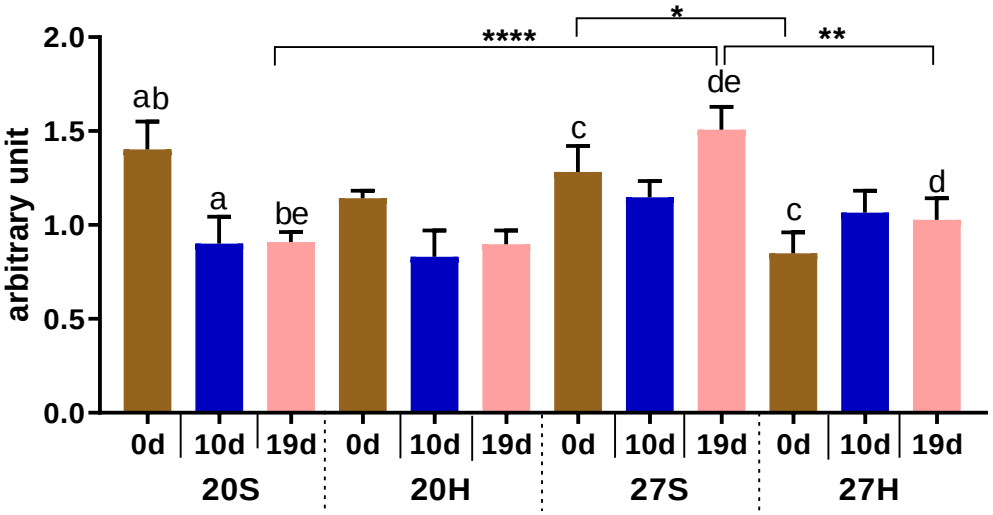


Figure 3.19 Adipose triglyceride lipase (ATGL) gene expression in the interscapular BAT

ATGL gene expression in the interscapular brown adipose tissue (BAT) of unmated (0), 10 and 19 days (d) pregnant rats housed at 20°C or 27°C and fed a standard (S) diet or high fat and sucrose (H) diet. Values are represented as mean ± SEM. Columns with the same superscripts are significantly different (P<.0.05); a, b, c: p<.05; d: p<.01; e: p<.0001.

At both temperatures, LPL showed high expression at 10 d/g in those dams fed the standard diet, its expression was also higher in the 27H compared to 27S group at mid-gestation (Figure 3.20). FATP4 gene expression increased significantly with pregnancy in all groups except in the 20H (Figure 3.21).

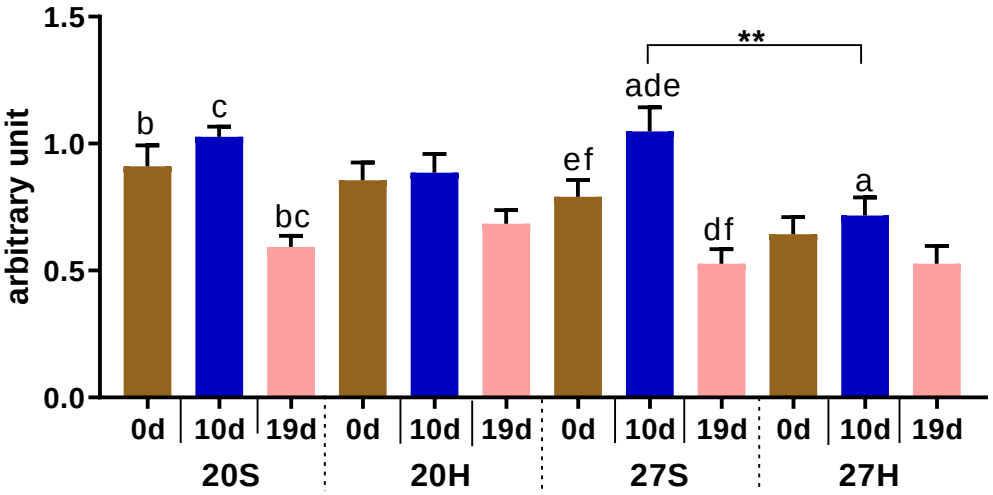


Figure 3.20 Lipoprotein lipase (LPL) gene expression in the interscapular BAT

LPL gene expression in the interscapular brown adipose tissue (BAT) of unmated (0), 10 and 19 days (d) pregnant rats housed at 20°C or 27°C and fed a standard (S) diet or high fat and sucrose (H) diet. Values are represented as mean ± SEM. Columns with the same superscripts are significantly different (P<.0.05); e, f: p<.05; a, b: p<.01; c,d: p<.001.

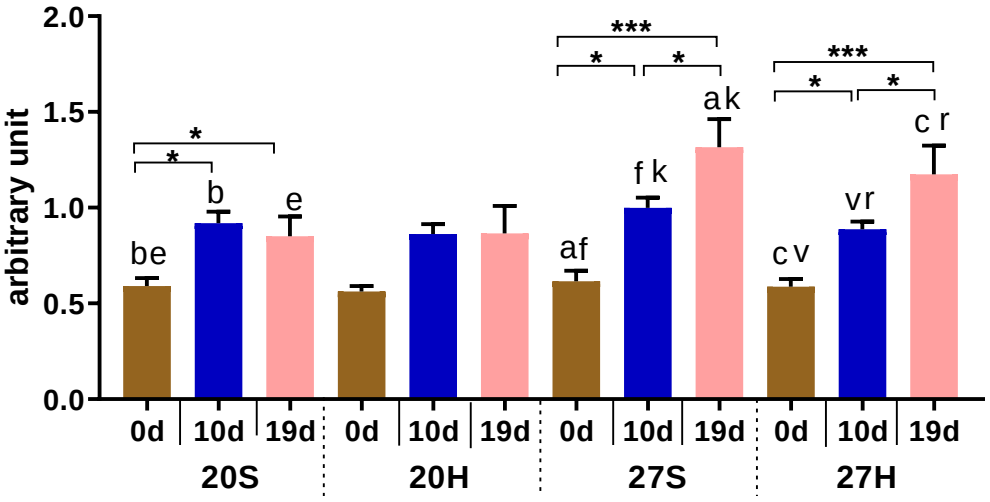


Figure 3.21 Fatty acid transport protein 4 (FATP4) gene expression in the interscapular BAT

FATP4 gene expression in the interscapular brown adipose tissue (BAT) of unmated (0), 10 and 19 days (d) pregnant rats housed at 20°C or 27°C and fed a standard (S) diet or high fat and sucrose (H) diet. Values are represented as mean ± SEM. Columns with the same superscripts are significantly different (P<.0.05); b, e, f, k, v, r: p<.05; a, c: p<.001.

3.5.4 Metabolic and endocrine profiles

Plasma glucose concentrations were notably higher in animals maintained at thermoneutrality before mating but were then similar between groups through pregnancy. Plasma triglyceride and leptin increased with gestation in all groups, whereas NEFA concentrations only increased at 19 d/g in the 20H group. Insulin was raised with the H diet before mating, only in animals kept at 20°C, and was then similar between groups through pregnancy with high variability. Additional details including p values can be found in Appendix 3.

3.6 Summary of main findings

Mainly, UCP1 protein expression was higher at mild cold than at thermoneutrality for the H fed diet while UCP1 gene expression was downregulated with pregnancy.

PPARγ, 11BHSD and leptin genes expression enhanced at thermoneutrality at different stages of gestation.

TCF7L2, IRS2, FATP4 genes were upregulated with pregnancy while PGC1-α gene was downregulated with pregnancy. TRPV1 and mTOR were upregulated in mid-pregnancy. PPARγ downregulated with pregnancy for the 20°C housed animals while LPL gene expression enhanced at mid-pregnancy for the standard diet fed animals

3.7 Discussion

Ambient temperature modulated the effect of a diet, this persisted into pregnancy and may have been caused by the reduction in the amount of UCP1 protein. This adaptation occurred in parallel with changes in the circulating glucose concentration that was raised at thermoneutrality prior to conception and could be caused in part by reduced thermogenesis in iBAT (Figure 3.22 A) (Zingaretti et al., 2009, Wang and Wahl, 2014). Pregnancy resulted in the effect of housing temperature on circulating glucose

concentration to disappear (Figure 3.22 B & C). This may be caused by metabolic adaptations associated with pregnancy that are mediated by hormones such as progesterone (Bell and Bauman, 1997, McIlvride et al., 2017), or by the changes in UCP1 (Figure 3.22 B & C). These results complement the previous findings of the effect of housing at thermoneutral temperature demonstrated in male mice, in which UCP1 expression reduced and effects on glucose and insulin diminish with time (Xiao et al., 2015, Small et al., 2018).

The downregulation of UCP1 and PGC-1α gene expression in iBAT with gestation was more pronounced at 20°C than at thermoneutrality, and was accompanied with a decline in UCP1 protein at 20°C only (Figure 3.22 A & B & C). A recent study in mice (McIlvride et al., 2017) suggested a reduction in UCP1 protein gene expression with gestation but this study has limitations in the procedures undertaken that may affect BAT properties. Firstly, no protein quantification was done and they depend on results from one immunohistochemistry slide to measure UCP1 protein abundance. Secondly, the same study suggested a reduction in the thermogenic response with gestation, but this was measured in terminally anaesthetised animals, such procedure can be a confounding factor that may affect brown fat characteristics due to its suppressive effect on the iBAT (Ohlson et al., 1994). In another report, UCP1 protein expression was suggested to decline with pregnancy (Qiao et al., 2018). However, in these studies, measures were made in total protein homogenates rather than mitochondrial preparations where the UCP1 presents (Aquila et al., 1985) and known to decline with pregnancy (Frontera et al., 2005).

The leptin gene which is considered as a white fat biomarker as its expression in WAT is 50 times higher than in BAT (Maffei et al., 1995) showed the largest relative change in gene expression with gestation in iBAT. This change was exclusive to animals housed at thermoneutrality while its expression in WAT was not affected by any intervention. Furthermore, in an in vitro study, cold exposure of UCP1-positive differentiated adipocytes enhanced leptin localization in their nuclei (Velickovic et al., 2018). In

another study, leptin treatment in vivo and in vitro caused increased lipolysis and glucose utilisation (Siegrist-Kaiser et al., 1997). Collectively, these data suggest a role of leptin in BAT function and development that is not yet fully established.

Consuming a high energy diet and/or a reduction in the ambient temperature activate the sympathetic nervous system would both be predicted to act on adrenoreceptors (e.g. β3AR*)* to promote thermogenesis (Bachman et al., 2002) (Figure 3.22 A). β3AR agonist administration stimulates the uptake of glucose and increases brown-like fat in WAT depots (Figure 3.22 A) (Cypess et al., 2015). In light of this, a reduction in β3AR gene expression in the 20H group in mid-gestation (Figure 3.22 B) was unexpected. There are, however, three subtypes of βeta adrenergic receptors (i.e. β1AR, β2AR, β3AR*)* (Collins and Surwit, 2001). Furthermore, in both rats and hamsters, α1 adrenergic receptors (α1AR) can modulate nonshivering thermogenesis in BAT after cold acclimation and with a high energy diet (Mohell, 1984). In addition, thermogenesis could be activated by β3AR treatment in adults in mature brown adipocytes not in preadipocytes as they possess β1AR *(*Nedergaard and Cannon, 2010*)*, so it would be worthwhile extending the measurements made on my animals accordingly.

As pregnancy progresses, pregnant rats have a longer time than virgin rats of exposure to the reduced ambient temperature and high energy diet which are both considered stimuli that activate brown fat and induce mitochondrial biogenesis (i.e. synthesis of mitochondrial proteins, mRNA and ribosomes) (Ouellet et al., 2012, Rothwell et al., 1982, Feldmann et al., 2009). Diet and cold could explain the significant increase in iBAT weight at 20°C housed rats and fed a high energy diet at each time point in pregnancy individually (mid and late gestation) (Figure 3.22 A & B & C). The lipoprotein lipase that acts as a triglycerides hydrolysis enzyme (He et al., 2018) peaked at 10 d/g to accompany the increase of triglycerides which is a common feature in pregnancy (Herrera, 2002b, Steingrimsdottir et al., 1980) (Figure 3.22 A & B & C). Previous studies showed that fructose supplementation to term altered the maternal microbiome and changed lipid and carbohydrate metabolism (Astbury et al., 2018), so it is possible that

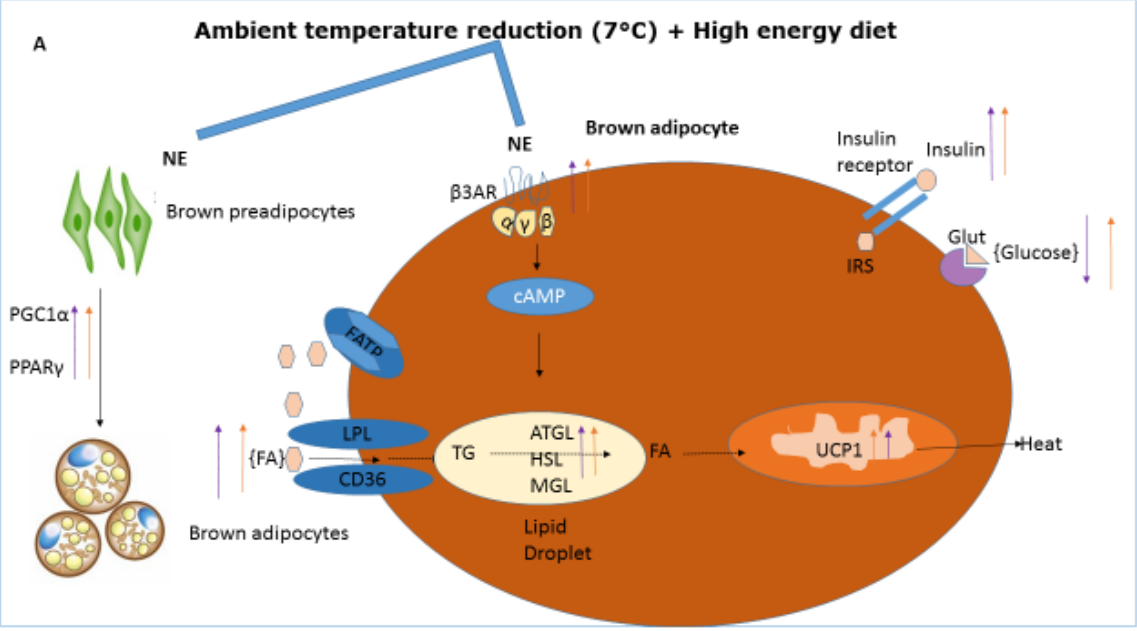
due to high sucrose diet used in my study such effect has been generated that cause the continuous rise of circulatory TG as pregnancy proceed even with the LPL rise in mid-gestation (Herrera et al., 1987). Reduced LPL expression in late pregnancy may be important to help in the diversion of lipid from storage in adipose tissue to mammary glands to help in milk formation for lactation (Hamosh et al., 1970) or to muscles to be oxidized (Knopp et al., 1986).

11βHSD is an enzyme that convert inactive cortisone to cortisol. It is highly active in adipose tissue of obese subjects. High expression of 11βHSD1 in subcutaneous adipose tissue and more weight gain which resulted from glucocorticoid administration, were accompanied with decreasing UCP1 expression in BAT. (Poggioli et al., 2013). 11βHSD1 was found to be highly expressed in mediastinal adipose tissue of patients with coronary artery diseases compared with those with no such disorder (Chechi et al., 2019). In the recent study, 11βHSD followed a pattern opposite to UCP1 protein expression pattern in virgin rats, as it showed higher expression in iBAT at thermoneutrality compared to mild cold for animals fed a high energy diet, this pattern continues with pregnancy. Furthermore, 11BHSD expression in the adipose tissue was reduced with HFD feeding in mice (Auvinen et al., 2012). In addition, 11BHSD induced expression impairs the metabolic activity of brown fat (Doig et al., 2017).

Fatty acids are the main activators for thermogenesis. The high serum concentration of NEFA in iBAT in late pregnancy is due to enhanced lipolysis. Possibly, this was activated by the action of cool temperature and high energy diet in the 20H group (Figure 3.22 C). Consequently, the proteins responsible for their uptake and processing in BAT (i.e. ATGL and CD36) should be upregulated in late pregnancy in the 20°C housed animals (Figure 3.22 A & B & C). Possible reasons for the reduced mRNA expression of these genes at mild cold for the standard diet-fed animals can be the pregnancy; it acts as a modulatory factor (Figure 3.22 B & C) that affects other interventions or interacts with them.

3.8 Conclusion

Prior to conception, a reduction in the ambient temperature triggers brown fat characteristics in the interscapular adipose tissue, an effect that is not found at thermoneutrality. The onset of pregnancy reduced the brown phenotype of the mild cold housed animals to be comparable to that seen in animals kept at thermoneutrality indicating that the surrounding temperature effect on lipid and carbohydrate metabolism, hormones and adipose tissue properties is little after gestation compared to before it. Additional details including gene expression, hormonal and metabolites concentrations, and p values can be found in Appendix 2 and Appendix 3.



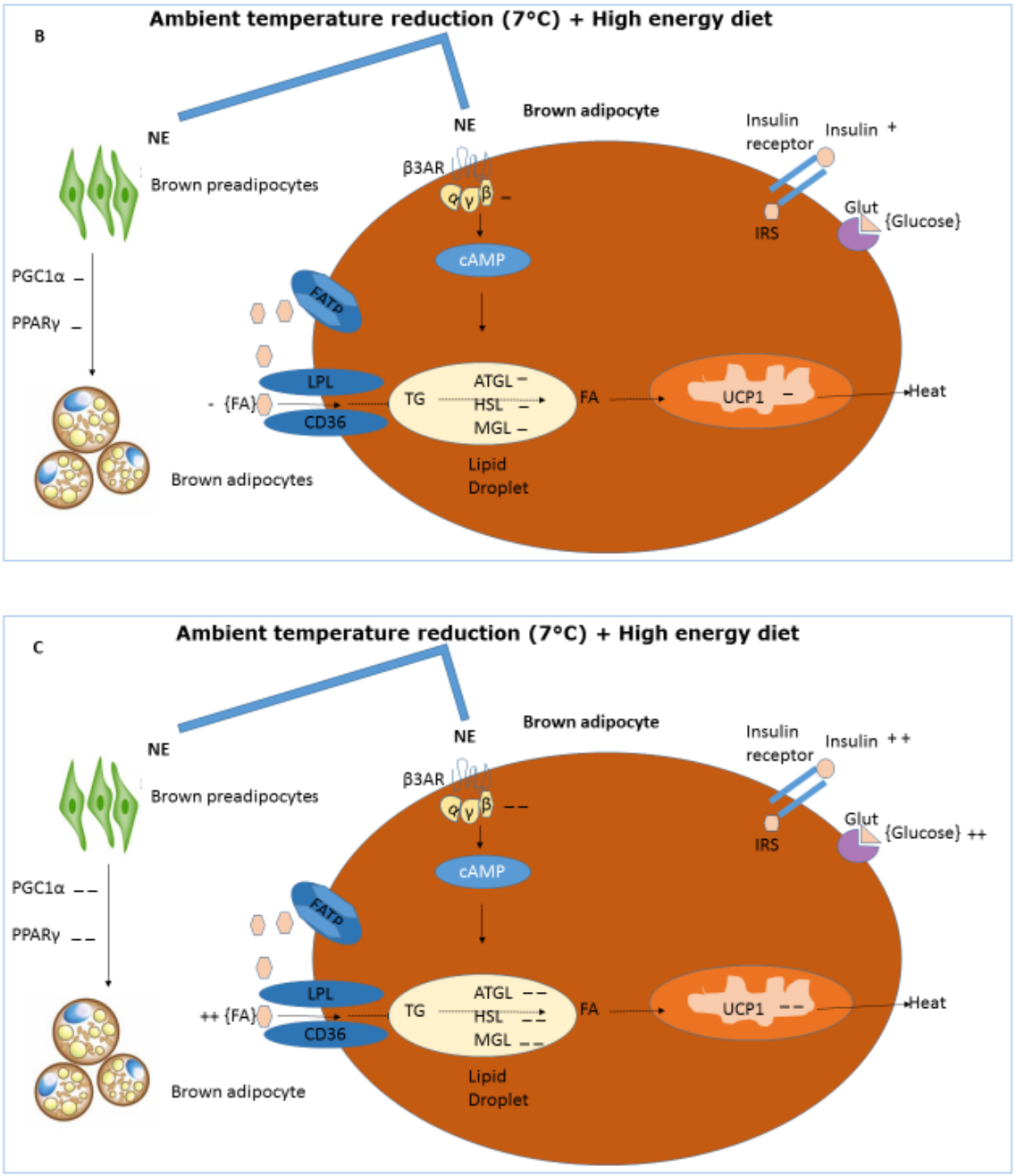


Figure 3.22 Illustration of changes in interscapular brown adipose tissue (iBAT)

Brown adipocytes characteristics and metabolites concentrations changes in response to a high energy diet consumption and ambient temperature reduction in unmated (0); A, 10 days; B and 19 days; C pregnant rats. Purple arrows indicate temp effect, orange arrows indicate diet effect, - & + indicate less or more expression or concentration with pregnancy, norepinephrine (NE), uncoupling protein 1 (UCP1), peroxisome proliferator-activated receptor gamma (PPARγ), peroxisome proliferator-activated receptor gamma coactivator 1-alpha (PGC-1α) , beta-3 adrenergic receptor (β3AR), insulin receptor substrates 1 and 2 (IRS1+2), fatty acid translocase (CD36), adipose triglyceride lipase (ATGL), lipoprotein lipase (LPL), fatty acid transport protein 4 (FATP4), hormone sensitive lipase (HSL), fatty acid (FA), triglyceride (TG), monoacylglycerol lipase (MGL), glucose transporter (GLUT).

Chapter 4. The response of inguinal adipose tissue to diet, housing temperature and pregnancy

4.1 Introduction

White adipose tissue is distributed through the body and according to anatomical location is divided into subcutaneous and visceral. It functions mainly in energy storage (Giralt and Villarroya, 2013) and also plays an important role in immunity (Fantuzzi, 2005) and secretes hormones (Avram et al., 2005, Wozniak et al., 2009). Each white fat depot differs phenotypically, as well as in their metabolic properties and potential to differentiate (Prunet-Marcassus et al., 2006).

White adipose tissue can respond to specific stimuli and may undergo a process called browning in which it acquires BAT characteristics, characterised by UCP1 expression in the mitochondria, plus the appearance of multilocular lipid droplets. The resulting adipocytes are called inducible, beige or brite as they are different from classical BAT in origin (Giralt and Villarroya, 2013). Understanding the browning process and the activating factors is important because as a thermogenic organ they could drive energy balance to a negative status and so participate in preventing or treating obesity (Lo and Sun, 2013). Cold exposure is the more established factor to induce browning (Nedergaard and Cannon, 2014).

Mammary gland is composed of connective tissue stroma, adipose tissue and epithelium. The epithelium consists of continuous branching ducts from the nipple leading to smaller ducts ending with alveolar buds or alveoli. The mammary gland in the rat extends from the cervical to the inguinal regions as six ventrolateral pairs, each with its own nipple. The development of mammary gland postnatally is characterised by rapid cellular proliferation and epithelial invasion that is increased at day 23 of age. With pregnancy, the alveolar epithelium also shows hypertrophy, as the cells accumulate intracellular lipid and increase their rough endoplasmic reticulum and Golgi and secretory vesicles. The

number of alveoli increases from day 5 of pregnancy and peaked at gestational day 20 (Masso-Welch et al., 2000). The high plasticity of adipocytes is revealed by events that occur during pregnancy. Recent evidence shows the ability of subcutaneous adipocytes (inguinal) to form alveolar epithelial cells in pregnancy which represent a component of the mammary gland to support subsequent lactation (Giordano et al., 2014). This process is reversible as these cells will convert back to adipocytes after lactation (Cinti, 2012).

In this chapter, I will explore the effect of housing at thermoneutrality compared to standard housing, together with high energy diet consumption on inguinal fat mass, as well as histological and molecular characteristics. This will be achieved by examining effects on genes involved in thermogenesis (*UCP1,β3AR, PPARG, OXTR*) (Shabalina et al., 2013, Bachman et al., 2002, Sell et al., 2004, Kasahara et al., 2006), glucose utilisation and insulin sensitivity (*IRS2*) (Saltiel and Kahn, 2001), lipid transport and fatty acid uptake from the circulation (*FATP4,FABP4*) (Nickerson et al., 2009) and appetite regulation (*LEPTIN*) (Blundell et al., 2001). Fat samples will be taken from virgin and pregnant rats at 50% and 90% of pregnancy (10 and 19 days of gestation; 10 d/g and 19 d/g) and I will also examine whether there is any interaction between the interventions. In addition, I examined the expression of genes that are considered to be mammary cell markers (*ELF5, WAP, STAT5A, OXTR*) (Zhou et al., 2005, Burdon et al., 1991, Liu et al., 1997, Soloff et al., 1979) and whether these are regulated through gestation and compare this with their expression in BAT and other white adipose tissues.

4.2 Hypothesis

I will test the hypotheses that:

- The housing of rats at a thermoneutral temperature will increase their susceptibility to store energy as fat. This will be due to the absence of a thermogenic stimulus to promote browning in the inguinal adipose tissue.

- Inguinal white fat of animals housed at standard husbandry temperature (20°C) will be influenced by mild cold which acts as a stimulus for browning in this tissue and consequently masks the effect of the dietary intervention (Xiao et al., 2015, Cui et al., 2016).
- Pre-conceptional induction of obesity by feeding a high energy diet in combination with housing at thermoneutrality will amplify the negative outcomes on dams by further increasing fat mass and reducing their insulin sensitivity (Shankar et al., 2008).
- Browning of the inguinal fat, potentially triggered by mild cold, will be compromised with pregnancy to reduce energy expenditure that could act to avoid exposing mothers and fetuses to nutrient shortage (McIlvride et al., 2017).
- Inguinal adipocytes will form alveolar structure similar to those composing mammary gland in response to pregnancy.

4.3 Aims

This chapter aims mainly to investigate the effect of housing at mild cold (standard husbandry temperature) on the browning capacity of the inguinal adipose tissue of rats by measuring the changes in UCP1 gene expression. It aims also to study the modulation for the genetic profile of this depot by pregnancy as previously published data suggested a possible differentiation of subcutaneous adipocytes to mammary cells phenotype.

4.4 Methods

All methods, laboratory protocols and statistical analysis used to produce the results of this chapter are detailed in chapter 2. I extracted mRNA using TRIZOl, transcribed it to cDNA and diluted it with nuclease-free water 1:10 and then ran the qPCR in a 96-well plate using primers or probes for gene expression quantification.

Representative samples from the 4 intervention groups at each of the three time points were processed, sectioned, stained and imaged as discussed in chapter 2 (section 2.3.3). All statistical analysis was performed as described in section 2.5.

4.5 Results

4.5.1 Gross anatomy of the inguinal adipose tissue

Photographic images were taken for the inguinal adipose tissue of virgin and pregnant rats during dissection of the animals as I noticed a different appearance of inguinal fat of pregnant rats (Figure 4.1).

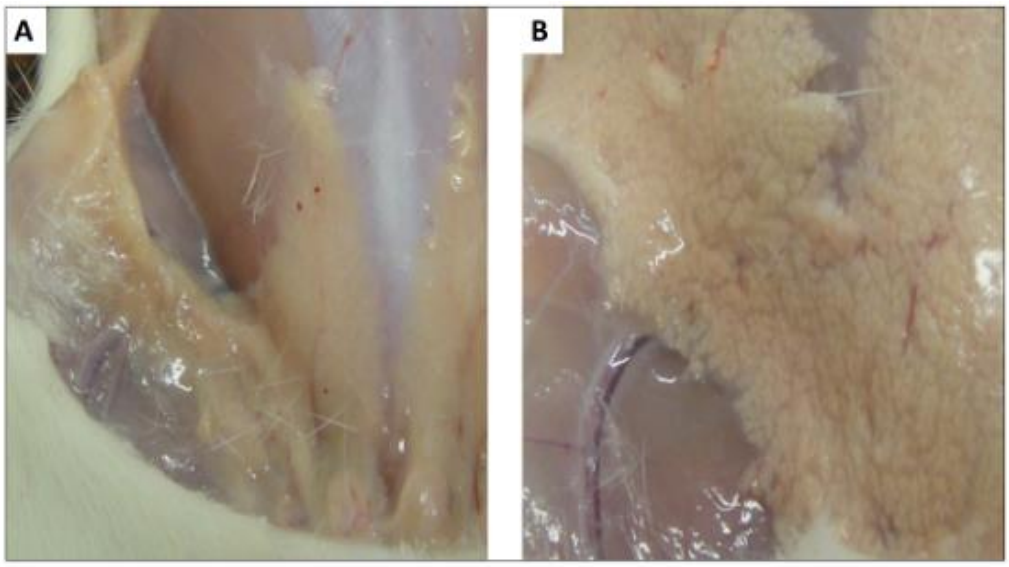


Figure 4.1 Representative images for inguinal fat of both Virgin (A) and Pregnant (B) rats during the tissues sampling process

4.5.2 Inguinal adipose tissue H & E stained histological sections

Sections from each time point were stained with H & E as shown in Figure 4.2.

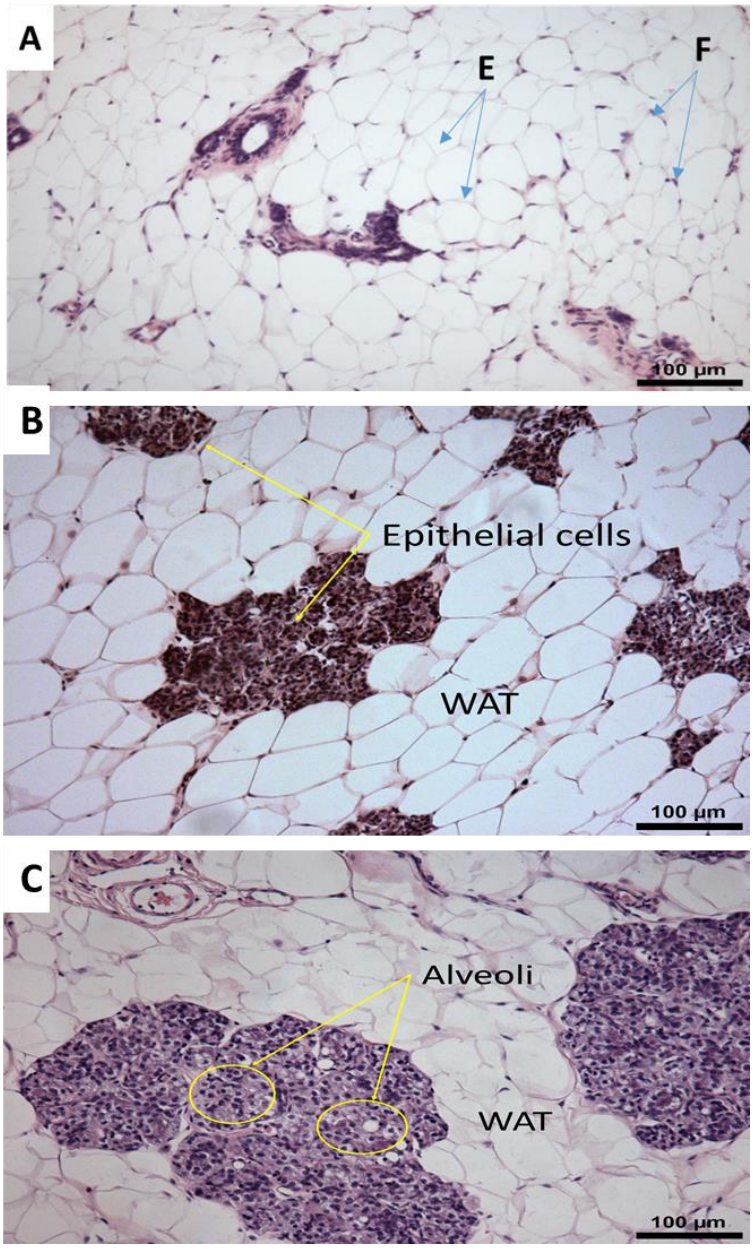


Figure 4.2 Representative microscopic slides of the inguinal adipose tissue

Representative microscopic slides of 5µm haematoxylin and eosin stained inguinal adipose tissue of unmated (A), 10 days (B) and 19 days (C) of gestation pregnant rats. A: Adipocyte membranes (pink stained boundaries) marked by arrow E. Blue stained nuclei squeesed to the periphery of the adipocyte membrane (arrow F). B: represents the first stage of alveoli development where it is constituted of epithelial cells devoid of lipid droplets. C: represent the second stage of mammary gland alveoli formation by the appearance of alveoli composed of lipid laden epithelial cells (pink adipocytes). Slides are displayed as 10X magnification.

4.5.3 Inguinal adipose tissue mass

Prior to conception, the high energy diet increased inguinal fat mass at both temperatures. In mid-gestation, more inguinal fat accumulate in the 27H compared to the 20H group. Effects of both temperature and diet on inguinal fat mass diminished at late pregnancy. Pregnancy further promoted the accumulation of inguinal fat in all groups. (Figure 4.3).

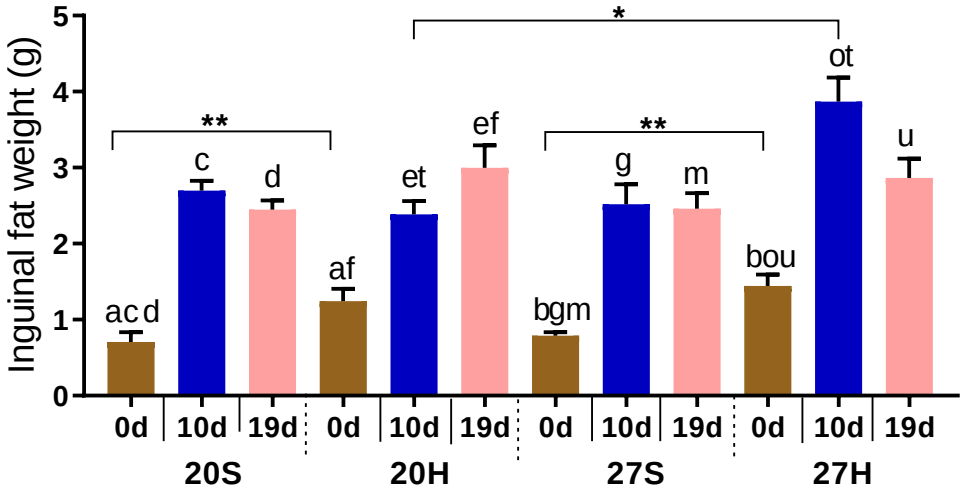


Figure 4.3 Effect of housing temperature, diet and pregnancy on inguinal fat mass

Inguinal fat mass of unmated (0), 10 and 19 days (d) pregnant rats housed at 20°C or 27°C and a standard (S) diet or high fat and sucrose (H) diet. Values are represented as mean ± SEM. Columns with the same superscripts are significantly different (P<.0.05); t: P<.05; a, b, e, o: p <.01; f, g, u: p<.001; c, d, m: p<.0001.

4.5.4 Expression of genes in the inguinal adipose tissue

4.5.4.1 Thermogenic genes

Gene expression of UCP1 was not found at any time point. There was no significant change in β3AR gene expression with diet or temperature prior to or at mid-gestation and it was not detectable at 19 d/g. In the 20S group, gene expression was higher in virgin rats compared with 10 d/g (Figure 4.4).

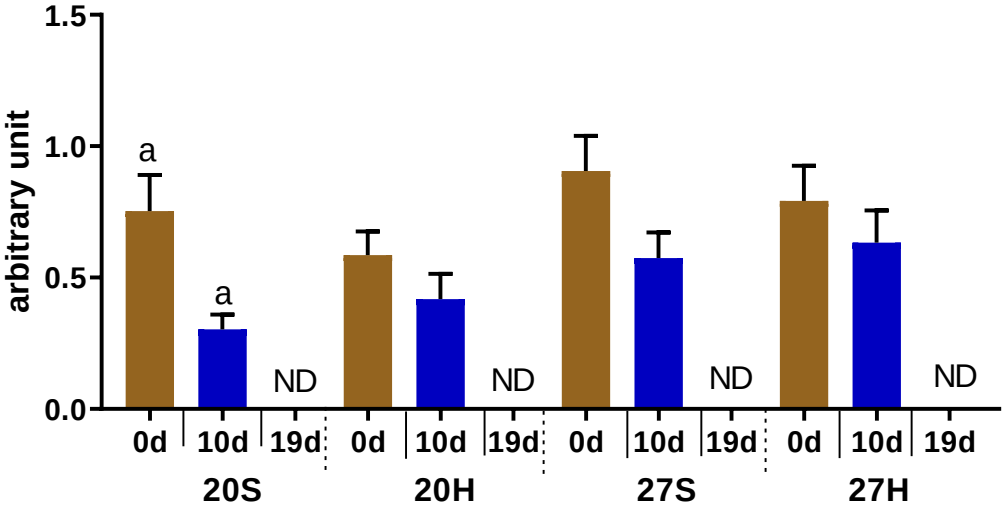


Figure 4.4 Beta-3 adrenergic receptor (β3AR) gene expression in the inguinal adipose tissue

β3AR gene expression in the inguinal adipose tissue of unmated (0), 10 and 19 days (d) pregnant rats housed at 20°C or 27°C and fed a standard (S) diet or high fat and sucrose (H) diet. Values are represented as mean ± SEM. ND denotes for Not Detected. Columns with the same superscripts are significantly different (P<.0.05); a: p<.05.

No significant effect of diet or temperature was found for PPARɣ gene expression in the inguinal fat of virgin or pregnant rats, and its expression decreased with pregnancy regardless of any intervention (Figure 4.5).

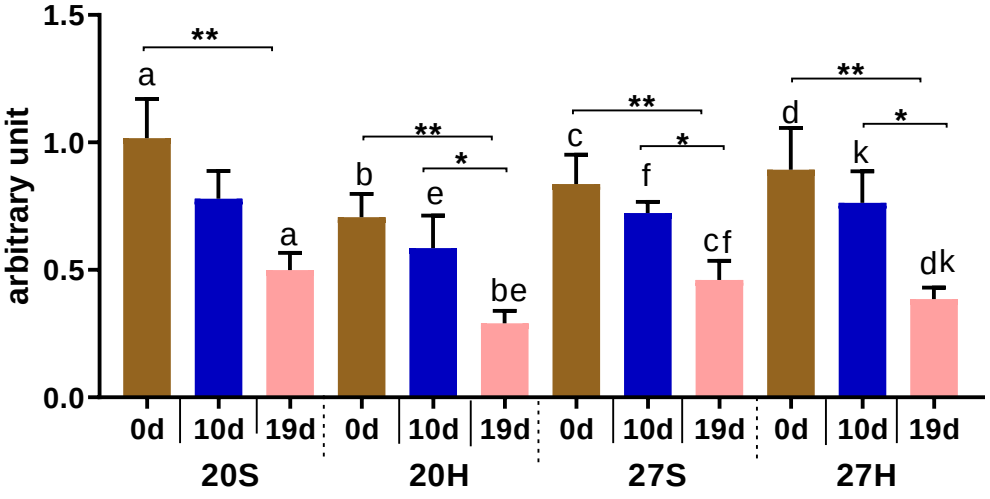


Figure 4.5 Peroxisome proliferator-activated receptor gamma (PPARɣ) gene expression in the inguinal adipose tissue

PPARɣ gene expression in the inguinal adipose tissue of unmated (0), 10 and 19 days (d) pregnant rats housed at 20°C or 27°C and fed a standard (S) diet or high fat and sucrose (H) diet. Values are represented as mean ± SEM. Columns with the same superscripts are significantly different (P<.0.05); k, e, f: p<.05; a, b, c, d: p<.01.

No significant effect of diet or temperature on gene expression of leptin was found at any time point but its expression decreased significantly at mid-gestation in the 20S group (Figure 4.6).

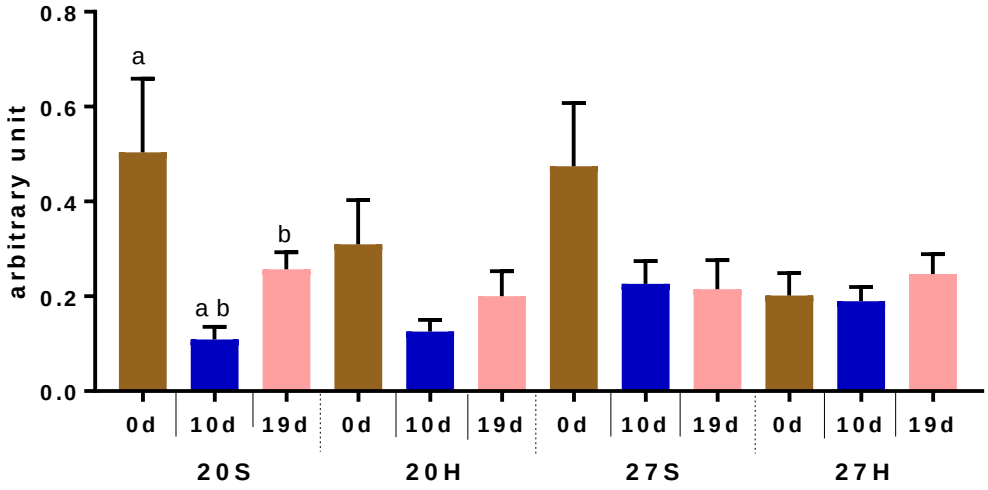


Figure 4.6 Leptin gene expression in the inguinal adipose tissue

Leptin gene expression in the inguinal adipose tissue of unmated (0), 10 and 19 days (d) pregnant rats housed at 20°C or 27°C and fed a standard (S) diet or high fat and sucrose (H) diet. Values are represented as mean ± SEM. Columns with the same superscripts are significantly different (P<.0.05); b: p<.05; a: p<.01.

4.5.4.2 Insulin sensitivity genes

IRS2 gene expression was not affected by the diet or temperature prior to or with gestation. It was downregulated in mid-pregnancy and then rose in late pregnancy in all groups (Figure 4.7).

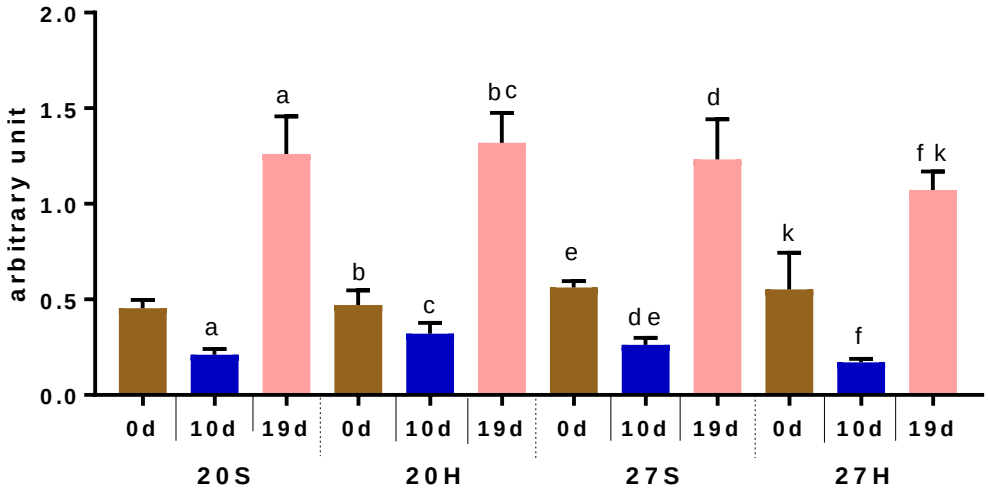


Figure 4.7 Insulin receptor substrate 2 (IRS2) gene expression in the inguinal adipose tissue

IRS2 gene expression in the inguinal adipose tissue of unmated (0), 10 and 19 days (d) pregnant rats housed at 20°C or 27°C and fed a standard (S) diet or high fat and sucrose (H) diet. Values are represented as mean ± SEM. Columns with the same superscripts are significantly different (P<.0.05); b, e, k: p<.05; a, c, f: p<.001; d: p<.0001.

4.5.4.3 Fat transport genes

FATP4 mRNA was not detected in any group of virgin or pregnant animals. FABP4 gene expression was not effected by any intervention, the only change was with the pregnancy and was confined to the standard diet-fed animals where it was downregulated in pregnant animals (Figure 4.8).

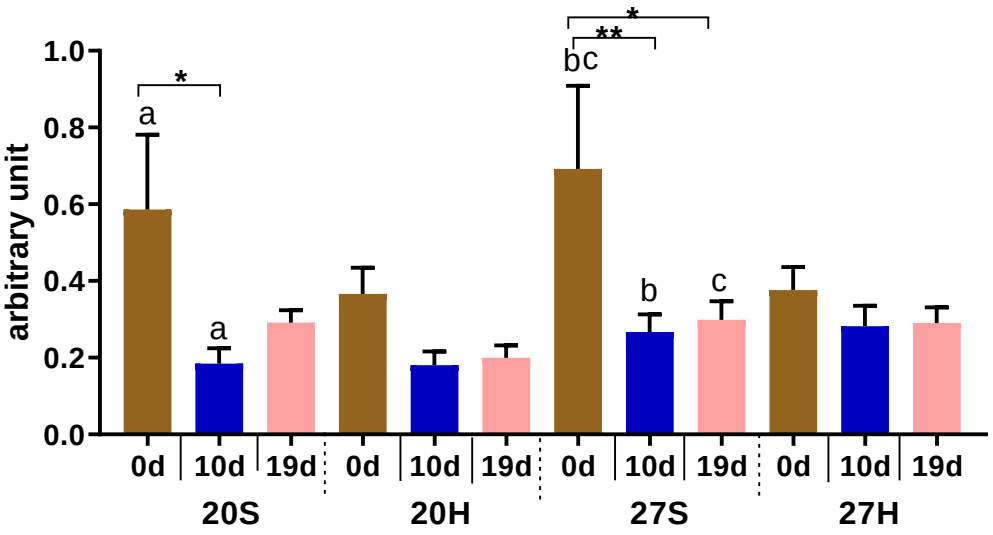


Figure 4.8 Fatty acid binding protein 4 (FABP4) gene expression in the inguinal adipose tissue

FABP4 gene expression in the inguinal adipose tissue of unmated (0), 10 and 19 days (d) pregnant rats housed at 20°C or 27°C and fed a standard (S) diet or high fat and sucrose (H) diet. Values are represented as mean ± SEM. Columns with the same superscripts are significantly different (P<.0.05); a, c: p<.05; b: p<.01.

4.5.4.4 Mammary cells biomarkers

Diet and ambient temperature reduction had no significant effect on ELF5 gene expression in the inguinal fat which increased with pregnancy in all groups (Figure 4.9).

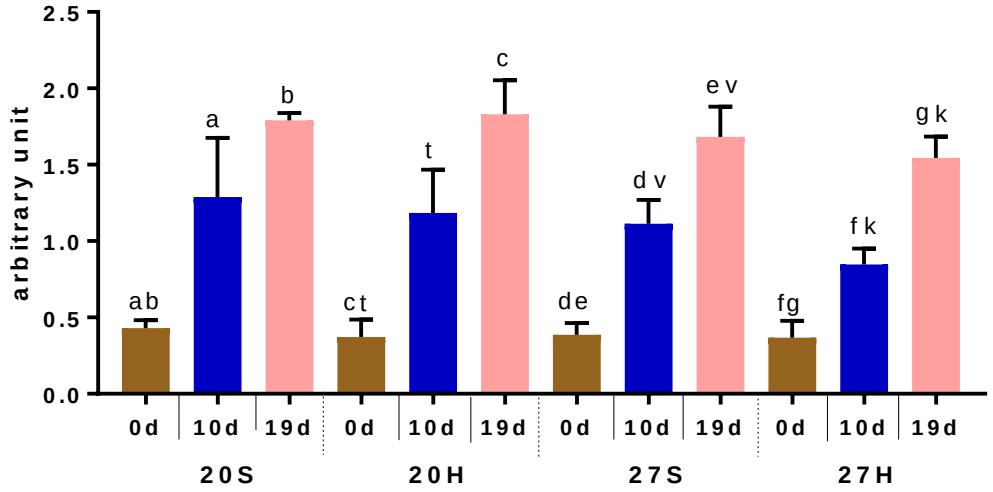


Figure 4.9 E74-Like ETS Transcription Factor 5 (ELF5) gene expression in the inguinal adipose tissue

ELF5 gene expression in the inguinal adipose tissue of unmated (0), 10 and 19 days (d) pregnant rats housed at 20°C or 27°C and fed a standard (S) diet or high fat and sucrose (H) diet. Values are represented as mean ± SEM. Columns with the same superscripts are significantly different (P<.0.05); a, f, t, v: p<.05; d: p<.01; b, c, k: p<.001; e, g: p<.0001.

The WAP gene was detected in low amounts in virgin rats, but its expression was upregulated with gestation without any difference between the groups at any time point (Figure 4.10).

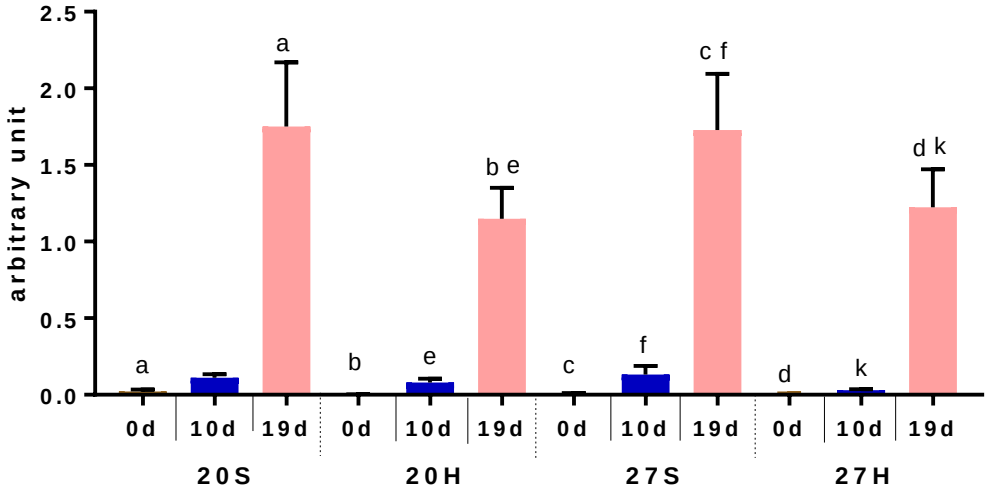


Figure 4.10 Whey Acidic Protein (WAP) gene expression in the inguinal adipose tissue

WAP gene expression in the inguinal adipose tissue of unmated (0), 10 and 19 days (d) pregnant rats housed at 20°C or 27°C and fed a standard (S) diet or high fat and sucrose (H) diet. Values are represented as mean ± SEM. Columns with the same superscripts are significantly different (P<.0.05); e, f, k: p<.05; a, d: p<.001; b, c: p<.0001.

Diet and housing temperature had no effect on STAT5A gene expression in virgin or pregnant rats, which increased with pregnancy in all groups (Figure 4.11).

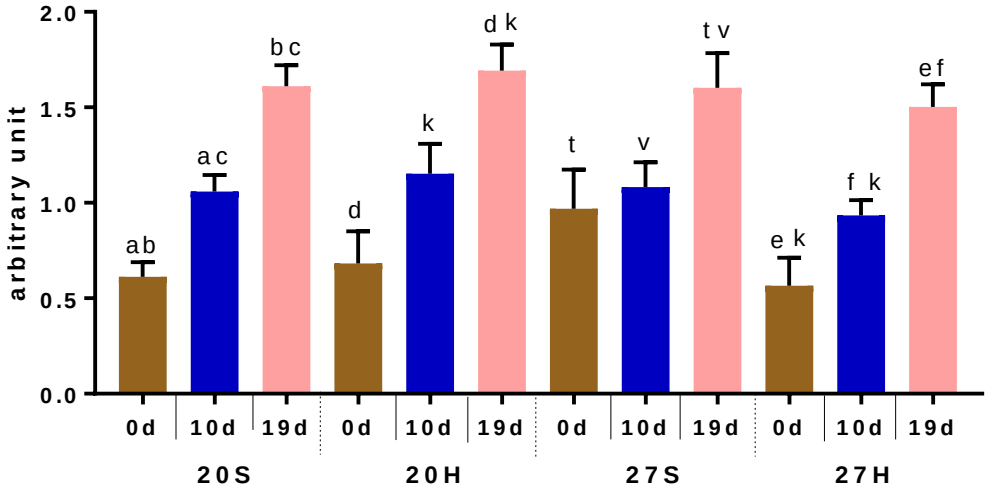


Figure 4.11 Signal transducer and activator of transcription 5A (STAT5A) gene expression in the inguinal adipose tissue

STAT5A gene expression in the inguinal adipose tissue of unmated (0), 10 and 19 days (d) pregnant rats housed at 20°C or 27°C and fed a standard (S) diet or high fat and sucrose (H) diet. Values are represented as mean ± SEM. Columns with the same superscripts are significantly different (P<.0.05); k, t, v: p<.05; a, c, f: p<.01; d, e: p<.001; b, e: p<.0001.

OXTR gene expression was affected by the diet in late gestation in those dams housed at 20°C in which it was raised in the 20S group. Pregnancy also increased *OXTR* expression in latter group (Figure 4.12).

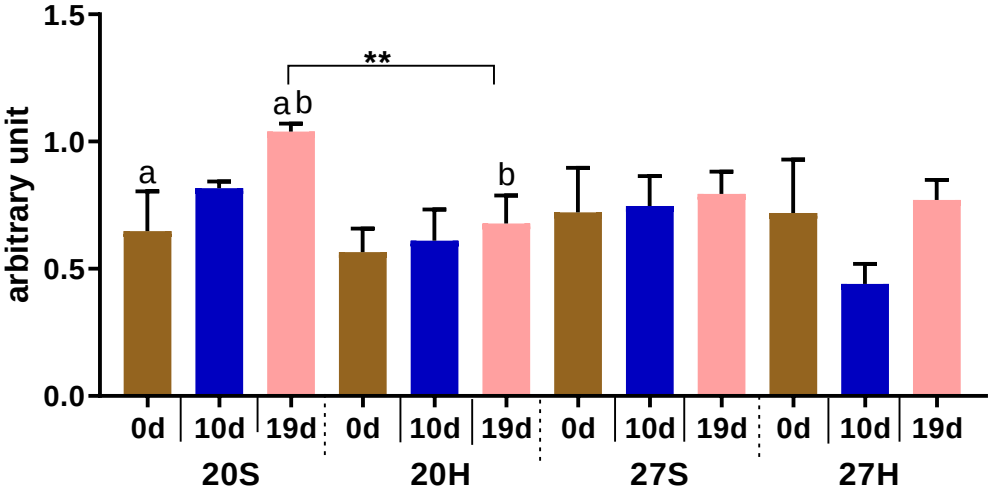


Figure 4.12 Oxytocin receptor (OXTR) gene expression in the inguinal adipose tissue

OXTR gene expression in the inguinal adipose tissue of unmated (0), 10 and 19 days (d) pregnant rats housed at 20°C or 27°C and fed a standard (S) diet or high fat and sucrose (H) diet. Values are represented as mean ± SEM. Columns with the same superscripts are significantly different (P<.0.05); a: p<.05, b :p <.01.

4.6 Summary of main findings

UCP1 gene expression was not detected in the inguinal adipose tissue of any group while b3-ar disappeared at late gestation. PPARγ expression decreased with pregnancy while FABP4 followed the same pattern but only for the standard diet fed animals. Pregnancy upregulated IRS2, ELF5, WAP, STAT5A genes in all interventional groups.

4.7 Discussion

Although the subcutaneous fat depot is more likely to acquire BAT characteristics in rodents than the omental fat depot (Zuriaga et al., 2017, Kim and Plutzky, 2016, Aldiss et al., 2017, Ferrannini et al., 2016), but I found no evidence of beiging in the inguinal adipose tissue. In other studies where UCP1 was found or browning in the inguinal fat depot was induced by mild cold acclimation (22C°) or exercise, only males were studied (Rogers et al., 2012, Poher et al., 2015, Knudsen et al., 2014, Wu et al., 2014, Cui et al., 2016, de Jong et al., 2015, Yang et al., 2017, Waldén et al., 2011) (Table 4.1). In the only study where UCP1 was found in the inguinal fat of females, the 129Sv mice strain was used (Rosell et al., 2014) (Table 4.1). This strain is known to be resistant to diet-induced obesity and exhibits distinct brown remodelling features possibly due to their higher metabolic rate and greater abundance of UCP1 in white fat compared to other mice strains (Almind et al., 2007, Ferrannini et al., 2016). It is also possible that the duration of the intervention (i.e. 4 weeks for virgin rats and with more 10 and 19 days for pregnant rats) was too short to trigger UCP1 gene expression in the inguinal fat. In a mouse study, males housed at cold (22°C) for 20 weeks caused UCP1 expression in the subcutaneous fat depot that was not seen at thermoneutrality (Cui et al., 2016) (Table 4.1).

Table 4.1 List of studies in rodents' inguinal adipose tissue where UCP1 was detected or induced.

Intervention	Old/Duration	Model/Sex	Change in UCP1		Comments	Reference
			gene	protein		
Housing temperature, (30°C) or (4°C)	Six weeks old/ 3 weeks	Mice-Male	Increase at 4°C			(de Jong et al., 2015)
Intermittent cold exposure	Different ages as captured/ 4 hours a day for 15 days	Pika		Not Changed	air-conditioned (5–6 °C)	(Bai et al., 2015)
Housing temperature, 4°C, –10°C, and –10°C/–20°C	Seven to eight weeks/different durations	Mice-Male		Increased in all groups relative to control	30°C used as a control	(Yang et al., 2017)
1. Housing temperature; 30°C or 22°C). 2. Diet (chow or HFD)	Not mentioned / 20 weeks	Mice-male	Decreased at 30°C	Decreased at 30°C	(HFD, 60% calories from fat)	(Cui et al., 2016)
Genetic manipulation ,3 strains; (C57BL/6J, 129/Sv , FVB/NJ)	Five-weeks old/ 8 days	Mice-male	Higher in FVB/NJ mice as compared to C57BL/6J.			(Ferrannini et al., 2016)
Housing Temperature; 28°C, 6°C, 22°C)	Ten weeks old/ 10 days	Mice-female	Increased after exposure to 6°C compared with either 28 or 22°C	increased with exposure to 6°C and 22°C compared with 28°C	129Sv mice strain is diabetes and obesity resistant	(Rosell et al., 2014)
Ageing	(6 weeks) (12 months)	Mice-male		276-fold reduction in 12 months compared to 6 weeks old		(Rogers et al., 2012)
1. Exercise (Sedentary, endurance trained. 2. Diet (low fat, high fat)	Eight weeks of interventions (Treadmill, 1h/day, 5	Rats- male		Almost undetectable in Sed HF. Ex LF > Sed LF.	Not detected in the Epid and Retro fat from all groups.	(Wu et al., 2014)

	days/week for 8 weeks)			Increased in Ex HF and Ex LF.		
Diet (high fat, control)	Three-weeks day pupil age /8 weeks interventio n on dams	Rats- male and female		Decreased in males of HFD- fed mothers. Not affected in females of HFD- fed mothers.		(Almeida et al., 2017)
Housing temperature (30°C, 4°C)	Six weeks old/ 3 weeks	Mice- male	Undetectab le at 30°C conditions. Expressed in 4°C mice			(Waldén et al., 2011)
Beta-3 agonist injection. Genetic manipulation(W istar rats, Lou/C.	Twelve weeks old/ 2 weeks	Rats-male	Increased in iWAT of Lou/C rats. Induced in iWAT of Wistar(=un treated Lou/C.	In the iWAT of the Lou/C-treated group only	Overexpression of UCP1 and Adrb3 in iWAT of Lou/C compared to Wistar rats	(Poher et al., 2015)

HFD: high fat diet; UCP1: uncoupling protein 1; iWAT: inguinal adipose tissue; LF: low fat; EX: endurance trained; Sed: sedentary; Adrb3: beta-3 adrenoreceptor; Epid: epididymal; Retro: retroperitoneal.

Inguinal adipose tissue has been shown to exhibit high plasticity that exceeds its capacity to differentiate to beige adipocytes (Giordano et al., 2014, Cinti, 2018). From assessment of the gross anatomy, histological and molecular composition, my study supports this proposal. Upon dissection, in pregnant rats, the subcutaneous inguinal fat depot was more compact and did not appear to be standard adipose tissue compared to the inguinal adipose tissue of virgin rats (Figure 4.12). H & E staining of sections revealed a normal appearance of unilocular adipocytes in the inguinal fat of virgin rats that with pregnancy was replaced by alveolar structure. The development of the mammary gland occurs in two stages. In the first stage of pregnancy, alveoli are composed of epithelial cells without lipid droplets (Figure 4.12 B) that are then filled with

lipids in later pregnancy (Figure 4.12 C) (Giordano et al., 2014). The process of alveologenesis suggested to start in the inguinal adipose tissue of rats during pregnancy has been referred to as "pinking" (Giordano et al., 2014, Cinti, 2017). This differentiation was accompanied with loss of *PPARɣ* that has an important role in white to pink differentiation (Giordano et al., 2014, Apostoli et al., 2014) and its loss was seen in my study. FABP4, is a protein that is highly expressed in adipocytes and macrophages (Furuhashi et al., 2014) and modulates inflammation and facilitates fatty acid transport (Zhang et al., 2014, Furuhashi et al., 2014). FABP4 is controlled at the transcriptional level by PPARɣ (Tan et al., 2002), so downregulation of the FABP4 gene in pregnancy may be linked to *PPARɣ* reduction and to adipocytes phenotype conversion into another cell type. Reduced FABP4 gene expression with gestation could also be due to its participation in the inflammation process in adipose tissue (referred to as meta inflammation (Hotamisligil, 2006)) that is partly suppressed with gestation to ensure the maintenance of pregnancy (Mor and Cardenas, 2010, Somerset et al., 2004).

At the gene expression level, the hypothesis of pinking of inguinal adipocytes is further supported by examining mammary cells biomarkers. Expression of *STAT5A* which is a principal mediator of mammary gland development (Liu et al., 1997) and regulates transcription of milk proteins (Suárez-Trujillo and Casey, 2016), increased through pregnancy. This was accompanied with a reduction in *β3AR* which was absent by 19 d/g. Previous studies demonstrated that the β3AR subtype is expressed only in adipose tissue (Muzzin et al., 1991) and its activity is reduced in subcutaneous compared to visceral fat (Van Harmelen et al., 1997). So, as the adipocytes exhibited alveoli formation at the histological and genetic profile level, this would explain the loss of adrenoreceptors in late gestation. In addition, ELF5 gene expression increases in the mammary glands during pregnancy and remains high during lactation (Lee and Ormandy, 2012). In my study, ELF5 mRNA level increased in the inguinal adipose tissue with gestation, which participates in alveoli formation of mammary cells (Zhou et al., 2005, Metzger et al., 2008).

The concept that inguinal adipocytes differentiation into another cell type with pregnancy is further supported by increased WAP mRNA expression (Burdon et al., 1991) through gestation with minimal expression in virgin rats. This could be due to the presence of inguinal adipose tissue adjacent to the mammary cells. It also suggests possible contamination during the excision of the inguinal fat as the mammary glands are enlarged during pregnancy and no distinct border is observed between them and the surrounding fat. The other reason is that white adipocytes can be a kind of "sleeping" mammary cells that are activated to differentiate and start milk production during late pregnancy. This was supported further by the presence of *ELF5* in the virgin inguinal fat and its absence in their omental and interscapular fat. Actually, an earlier study suggested a role of ELF5 in the WAP gene expression induction by binding directly to its promoter in mammary cells (Lee and Ormandy, 2012). Although leptin is considered as a white fat biomarker, earlier studies showed that mammary cells can express leptin (Smith-Kirwin et al., 1998). This would explain its continuous presence later in pregnancy when adipocytes are replaced with alveoli but with low expression compared to virgin rat inguinal fat. In a previous study, serum and tissue content of leptin were upregulated after mid-pregnancy compared to virgin rats which was attributed to the need for building up of nutrient stores for fetal development and lactation (Mounzih et al., 1998, Tomimatsu et al., 1997). A role of leptin in UCP1 thermogenesis and glucose homeostasis has been suggested in many studies (Campfield et al., 1995, Halaas et al., 1995, Pelleymounter et al., 1995, Velickovic et al., 2018, Covey et al., 2006).

OXTR is also present in both adipose tissue and mammary cells and plays a role in milk ejection in mammary cells (Zingg and Laporte, 2003) and in regulating energy balance. OXTR gene deficient male mice show impaired thermogenesis in BAT and late-onset obesity (Takayanagi et al., 2008). However, OXTR mRNA was affected by diet at late pregnancy but I think this was due to its role in energy homeostasis regulation which is not well-established yet (Takayanagi et al., 2008) rather than to its role in mammary cells development. Overall, my observations support the hypothesis that inguinal adipose

tissue differentiates into alveolar structure representing a type of mammary gland cellular composition with pregnancy.

4.8 Conclusion

Beiging was not found in inguinal adipocytes that in females appear to exhibit a pronounced ability to form alveoli which is a part of the mammary cells structure with gestation. These mammary biomarkers were not affected by diet or temperature intervention (Figure 4.13). Additional details including gene expression and p values can be found in Appendix 4.

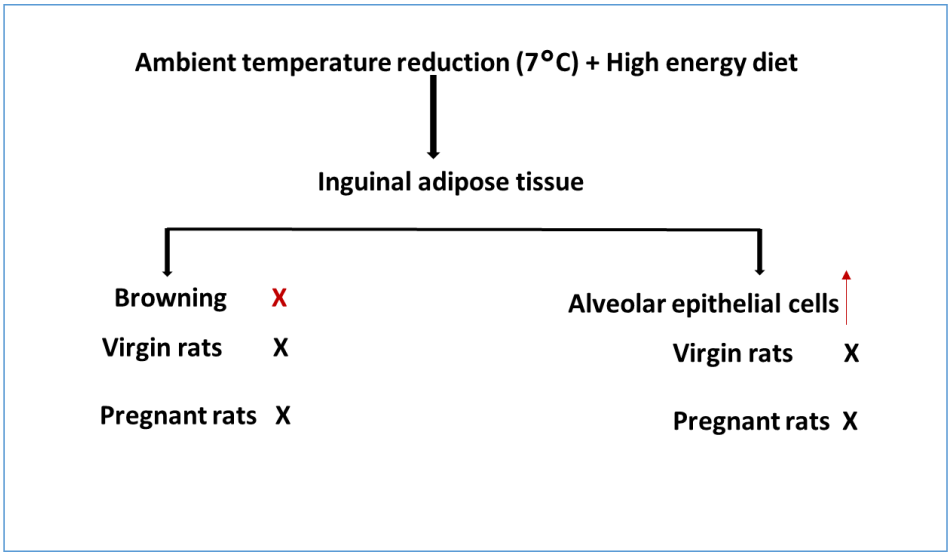


Figure 4.13 Summary diagram of inguinal adipose tissue analysis findings.

Black X: no effect of diet or temperature; red X: no effect of pregnancy; upward arrow: stimulatory effect of pregnancy.

Chapter 5. The response of omental adipose tissue to diet, housing temperature and pregnancy

5.1 Introduction

Visceral fat represents a major depot of white adipose tissue, whose main role is energy storage (Giralt and Villarroya, 2013). It also participates in immunity (Fantuzzi, 2005) and acts as an endocrine organ (Avram et al., 2005, Wozniak et al., 2009). Unlike the subcutaneous fat depot, excess visceral fat accumulation is usually linked with impaired glucose and lipid metabolism and cardiovascular disorders (Matsuzawa et al., 1995); this can be attributed to differences in metabolic properties and differentiation potentials between the two depots (Prunet-Marcassus et al., 2006, Hellmer et al., 1992). Visceral fat which includes mesenteric and omental fat is more metabolically active than subcutaneous i.e. it is more sensitive to lipolysis and more insulin resistant, and has greater infiltration by immune cells (Ibrahim, 2010).

In this chapter, I will explore the effect of exposure to mild cold and a high energy diet on omental adipose tissue mass, histological and molecular characteristics. I will examine the effects on expression of genes involved in thermogenesis (UCP1, β3AR, SERCA2B, RYR2), glucose mobilisation and insulin release (IRS1, IRS2), lipid transport and fatty acid uptake from the circulation (FATP4, FABP4), plus appetite regulation (LEPTIN) of virgin and pregnant rats at 50% and 90% of pregnancy (10 and 19 days of gestation; 10 d/g and 19 d/g) and if there is any interaction between the interventions. I will also measure the expression of genes that are involved in the immune response (NFKB, TNFα, MCP1, IL6, IL10) and whether they are regulated through gestation.

5.2 Hypothesis

The hypotheses were:

- Housing of rats at a thermoneutral temperature will increase the susceptibility to excess energy storage as fat and consequently initiates an inflammation process in omental adipose tissue due to the absence of a thermogenic stimulus to promote browning.
- Omental white fat of animals housed at a standard husbandry temperature (20°C) will be influenced by a mild cold, which acts as a stimulus for browning process and consequently limits the adverse effect of dietary induced obesity.
- Pre-conceptional induction of obesity by feeding a high energy diet in combination with living at thermoneutrality will amplify the negative impact of increased omental fat accumulation, impairment in lipid and glucose metabolism and reduced insulin sensitivity.
- Browning of the omental fat triggered by mild cold will be reduced with pregnancy to reduce energy expenditure that could act to avoid exposing mothers and foetuses to a shortage of nutrients (McIlvride et al., 2017).

5.3 Aims

The main aim of this chapter is to explore whether a reduction in the ambient temperature (housing at standard husbandry temperature) will enhance browning that will be indicated by upregulation of UCP1 gene expression in the omental adipose tissue. This chapter will also test if such browning will reduce the inflammatory biomarkers in the adipose tissue and how both (browning and inflammatory) biomarkers are modulated with pregnancy.

5.4 Methods

Methods, laboratory protocols, and statistical analysis used to produce the results of this chapter were detailed in Chapter 2. I extracted mRNA using TRIZOl, transcribed it to cDNA and diluted it with nuclease-free water 1:10 then I ran in a qPCR 96-well plate using primers for gene expression quantification.

Representative samples from the four intervention groups at each of the three time points were processed, sectioned, stained and imaged as discussed in chapter 2 (sections 2.3.3). All statistical analysis was performed as described in Section 2.5. All animal experimentations, i.e. dissection, tissue weighing, plasma analysis, histological and molecular analysis were supervised by Professor Michael Symonds, Professor Helen Budge and Dr Neele Dellschaft.

5.5 Results

5.5.1 Histology of the omental adipose tissue

Sections from the omental fat of the four interventions groups at each time point were stained with H & E as shown in Figure 5.1.

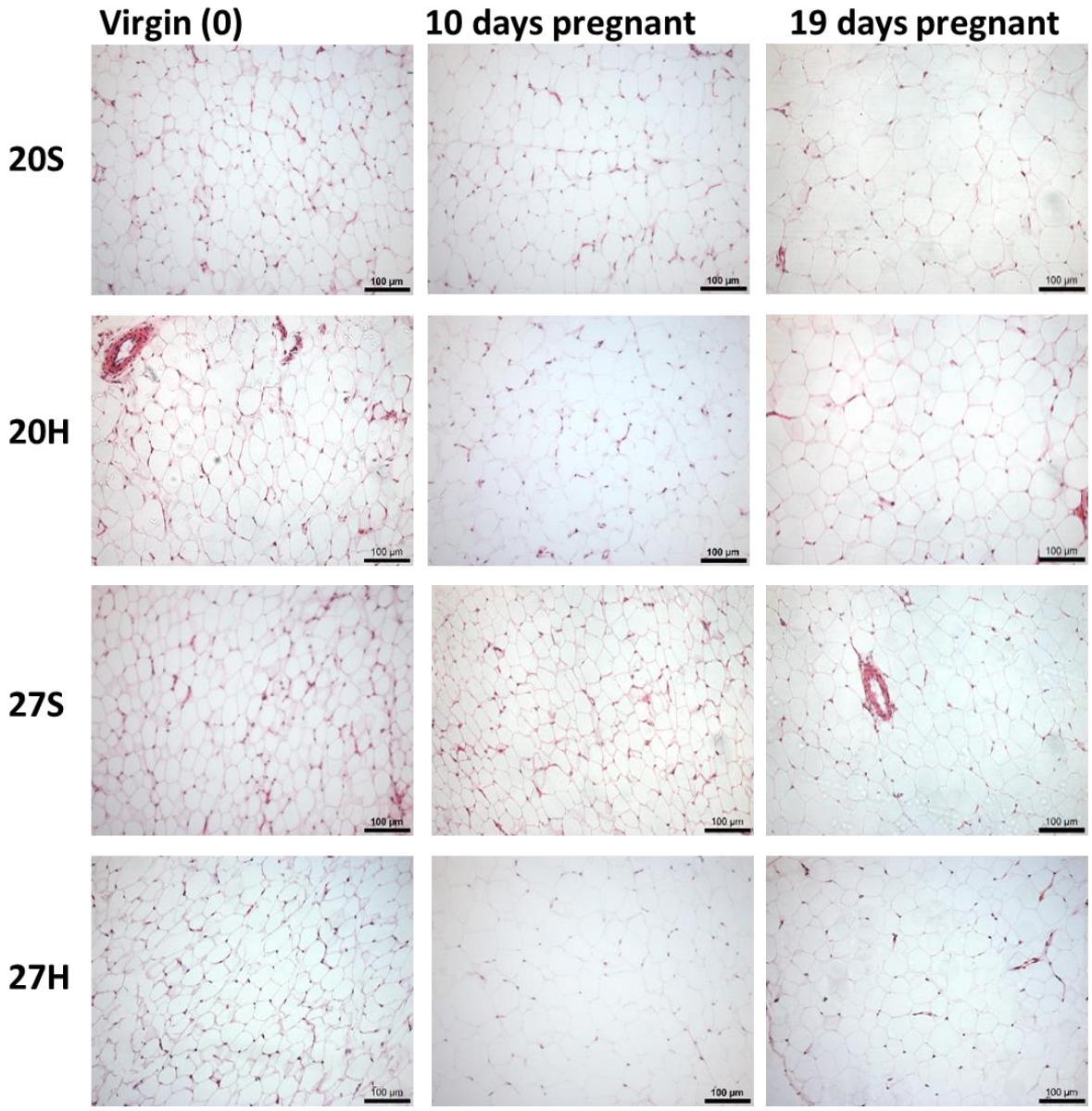


Figure 5.1 Representative Haematoxylin and Eosin stained-microscopic slides of the omental adipose tissue

H & E stained microscopic sections of the omental fat of virgin (0), 10 and 19 days pregnant rats housed at 20°C or 27°C and fed a standard (S), or high fat and sucrose diet (H).

5.5.2 Omental fat mass

Prior to conception, the high energy diet increased omental fat mass at thermoneutrality. At 10 days of gestation (10 d/g), this effect continued in addition to the temperature effect which appeared in high energy diet fed rats where more fat accumulated at thermoneutrality compared to 20°C housed animals. Both the effects of temperature and diet diminished at late pregnancy, which further promoted the accumulation of omental fat in all groups (Figure 5.2).

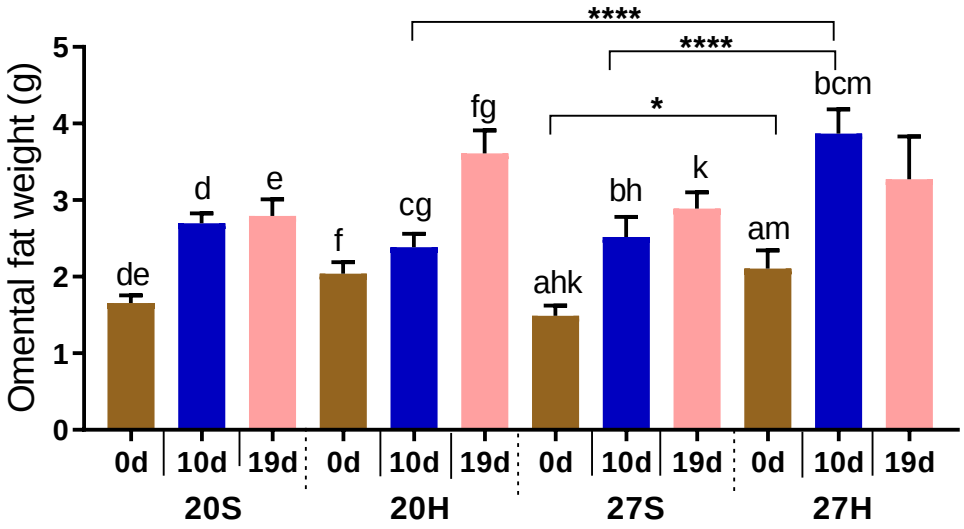


Figure 5.2 Effect of housing temperature, diet and pregnancy on omental adipose tissue mass

Omental fat mass of unmated (0), 10 and 19 days (d) pregnant rats housed at 20°C or 27°C and fed a standard (S) diet or high fat and sucrose (H) diet. Values are represented as mean ± SEM. Columns with the same superscripts are significantly different (P<.0.05); a: p <.05, g, h, m k: p<.01, d, e, f, k: p<.001, b, c: p<.0001.

5.5.3 Expression of genes in the omental adipose tissue

5.5.3.1 Thermogenic genes

Gene expression of UCP1 was not found at any time point. There was no significant change in β3AR gene expression with diet or temperature before or with gestation. In the 27S group, gene expression was higher in 10 d/g compared to 19 days of gestation (19 d/g) (Figure 5.3).

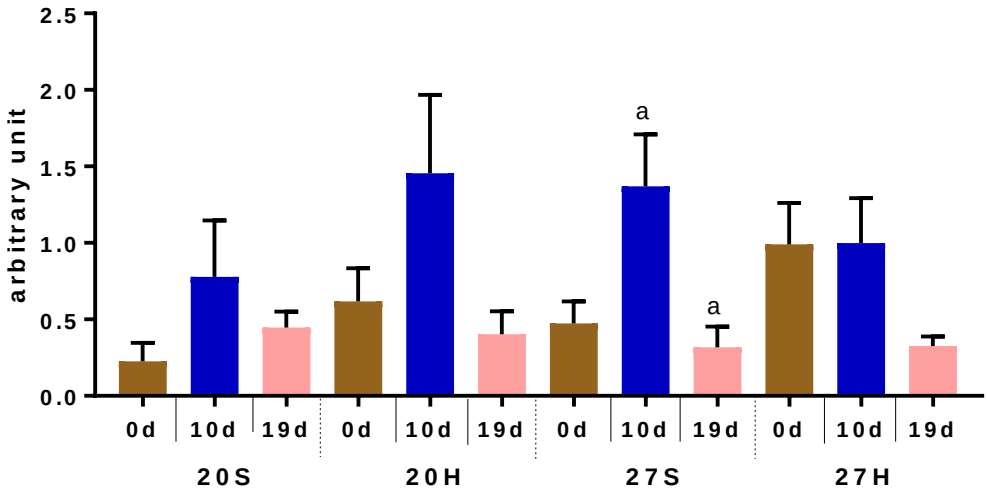


Figure 5.3 Beta-3 adrenergic receptor (β3AR) gene expression in the omental adipose tissue

β3AR gene expression in the omental fat of unmated (0), 10 and 19 days (d) pregnant rats housed at 20°C or 27°C and fed a standard (S) diet or high fat and sucrose (H) diet. Values are represented as mean ± SEM. Columns with the same superscripts are significantly different (P<.0.05); a: p<.05.

No significant effect of diet or temperature was found for leptin gene expression in the omental fat of virgin or pregnant rats, and its expression was unaffected by pregnancy in any group (Figure 5.4).

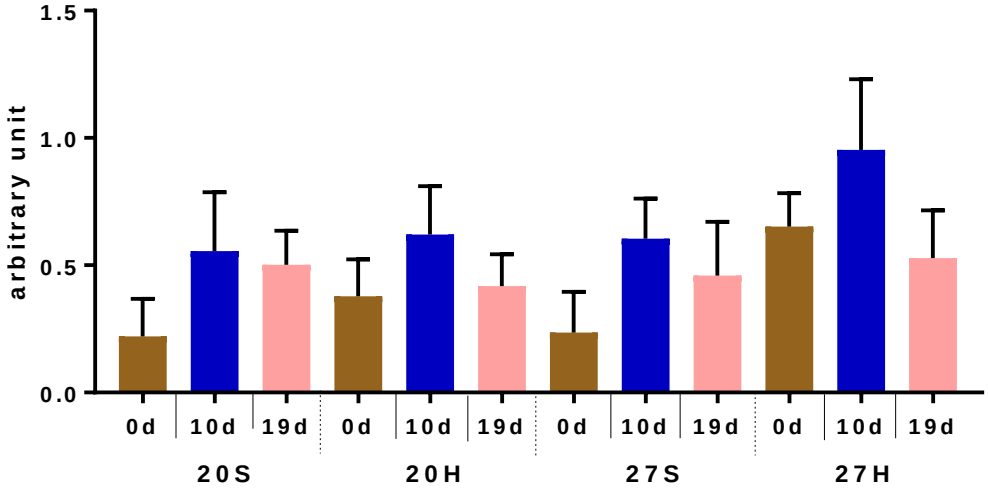


Figure 5.4 Leptin gene expression in the omental fat

Leptin gene expression in the omental fat of unmated (0), 10 and 19 days (d) pregnant rats housed at 20°C or 27°C and fed a standard (S) diet or high fat and sucrose (H) diet. Values are represented as mean ± SEM. There were no significant differences (P≥.0.05).

SERCA2B and RYR2 gene expression were not affected by diet or temperature at any time point. Pregnancy did not affect the SERCA2B gene expression (Figure 5.5) but caused a reduction in RYR2 expression (Figure 5.6).

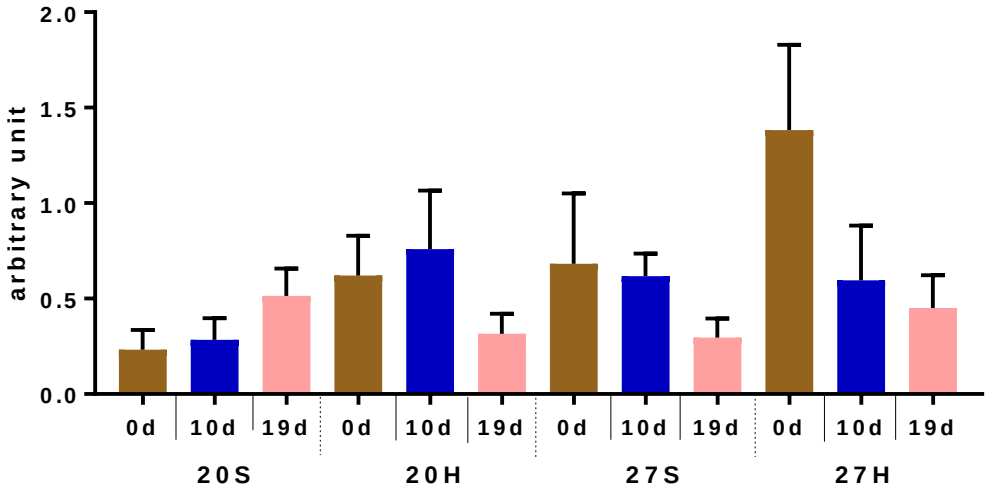


Figure 5.5 Sarcoplasmic/endoplasmic reticulum Ca2+ transporting 2 B (SERCA2B) gene expression in the omental adipose tissue

SERCA2B gene expression in the omental fat of unmated (0), 10 and 19 days (d) pregnant rats housed at 20°C or 27°C and fed a standard (S) diet or high fat and sucrose (H) diet. Values are represented as mean ± SEM. There were no significant differences (P≥.0.05).

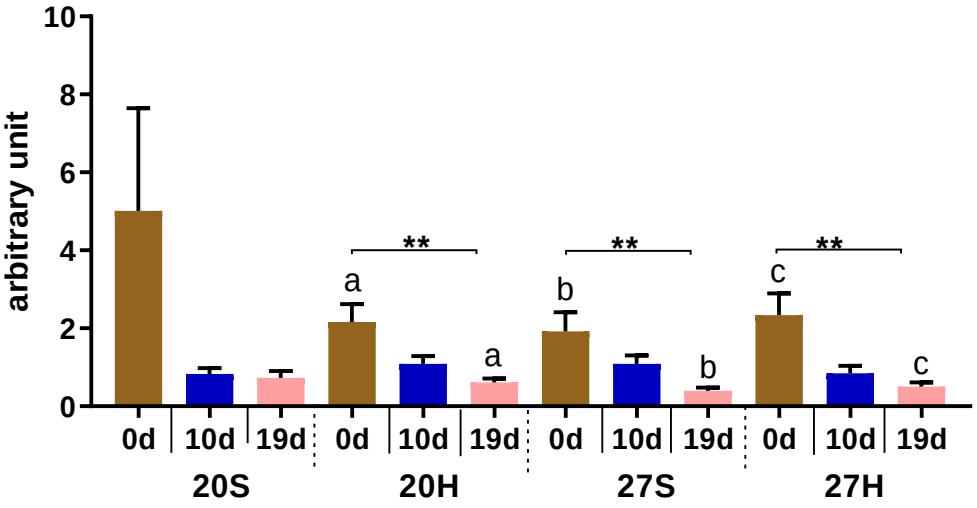


Figure 5.6 Ryanodine receptor 2 (RYR2) gene expression in the omental adipose tissue

RYR2 gene expression in the omental fat of unmated (0), 10 and 19 days (d) pregnant rats housed at 20°C or 27°C and fed a standard (S) diet or high fat and sucrose (H) diet. Values are represented as mean ± SEM. Columns with the same superscripts are significantly different (P<.0.05); a, b, c: p<.01.

Temperature and diet had no significant effect on VEGFA gene expression in virgin or pregnant rats, and its expression with pregnancy was affected only in the 27H group where it was lower in late gestation compared to virgin rats (Figure 5.7).

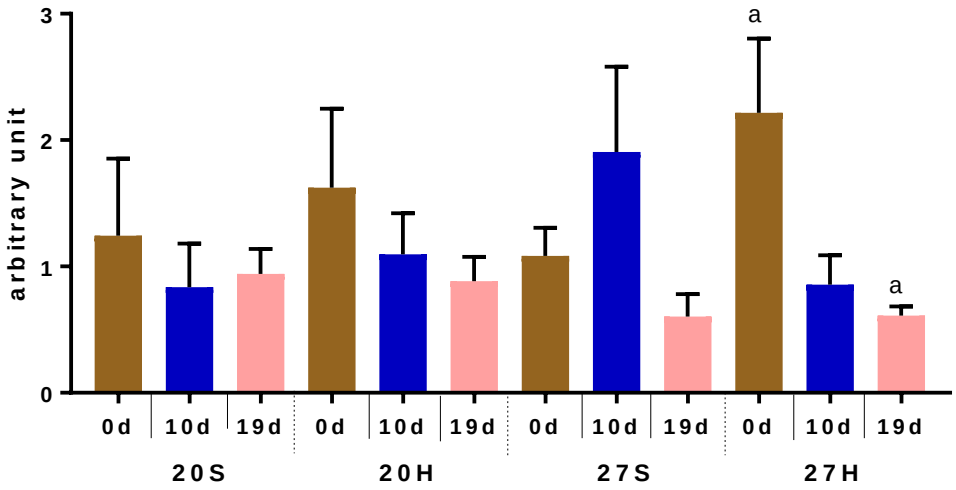


Figure 5.7 Vascular endothelium growth factor A (VEGFA) gene expression in the omental adipose tissue

VEGFA gene expression in the omental fat of unmated (0), 10 and 19 days (d) pregnant rats housed at 20°C or 27°C and fed a standard (S) diet or high fat and sucrose (H) diet. Values are represented as mean ± SEM. Columns with the same superscripts are significantly different (P<.0.05); a: p<.05.

5.5.3.2 Insulin sensitivity genes.

No significant changes in the IRS1 gene expression in response to temperature or diet interventions were detected. Also, pregnancy did not affect this gene expression at any of the four groups (Figure 5.8).

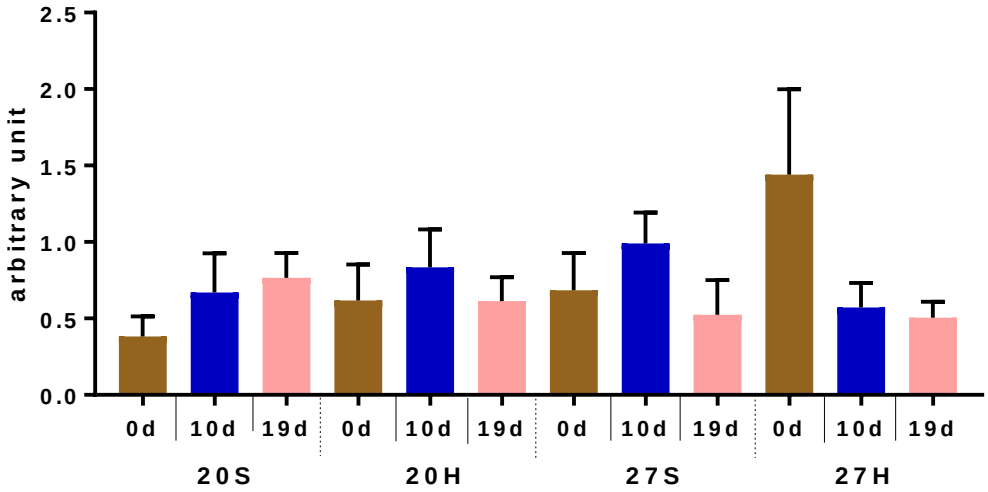


Figure 5.8 Insulin receptor substrate 1 (IRS1) gene expression in the omental adipose tissue

IRS1 gene expression in the omental fat of unmated (0), 10 and 19 days (d) pregnant rats housed at 20°C or 27°C and fed a standard (S) diet or high fat and sucrose (H) diet. Values are represented as mean ± SEM. There were no significant differences (P≥.0.05).

IRS2 gene expression was unaffected by any intervention, the only change was with the pregnancy and was confined to the 20°C animals where it was higher in virgin than in pregnant rats (Figure 5.9).

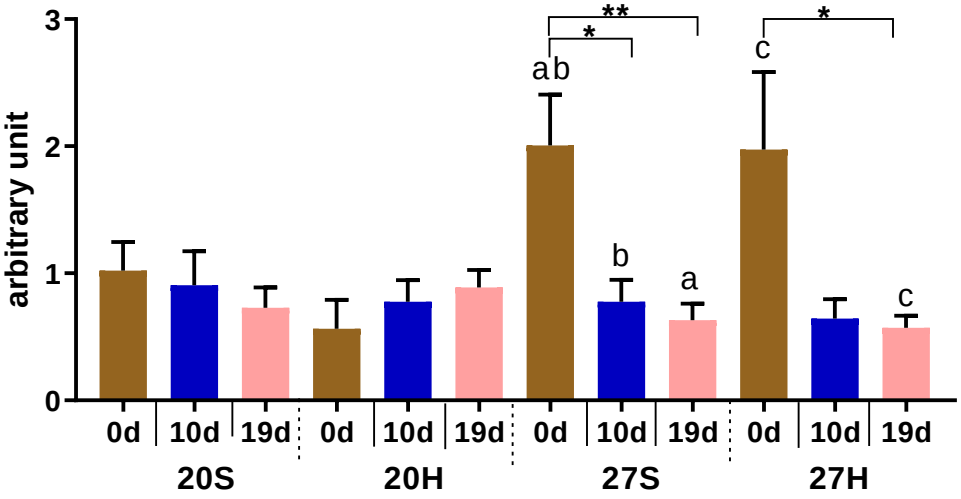


Figure 5.9 Insulin receptor substrate (IRS2) gene expression in the omental adipose tissue

IRS2 gene expression in the omental fat of unmated (0), 10 and 19 days (d) pregnant rats housed at 20°C or 27°C and fed a standard (S) diet or high fat and sucrose (H) diet. Values are represented as mean ± SEM. Columns with the same superscripts are significantly different (P<.0.05); a: p<.01, b, c: p<.05.

5.5.3.3 Fat transport genes

FABP4 gene expression in virgin and pregnant rat's omental fat was not affected by the temperature or diet. The pregnancy resulted in a significant change in gene expression in the 27S group where it was higher at 10 d/g compared to virgin and 19 d/g rats (Figure 5.10).

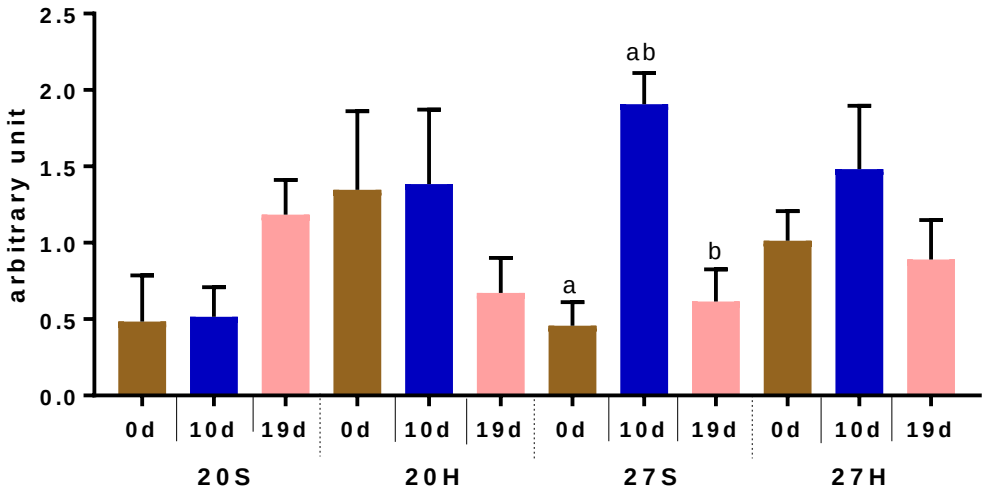


Figure 5.10 Fatty acid binding protein 4 (FABP4) gene expression in the omental adipose tissue

FABP4 gene expression in the omental fat of unmated (0), 10 and 19 days (d) pregnant rats housed at 20°C or 27°C and fed a standard (S) diet or high fat and sucrose (H) diet. Values are represented as mean ± SEM. Columns with the same superscripts are significantly different (P<.0.05); b: p<.001**,** a: p<.0001

FATP4 gene expression was unaffected by temperature or diet at any time point, but pregnancy caused a significant rise in its expression at mid-gestation compared to late gestation in standard diet-fed animals only (Figure 5.11).

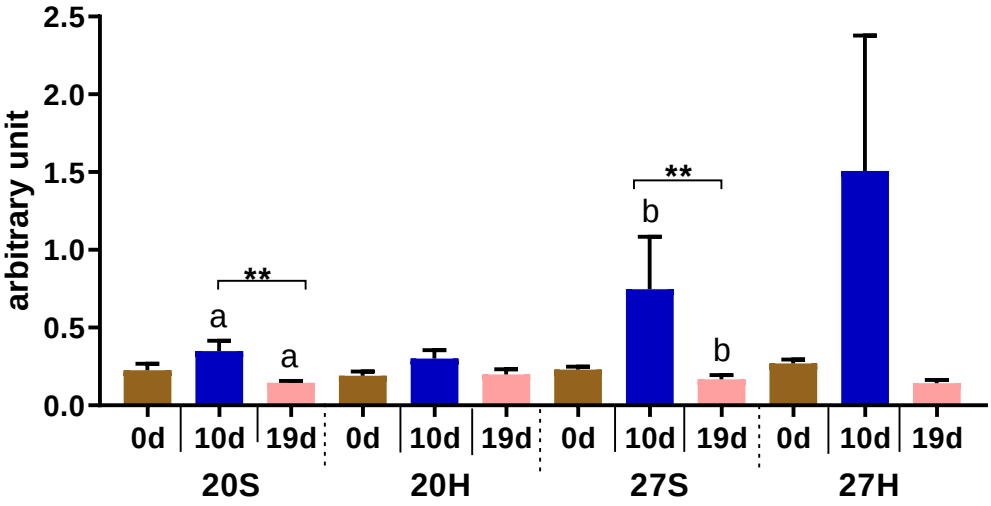


Figure 5.11 Fatty acid transport protein 4 (FATP4) gene expression in the omental adipose tissue

FATP4 gene expression in the omental fat of unmated (0), 10 and 19 days (d) pregnant rats housed at 20°C or 27°C and fed a standard (S) diet or high fat and sucrose (H) diet. Values are represented as mean ± SEM. Columns with the same superscripts are significantly different (P<.0.05); a, b: p<.01.

5.5.3.4 Immune cells biomarker genes.

Interleukin 10 (IL10) gene expression was detected only in 19 days omental fat and was not affected by any intervention (Figure 5.12).

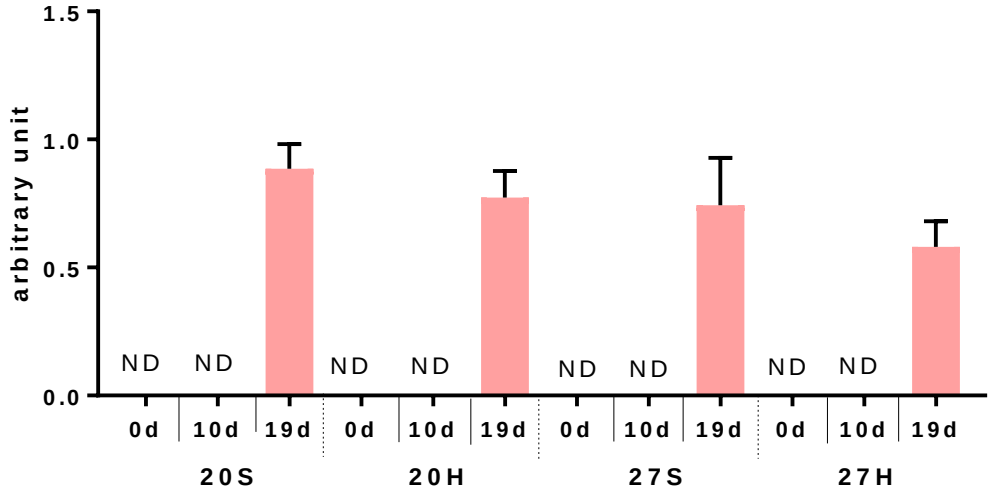


Figure 5.12 Interleukin 10 (IL10) gene expression in the omental adipose tissue

IL10 gene expression in the omental fat of unmated (0), 10 and 19 days (d) pregnant rats housed at 20°C or 27°C and fed a standard (S) diet or high fat and sucrose (H) diet. Values are represented as mean ± SEM. ND denotes for Not Detected. There were no significant differences (P≥.0.05).

Temperature and diet interventions had no effect on Interleukin 6 (IL6) expression at any time point. Only in the 20S group, pregnancy caused a reduction in IL6 gene expression in pregnant rats (Figure 5.13).

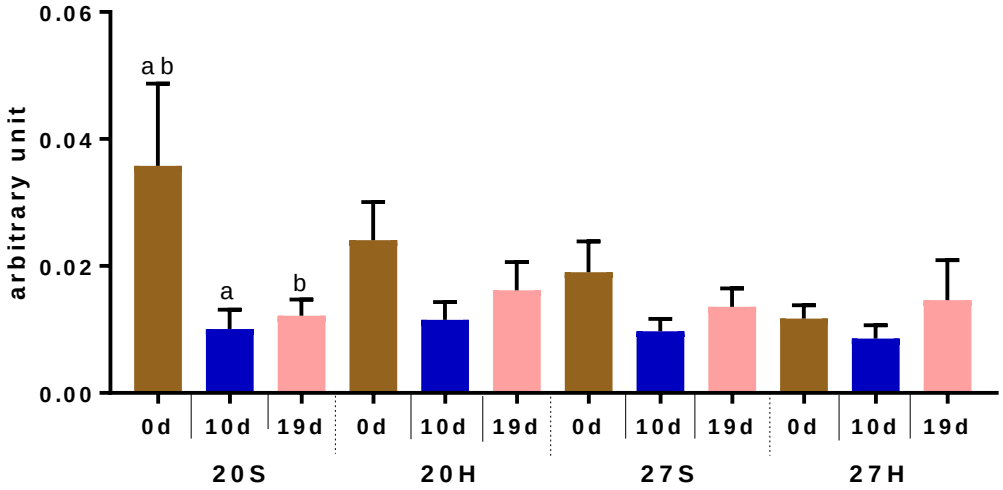


Figure 5.13 Interleukin 6 (IL6) gene expression in the omental adipose tissue

IL6 gene expression in the omental fat of unmated (0), 10 and 19 days (d) pregnant rats housed at 20°C or 27°C and fed a standard (S) diet or high fat and sucrose (H) diet. Values are represented as mean ± SEM. Columns with the same superscripts are significantly different (P<.0.05); *b: p<.05, a: p<.01.*

Nuclear factor kappa-light-chain-enhancer of activated B cells (NF-kB) gene expression was unaffected by the interventions at any time point but was downregulated with pregnancy in all groups (Figure 5.14).

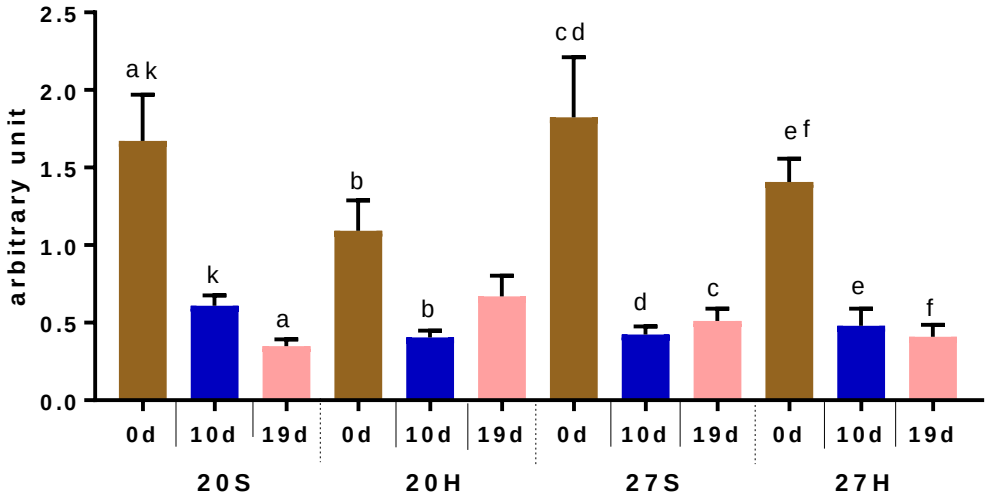


Figure 5.14 Nuclear factor kappa B subunit (NF-kB) gene expression in the omental adipose tissue

NF-kB gene expression in the omental fat of unmated (0), 10 and 19 days (d) pregnant rats housed at 20°C or 27°C and fed a standard (S) diet or high fat and sucrose (H) diet. Values are represented as mean ± SEM. Columns with the same superscripts are significantly different (P<.0.05); k: p<.05; b, c, e, f: p<.01; a, d: p<.001.

MCP1 gene expression was affected only at late gestation where it was significantly higher in the 20S group compared to both 20H and 27S groups. MCP1 gene was downregulated with pregnancy in all groups (Figure 5.15)

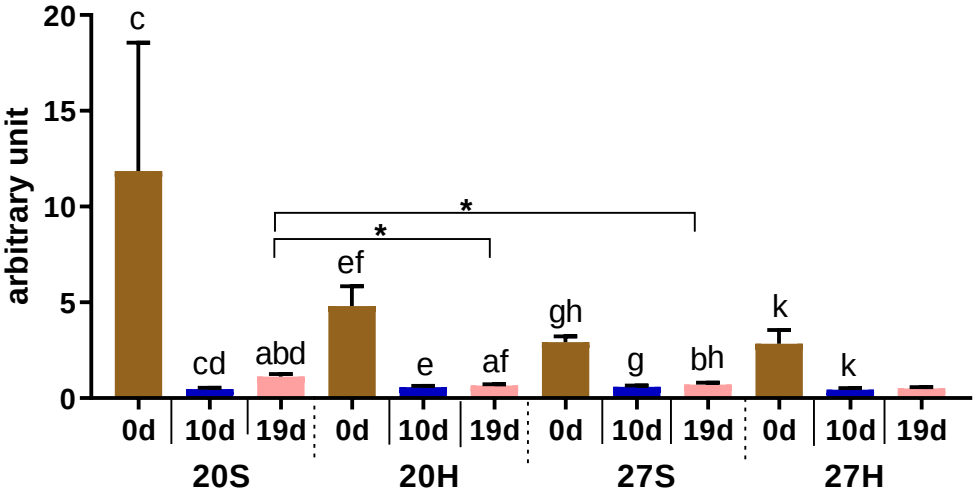


Figure 5.15 Monocyte chemoattractant protein1 (MCP1) gene expression in the omental adipose tissue

MCP1 gene expression in the omental fat of unmated (0), 10 and 19 days (d) pregnant rats housed at 20°C or 27°C and fed a standard (S) diet or high fat and sucrose (H) diet. Values are represented as mean ± SEM. Columns with the same superscripts are significantly different (P<.0.05); a, b, d, f, h: p<.05; a, c, e, g, k: p<.01.

TNFα gene expression was unaffected by the diet or temperature interventions and the only significant change in its expression with gestation was confined to the 20S group animals where it was downregulated at late pregnancy compared to before conception (Figure 5.16).

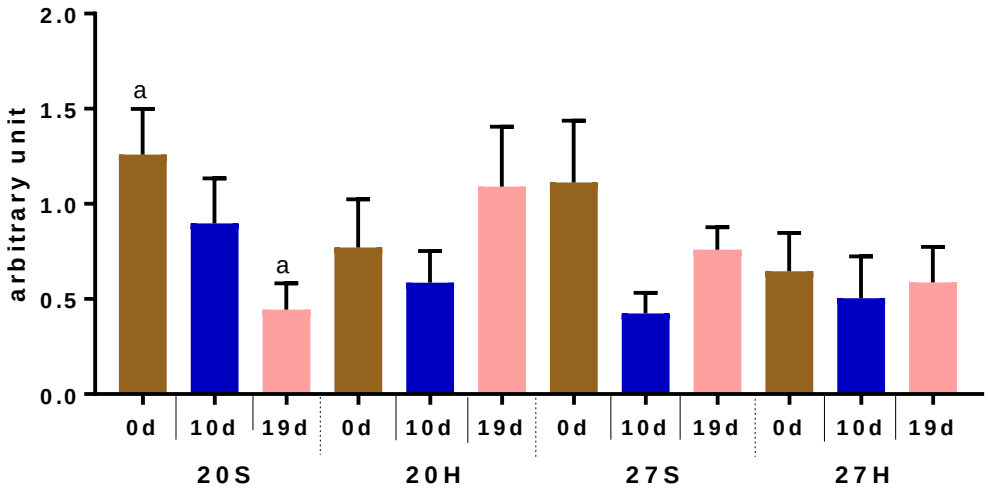


Figure 5.16 Tumour necrosis factor alpha (TNFα) gene expression in the omental adipose tissue

MCP1 gene expression in the omental fat of unmated (0), 10 and 19 days (d) pregnant rats housed at 20°C or 27°C and fed a standard (S) diet or high fat and sucrose (H) diet. Values are represented as mean ± SEM. Columns with the same superscripts are significantly different (P<.0.05); a: p<.05.

5.6 Summary of main findings

No UCP1 gene expression was found in any interventional group at any time point. Leptin and b3-ar genes were not affected by the diet or temperature. Pregnancy downregulated RYR2, MCP1, and NFkB gene expression in all interventional groups while it downregulated IRS2 but only in animals housed at thermoneutrality. FATP4 gene expression was higher in mid-gestation for standard diet fed animals.

Discussion

UCP1 was not detected within the omental adipose tissue in this study, which may have several explanations. Firstly, many studies suggest less susceptibility of visceral adipose tissue to browning compared to subcutaneous fat in rodents (Kim and Plutzky, 2016, Bargut et al., 2017, Cohen et al., 2014); this was attributed at least partly to the differential expression of the Prdm16 between fat depots, which is a factor considered to be a key determinant for adipose tissues browning capacity (Zuriaga et al., 2017). Prdm16 gene expression was higher in subcutaneous than in visceral fat of rodents (Seale et al., 2011). Secondly, in the few studies where browning was triggered in the visceral fat depot, only males were studied (de Jong et al., 2015, Ferrannini et al., 2016, Rosell et al., 2014, Yang et al., 2017, Cui et al., 2016). Thirdly, it can be the genetic background that determines WAT susceptibility to browning. In a study where three mice strains (C57BL/6J, 129/Sv and FVB/NJ) were exposed to cold, FVB/NJ showed more browning in the inguinal compared to more browning in the visceral exhibited by 129/Sv mice, whereas C57BL/6J did not exhibit any UCP1 expression in their visceral fat in response to cold (Ferrannini et al., 2016). Finally, it is also possible that more reduction in temperature is needed to induce browning in the omental adipose tissue, a proposal supported by a mice study where browning phenotype was not enhanced unless exposed to a very low temperature of between -10°C to -20°C (Yang et al., 2017) (Table 5.1).

Table 5.1 List of published studies where UCP1 was detected or induced in the omental adipose tissue

Intervention	Old/ Duration	Model/ Sex	Change in UCP1		Comment	Reference
			gene	protein		
Housing temperature, thermoneutrality (30°C) or cold (4°C)	Six weeks /3 weeks	Mice-male	Increased with 4°C			(de Jong et al., 2015)
Intermittent cold exposure	Different ages as captured/ 4 hours a day for 15 days	Pika		Expressed but not changed	Air-conditioned (5–6 °C)	(Bai et al., 2015)
Housing temperature, 4°C, –10°C, and –10°C/–20°C	Seven-eight weeks /different durations	Mice-male	Increased in all groups relative to control	Increased At –10°C and –10°C/–20°C. Not changed at 4°C.	30°C used as a control	(Yang et al., 2017)
1. Housing temperature; thermoneutrality (30°C) or mild cold (22°C). 2. Diet (chow or HFD).	Not mentioned/ 20 weeks	Mice-male	Decreased at 30°C	Decreased at 30°C		(Cui et al., 2016)
Genetic manipulation ;3 strains (C57BL/6J, 129/Sv,FVB/NJ)	Five weeks old/ 8 days duration	Mice-male	400-fold higher in 129/Sv than in C57BL/6J mice			(Ferrannini et al., 2016)
Housing Temperature; 28°C, 6°C,22°C)	Ten weeks old/ 10 days	Mice-female	Increased after exposure to 6°C compared with either 28 or22°C	increased with exposure to 6°C and 22°C compared with 28 °C	129Sv mice strain is diabetes and obesity resistant	(Rosell et al., 2014)

UCP1: uncoupling protein 1; HFD: high fat diet

In the absence of UCP1, a pathway that is UCP1-independent which functions through ATP-dependent calcium cycling has been suggested (Ikeda et al., 2017). In this mechanism, the calcium released by the serca2b pump is taken back by the ryanodine receptor (RYR)2 (Ikeda et al., 2017, Mottillo et al., 2018). As the action of RYR2 is ATP-

dependent, its reduction with pregnancy represents an adaptation in the mother that could ensure the increased nutrient demands by the foetus through gestation are met (McIlvride et al., 2017). According to a recent study, central obesity would result in poor pregnancy outcomes because of the altered and unhealthy concentrations of adipokines produced by omental fat (Hayward et al., 2018). So, the presence of this alternative pathway especially in the omental fat depot in the absence of UCP1 may enable adaptations in whole body metabolism to protect the foetus from being exposed to harmful concentrations of adipokines.

Due to the widely known inflammatory properties of omental fat (Chatterjee et al., 2009), i.e. infiltration of macrophages is doubled in omental compared to subcutaneous fat (Cancello et al., 2006, Palou et al., 2009), I examined some biomarkers of pro- and anti-inflammatory cells. The absence of any temperature or diet effect on those examined could be due to the difference in the sex of animals used. For mice studies in which inflammatory biomarkers in the omental fat were reduced with temperature reduction from 29°C to 22°C (van der Stelt et al., 2017) or when a chow diet was compared to high fat feeding (Kim et al., 2012), males were used. Furthermore, in previous studies where the inflammation process was triggered in a female's omental fat, human's tissues were used (Poulain-Godefroy et al., 2008, Cancello et al., 2006, Terra et al., 2010). Genetic manipulation intervention of the model used can also be a factor as the susceptibility to express inflammatory genes in adipose tissue differs between strains (Kim et al., 2012, Xu et al., 2003) (Table 5.2).

Table 5.2 List of studies about meta-inflammation in omental adipose tissue

Intervention	Old/Duration	Model/ sex	Change in inflammation		Reference
			gene	protein	
1. Diet (Standard, high fat). 2.Genetic manipulation (*ob/ob*, controls) mice	Five weeks old/12 weeks	Mice - male	TNFα and IL-6 were higher in HFD than chow. TNFα and IL-6 were higher in ob/ob mice than controls.		(Kim et al., 2012)
1.Genetic manipulation (*ob/ob, db/db*, agouti , tubby), DIO, controls)	4–5 weeks of age, wildtype/16 weeks. (ob/ob,db/db), sacrificed at 15 weeks of age, agouti, tubby, sacrificed at 25 weeks of age.	Mice- male	MCP1, EMR1 upregulated in ob /ob,db/db and DIO. MCP-1, EMR1 downregulated in controls than in DIO.		(Xu et al., 2003)
1. Housing temperature, thermoneutrality (30°C) or mild cold (22°C).	Nine weeks age/3 weeks of low-fat diet followed by 12 weeks of HDF/5 days of intervention.	Mice- male	Pro-inflammatory markers were downregulated or showed a trend toward in the 22◦C mice		(van der Stelt et al., 2017)

HFD: high fat diet; DIO: diet induced obesity; TNFα: tumour necrosis factor; *EMR1:* Mucin-Like Hormone Receptor-Like 1; MCP1: monocyte attractant protein 1; IL6: interleukin 6.

The reduction of pro-inflammatory biomarkers (e.g. NFKB, MCP1, IL6) and the upregulation of the anti-inflammatory biomarkers (IL10) in the omental fat with pregnancy are likely to be driven by changes in oestrogen and progesterone secretion (Zen et al., 2010), thereby modulating the immune system in order to sustain pregnancy (Somerset et al., 2004, Mor and Cardenas, 2010). Both hormones affect the maturation of immune cells and can alter some cytokines production, e.g. oestrogen stimulates IL10 production and decreases TNFα secretion (Straub, 2007). Progesterone increases IL10 production and inhibits IL6 secretion (Straub, 2007). The different patterns of expression

through pregnancy exhibited by the FABP4 in omental fat may be due to its role in the inflammation process and its presence in macrophages as well as in adipocytes especially that the inflammation process is modulated with pregnancy (Furuhashi et al., 2014, Zhang et al., 2014, Mor and Cardenas, 2010). The absence of diet and temperature effects on fat transport and binding proteins genes expression (FABP4, FATP4) can be due to the absence of UCP1 that drives the thermogenesis where the fatty acids represent the activators of it.

5.7 Conclusion

Browning was not detected in the omental fat in the current study which can be due to the use of females rather than males as in other studies where browning was induced. No effect of the interventions on the inflammation process was found while this process biomarkers were changing according to different phases of pregnancy (Figure 5.17). Additional details including gene expression and p values can be found in Appendix 5.

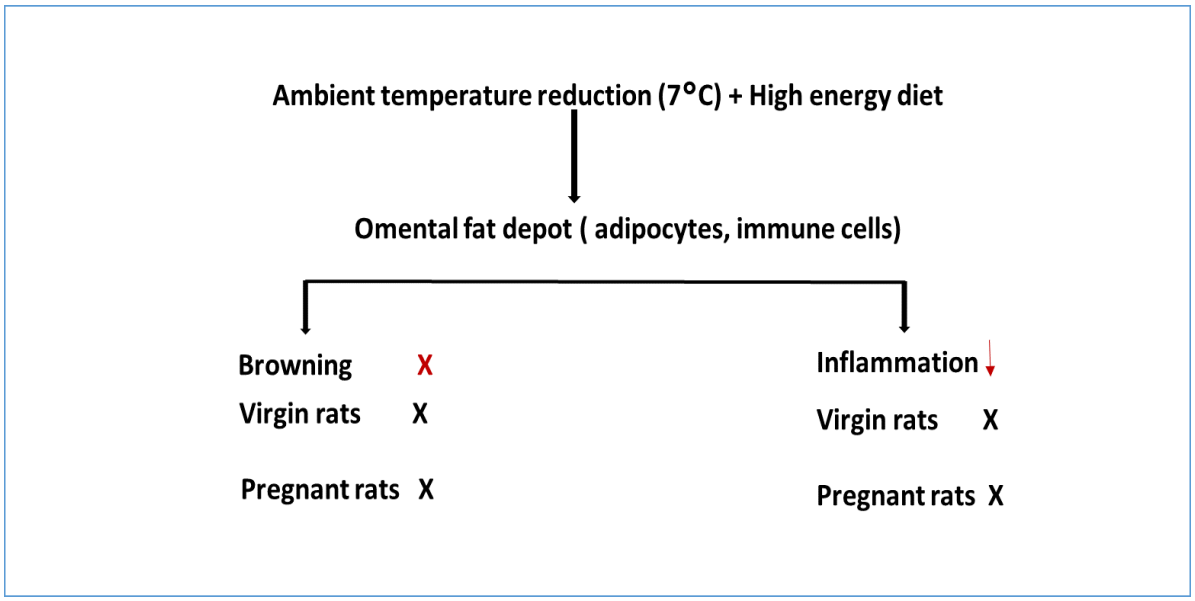


Figure 5.17 Summary diagram of omental adipose tissue analysis findings.
Black X: no effect of diet or temperature; red X: no effect of pregnancy; downward arrow: inhibitory effect of pregnancy.

Chapter 6. Conclusion

6.1 Hypothesis

In my thesis, I hypothesised that housing rats at 20°C compared with 27°C will act as a cold stimulus that induces browning in WAT and causes induction of classical BAT activity which then masks the effect of the obesogenic dietary intervention. Furthermore, animals housed at 20°C will exhibit less inflammatory biomarker infiltration in their omental fat depot. This depot as part of the visceral fat has a unique inflammatory profile compared to subcutaneous adipose tissue (Alvehus et al., 2010) and visceral fat accumulation is known as a risk factor for obesity-related adverse inflammatory and metabolic outcomes (Magnuson et al., 2015).

In addition, pregnancy will modulate adipose tissue activity and metabolism. WAT browning and classical BAT activity will be reduced with gestation. I also hypothesised that Inguinal fat would differentiate to mammary cells during gestation to support milk production and lactation because of their presence as adjacent to mammary glands, suggesting the plasticity of adipose tissue exceeds their capability to switch between white and brown, an observation that has been detected previously in pregnant mice. Inflammatory biomarkers will be downregulated in omental fat with pregnancy.

6.2 Methods

Four weeks old Sprague Dawley rats were fed either a chow or a high-fat high sucrose diet and housed at either 27°C or 20°C. Food intake for virgin animals and body weight for all animals were measured three times a week. Virgin rats were tissue sampled at 10 weeks of age while the rest of the animals were mated and sampled at 50% and 90% of pregnancy (10 and 19 days of pregnancy, respectively). Blood was collected while tissues and foetuses were sampled and weighted. Gene expression was studied in the

iBAT, omental and inguinal adipose tissue using qPCR. Immunohistochemistry was used to explore UCP1 protein abundance in iBAT while plasma metabolites and hormones were measured with commercial assays. Omental and inguinal sections were stained with H&E for examination of histological appearance.

6.3 Summary of main findings

6.3.1 Mild cold ambient temperature enhances a thermogenic activity of BAT that is modulated with pregnancy

In agreement with published studies (Iwen et al., 2017, van der Lans et al., 2013, Vijgen et al., 2011, Chondronikola et al., 2014, Small et al., 2018, Saito et al., 2009, Ouellet et al., 2011), a reduction in the ambient temperature triggers UCP1 protein expression in classical BAT depot in virgin rats and reduces circulating glucose, an effect not found at thermoneutrality. Pregnancy reduced the brown phenotype induced by rearing at a cool ambient temperature (Wade et al., 1986). This reduction in brown phenotype is thought to be an adaptation that causes less energy expenditure to ensure availability of nutrients through gestation for both the mother and fetal development (Wade et al., 1986). As expected, ambient temperature modulates metabolism, hormones, and adipose tissue function, a response that is diminished after conception.

6.3.2 No browning was detected in the inguinal adipose tissue

UCP1 was not detected in the inguinal adipose at any temperature of both virgin and pregnant rats. Previous studies which found UCP1 in this depot after interventions like mild cold, were undertaken on males (Rogers et al., 2012, Poher et al., 2015, Knudsen et al., 2014, Wu et al., 2014, Cui et al., 2016, de Jong et al., 2015, Yang et al., 2017, Waldén et al., 2011); this suggests that the capacity of browning in WAT can be sex-specific in some species.

6.3.3 Inguinal adipocytes differentiate to mammary cells with pregnancy

The current study, as well as previous studies (De Matteis et al., 2009, Morroni et al., 2004, Prokesch et al., 2014), showed that there was a differentiation of the subcutaneous adipocytes into alveoli composed of epithelial cells which constitute the mammary gland with gestation which was supported by evidence at the molecular and histological levels. Gene expression revealed a high expression of whey acidic protein and ELF5 genes during pregnancy; both are considered unique for milk formation and alveologenesis regulation, respectively. These two genes were absent in the virgin rats' interscapular and omental fat depots. The histological sections showed the formation of alveoli as pregnancy proceeds while a gross anatomy evidence in my study supports this observation further as inguinal fat depot appeared more compact in pregnant compared to virgin rats.

6.3.4 Absence of browning and inflammatory biomarkers downregulation in the omental fat in response to mild cold exposure

No signs of browning were detected at any group of the three time points. This can be due to the use of females because browning was triggered in the omental fat in response to cold when males were used in previous studies (de Jong et al., 2015, Ferrannini et al., 2016, Rosell et al., 2014, Yang et al., 2017, Cui et al., 2016). The same explanation applies to the absence of an effect of ambient temperature on omental fat infiltration by immune cells as males were used in other studies, that demonstrated reduced meta-inflammation with cold exposure (van der Stelt et al., 2017, Kim et al., 2012). The model used can also be a reason as browning was enhanced in omental fat of human females (Poulain-Godefroy et al., 2008, Cancello et al., 2006, Terra et al., 2010)

6.3.5 Inflammation process in omental fat is suppressed with gestation.

A significant reduction in inflammatory biomarkers of omental fat was found with gestation and may be necessary for sustaining the pregnancy. This change is driven by changes in the secretion of some hormones such as oestrogen and progesterone (Somerset et al., 2004, Mor and Cardenas, 2010, Zen et al., 2010)

6.4 Limitations

6.4.1 Small amount of iBAT in rats

Due to the relatively small size of rat iBAT, the sampled tissues were only enough for gene expression and histological analysis. The inclusion of more animals would help to provide sufficient amounts of iBAT for further analysis by techniques like western blotting for mitochondrial proteins analysis (Mahmood and Yang, 2012) or seahorse assay for oxygen consumption measurements (Shin et al., 2017, Rogers et al., 2011)

6.4.2 Technical limitations

6.4.2.1 Food intake Measurement

As conception occurred at different times, cages contained rats at different stages of pregnancy which meant it was not possible to measure the food intake for rats during gestation.

6.4.2.2 Relative weights of pregnant rats

Rats were pregnant with different numbers of foetuses. I did not take the whole weights of foetuses and uterus which made it difficult to calculate the relative weight of tissues; assuming that the only increase in body weight during pregnancy was due to the fetal weight.

6.4.2.3 Glucose and NEFA measurement

Due to stressful sacrifice procedure, changes in glucose or NEFA levels may be influenced by hypoxia and thus not reflect the metabolic/BAT status.

6.5 Future work

This thesis indicates a need for further research to investigate the anatomical changes in the development of adipose tissue, particularly for the brown and beige adipocytes in response to temperature and diet, and how these are modulated with pregnancy. The following are suggested to be performed in order to achieve this:

6.5.1 Maternal obesity programming effect on offspring postnatally

The impact of maternal obesity, as a risk factor for obesity in the offspring, needs to be investigated at thermoneutrality; this should be carried through different developmental windows, i.e. before conception, during pregnancy, lactation and different stages of postnatal life. It would be worthy of running a similar study at standard housing temperature to compare birth weights, fat mass, BAT characteristics and browning capacity in WAT between the two temperatures.

6.5.2 Postnatal effects of maternal diet in relation to the sex of offspring

As previous studies have shown a difference between males and females in the postnatal response to maternal diet during gestation and lactation, a natural progression of this work would be to identify these differences and their specific patterns of weight gain and metabolic differences.

6.5.3 BAT and WAT plasticity in lactation and beyond.

Mammary cells, which originally were adipocytes before pregnancy convert back to adipocytes after lactation (Cinti, 2009). A recent study suggests a possible differentiation of milk-producing cells to brown adipocytes (Giordano et al., 2017) indicating a unique type of adipose tissue plasticity that needs to be further explored. It would be interesting to investigate the genetic profile of different adipose tissue depots especially in unique physiological cases, i.e. pregnancy and lactation.

6.5.4 Browning and inflammation in male adipose tissues.

Further studies are needed to evaluate the effect of housing temperature on interscapular BAT activation and the capacity of WAT to undergo browning in males.

6.5.5 Standard housing temperature precautions

The standard housing temperature of the animals should be considered during metabolic studies as such a small reduction in temperature was enough to trigger browning in the interscapular BAT. This response may confound the effect of the dietary intervention introduced for obesity induction as well as the capacity of programming by maternal diet on the offspring postnatally.

6.5.6 Staining virgin inguinal fat with mammary cells biomarker

It would be interesting to stain the virgin rat's inguinal fat with ELF5 antibodies in order to reveal the nature of these cells.

6.5.7 Measuring deiodinase 2 (MDI 2) expression in iBAT

As my study concentrated mainly on the investigation of any change in UCP1 expression in different adipose tissue depots in response to changes in the diet and ambient

temperature, I didn't explore the expression of factors that mediate the detailed mechanism of cold induced thermogenesis. Measuring MDI 2 expression in BAT may provide insight about the mechanism underlying NST in as it is locally produced by BAT.

6.6 Summary of the thesis

The diagram summary explains, in brief, my study design, methods used and the major findings (Figure 6.1).

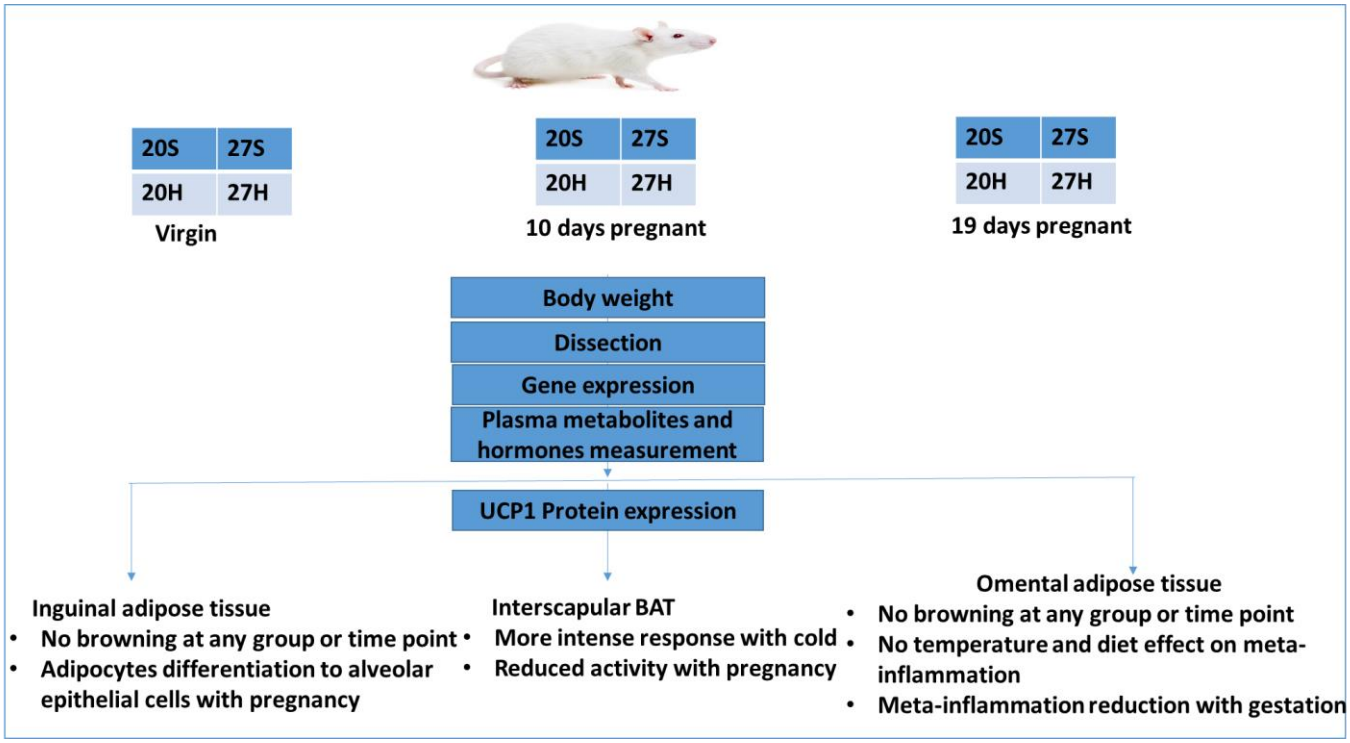


Figure 6.1 Summary diagram of study design, methods and main findings

20°C and standard diet (20S), 20°C and high energy diet (20H), 27°C and standard diet (27S), 27°C and high energy diet (27H), brown adipose tissue (BAT), uncoupling protein 1 (UCP1).

References

ADEREM, A. & ULEVITCH, R. J. 2000. Toll-like receptors in the induction of the innate immune response. *Nature,* 406**,** 782.

ALDISS, P., BETTS, J., SALE, C., POPE, M. & SYMONDS, M. E. 2017. Exercise-induced 'browning'of adipose tissues. *Metabolism*.

ALMEIDA, M. M., DIAS-ROCHA, C. P., SOUZA, A. S., MUROS, M. F., MENDONCA, L. S., PAZOS-MOURA, C. C. & TREVENZOLI, I. H. 2017. Perinatal maternal high-fat diet induces early obesity and sex-specific alterations of the endocannabinoid system in white and brown adipose tissue of weanling rat offspring. *British Journal of Nutrition,* 118**,** 788-803.

ALMIND, K., MANIERI, M., SIVITZ, W. I., CINTI, S. & KAHN, C. R. 2007. Ectopic brown adipose tissue in muscle provides a mechanism for differences in risk of metabolic syndrome in mice. *Proceedings of the National Academy of Sciences,* 104**,** 2366-2371.

ALVEHUS, M., BURÉN, J., SJÖSTRÖM, M., GOEDECKE, J. & OLSSON, T. 2010. The human visceral fat depot has a unique inflammatory profile. *Obesity,* 18**,** 879-883.

ANDREOLLO, N. A., SANTOS, E. F. D., ARAÚJO, M. R. & LOPES, L. R. 2012. Rat's age versus human's age: what is the relationship? *ABCD. Arquivos Brasileiros de Cirurgia Digestiva (São Paulo),* 25**,** 49-51.

APOSTOLI, A. J., SKELHORNE-GROSS, G. E., RUBINO, R. E., PETERSON, N. T., DI LENA, M. A., SCHNEIDER, M. M., SENGUPTA, S. K. & NICOL, C. J. 2014. Loss of PPARγ expression in mammary secretory epithelial cells creates a pro-breast tumorigenic environment. *International journal of cancer,* 134**,** 1055-1066.

AQUILA, H., LINK, T. A. & KLINGENBERG, M. 1985. The uncoupling protein from brown fat mitochondria is related to the mitochondrial ADP/ATP carrier. Analysis of sequence homologies and of folding of the protein in the membrane. *The EMBO journal,* 4**,** 2369-2376.

ARAI, Y. & MATSUMOTO, A. 1978. Synapse formation of the hypothalamic arcuate nucleus during post-natal development in the female rat and its modification by neonatal estrogen treatment. *Psychoneuroendocrinology,* 3**,** 31-45.

ARYA, M., SHERGILL, I. S., WILLIAMSON, M., GOMMERSALL, L., ARYA, N. & PATEL, H. R. 2005. Basic principles of real-time quantitative PCR. *Expert review of molecular diagnostics,* 5**,** 209-219.

ASTBURY, S., SONG, A., ZHOU, M., NIELSEN, B., HOEDL, A., WILLING, B. P., SYMONDS, M. E. & BELL, R. C. 2018. High fructose intake during pregnancy in rats influences the maternal microbiome and gut development in the offspring. *Frontiers in genetics,* 9.

AUVINEN, H. E., ROMIJN, J. A., BIERMASZ, N. R., PIJL, H., HAVEKES, L. M., SMIT, J. W., RENSEN, P. C. & PEREIRA, A. M. 2012. The effects of high fat diet on the basal activity of the hypothalamuspituitaryadrenal axis in mice. *Journal of Endocrinology,* 214**,** 191.

AVRAM, A. S., AVRAM, M. M. & JAMES, W. D. J. J. O. T. A. A. O. D. 2005. Subcutaneous fat in normal and diseased states: 2. Anatomy and physiology of white and brown adipose tissue. 53**,** 671-683.

AWADA, R., PARIMISETTY, A. & D'HELLENCOURT, C. L. 2013. Influence of obesity on neurodegenerative diseases. *Neurodegenerative Diseases.* InTech.

BACHMAN, E. S., DHILLON, H., ZHANG, C.-Y., CINTI, S., BIANCO, A. C., KOBILKA, B. K. & LOWELL, B. B. 2002. βAR signaling required for diet-induced thermogenesis and obesity resistance. *Science,* 297**,** 843-845.

BAI, Z., WUREN, T., LIU, S., HAN, S., CHEN, L., MCCLAIN, D. & GE, R.-L. 2015. Intermittent cold exposure results in visceral adipose tissue "browning" in the plateau pika (Ochotona curzoniae). *Comparative Biochemistry and Physiology Part A: Molecular & Integrative Physiology,* 184**,** 171-178.

BAKER, R. G., HAYDEN, M. S. & GHOSH, S. 2011. NF-κB, inflammation, and metabolic disease. *Cell metabolism,* 13**,** 11-22.
BAMIAS, G., GOUKOS, D., LAOUDI, E., BALLA, I. G., SIAKAVELLAS, S. I., DAIKOS, G. L. & LADAS, S. D. 2013. Comparative Study of Candidate Housekeeping Genes for Quantification of Target Gene Messenger RNA Expression by Real-Time PCR in Patients with Inflammatory Bowel Disease. *Inflammatory Bowel Diseases,* 19**,** 2840-2847.
BARGUT, T. C. L., SOUZA-MELLO, V., AGUILA, M. B. & MANDARIM-DE-LACERDA, C. A. 2017. Browning of white adipose tissue: lessons from experimental models. *Hormone molecular biology and clinical investigation,* 31.
BARON, S. & ALBRECHT, T. 1996. *Medical microbiology / edited by Samuel Baron ; co-editors, Thomas Albrecht ... [et al.] ; scientific illustrator, Steve Schuenke.,* United States, Galveston, Tex. : University of Texas Medical Branch at Galveston, Dept. of Microbiology & Immunology, 1996.
BARTELT, A., BRUNS, O. T., REIMER, R., HOHENBERG, H., ITTRICH, H., PELDSCHUS, K., KAUL, M. G., TROMSDORF, U. I., WELLER, H. & WAURISCH, C. 2011. Brown adipose tissue activity controls triglyceride clearance. *Nature medicine,* 17**,** 200.
BARTELT, A. & HEEREN, J. 2014. Adipose tissue browning and metabolic health. *Nature Reviews Endocrinology,* 10**,** 24.
BARTNESS, T., VAUGHAN, C. & SONG, C. J. I. J. O. O. 2010. Sympathetic and sensory innervation of brown adipose tissue. 34**,** S36.
BASKARAN, P., KRISHNAN, V., REN, J. & THYAGARAJAN, B. 2016. Capsaicin induces browning of white adipose tissue and counters obesity by activating TRPV1 channel-dependent mechanisms. *British journal of pharmacology,* 173**,** 2369-2389.
BASKARAN, P., ZHANG, Z. & THYAGARAJAN, B. 2017. TRPV1 Activation Stimulates Brown Adipose Tissue Activation and Enhances Mitochondrial Biogenesis to Counteract Diet-Induced Obesity. *Biophysical Journal,* 112**,** 408a.
BASTARD, J.-P., MAACHI, M., LAGATHU, C., KIM, M. J., CARON, M., VIDAL, H., CAPEAU, J. & FEVE, B. 2006. Recent advances in the relationship between obesity, inflammation, and insulin resistance. *European cytokine network,* 17**,** 4-12.
BAYOL, S. A., FARRINGTON, S. J. & STICKLAND, N. C. 2007. A maternal 'junk food'diet in pregnancy and lactation promotes an exacerbated taste for 'junk food'and a greater propensity for obesity in rat offspring. *British Journal of Nutrition,* 98**,** 843-851.
BELL, A. W. & BAUMAN, D. E. 1997. Adaptations of glucose metabolism during pregnancy and lactation. *Journal of mammary gland biology and neoplasia,* 2**,** 265-278.
BIANCO, A. C. & KIM, B. W. 2006. Deiodinases: implications of the local control of thyroid hormone action. *The Journal of clinical investigation,* 116**,** 2571-2579.
BIESWAL, F., AHN, M. T., REUSENS, B., HOLVOET, P., RAES, M., REES, W. D. & REMACLE, C. 2006. The importance of catch-up growth after early malnutrition for the programming of obesity in male rat. *Obesity,* 14**,** 1330-1343.
BILLON, N. & DANI, C. 2012. Developmental origins of the adipocyte lineage: new insights from genetics and genomics studies. *Stem Cell Reviews and Reports,* 8**,** 55-66.
BIRERDINC, A., JARRAR, M., STOTISH, T., RANDHAWA, M. & BARANOVA, A. 2013. Manipulating molecular switches in brown adipocytes and their precursors: a therapeutic potential. *Progress in lipid research,* 52**,** 51-61.
BLAIR, N. J., THOMPSON, J. M., BLACK, P., BECROFT, D., CLARK, P., HAN, D. Y., ROBINSON, E., WALDIE, K., WILD, C. & MITCHELL, E. A. 2007. Risk factors for obesity in 7 year old European children: The Auckland birthweight collaborative Study. *Archives of disease in childhood*.
BLÜHER, M., FASSHAUER, M., TÖNJES, A., KRATZSCH, J., SCHÖN, M. & PASCHKE, R. 2005. Association of interleukin-6, C-reactive protein, interleukin-10 and adiponectin plasma concentrations with measures of obesity, insulin sensitivity

and glucose metabolism. *Experimental and clinical endocrinology & diabetes,* 113**,** 534-537.
BLUNDELL, J., GOODSON, S. & HALFORD, J. 2001. Regulation of appetite: role of leptin in signalling systems for drive and satiety. *International Journal of Obesity,* 25**,** S29.
BOLLEPALLI, S. & ROSE, S. R. 2012. Disorders of the thyroid gland. *Avery's Diseases of the Newborn.* Elsevier.
BONET, M. L., OLIVER, P. & PALOU, A. 2013. Pharmacological and nutritional agents promoting browning of white adipose tissue. *Biochimica et Biophysica Acta (BBA)-Molecular and Cell Biology of Lipids,* 1831**,** 969-985.
BRUN, R. P., TONTONOZ, P., FORMAN, B. M., ELLIS, R., CHEN, J., EVANS, R. M. & SPIEGELMAN, B. M. 1996. Differential activation of adipogenesis by multiple PPAR isoforms. *Genes & development,* 10**,** 974-984.
BRYCHTA, R. & CHEN, K. 2017. Cold-induced thermogenesis in humans. *European journal of clinical nutrition,* 71**,** 345.
BUCHANAN, T. A. & XIANG, A. H. 2005. Gestational diabetes mellitus. *The Journal of clinical investigation,* 115**,** 485-491.
BUETTNER, R., SCHÖLMERICH, J. & BOLLHEIMER, L. C. 2007. High-fat diets: modeling the metabolic disorders of human obesity in rodents. *Obesity,* 15**,** 798-808.
BURDETTE, H. L., WHITAKER, R. C., HALL, W. C. & DANIELS, S. R. 2006. Maternal infant-feeding style and children's adiposity at 5 years of age. *Archives of pediatrics & adolescent medicine,* 160**,** 513-520.
BURDON, T., SANKARAN, L., WALL, R., SPENCER, M. & HENNIGHAUSEN, L. 1991. Expression of a whey acidic protein transgene during mammary development. Evidence for different mechanisms of regulation during pregnancy and lactation. *Journal of Biological Chemistry,* 266**,** 6909-6914.
BUSTIN, S. A. & NOLAN, T. 2004. Pitfalls of quantitative real-time reverse-transcription polymerase chain reaction. *Journal of biomolecular techniques: JBT,* 15**,** 155.
BUTTE, N. F. 2000. Carbohydrate and lipid metabolism in pregnancy: normal compared with gestational diabetes mellitus–. *The American journal of clinical nutrition,* 71**,** 1256S-1261S.
CALDERON-DOMINGUEZ, M., MIR, J. F., FUCHO, R., WEBER, M., SERRA, D. & HERRERO, L. 2016. Fatty acid metabolism and the basis of brown adipose tissue function. *Adipocyte,* 5**,** 98-118.
CAMPFIELD, L. A., SMITH, F. J., GUISEZ, Y., DEVOS, R. & BURN, P. 1995. Recombinant mouse OB protein: evidence for a peripheral signal linking adiposity and central neural networks. *Science,* 269**,** 546-549.
CANCELLO, R., TORDJMAN, J., POITOU, C., GUILHEM, G., BOUILLOT, J. L., HUGOL, D., COUSSIEU, C., BASDEVANT, A., HEN, A. B. & BEDOSSA, P. 2006. Increased infiltration of macrophages in omental adipose tissue is associated with marked hepatic lesions in morbid human obesity. *Diabetes,* 55**,** 1554-1561.
CANNON, B. & NEDERGAARD, J. 2004. Brown adipose tissue: function and physiological significance. *Physiological reviews,* 84**,** 277-359.
CAPUTO, T., GILARDI, F. & DESVERGNE, B. 2017. From chronic overnutrition to metaflammation and insulin resistance: adipose tissue and liver contributions. *FEBS letters,* 591**,** 3061-3088.
CATALANO, P. M., PRESLEY, L., MINIUM, J. & HAUGUEL-DE MOUZON, S. 2009. Fetuses of obese mothers develop insulin resistance in utero. *Diabetes care,* 32**,** 1076-1080.
CATALANO, P. M., TYZBIR, E. D., ROMAN, N. M., AMINI, S. B. & SIMS, E. A. 1991. Longitudinal changes in insulin release and insulin resistance in nonobese pregnant women. *American Journal of Obstetrics & Gynecology,* 165**,** 1667-1672.
CATALANO, P. M., TYZBIR, E. D., WOLFE, R. R., CALLES, J., ROMAN, N. M., AMINI, S. B. & SIMS, E. 1993. Carbohydrate metabolism during pregnancy in control subjects and women with gestational diabetes. *American Journal of Physiology-Endocrinology And Metabolism,* 264**,** E60-E67.

CATALANO, P. M., TYZBIR, E. D., WOLFE, R. R., ROMAN, N. M., AMINI, S. B. & SIMS, E. A. 1992. Longitudinal changes in basal hepatic glucose production and suppression during insulin infusion in normal pregnant women. *American Journal of Obstetrics & Gynecology,* 167**,** 913-919.
CHATTERJEE, T. K., STOLL, L. L., DENNING, G. M., HARRELSON, A., BLOMKALNS, A. L., IDELMAN, G., ROTHENBERG, F. G., NELTNER, B., ROMIG-MARTIN, S. A. & DICKSON, E. W. 2009. Proinflammatory phenotype of perivascular adipocytes: influence of high-fat feeding. *Circulation research,* 104**,** 541-549.
CHAUDHRI, O. B., SALEM, V., MURPHY, K. G. & BLOOM, S. R. J. A. R. P. 2008. Gastrointestinal satiety signals. 70**,** 239-255.
CHECHI, K., VIJAY, J., VOISINE, P., MATHIEU, P., BOSSÉ, Y., TCHERNOF, A., GRUNDBERG, E. & RICHARD, D. 2019. UCP1 expression–associated gene signatures of human epicardial adipose tissue. *JCI insight,* 4.
CHEN, H., SIMAR, D., LAMBERT, K., MERCIER, J. & MORRIS, M. J. 2008. Maternal and postnatal overnutrition differentially impact appetite regulators and fuel metabolism. *Endocrinology,* 149**,** 5348-5356.
CHOI, Y. S., CHAKRABARTI, R., ESCAMILLA-HERNANDEZ, R. & SINHA, S. 2009. Elf5 conditional knockout mice reveal its role as a master regulator in mammary alveolar development: failure of Stat5 activation and functional differentiation in the absence of Elf5. *Developmental biology,* 329**,** 227-241.
CHONDRONIKOLA, M., VOLPI, E., BØRSHEIM, E., PORTER, C., ANNAMALAI, P., ENERBÄCK, S., LIDELL, M. E., SARAF, M. K., LABBE, S. M. & HURREN, N. M. 2014. Brown adipose tissue improves whole body glucose homeostasis and insulin sensitivity in humans. *Diabetes***,** DB_140746.
CHU, S. Y., CALLAGHAN, W. M., KIM, S. Y., SCHMID, C. H., LAU, J., ENGLAND, L. J. & DIETZ, P. M. 2007. Maternal obesity and risk of gestational diabetes mellitus. *Diabetes care,* 30**,** 2070-2076.
CINTI, S. 2009. Reversible physiological transdifferentiation in the adipose organ: Symposium on 'Frontiers in adipose tissue biology'. *Proceedings of the Nutrition Society,* 68**,** 340-349.
CINTI, S. 2012. The adipose organ at a glance. *Disease models & mechanisms,* 5**,** 588-594.
CINTI, S. 2017. UCP1 protein: The molecular hub of adipose organ plasticity. *Biochimie,* 134**,** 71-76.
CINTI, S. 2018. White, Brown, Beige and Pink: A Rainbow in the Adipose Organ. *Current Opinion in Endocrine and Metabolic Research*.
CINTI, S., FREDERICH, R. C., ZINGARETTI, M. C., DE MATTEIS, R., FLIER, J. S. & LOWELL, B. B. 1997. Immunohistochemical localization of leptin and uncoupling protein in white and brown adipose tissue. *Endocrinology,* 138**,** 797-804.
COHEN, P., LEVY, J. D., ZHANG, Y., FRONTINI, A., KOLODIN, D. P., SVENSSON, K. J., LO, J. C., ZENG, X., YE, L. & KHANDEKAR, M. J. 2014. Ablation of PRDM16 and beige adipose causes metabolic dysfunction and a subcutaneous to visceral fat switch. *Cell,* 156**,** 304-316.
COLLINS, S. & SURWIT, R. S. 2001. The beta-adrenergic receptors and the control of adipose tissue metabolism and thermogenesis. *Recent progress in hormone research,* 56**,** 309-328.
COMMINS, S. P., WATSON, P. M., PADGETT, M. A., DUDLEY, A., ARGYROPOULOS, G. & GETTYS, T. W. 1999. Induction of uncoupling protein expression in brown and white adipose tissue by leptin. *Endocrinology,* 140**,** 292-300.
COONS, A. H., LEDUC, E. H. & CONNOLLY, J. M. 1955. Studies on antibody production: I. A method for the histochemical demonstration of specific antibody and its application to a study of the hyperimmune rabbit. *Journal of Experimental Medicine,* 102**,** 49-60.
COUSIN, B., CINTI, S., MORRONI, M., RAIMBAULT, S., RICQUIER, D., PENICAUD, L. & CASTEILLA, L. 1992. Occurrence of brown adipocytes in rat white adipose tissue:

molecular and morphological characterization. *Journal of cell science,* 103**,** 931-942.
COVEY, S. D., WIDEMAN, R. D., MCDONALD, C., UNNIAPPAN, S., HUYNH, F., ASADI, A., SPECK, M., WEBBER, T., CHUA, S. C. & KIEFFER, T. J. 2006. The pancreatic β cell is a key site for mediating the effects of leptin on glucose homeostasis. *Cell metabolism,* 4**,** 291-302.
CUI, X., NGUYEN, N. L. T., ZAREBIDAKI, E., CAO, Q., LI, F., ZHA, L., BARTNESS, T., SHI, H. & XUE, B. 2016. Thermoneutrality decreases thermogenic program and promotes adiposity in high-fat diet-fed mice. *Physiological reports,* 4**,** e12799.
CYPESS, A. M., WEINER, L. S., ROBERTS-TOLER, C., ELÍA, E. F., KESSLER, S. H., KAHN, P. A., ENGLISH, J., CHATMAN, K., TRAUGER, S. A. & DORIA, A. 2015. Activation of human brown adipose tissue by a β3-adrenergic receptor agonist. *Cell metabolism,* 21**,** 33-38.
D'HAENE, B. & HELLEMANS, J. 2010. The importance of quality control during qPCR data analysis. *Int Drug Disc,* 18**,** 24.
DE JONEE, L. & BRAY, G. A. 1997. The thermic effect of food and obesity: a critical review. *Obesity Research,* 5**,** 622-631.
DE JONG, J. M., LARSSON, O., CANNON, B. & NEDERGAARD, J. 2015. A stringent validation of mouse adipose tissue identity markers. *American Journal of Physiology-Endocrinology and Metabolism,* 308**,** E1085-E1105.
DE MATTEIS, R., ZINGARETTI, M. C., MURANO, I., VITALI, A., FRONTINI, A., GIANNULIS, I., BARBATELLI, G., MARCUCCI, F., BORDICCHIA, M. & SARZANI, R. 2009. In vivo physiological transdifferentiation of adult adipose cells. *Stem Cells,* 27**,** 2761-2768.
DESAI, M., JELLYMAN, J. K., HAN, G., BEALL, M., LANE, R. H. & ROSS, M. G. 2014. Maternal obesity and high-fat diet program offspring metabolic syndrome. *American journal of obstetrics and gynecology,* 211**,** 237. e1-237. e13.
DOIG, C. L., FLETCHER, R. S., MORGAN, S. A., MCCABE, E. L., LARNER, D. P., TOMLINSON, J. W., STEWART, P. M., PHILP, A. & LAVERY, G. G. 2017. 11β-HSD1 Modulates the Set Point of Brown Adipose Tissue Response to Glucocorticoids in Male Mice. *Endocrinology,* 158**,** 1964-1976.
DRAKE, A. J. & REYNOLDS, R. M. 2010. Impact of maternal obesity on offspring obesity and cardiometabolic disease risk. *Reproduction,* 140**,** 387-398.
EL-JACK, A. K., HAMM, J. K., PILCH, P. F. & FARMER, S. R. 1999. Reconstitution of insulin-sensitive glucose transport in fibroblasts requires expression of both PPARγ and C/EBPα. *Journal of Biological Chemistry,* 274**,** 7946-7951.
FAGUNDES, D. J. & TAHA, M. O. 2004. Animal disease model: choice´ s criteria and current animals specimens. *Acta Cirurgica Brasileira,* 19**,** 59-65.
FÅHRAEUS, L., LARSSON-COHN, U. & WALLENTIN, L. 1985. Plasma lipoproteins including high density lipoprotein subfractions during normal pregnancy. *Obstetrics and gynecology,* 66**,** 468-472.
FANTUZZI, G. 2005. Adipose tissue, adipokines, and inflammation. *Journal of Allergy and Clinical Immunology,* 115**,** 911-919.
FARMER, S. R. 2008. Molecular determinants of brown adipocyte formation and function. *Genes & development,* 22**,** 1269-1275.
FELDMANN, H. M., GOLOZOUBOVA, V., CANNON, B. & NEDERGAARD, J. 2009. UCP1 ablation induces obesity and abolishes diet-induced thermogenesis in mice exempt from thermal stress by living at thermoneutrality. *Cell metabolism,* 9**,** 203-209.
FERRANNINI, G., NAMWANJE, M., FANG, B., DAMLE, M., LI, D., LIU, Q., LAZAR, M. A. & QIANG, L. 2016. Genetic backgrounds determine brown remodeling of white fat in rodents. *Molecular metabolism,* 5**,** 948-958.
FIALA, J. & BRÁZDOVÁ, Z. J. C. E. J. O. P. H. 2000. A comparison between the lifestyles of men and women--parents of school age children. 8**,** 94-100.

FISCHER, A. H., JACOBSON, K. A., ROSE, J. & ZELLER, R. 2008. Hematoxylin and eosin staining of tissue and cell sections. *Cold Spring Harbor Protocols,* 2008**,** pdb. prot4986.
FROMME, T. & KLINGENSPOR, M. 2010. Uncoupling protein 1 expression and high-fat diets. *American Journal of Physiology-Regulatory, Integrative and Comparative Physiology,* 300**,** R1-R8.
FRONTERA, M., PUJOL, E., RODRÍGUEZ-CUENCA, S., CATALÀ-NIELL, A., ROCA, P., GARCÍA-PALMER, F. & GIANOTTI, M. 2005. Rat brown adipose tissue thermogenic features are altered during mid-pregnancy. *Cellular Physiology and Biochemistry,* 15**,** 203-210.
FRÜHBECK, G., BECERRIL, S., SÁINZ, N., GARRASTACHU, P. & GARCÍA-VELLOSO, M. J. J. T. I. P. S. 2009. BAT: a new target for human obesity? 30**,** 387-396.
FURUHASHI, M., SAITOH, S., SHIMAMOTO, K. & MIURA, T. 2014. Fatty acid-binding protein 4 (FABP4): pathophysiological insights and potent clinical biomarker of metabolic and cardiovascular diseases. *Clinical Medicine Insights: Cardiology,* 8**,** CMC. S17067.
GALE, C. R., JAVAID, M. K., ROBINSON, S. M., LAW, C. M., GODFREY, K. M. & COOPER, C. 2007. Maternal size in pregnancy and body composition in children. *The Journal of Clinical Endocrinology & Metabolism,* 92**,** 3904-3911.
GASPARETTI, A. L., DE SOUZA, C. T., PEREIRA-DA-SILVA, M., OLIVEIRA, R. L., SAAD, M. J., CARNEIRO, E. M. & VELLOSO, L. A. 2003. Cold exposure induces tissue-specific modulation of the insulin-signalling pathway in Rattus norvegicus. *The Journal of physiology,* 552**,** 149-162.
GENECARDSDATABASE. *TRPV1 Gene (Protein Coding)* [Online]. Available: https://www.genecards.org/cgi-bin/carddisp.pl?gene=TRPV1 [Accessed 2019].
GESTA, S., TSENG, Y.-H. & KAHN, C. R. 2007. Developmental origin of fat: tracking obesity to its source. *Cell,* 131**,** 242-256.
GIMENO, R. E. 2007. Fatty acid transport proteins. *Current opinion in lipidology,* 18**,** 271-276.
GIORDANO, A., FRONTINI, A., CASTELLUCCI, M., CINTI, S. J. J. O. H. & CYTOCHEMISTRY 2004. Presence and distribution of cholinergic nerves in rat mediastinal brown adipose tissue. 52**,** 923-930.
GIORDANO, A., PERUGINI, J., KRISTENSEN, D. M., SARTINI, L., FRONTINI, A., KAJIMURA, S., KRISTIANSEN, K. & CINTI, S. 2017. Mammary alveolar epithelial cells convert to brown adipocytes in post-lactating mice. *Journal of cellular physiology,* 232**,** 2923-2928.
GIORDANO, A., SMORLESI, A., FRONTINI, A., BARBATELLI, G. & CINTI, S. 2014. White, brown and pink adipocytes: the extraordinary plasticity of the adipose organ. *European Journal of Endocrinology***,** EJE-13-0945.
GIRALT, M. & VILLARROYA, F. 2013. White, brown, beige/brite: different adipose cells for different functions? *Endocrinology,* 154**,** 2992-3000.
GONZÁLEZ-BARROSO, M. M., FLEURY, C., BOUILLAUD, F., NICHOLLS, D. G. & RIAL, E. 1998. The uncoupling protein UCP1 does not increase the proton conductance of the inner mitochondrial membrane by functioning as a fatty acid anion transporter. *Journal of Biological Chemistry,* 273**,** 15528-15532.
GUSTAFSON, B., HAMMARSTEDT, A., HEDJAZIFAR, S., HOFFMANN, J. M., SVENSSON, P.-A., GRIMSBY, J., RONDINONE, C. & SMITH, U. 2015. BMP4 and BMP antagonists regulate human white and beige adipogenesis. *Diabetes***,** db141127.
HAGBERG, C. E., FALKEVALL, A., WANG, X., LARSSON, E., HUUSKO, J., NILSSON, I., VAN MEETEREN, L. A., SAMEN, E., LU, L. & VANWILDEMEERSCH, M. 2010. Vascular endothelial growth factor B controls endothelial fatty acid uptake. *Nature,* 464**,** 917.
HALAAS, J. L., GAJIWALA, K. S., MAFFEI, M., COHEN, S. L., CHAIT, B. T., RABINOWITZ, D., LALLONE, R. L., BURLEY, S. K. & FRIEDMAN, J. M. 1995. Weight-reducing effects of the plasma protein encoded by the obese gene. *Science,* 269**,** 543-546.

HALFORD, J. C. & BLUNDELL, J. E. J. A. O. M. 2000. Separate systems for serotonin and leptin in appetite control. 32**,** 222-232.
HAMOSH, M., CLARY, T. R., CHERNICK, S. S. & SCOW, R. O. 1970. Lipoprotein lipase activity of adipose and mammary tissue and plasma triglyceride in pregnant and lactating rats. *Biochimica et Biophysica Acta (BBA)-Lipids and Lipid Metabolism,* 210**,** 473-482.
HANSEN, J. B., JØRGENSEN, C., PETERSEN, R. K., HALLENBORG, P., DE MATTEIS, R., BØYE, H. A., PETROVIC, N., ENERBÄCK, S., NEDERGAARD, J. & CINTI, S. 2004. Retinoblastoma protein functions as a molecular switch determining white versus brown adipocyte differentiation. *Proceedings of the National Academy of Sciences,* 101**,** 4112-4117.
HARMS, M. & SEALE, P. 2013. Brown and beige fat: development, function and therapeutic potential. *Nature medicine,* 19**,** 1252.
HAUSMAN, D., DIGIROLAMO, M., BARTNESS, T., HAUSMAN, G. & MARTIN, R. 2001. The biology of white adipocyte proliferation. *Obesity reviews,* 2**,** 239-254.
HAYWARD, C. E., COWLEY, E. J., SIBLEY, C. P., MYERS, J. E. & WAREING, M. 2018. Exposure to omentum adipose tissue conditioned medium from obese pregnant women promotes myometrial artery dysfunction. *Journal of Obstetrics and Gynaecology Research,* 44**,** 124-133.
HE, P.-P., JIANG, T., OUYANG, X.-P., LIANG, Y.-Q., ZOU, J.-Q., WANG, Y., SHEN, Q.-Q., LIAO, L. & ZHENG, X.-L. 2018. Lipoprotein lipase: biosynthesis, regulatory factors, and its role in atherosclerosis and other diseases. *Clinica Chimica Acta*.
HEATON, G. M., WAGENVOORD, R. J., KEMP JR, A. & NICHOLLS, D. G. 1978. brown-adipose-tissue mitochondria: photoaffinity labelling of the regulatory site of energy dissipation. *European Journal of Biochemistry,* 82**,** 515-521.
HEATON, J. M. 1972. The distribution of brown adipose tissue in the human. *Journal of anatomy,* 112**,** 35.
HEID, C. A., STEVENS, J., LIVAK, K. J. & WILLIAMS, P. M. 1996. Real time quantitative PCR. *Genome research,* 6**,** 986-994.
HELLMER, J., MARCUS, C., SONNENFELD, T. & ARNER, P. 1992. Mechanisms for differences in lipolysis between human subcutaneous and omental fat cells. *The Journal of Clinical Endocrinology & Metabolism,* 75**,** 15-20.
HERRERA, E. 2002a. Implications of dietary fatty acids during pregnancy on placental, fetal and postnatal development—a review. *Placenta,* 23**,** S9-S19.
HERRERA, E. 2002b. Lipid metabolism in pregnancy and its consequences in the fetus and newborn. *Endocrine,* 19**,** 43-55.
HERRERA, E., GOMEZ-CORONADO, D. & LASUNCIÓN, M. A. 1987. Lipid metabolism in pregnancy. *Neonatology,* 51**,** 70-77.
HERRERA, E. & ORTEGA-SENOVILLA, H. 2014. Lipid metabolism during pregnancy and its implications for fetal growth. *Current pharmaceutical biotechnology,* 15**,** 24-31.
HIMMS-HAGEN, J. 1990. Brown adipose tissue thermogenesis: interdisciplinary studies. *The FASEB Journal,* 4**,** 2890-2898.
HONDARES, E., IGLESIAS, R., GIRALT, A., GONZALEZ, F. J., GIRALT, M., MAMPEL, T. & VILLARROYA, F. 2011. Thermogenic activation induces FGF21 expression and release in brown adipose tissue. *Journal of Biological Chemistry***,** jbc. M110. 215889.
HOTAMISLIGIL, G. 2003. Inflammatory pathways and insulin action. *International Journal of Obesity,* 27**,** S53.
HOTAMISLIGIL, G. S. 2006. Inflammation and metabolic disorders. *Nature,* 444**,** 860.
HOTAMISLIGIL, G. S. 2017. Inflammation, metaflammation and immunometabolic disorders. *Nature,* 542**,** 177.
HOTMANSGILI, G., SHARGILL, N. & SPIEGELMAN, B. 1993. Adipose expression of tumor necrosis factor-alpha: direct role in obesity-linked insulin resistamce. *Science,* 259**,** 87-91.

HULL, H. R., DINGER, M. K., KNEHANS, A. W., THOMPSON, D. M. & FIELDS, D. A. 2008. Impact of maternal body mass index on neonate birthweight and body composition. *American journal of obstetrics and gynecology,* 198**,** 416. e1-416. e6.
IBRAHIM, M. M. 2010. Subcutaneous and visceral adipose tissue: structural and functional differences. *Obesity reviews,* 11**,** 11-18.
IKEDA, K., KANG, Q., YONESHIRO, T., CAMPOREZ, J. P., MAKI, H., HOMMA, M., SHINODA, K., CHEN, Y., LU, X. & MARETICH, P. 2017. UCP1-independent signaling involving SERCA2b-mediated calcium cycling regulates beige fat thermogenesis and systemic glucose homeostasis. *Nature medicine,* 23**,** 1454.
IMAI, T., TAKAKUWA, R., MARCHAND, S., DENTZ, E., BORNERT, J.-M., MESSADDEQ, N., WENDLING, O., MARK, M., DESVERGNE, B. & WAHLI, W. 2004. Peroxisome proliferator-activated receptor γ is required in mature white and brown adipocytes for their survival in the mouse. *Proceedings of the National Academy of Sciences,* 101**,** 4543-4547.
IWASAKI, Y., TAMURA, Y., INAYOSHI, K., NARUKAWA, M., KOBATA, K., CHIBA, H., MURAKI, E., TSUNODA, N. & WATANABE, T. 2011. TRPV1 agonist monoacylglycerol increases UCP1 content in brown adipose tissue and suppresses accumulation of visceral fat in mice fed a high-fat and high-sucrose diet. *Bioscience, biotechnology, and biochemistry,* 75**,** 904-909.
IWEN, K. A., BACKHAUS, J., CASSENS, M., WALTL, M., HEDESAN, O. C., MERKEL, M., HEEREN, J., SINA, C., RADEMACHER, L. & WINDJÄGER, A. 2017. Cold-induced brown adipose tissue activity alters plasma fatty acids and improves glucose metabolism in men. *The Journal of Clinical Endocrinology & Metabolism,* 102**,** 4226-4234.
JIMENEZ, M., BARBATELLI, G., ALLEVI, R., CINTI, S., SEYDOUX, J., GIACOBINO, J. P., MUZZIN, P. & PREITNER, F. 2003. β3-Adrenoceptor knockout in C57BL/6J mice depresses the occurrence of brown adipocytes in white fat. *European Journal of Biochemistry,* 270**,** 699-705.
KADOWAKI, T., YAMAUCHI, T., KUBOTA, N., HARA, K., UEKI, K. & TOBE, K. 2006. Adiponectin and adiponectin receptors in insulin resistance, diabetes, and the metabolic syndrome. *The Journal of clinical investigation,* 116**,** 1784-1792.
KAJIMURA, S., SEALE, P., KUBOTA, K., LUNSFORD, E., FRANGIONI, J. V., GYGI, S. P. & SPIEGELMAN, B. M. 2009. Initiation of myoblast to brown fat switch by a PRDM16–C/EBP-β transcriptional complex. *Nature,* 460**,** 1154.
KAJIMURA, S., SEALE, P. & SPIEGELMAN, B. M. 2010. Transcriptional control of brown fat development. *Cell metabolism,* 11**,** 257-262.
KALINOVICH, A. V., DE JONG, J. M., CANNON, B. & NEDERGAARD, J. 2017. UCP1 in adipose tissues: two steps to full browning. *Biochimie,* 134**,** 127-137.
KANDA, H., TATEYA, S., TAMORI, Y., KOTANI, K., HIASA, K.-I., KITAZAWA, R., KITAZAWA, S., MIYACHI, H., MAEDA, S. & EGASHIRA, K. 2006. MCP-1 contributes to macrophage infiltration into adipose tissue, insulin resistance, and hepatic steatosis in obesity. *The Journal of clinical investigation,* 116**,** 1494-1505.
KAROPKA, T., FLUCK, J., MEVISSEN, H.-T. & GLASS, Ä. 2006. The Autoimmune Disease Database: a dynamically compiled literature-derived database. *BMC bioinformatics,* 7**,** 325.
KASAHARA, Y., TAKAYANAGI, Y., KAWADA, T., ITOI, K. & NISHIMORI, K. Cold-sensitive phenotype in mice lacking oxytocin receptor gene. Proceedings of Annual Meeting of the Physiological Society of Japan Proceedings of Annual Meeting of the Physiological Society of Japan, 2006. PHYSIOLOGICAL SOCIETY OF JAPAN, 230-230.
KERN, P. A. 1997. Potential role of TNFα and lipoprotein lipase as candidate genes for obesity. *The Journal of nutrition,* 127**,** 1917S-1922S.
KIM, S.-J., CHOI, Y., CHOI, Y.-H. & PARK, T. 2012. Obesity activates toll-like receptor-mediated proinflammatory signaling cascades in the adipose tissue of mice. *The Journal of nutritional biochemistry,* 23**,** 113-122.

KIM, S. H. & PLUTZKY, J. 2016. Brown fat and browning for the treatment of obesity and related metabolic disorders. *Diabetes & metabolism journal,* 40**,** 12-21.
KIRK, S. L., SAMUELSSON, A.-M., ARGENTON, M., DHONYE, H., KALAMATIANOS, T., POSTON, L., TAYLOR, P. D. & COEN, C. W. 2009. Maternal obesity induced by diet in rats permanently influences central processes regulating food intake in offspring. *PloS one,* 4**,** e5870.
KNOPP, R. H., WARTH, M. R., CHARLES, D., CHILDS, M., LI, J. R., MABUCHI, H. & VAN ALLEN, M. I. 1986. Lipoprotein metabolism in pregnancy, fat transport to the fetus, and the effects of diabetes. *Neonatology,* 50**,** 297-317.
KNUDSEN, J. G., MURHOLM, M., CAREY, A. L., BIENSØ, R. S., BASSE, A. L., ALLEN, T. L., HIDALGO, J., KINGWELL, B. A., FEBBRAIO, M. A. & HANSEN, J. B. 2014. Role of IL-6 in exercise training-and cold-induced UCP1 expression in subcutaneous white adipose tissue. *PloS one,* 9**,** e84910.
KOUPIL, I. & TOIVANEN, P. 2008. Social and early-life determinants of overweight and obesity in 18-year-old Swedish men. *International Journal of Obesity,* 32**,** 73.
KRIEF, S., LÖNNQVIST, F., RAIMBAULT, S., BAUDE, B., VAN SPRONSEN, A., ARNER, P., STROSBERG, A. D., RICQUIER, D. & EMORINE, L. J. 1993. Tissue distribution of beta 3-adrenergic receptor mRNA in man. *The Journal of clinical investigation,* 91**,** 344-349.
KWOK, K. H. M., LAM, K. S. L. & XU, A. 2016. Heterogeneity of white adipose tissue: molecular basis and clinical implications. *Experimental &Amp; Molecular Medicine,* 48**,** e215.
LABBÉ, S. M., CARON, A., LANFRAY, D., MONGE-ROFARELLO, B., BARTNESS, T. J. & RICHARD, D. 2015. Hypothalamic control of brown adipose tissue thermogenesis. *Frontiers in systems neuroscience,* 9**,** 150.
LAIN, K. Y. & CATALANO, P. M. 2007. Metabolic changes in pregnancy. *Clinical obstetrics and gynecology,* 50**,** 938-948.
LANDSBERG, L., ARONNE, L. J., BEILIN, L. J., BURKE, V., IGEL, L. I., LLOYD-JONES, D. & SOWERS, J. J. T. J. O. C. H. 2013. Obesity-related hypertension: pathogenesis, cardiovascular risk, and treatment: a position paper of the Obesity Society and the American Society of Hypertension. 15**,** 14-33.
LANGLEY-EVANS, S. C. & NWAGWU, M. 1998. Impaired growth and increased glucocorticoid-sensitive enzyme activities in tissues of rat fetuses exposed to maternal low protein diets. *Life sciences,* 63**,** 605-615.
LARA-CASTRO, C., WEINSIER, R. L., HUNTER, G. R. & DESMOND, R. J. O. R. 2002. Visceral adipose tissue in women: longitudinal study of the effects of fat gain, time, and race. 10**,** 868-874.
LAWRENCE, T. 2009. The nuclear factor NF-κB pathway in inflammation. *Cold Spring Harbor perspectives in biology***,** a001651.
LEAN, M., JAMES, W., JENNINGS, G. & TRAYHURN, P. 1986. Brown adipose tissue in patients with phaeochromocytoma. *International journal of obesity,* 10**,** 219-227.
LEE, H. J. & ORMANDY, C. J. 2012. Elf5, hormones and cell fate. *Trends in Endocrinology & Metabolism,* 23**,** 292-298.
LEE, J.-Y., TAKAHASHI, N., YASUBUCHI, M., KIM, Y.-I., HASHIZAKI, H., KIM, M.-J., SAKAMOTO, T., GOTO, T. & KAWADA, T. 2011. Triiodothyronine induces UCP-1 expression and mitochondrial biogenesis in human adipocytes. *American Journal of Physiology-Cell Physiology,* 302**,** C463-C472.
LEE, Y. S., KIM, J.-W., OSBORNE, O., SASIK, R., SCHENK, S., CHEN, A., CHUNG, H., MURPHY, A., WATKINS, S. M. & QUEHENBERGER, O. 2014. Increased adipocyte O 2 consumption triggers HIF-1α, causing inflammation and insulin resistance in obesity. *Cell,* 157**,** 1339-1352.
LI, C., KAUR, H., CHOI, W. S., HUANG, T. T. K., LEE, R. E. & AHLUWALIA, J. S. 2005. Additive interactions of maternal prepregnancy BMI and breast-feeding on childhood overweight. *Obesity research,* 13**,** 362-371.
LIEBERMAN, M. & MARKS, A. D. 2009. *Marks' basic medical biochemistry: a clinical approach*, Lippincott Williams & Wilkins.

LIU, X., ROBINSON, G. W., WAGNER, K.-U., GARRETT, L., WYNSHAW-BORIS, A. & HENNIGHAUSEN, L. 1997. Stat5a is mandatory for adult mammary gland development and lactogenesis. *Genes & development,* 11**,** 179-186.
LIVAK, K. J. & SCHMITTGEN, T. D. 2001. Analysis of relative gene expression data using real-time quantitative PCR and the 2− ΔΔCT method. *methods,* 25**,** 402-408.
LO, K. A. & SUN, L. 2013. Turning WAT into BAT: a review on regulators controlling the browning of white adipocytes. *Bioscience reports,* 33**,** e00065.
LONG, J. Z., SVENSSON, K. J., TSAI, L., ZENG, X., ROH, H. C., KONG, X., RAO, R. R., LOU, J., LOKURKAR, I. & BAUR, W. 2014. A smooth muscle-like origin for beige adipocytes. *Cell metabolism,* 19**,** 810-820.
LOWELL, B. B. & BACHMAN, E. S. 2003. β-Adrenergic receptors, diet-induced thermogenesis, and obesity. *Journal of Biological Chemistry,* 278**,** 29385-29388.
LUKASZEWSKI, M.-A., EBERLÉ, D., VIEAU, D. & BRETON, C. 2013. Nutritional manipulations in the perinatal period program adipose tissue in offspring. *American Journal of Physiology-Endocrinology and Metabolism,* 305**,** E1195-E1207.
LUMENG, C. N., BODZIN, J. L. & SALTIEL, A. R. 2007a. Obesity induces a phenotypic switch in adipose tissue macrophage polarization. *The Journal of clinical investigation,* 117**,** 175-184.
LUMENG, C. N., DEYOUNG, S. M., BODZIN, J. L. & SALTIEL, A. R. 2007b. Increased inflammatory properties of adipose tissue macrophages recruited during diet-induced obesity. *Diabetes,* 56**,** 16-23.
MAACHI, M., PIERONI, L., BRUCKERT, E., JARDEL, C., FELLAHI, S., HAINQUE, B., CAPEAU, J. & BASTARD, J. 2004. Systemic low-grade inflammation is related to both circulating and adipose tissue TNFα, leptin and IL-6 levels in obese women. *International journal of obesity,* 28**,** 993.
MAEKAWA, R., SEINO, Y., OGATA, H., MURASE, M., IIDA, A., HOSOKAWA, K., JOO, E., HARADA, N., TSUNEKAWA, S. & HAMADA, Y. 2017. Chronic high-sucrose diet increases fibroblast growth factor 21 production and energy expenditure in mice. *The Journal of nutritional biochemistry,* 49**,** 71-79.
MAFFEI, M., FEI, H., LEE, G.-H., DANI, C., LEROY, P., ZHANG, Y., PROENCA, R., NEGREL, R., AILHAUD, G. & FRIEDMAN, J. M. 1995. Increased expression in adipocytes of ob RNA in mice with lesions of the hypothalamus and with mutations at the db locus. *Proceedings of the National Academy of Sciences,* 92**,** 6957-6960.
MAGNUSON, A., FOUTS, J., BOOTH, A. & FOSTER, M. 2015. Obesity-induced chronic low grade inflammation: Gastrointestinal and adipose tissue crosstalk. *Integrative Obesity and Diabetes,* 1**,** 103-108.
MAHMOOD, T. & YANG, P.-C. 2012. Western blot: technique, theory, and trouble shooting. *North American journal of medical sciences,* 4**,** 429.
MARCADENTI, A., FUCHS, F. D., MATTE, U., SPERB, F., MOREIRA, L. B. & FUCHS, S. C. J. C. D. 2013. Effects of FTO RS9939906 and MC4R RS17782313 on obesity, type 2 diabetes mellitus and blood pressure in patients with hypertension. 12**,** 103.
MARTINEAU, L. & JACOBS, I. 1988. Muscle glycogen utilization during shivering thermogenesis in humans. *Journal of Applied Physiology,* 65**,** 2046-2050.
MASSO-WELCH, P. A., DARCY, K. M., STANGLE-CASTOR, N. C. & IP, M. M. 2000. A developmental atlas of rat mammary gland histology. *Journal of mammary gland biology and neoplasia,* 5**,** 165-185.
MATSUZAWA, Y., SHIMOMURA, I., NAKAMURA, T., KENO, Y., KOTANI, K. & TOKUNAGA, K. 1995. Pathophysiology and pathogenesis of visceral fat obesity. *Obesity research,* 3**,** 187s-194s.
MATTHIAS, A., OHLSON, K. B., FREDRIKSSON, J. M., JACOBSSON, A., NEDERGAARD, J. & CANNON, B. 2000. Thermogenic responses in brown fat cells are fully Ucp1-dependent UCP2 or UCP3 do not substitute for UCP1 in adrenergically or fatty acid-induced thermogenesis. *Journal of Biological Chemistry,* 275**,** 25073-25081.

MCILVRIDE, S., MUSHTAQ, A., PAPACLEOVOULOU, G., HURLING, C., STEEL, J., JANSEN, E., ABU-HAYYEH, S. & WILLIAMSON, C. 2017. A progesterone-brown fat axis is involved in regulating fetal growth. *Scientific reports,* 7**,** 10671.
MCMANUS, L. M. & MITCHELL, R. N. 2014. *Pathobiology of human disease: a dynamic encyclopedia of disease mechanisms*, Elsevier.
MERCER, S. W. & TRAYHURN, P. 1987. Effect of high fat diets on energy balance and thermogenesis in brown adipose tissue of lean and genetically obese ob/ob mice. *The Journal of nutrition,* 117**,** 2147-2153.
METZGER, D. E., STAHLMAN, M. T. & SHANNON, J. M. 2008. Misexpression of ELF5 disrupts lung branching and inhibits epithelial differentiation. *Developmental biology,* 320**,** 149-160.
MILLS, J. L., JOVANOVIC, L., KNOPP, R., AARONS, J., CONLEY, M., PARK, E., LEE, Y. J., HOLMES, L., SIMPSON, J. L. & METZGER, B. 1998. Physiological reduction in fasting plasma glucose concentration in the first trimester of normal pregnancy: the diabetes in early pregnancy study. *Metabolism-Clinical and Experimental,* 47**,** 1140-1144.
MINOKOSHI, Y., ALQUIER, T., FURUKAWA, N., KIM, Y.-B., LEE, A., XUE, B., MU, J., FOUFELLE, F., FERRÉ, P. & BIRNBAUM, M. J. 2004. AMP-kinase regulates food intake by responding to hormonal and nutrient signals in the hypothalamus. *Nature,* 428**,** 569.
MOHELL, N. 1984. Alpha 1-adrenergic receptors in brown adipose tissue. Thermogenic significance and mode of action.
MOR, G. & CARDENAS, I. 2010. The immune system in pregnancy: a unique complexity. *American journal of reproductive immunology,* 63**,** 425-433.
MORRONI, M., GIORDANO, A., ZINGARETTI, M. C., BOIANI, R., DE MATTEIS, R., KAHN, B. B., NISOLI, E., TONELLO, C., PISOSCHI, C. & LUCHETTI, M. M. 2004. Reversible transdifferentiation of secretory epithelial cells into adipocytes in the mammary gland. *Proceedings of the National Academy of Sciences,* 101**,** 16801-16806.
MOTTILLO, E. P., RAMSEYER, V. D. & GRANNEMAN, J. G. 2018. SERCA2b Cycles Its Way to UCP1-Independent Thermogenesis in Beige Fat. *Cell metabolism,* 27**,** 7-9.
MOUNZIH, K., QIU, J., EWART-TOLAND, A. & CHEHAB, F. F. 1998. Leptin is not necessary for gestation and parturition but regulates maternal nutrition via a leptin resistance state. *Endocrinology,* 139**,** 5259-5262.
MÜHLHÄUSLER, B., MCMILLEN, I. C., ROUZAUD, G., FINDLAY, P., MARROCCO, E., RHIND, S. & ADAM, C. L. 2004. Appetite regulatory neuropeptides are expressed in the sheep hypothalamus before birth. *Journal of neuroendocrinology,* 16**,** 502-507.
MUZZIN, P., REVELLI, J., KUHNE, F., GOCAYNE, J., MCCOMBIE, W., VENTER, J., GIACOBINO, J. & FRASER, C. 1991. An adipose tissue-specific beta-adrenergic receptor. Molecular cloning and down-regulation in obesity. *Journal of Biological Chemistry,* 266**,** 24053-24058.
NAKAMURA, K., MORRISON, S. F. J. A. J. O. P.-R., INTEGRATIVE & PHYSIOLOGY, C. 2007. Central efferent pathways mediating skin cooling-evoked sympathetic thermogenesis in brown adipose tissue. 292**,** R127-R136.
NEDERGAARD, J. & CANNON, B. 2010. The changed metabolic world with human brown adipose tissue: therapeutic visions. *Cell metabolism,* 11**,** 268-272.
NEDERGAARD, J. & CANNON, B. 2014. The browning of white adipose tissue: some burning issues. *Cell metabolism,* 20**,** 396-407.
NELSON, S. M., MATTHEWS, P. & POSTON, L. 2009. Maternal metabolism and obesity: modifiable determinants of pregnancy outcome. *Human reproduction update,* 16**,** 255-275.
NICKERSON, J. G., ALKHATEEB, H., BENTON, C. R., LALLY, J., NICKERSON, J., HAN, X.-X., WILSON, M. H., JAIN, S. S., SNOOK, L. A. & GLATZ, J. F. 2009. Greater transport efficiencies of the membrane fatty acid transporters FAT/CD36 and FATP4 than FABPPM and FATP, and differential effects on fatty acid esterification

and oxidation in rat skeletal muscle. *Journal of Biological Chemistry*, jbc. M109. 004788.
NIVOIT, P., MORENS, C., VAN ASSCHE, F., JANSEN, E., POSTON, L., REMACLE, C. & REUSENS, B. 2009. Established diet-induced obesity in female rats leads to offspring hyperphagia, adiposity and insulin resistance. *Diabetologia,* 52**,** 1133-1142.
NORRIS, D. O. & CARR, J. A. 2013. *Vertebrate endocrinology*, Academic Press.
NYGARD, A.-B., JØRGENSEN, C. B., CIRERA, S. & FREDHOLM, M. 2007. Selection of reference genes for gene expression studies in pig tissues using SYBR green qPCR. *BMC molecular biology,* 8**,** 67.
OBSTETRICS, I. J. O. G. 1995. Diabetes and pregnancy. *International Journal of Gynecology & Obstetrics,* 48**,** 331-339.
OHKUMA, T., HIRAKAWA, Y., NAKAMURA, U., KIYOHARA, Y., KITAZONO, T. & NINOMIYA, T. J. I. J. O. O. 2015. Association between eating rate and obesity: a systematic review and meta-analysis. 39**,** 1589.
OHLSON, K., MOHELL, N., CANNON, B., LINDAHL, S. & NEDERGAARD, J. 1994. Thermogenesis in brown adipocytes is inhibited by volatile anesthetic agents. A factor contributing to hypothermia in infants? *Anesthesiology,* 81**,** 176-183.
OHNO, H., SHINODA, K., SPIEGELMAN, B. M. & KAJIMURA, S. 2012. PPARγ agonists induce a white-to-brown fat conversion through stabilization of PRDM16 protein. *Cell metabolism,* 15**,** 395-404.
OKAMATSU-OGURA, Y., FUKANO, K., TSUBOTA, A., UOZUMI, A., TERAO, A., KIMURA, K. & SAITO, M. 2013. Thermogenic ability of uncoupling protein 1 in beige adipocytes in mice. *PloS one,* 8**,** e84229.
OKLA, M., KIM, J., KOEHLER, K. & CHUNG, S. 2017. Dietary factors promoting brown and beige fat development and thermogenesis. *Advances in Nutrition,* 8**,** 473-483.
OUELLET, V., LABBÉ, S. M., BLONDIN, D. P., PHOENIX, S., GUÉRIN, B., HAMAN, F., TURCOTTE, E. E., RICHARD, D. & CARPENTIER, A. C. 2012. Brown adipose tissue oxidative metabolism contributes to energy expenditure during acute cold exposure in humans. *The Journal of clinical investigation,* 122**,** 545-552.
OUELLET, V., ROUTHIER-LABADIE, A., BELLEMARE, W., LAKHAL-CHAIEB, L., TURCOTTE, E., CARPENTIER, A. C. & RICHARD, D. 2011. Outdoor temperature, age, sex, body mass index, and diabetic status determine the prevalence, mass, and glucose-uptake activity of 18F-FDG-detected BAT in humans. *The Journal of Clinical Endocrinology & Metabolism,* 96**,** 192-199.
OVALLE, W. K. & NAHIRNEY, P. C. 2013. *Netter's Essential Histology E-Book*, Elsevier Health Sciences.
PALOU, M., PRIEGO, T., SÁNCHEZ, J., RODRÍGUEZ, A. M., PALOU, A. & PICÓ, C. 2009. Gene expression patterns in visceral and subcutaneous adipose depots in rats are linked to their morphologic features. *Cellular Physiology and Biochemistry,* 24**,** 547-556.
PASARICA, M., SEREDA, O. R., REDMAN, L. M., ALBARADO, D. C., HYMEL, D. T., ROAN, L. E., ROOD, J. C., BURK, D. H. & SMITH, S. R. 2009. Reduced adipose tissue oxygenation in human obesity: evidence for rarefaction, macrophage chemotaxis, and inflammation without an angiogenic response. *Diabetes,* 58**,** 718-725.
PASCHOS, G. K., TANG, S. Y., THEKEN, K. N., LI, X., VERGINADIS, I., LEKKAS, D., HERMAN, L., YAN, W., LAWSON, J. & FITZGERALD, G. A. 2018. Cold-induced browning of inguinal white adipose tissue is independent of adipose tissue cyclooxygenase-2. *Cell reports,* 24**,** 809-814.
PEIRSON, S. N., BUTLER, J. N. & FOSTER, R. G. 2003. Experimental validation of novel and conventional approaches to quantitative real-time PCR data analysis. *Nucleic acids research,* 31**,** e73-e73.
PELLEYMOUNTER, M. A., CULLEN, M. J., BAKER, M. B., HECHT, R., WINTERS, D., BOONE, T. & COLLINS, F. 1995. Effects of the obese gene product on body weight regulation in ob/ob mice. *Science,* 269**,** 540-543.

PETROVIC, N., WALDEN, T. B., SHABALINA, I. G., TIMMONS, J. A., CANNON, B. & NEDERGAARD, J. 2010. Chronic peroxisome proliferator-activated receptor γ (PPARγ) activation of epididymally derived white adipocyte cultures reveals a population of thermogenically competent, UCP1-containing adipocytes molecularly distinct from classic brown adipocytes. *Journal of Biological Chemistry,* 285**,** 7153-7164.

PICO, C., BONET, M. & PALOU, A. 1998. Stimulation of uncoupling protein synthesis in white adipose tissue of mice treated with the β3-adrenergic agonist CGP-12177. *Cellular and Molecular Life Sciences CMLS,* 54**,** 191-195.

PILLAY, V., CROWTHER, N., RAMSAY, M., SMITH, G., NORRIS, S., LOMBARD, Z. J. N. & DIABETES 2015. Exploring genetic markers of adult obesity risk in black adolescent South Africans—the Birth to Twenty Cohort. 5**,** e157.

POGGIOLI, R., UETA, C. B., E DRIGO, R. A., CASTILLO, M., FONSECA, T. L. & BIANCO, A. C. 2013. Dexamethasone reduces energy expenditure and increases susceptibility to diet-induced obesity in mice. *Obesity,* 21**,** E415-E420.

POHER, A.-L., VEYRAT-DUREBEX, C., ALTIRRIBA, J., MONTET, X., COLIN, D. J., CAILLON, A., LYAUTEY, J. & ROHNER-JEANRENAUD, F. 2015. Ectopic UCP1 overexpression in white adipose tissue improves insulin sensitivity in Lou/C rats, a model of obesity resistance. *Diabetes***,** db150210.

POULAIN-GODEFROY, O., LECOEUR, C., PATTOU, F., FRUHBECK, G. & FROGUEL, P. 2008. Inflammation is associated with a decrease of lipogenic factors in omental fat in women. *American Journal of Physiology-Regulatory, Integrative and Comparative Physiology,* 295**,** R1-R7.

PREVIS, S. F., WITHERS, D. J., REN, J.-M., WHITE, M. F. & SHULMAN, G. I. 2000. Contrasting effects of IRS-1 vs IRS-2 gene disruption on carbohydrate and lipid metabolism in vivo. *Journal of Biological Chemistry*.

PROKESCH, A., SMORLESI, A., PERUGINI, J., MANIERI, M., CIARMELA, P., MONDINI, E., TRAJANOSKI, Z., KRISTIANSEN, K., GIORDANO, A. & BOGNER-STRAUSS, J. G. 2014. Molecular aspects of adipoepithelial transdifferentiation in mouse mammary gland. *Stem Cells,* 32**,** 2756-2766.

PRUNET-MARCASSUS, B., COUSIN, B., CATON, D., ANDRÉ, M., PÉNICAUD, L. & CASTEILLA, L. 2006. From heterogeneity to plasticity in adipose tissues: site-specific differences. *Experimental cell research,* 312**,** 727-736.

PUIGSERVER, P., WU, Z., PARK, C. W., GRAVES, R., WRIGHT, M. & SPIEGELMAN, B. M. 1998. A cold-inducible coactivator of nuclear receptors linked to adaptive thermogenesis. *Cell,* 92**,** 829-839.

QIAO, L., LEE, S., NGUYEN, A., HAY JR, W. W. & SHAO, J. 2018. The Regulatory Effects of Brown Adipose Tissue Thermogenesis on Maternal Metabolic Adaptation, Placental Efficiency, and Fetal Growth in Mice. *American Journal of Physiology-Endocrinology and Metabolism*.

RAMOS-VARA, J. 2005. Technical aspects of immunohistochemistry. *Veterinary pathology,* 42**,** 405-426.

RANDHAWA, M., HUFF, T., VALENCIA, J. C., YOUNOSSI, Z., CHANDHOKE, V., HEARING, V. J. & BARANOVA, A. 2009. Evidence for the ectopic synthesis of melanin in human adipose tissue. *The FASEB Journal,* 23**,** 835-843.

RAVELLI, A. C., VAN DER MEULEN, J. H., MICHELS, R., OSMOND, C., BARKER, D. J., HALES, C. & BLEKER, O. P. 1998. Glucose tolerance in adults after prenatal exposure to famine. *The Lancet,* 351**,** 173-177.

RAVELLI, A. C., VAN DER MEULEN, J. H., OSMOND, C., BARKER, D. J. & BLEKER, O. P. 1999. Obesity at the age of 50 y in men and women exposed to famine prenatally–. *The American journal of clinical nutrition,* 70**,** 811-816.

RENEHAN, A. G., ZWAHLEN, M. & EGGER, M. J. N. R. C. 2015. Adiposity and cancer risk: new mechanistic insights from epidemiology. 15**,** 484.

RICHARD, D. J. N. R. E. 2015. Cognitive and autonomic determinants of energy homeostasis in obesity. 11**,** 489.

ROBERTSON, A. F. & SPRECHER, H. 1968. A review of human placental lipid metabolism and transport. *Acta Pædiatrica,* 57**,** 1-18.
ROGERS, G. W., BRAND, M. D., PETROSYAN, S., ASHOK, D., ELORZA, A. A., FERRICK, D. A. & MURPHY, A. N. 2011. High throughput microplate respiratory measurements using minimal quantities of isolated mitochondria. *PloS one,* 6**,** e21746.
ROGERS, N. H., LANDA, A., PARK, S. & SMITH, R. G. 2012. Aging leads to a programmed loss of brown adipocytes in murine subcutaneous white adipose tissue. *Aging cell,* 11**,** 1074-1083.
ROLLS, B., GURR, M., VAN DUIJVENVOORDE, P., ROLLS, B. J. & ROWE, E. 1986. Lactation in lean and obese rats: effect of cafeteria feeding and of dietary obesity on milk composition. *Physiology & behavior,* 38**,** 185-190.
RONDINONE, C. M., WANG, L.-M., LONNROTH, P., WESSLAU, C., PIERCE, J. H. & SMITH, U. 1997. Insulin receptor substrate (IRS) 1 is reduced and IRS-2 is the main docking protein for phosphatidylinositol 3-kinase in adipocytes from subjects with non-insulin-dependent diabetes mellitus. *Proceedings of the National Academy of Sciences,* 94**,** 4171-4175.
ROSELL, M., KAFOROU, M., FRONTINI, A., OKOLO, A., CHAN, Y.-W., NIKOLOPOULOU, E., MILLERSHIP, S., FENECH, M. E., MACINTYRE, D. & TURNER, J. O. 2014. Brown and white adipose tissues: intrinsic differences in gene expression and response to cold exposure in mice. *American Journal of Physiology-Endocrinology and Metabolism,* 306**,** E945-E964.
ROSEN, E. D. 2005. The transcriptional basis of adipocyte development. *Prostaglandins, Leukotrienes and Essential Fatty Acids,* 73**,** 31-34.
ROSEN, E. D. & SPIEGELMAN, B. M. 2006. Adipocytes as regulators of energy balance and glucose homeostasis. *Nature,* 444**,** 847.
ROTHWELL, N., STOCK, M. & STRIBLING, D. 1982. Diet-induced thermogenesis. *Pharmacology & therapeutics,* 17**,** 251-268.
ROTHWELL, N. J. & STOCK, M. J. 1979. A role for brown adipose tissue in diet-induced thermogenesis. *Nature,* 281**,** 31.
ROTHWELL, N. J. & STOCK, M. J. 1981a. Brown adipose tissue and diet-induced thermogenesis (reply). *Nature,* 289**,** 699.
ROTHWELL, N. J. & STOCK, M. J. 1981b. Influence of noradrenaline on blood flow to brown adipose tissue in rats exhibiting diet-induced thermogenesis. *Pflügers Archiv European Journal of Physiology,* 389**,** 237-242.
RYAN, E. A., O'SULLIVAN, M. J. & SKYLER, J. S. 1985. Insulin action during pregnancy: studies with the euglycemic clamp technique. *Diabetes,* 34**,** 380-389.
SAIKI, R. K., GELFAND, D. H., STOFFEL, S., SCHARF, S. J., HIGUCHI, R., HORN, G. T., MULLIS, K. B. & ERLICH, H. A. 1988. Primer-directed enzymatic amplification of DNA with a thermostable DNA polymerase. *Science,* 239**,** 487-491.
SAITO, M., OKAMATSU-OGURA, Y., MATSUSHITA, M., WATANABE, K., YONESHIRO, T., NIO-KOBAYASHI, J., IWANAGA, T., MIYAGAWA, M., KAMEYA, T. & NAKADA, K. 2009. High incidence of metabolically active brown adipose tissue in healthy adult humans: effects of cold exposure and adiposity. *Diabetes*.
SAITO, M. & YONESHIRO, T. 2013. Capsinoids and related food ingredients activating brown fat thermogenesis and reducing body fat in humans. *Current opinion in lipidology,* 24**,** 71-77.
SALTIEL, A. R. & KAHN, C. R. 2001. Insulin signalling and the regulation of glucose and lipid metabolism. *Nature,* 414**,** 799.
SCHÄFER, M.-H., EIDEN, L. & WEIHE, E. J. N. 1998. Cholinergic neurons and terminal fields revealed by immunohistochemistry for the vesicular acetylcholine transporter. II. The peripheral nervous system. 84**,** 361-376.
SCHUTZ, Y., BESSARD, T. & JEQUIER, E. 1984. Diet-induced thermogenesis measured over a whole day in obese and nonobese women. *The American journal of clinical nutrition,* 40**,** 542-552.

SCHWARTZ, M. W., PESKIND, E., RASKIND, M., BOYKO, E. J. & PORTE JR, D. J. N. M. 1996. Cerebrospinal fluid leptin levels: relationship to plasma levels and to adiposity in humans. 2**,** 589.
SCIMÈ, A., GRENIER, G., HUH, M. S., GILLESPIE, M. A., BEVILACQUA, L., HARPER, M.-E. & RUDNICKI, M. A. 2005. Rb and p107 regulate preadipocyte differentiation into white versus brown fat through repression of PGC-1α. *Cell metabolism,* 2**,** 283-295.
SCOTT, C. B. & DEVORE, R. 2005. Diet-induced thermogenesis: variations among three isocaloric meal-replacement shakes. *Nutrition,* 21**,** 874-877.
SEALE, P., BJORK, B., YANG, W., KAJIMURA, S., CHIN, S., KUANG, S., SCIME, A., DEVARAKONDA, S., CONROE, H. M. & ERDJUMENT-BROMAGE, H. 2008. PRDM16 controls a brown fat/skeletal muscle switch. *Nature,* 454**,** 961.
SEALE, P., CONROE, H. M., ESTALL, J., KAJIMURA, S., FRONTINI, A., ISHIBASHI, J., COHEN, P., CINTI, S. & SPIEGELMAN, B. M. 2011. Prdm16 determines the thermogenic program of subcutaneous white adipose tissue in mice. *The Journal of clinical investigation,* 121**,** 96-105.
SEALE, P., KAJIMURA, S., YANG, W., CHIN, S., ROHAS, L. M., ULDRY, M., TAVERNIER, G., LANGIN, D. & SPIEGELMAN, B. M. 2007. Transcriptional control of brown fat determination by PRDM16. *Cell metabolism,* 6**,** 38-54.
SELL, H., BERGER, J. P., SAMSON, P., CASTRIOTA, G., LALONDE, J. E., DESHAIES, Y. & RICHARD, D. 2004. Peroxisome proliferator-activated receptor γ agonism increases the capacity for sympathetically mediated thermogenesis in lean and ob/ob mice. *Endocrinology,* 145**,** 3925-3934.
SENGUPTA, P. 2013. The laboratory rat: relating its age with human's. *International journal of preventive medicine,* 4**,** 624.
SEWELL, M. F., HUSTON-PRESLEY, L., SUPER, D. M. & CATALANO, P. 2006. Increased neonatal fat mass, not lean body mass, is associated with maternal obesity. *American journal of obstetrics and gynecology,* 195**,** 1100-1103.
SHABALINA, I. G., PETROVIC, N., DE JONG, J. M., KALINOVICH, A. V., CANNON, B. & NEDERGAARD, J. 2013. UCP1 in brite/beige adipose tissue mitochondria is functionally thermogenic. *Cell reports,* 5**,** 1196-1203.
SHANKAR, K., HARRELL, A., LIU, X., GILCHRIST, J. M., RONIS, M. J. & BADGER, T. M. 2008. Maternal obesity at conception programs obesity in the offspring. *American Journal of Physiology-Regulatory, Integrative and Comparative Physiology,* 294**,** R528-R538.
SHIN, H., MA, Y., CHANTURIYA, T., CAO, Q., WANG, Y., KADEGOWDA, A. K., JACKSON, R., RUMORE, D., XUE, B. & SHI, H. 2017. Lipolysis in brown adipocytes is not essential for cold-induced thermogenesis in mice. *Cell metabolism,* 26**,** 764-777. e5.
SHORE, A. M., KARAMITRI, A., KEMP, P., SPEAKMAN, J. R., GRAHAM, N. S. & LOMAX, M. A. 2013. Cold-induced changes in gene expression in brown adipose tissue, white adipose tissue and liver. *PloS one,* 8**,** e68933.
SIDOSSIS, L. S., PORTER, C., SARAF, M. K., BØRSHEIM, E., RADHAKRISHNAN, R. S., CHAO, T., ALI, A., CHONDRONIKOLA, M., MLCAK, R. & FINNERTY, C. C. J. C. M. 2015. Browning of subcutaneous white adipose tissue in humans after severe adrenergic stress. 22**,** 219-227.
SIEGRIST-KAISER, C. A., PAULI, V., JUGE-AUBRY, C. E., BOSS, O., PERNIN, A., CHIN, W. W., CUSIN, I., ROHNER-JEANRENAUD, F., BURGER, A. G. & ZAPF, J. 1997. Direct effects of leptin on brown and white adipose tissue. *The journal of clinical investigation,* 100**,** 2858-2864.
SIEMELINK, M., VERHOEF, A., DORMANS, J., SPAN, P. & PIERSMA, A. 2002. Dietary fatty acid composition during pregnancy and lactation in the rat programs growth and glucose metabolism in the offspring. *Diabetologia,* 45**,** 1397-1403.
SILVER, N., BEST, S., JIANG, J. & THEIN, S. L. 2006. Selection of housekeeping genes for gene expression studies in human reticulocytes using real-time PCR. *BMC Molecular Biology,* 7**,** 33.

SMALL, L., GONG, H., YASSMIN, C., COONEY, G. J. & BRANDON, A. E. 2018. Thermoneutral housing does not influence fat mass or glucose homeostasis in C57BL/6 mice. *Journal of Endocrinology,* 239**,** 313-324.
SMITH-KIRWIN, S. M., O'CONNOR, D. M., JOHNSTON, J., DE LANCY, E., HASSINK, S. G. & FUNANAGE, V. L. 1998. Leptin expression in human mammary epithelial cells and breast milk. *The Journal of Clinical Endocrinology & Metabolism,* 83**,** 1810-1810.
SOLOFF, M. S., ALEXANDROVA, M. & FERNSTROM, M. J. 1979. Oxytocin receptors: triggers for parturition and lactation? *Science,* 204**,** 1313-1315.
SOMERSET, D. A., ZHENG, Y., KILBY, M. D., SANSOM, D. M. & DRAYSON, M. T. 2004. Normal human pregnancy is associated with an elevation in the immune suppressive CD25+ CD4+ regulatory T-cell subset. *Immunology,* 112**,** 38-43.
SOTTILE, V. & SEUWEN, K. 2000. Bone morphogenetic protein-2 stimulates adipogenic differentiation of mesenchymal precursor cells in synergy with BRL 49653 (rosiglitazone). *FEBS letters,* 475**,** 201-204.
SPIEGELMAN, B. 1998. PPAR-gamma: adipogenic regulator and thiazolidinedione receptor. *Diabetes,* 47**,** 507-514.
SPITALNIK, P. F. 2016. *Histology Laboratory Manual*, College of Physicians and Surgeons Columbia University.
STANFORD, K. I., MIDDELBEEK, R. J., TOWNSEND, K. L., AN, D., NYGAARD, E. B., HITCHCOX, K. M., MARKAN, K. R., NAKANO, K., HIRSHMAN, M. F. & TSENG, Y.-H. 2012. Brown adipose tissue regulates glucose homeostasis and insulin sensitivity. *The Journal of clinical investigation,* 123.
STEINGRIMSDOTTIR, L., BRASEL, J. A. & GREENWOOD, M. 1980. Diet, pregnancy, and lactation: effects on adipose tissue, lipoprotein lipase, and fat cell size. *Metabolism-Clinical and Experimental,* 29**,** 837-841.
STRAUB, R. H. 2007. The complex role of estrogens in inflammation. *Endocrine reviews,* 28**,** 521-574.
STUEBE, A. M., FORMAN, M. R. & MICHELS, K. B. 2009. Maternal-recalled gestational weight gain, pre-pregnancy body mass index, and obesity in the daughter. *International journal of obesity,* 33**,** 743.
SU, X. & ABUMRAD, N. A. 2009. Cellular fatty acid uptake: a pathway under construction. *Trends in Endocrinology & Metabolism,* 20**,** 72-77.
SUÁREZ-TRUJILLO, A. & CASEY, T. M. 2016. Serotoninergic and circadian systems: driving mammary gland development and function. *Frontiers in physiology,* 7**,** 301.
SYMONDS, M. E. & BUDGE, H. 2009. Nutritional models of the developmental programming of adult health and disease: Workshop on 'Nutritional models of the developmental origins of adult health and disease'. *Proceedings of the Nutrition Society,* 68**,** 173-178.
SYMONDS, M. E., SEBERT, S. & BUDGE, H. J. F. I. G. 2011. The obesity epidemic: from the environment to epigenetics–not simply a response to dietary manipulation in a thermoneutral environment. 2**,** 24.
SYMONDS, M. E., SEBERT, S. P. & BUDGE, H. 2009. The impact of diet during early life and its contribution to later disease: critical checkpoints in development and their long-term consequences for metabolic health: Symposium on 'Early nutrition and later disease: current concepts, research and implications'. *Proceedings of the Nutrition Society,* 68**,** 416-421.
SYMONDS, M. E., STEPHENSON, T., GARDNER, D. S. & BUDGE, H. 2006. Long-term effects of nutritional programming of the embryo and fetus: mechanisms and critical windows. *Reproduction, Fertility and Development,* 19**,** 53-63.
TAI, M. M., CASTILLO, P. & PI-SUNYER, F. X. 1991. Meal size and frequency: effect on the thermic effect of food. *The American journal of clinical nutrition,* 54**,** 783-787.

TAKAYANAGI, Y., KASAHARA, Y., ONAKA, T., TAKAHASHI, N., KAWADA, T. & NISHIMORI, K. 2008. Oxytocin receptor-deficient mice developed late-onset obesity. *Neuroreport,* 19**,** 951-955.
TAN, N.-S., SHAW, N. S., VINCKENBOSCH, N., LIU, P., YASMIN, R., DESVERGNE, B., WAHLI, W. & NOY, N. 2002. Selective cooperation between fatty acid binding proteins and peroxisome proliferator-activated receptors in regulating transcription. *Molecular and cellular biology,* 22**,** 5114-5127.
TEQUEANES, A. L. L., GIGANTE, D. P., ASSUNÇÃO, M. C. F., CHICA, D. A. G. & HORTA, B. L. 2009. Maternal anthropometry is associated with the body mass index and waist: height ratio of offspring at 23 years of age. *The Journal of nutrition,* 139**,** 750-754.
TERRA, X., AUGUET, T., PORRAS, J. A., QUINTERO, Y., AGUILAR, C., LUNA, A. M., HERNÁNDEZ, M., SABENCH, F., DEL CASTILLO, D. & RICHART, C. 2010. Anti-inflammatory profile of FTO gene expression in adipose tissues from morbidly obese women. *Cellular Physiology and Biochemistry,* 26**,** 1041-1050.
THERMOFISHERSCIENTIFIC. 2019. *https://www.thermofisher.com/uk/en/home/life-science/cloning/cloning-learning-center/invitrogen-school-of-molecular-biology/rt-education/reverse-transcription-applications.html* [Online]. [Accessed april 2019].
THYAGARAJAN, B. & BASKARAN, P. 2017. TRPV1 Expression in Adipose Tissues Determines Metabolic Activity and Energy Expression to Counter Diet-Induced Obesity. *Biophysical Journal,* 112**,** 408a-409a.
TOMIMATSU, T., YAMAGUCHI, M., MURAKAMI, T., OGURA, K., SAKATA, M., MITSUDA, N., KANZAKI, T., KURACHI, H., IRAHARA, M. & MIYAKE, A. 1997. Increase of mouse leptin production by adipose tissue after midpregnancy: gestational profile of serum leptin concentration. *Biochemical and Biophysical Research Communications,* 240**,** 213-215.
TRAYHURN, P. & BEATTIE, J. H. J. P. O. T. N. S. 2001. Physiological role of adipose tissue: white adipose tissue as an endocrine and secretory organ. 60**,** 329-339.
TRAYHURN, P. & WOOD, I. S. 2004. Adipokines: inflammation and the pleiotropic role of white adipose tissue. *British Journal of Nutrition,* 92**,** 347-355.
TSENG, Y.-H., KOKKOTOU, E., SCHULZ, T. J., HUANG, T. L., WINNAY, J. N., TANIGUCHI, C. M., TRAN, T. T., SUZUKI, R., ESPINOZA, D. O. & YAMAMOTO, Y. 2008. New role of bone morphogenetic protein 7 in brown adipogenesis and energy expenditure. *Nature,* 454**,** 1000.
UKROPEC, J., ANUNCIADO, R. P., RAVUSSIN, Y., HULVER, M. W. & KOZAK, L. P. 2006. UCP1-independent thermogenesis in white adipose tissue of cold-acclimated Ucp1-/-mice. *Journal of Biological Chemistry,* 281**,** 31894-31908.
ULDRY, M., YANG, W., ST-PIERRE, J., LIN, J., SEALE, P. & SPIEGELMAN, B. M. 2006. Complementary action of the PGC-1 coactivators in mitochondrial biogenesis and brown fat differentiation. *Cell metabolism,* 3**,** 333-341.
URSINO, M. G., VASINA, V., RASCHI, E., CREMA, F. & DE PONTI, F. 2009. The β3-adrenoceptor as a therapeutic target: current perspectives. *Pharmacological research,* 59**,** 221-234.
VAN DER LANS, A. A., HOEKS, J., BRANS, B., VIJGEN, G. H., VISSER, M. G., VOSSELMAN, M. J., HANSEN, J., JÖRGENSEN, J. A., WU, J. & MOTTAGHY, F. M. J. T. J. O. C. I. 2013. Cold acclimation recruits human brown fat and increases nonshivering thermogenesis. 123**,** 3395-3403.
VAN DER STELT, I., HOEVENAARS, F., ŠIROKÁ, J., DE RONDE, L., FRIEDECKÝ, D., KEIJER, J. & VAN SCHOTHORST, E. 2017. Metabolic response of visceral white adipose tissue of obese mice exposed for 5 days to human room temperature compared to mouse thermoneutrality. *Frontiers in physiology,* 8**,** 179.
VAN HARMELEN, V., LÖNNQVIST, F., THÖRNE, A., WENNLUND, A., LARGE, V., REYNISDOTTIR, S. & ARNER, P. 1997. Noradrenaline-induced lipolysis in isolated mesenteric, omental and subcutaneous adipocytes from obese subjects. *International journal of obesity,* 21**,** 972.

VAN MARKEN LICHTENBELT, W. D., VANHOMMERIG, J. W., SMULDERS, N. M., DROSSAERTS, J. M., KEMERINK, G. J., BOUVY, N. D., SCHRAUWEN, P. & TEULE, G. J. 2009. Cold-activated brown adipose tissue in healthy men. *New England Journal of Medicine,* 360**,** 1500-1508.
VANDESOMPELE, J., DE PRETER, K., PATTYN, F., POPPE, B., VAN ROY, N., DE PAEPE, A. & SPELEMAN, F. 2002. Accurate normalization of real-time quantitative RT-PCR data by geometric averaging of multiple internal control genes. *Genome Biology,* 3**,** research0034.1.
VELICKOVIC, K., LEIJA, H. A. L., BLOOR, I., LAW, J., SACKS, H., SYMONDS, M. & SOTTILE, V. 2018. Low temperature exposure induces browning of bone marrow stem cell derived adipocytes in vitro. *Scientific reports,* 8**,** 4974.
VIJGEN, G. H., BOUVY, N. D., TEULE, G. J., BRANS, B., SCHRAUWEN, P. & VAN MARKEN LICHTENBELT, W. D. 2011. Brown adipose tissue in morbidly obese subjects. *PloS one,* 6**,** e17247.
VIRTANEN, K. A., LIDELL, M. E., ORAVA, J., HEGLIND, M., WESTERGREN, R., NIEMI, T., TAITTONEN, M., LAINE, J., SAVISTO, N.-J. & ENERBÄCK, S. J. N. E. J. O. M. 2009. Functional brown adipose tissue in healthy adults. 360**,** 1518-1525.
VITSEVA, O. I., TANRIVERDI, K., TCHKONIA, T. T., KIRKLAND, J. L., MCDONNELL, M. E., APOVIAN, C. M., FREEDMAN, J. & GOKCE, N. 2008. Inducible Toll-like receptor and NF-κB regulatory pathway expression in human adipose tissue. *Obesity,* 16**,** 932-937.
WADE, G. N., JENNINGS, G. & TRAYHURN, P. 1986. Energy balance and brown adipose tissue thermogenesis during pregnancy in Syrian hamsters. *American Journal of Physiology-Regulatory, Integrative and Comparative Physiology,* 250**,** R845-R850.
WALDÉN, T. B., HANSEN, I. R., TIMMONS, J. A., CANNON, B. & NEDERGAARD, J. 2011. Recruited vs. nonrecruited molecular signatures of brown,"brite," and white adipose tissues. *American Journal of Physiology-Endocrinology and Metabolism,* 302**,** E19-E31.
WANG, H. & SIEMENS, J. 2015. TRP ion channels in thermosensation, thermoregulation and metabolism. *Temperature,* 2**,** 178-187.
WANG, S. P., LAURIN, N., HIMMS-HAGEN, J., RUDNICKI, M. A., LEVY, E., ROBERT, M. F., PAN, L., OLIGNY, L. & MITCHELL, G. A. 2001. The adipose tissue phenotype of hormone-sensitive lipase deficiency in mice. *Obesity research,* 9**,** 119-128.
WANG, X. & WAHL, R. 2014. Responses of the insulin signaling pathways in the brown adipose tissue of rats following cold exposure. *PloS one,* 9**,** e99772.
WARTH, M. R., ARKY, R. A. & KNOPP, R. H. 1975. Lipid metabolism in pregnancy. III. Altered lipid composition in intermediate, very low, low, and high-density lipoprotein fractions. *The Journal of Clinical Endocrinology & Metabolism,* 41**,** 649-655.
WEAVER, R. F. 2012. *Molecular Biology*, McGraw-Hill.
WEISBERG, S. P., MCCANN, D., DESAI, M., ROSENBAUM, M., LEIBEL, R. L. & FERRANTE, A. W. 2003. Obesity is associated with macrophage accumulation in adipose tissue. *The Journal of clinical investigation,* 112**,** 1796-1808.
WERNER, M., CHOTT, A., FABIANO, A. & BATTIFORA, H. 2000. Effect of formalin tissue fixation and processing on immunohistochemistry. *The American journal of surgical pathology,* 24**,** 1016-1019.
WESTERTERP, K., WILSON, S. & ROLLAND, V. 1999. Diet induced thermogenesis measured over 24h in a respiration chamber: effect of diet composition. *International journal of obesity,* 23**,** 287.
WHITAKER, R. C. 2004. Predicting preschooler obesity at birth: the role of maternal obesity in early pregnancy. *Pediatrics,* 114**,** e29-e36.
WHO. 2014. *http://www.who.int/gho/ncd/risk_factors/overweight/en/index1.html* [Online]. [Accessed 10.09.2015].
WHO. 2018. *Obesity and overweight* [Online]. Available: https://www.who.int/news-room/fact-sheets/detail/obesity-and-overweight [Accessed 2018].

WHO. 2019a. *Fact sheets. obesity and overweight* [Online]. Available: https://www.who.int/en/news-room/fact-sheets/detail/obesity-and-overweight [Accessed 2019].
WHO 2019b. Overweight among adults.
WIRSEN, C. 1965. Distribution of adrenergic nerve fibers in brown and white adipose tissue. *Handbook of physiology.* American Physiological Society, Washington, DC.
WITHERS, D. J., GUTIERREZ, J. S., TOWERY, H., BURKS, D. J., REN, J.-M., PREVIS, S., ZHANG, Y., BERNAL, D., PONS, S. & SHULMAN, G. I. 1998. Disruption of IRS-2 causes type 2 diabetes in mice. *Nature,* 391**,** 900.
WOOD, P. A. 2006. *How fat works*, Harvard University Press.
WOZNIAK, S. E., GEE, L. L., WACHTEL, M. S., FREZZA, E. E. J. D. D. & SCIENCES 2009. Adipose tissue: the new endocrine organ? A review article. 54**,** 1847-1856.
WU, J., BOSTRÖM, P., SPARKS, L. M., YE, L., CHOI, J. H., GIANG, A.-H., KHANDEKAR, M., VIRTANEN, K. A., NUUTILA, P. & SCHAART, G. 2012a. Beige adipocytes are a distinct type of thermogenic fat cell in mouse and human. *Cell,* 150**,** 366-376.
WU, J., BOSTRÖM, P., SPARKS, L. M., YE, L., CHOI, J. H., GIANG, A.-H., KHANDEKAR, M., VIRTANEN, K. A., NUUTILA, P. & SCHAART, G. J. C. 2012b. Beige adipocytes are a distinct type of thermogenic fat cell in mouse and human. 150**,** 366-376.
WU, M. V., BIKOPOULOS, G., HUNG, S. & CEDDIA, R. B. 2014. Thermogenic capacity is antagonistically regulated in classical brown and white subcutaneous fat depots by high-fat diet and endurance training in rats: Impact on whole-body energy expenditure. *Journal of Biological Chemistry***,** jbc. M114. 591008.
XIAO, C., GOLDGOF, M., GAVRILOVA, O. & REITMAN, M. L. 2015. Anti-obesity and metabolic efficacy of the β3-adrenergic agonist, CL316243, in mice at thermoneutrality compared to 22° C. *Obesity,* 23**,** 1450-1459.
XU, H., BARNES, G. T., YANG, Q., TAN, G., YANG, D., CHOU, C. J., SOLE, J., NICHOLS, A., ROSS, J. S. & TARTAGLIA, L. A. 2003. Chronic inflammation in fat plays a crucial role in the development of obesity-related insulin resistance. *The Journal of clinical investigation,* 112**,** 1821-1830.
YANG, X., SUI, W., ZHANG, M., DONG, M., LIM, S., SEKI, T., GUO, Z., FISCHER, C., LU, H. & ZHANG, C. 2017. Switching harmful visceral fat to beneficial energy combustion improves metabolic dysfunctions. *JCI insight,* 2.
YE, J. 2011. Adipose tissue vascularization: its role in chronic inflammation. *Current diabetes reports,* 11**,** 203-210.
YE, J., COULOURIS, G., ZARETSKAYA, I., CUTCUTACHE, I., ROZEN, S. & MADDEN, T. L. 2012. Primer-BLAST: a tool to design target-specific primers for polymerase chain reaction. *BMC bioinformatics,* 13**,** 134.
YıLMAZ, M., OZIC, C. & GOK, İ. 2012. Principles of nucleic acid separation by agarose gel electrophoresis. *Gel Electrophoresis-Principles and Basics.* InTech.
ZECHNER, R., KIENESBERGER, P. C., HAEMMERLE, G., ZIMMERMANN, R. & LASS, A. 2009. Adipose triglyceride lipase and the lipolytic catabolism of cellular fat stores. *Journal of lipid research,* 50**,** 3-21.
ZEN, M., GHIRARDELLO, A., IACCARINO, L., TONON, M., CAMPANA, C., ARIENTI, S., RAMPUDDA, M., CANOVA, M. & DORIA, A. 2010. Hormones, immune response, and pregnancy in healthy women and SLE patients. *Swiss Medical Weekly,* 140**,** 187.
ZHANG, M., ZHU, W. & LI, Y. 2014. Small molecule inhibitors of human adipocyte fatty acid binding protein (FABP4). *Medicinal chemistry,* 10**,** 339-347.
ZHAO, J., BRADFIELD, J. P., LI, M., WANG, K., ZHANG, H., KIM, C. E., ANNAIAH, K., GLESSNER, J. T., THOMAS, K. & GARRIS, M. J. O. 2009. The role of obesity-associated loci identified in genome-wide association studies in the determination of pediatric BMI. 17**,** 2254-2257.
ZHOU, J., CHEHAB, R., TKALCEVIC, J., NAYLOR, M. J., HARRIS, J., WILSON, T. J., TSAO, S., TELLIS, I., ZAVARSEK, S. & XU, D. 2005. Elf5 is essential for early embryogenesis and mammary gland development during pregnancy and lactation. *The EMBO journal,* 24**,** 635-644.

ZHOU, J., NG, A. Y., TYMMS, M. J., JERMIIN, L. S., SETH, A. K., THOMAS, R. S. & KOLA, I. 1998. A novel transcription factor, ELF5, belongs to the ELF subfamily of ETS genes and maps to human chromosome 11p13–15, a region subject to LOH and rearrangement in human carcinoma cell lines. *Oncogene,* 17**,** 2719.

ZIMMERMANN, R., STRAUSS, J. G., HAEMMERLE, G., SCHOISWOHL, G., BIRNER-GRUENBERGER, R., RIEDERER, M., LASS, A., NEUBERGER, G., EISENHABER, F. & HERMETTER, A. 2004. Fat mobilization in adipose tissue is promoted by adipose triglyceride lipase. *Science,* 306**,** 1383-1386.

ZINGARETTI, M. C., CROSTA, F., VITALI, A., GUERRIERI, M., FRONTINI, A., CANNON, B., NEDERGAARD, J. & CINTI, S. 2009. The presence of UCP1 demonstrates that metabolically active adipose tissue in the neck of adult humans truly represents brown adipose tissue. *The FASEB Journal,* 23**,** 3113-3120.

ZINGG, H. H. & LAPORTE, S. A. 2003. The oxytocin receptor. *Trends in Endocrinology & Metabolism,* 14**,** 222-227.

ZURIAGA, M. A., FUSTER, J. J., GOKCE, N. & WALSH, K. 2017. Humans and mice display opposing patterns of "browning" gene expression in visceral and subcutaneous white adipose tissue depots. *Frontiers in cardiovascular medicine,* 4**,** 27.

Appendices

Appendix 1 Probes and primers sequences

Probes and primers used for measurements of gene expression. For each gene, the nucleotide sequence of the primer pair is stated, together with the length of the amplicon (in base pairs) and accession number.

Pathway	Gene	Sequence (5'->3')	Product length	Accession number
Thermogenesis	UCP1	GCCTAGCAGACATCATCACCT	147	NM_012682.2
		GTTTCGGCAATCCTTCTGTC		
	PPARG	CCCAATGGTTGCTGATTACA	76	XM_006237009.3
		GGACGCAGGCTCTACTTTGA		
	PGC-1α	Bio-Rad probe qRnoCIP0022855	102	NM_031347
	Leptin	TTCACACACGCAGTCGGTAT	186	XM_008762762.2
		AGGTCTCGCAGGTTCTCCAG		
	β3AR	TAGCAAGGAGCCTGACTTCTG	133	NM_013108.2
		TTCTGGAGAGTTGCGGTTCC		
	VEGFA	TGAGTTAAACGAACGTACTTGCAG	91	NM_001287113.1
		TCTAGTTCCCGAAACCCTGA		
	TRPV1	CATGGGTGAGACCGTCAACA	116	NM_031982.1
		AGGCCTTCCTCATGCACTTC		
	BHSD11	Bio-Rad probe qRnoCEP0023342	103	NM_017080
	SERCA2B	TCATGGACGAGACGCTCAAG	163	NM_001110139.2
		TTCCCCAAGCTCAGTCATGC		
	RYR2	GGAAGTGAAGCAGCCCAAG	71	NM_001191043.1
		TCATCCATGTGTCCATGTAGC		
	IRS-1	GAAGTTCCTTCCGCAGTGTC	155	NM_012969.1

Insulin sensitivity and energy sensing		GTTGCCACCCCTAGACAAAA		
	IRS-2	CTACCCACTGAGCCCAAGAG	151	NM_001168633.1
		CCAGGGATGAAGCAGGACTA		
	mTOR	TGGAGGGAGAGCGTCTGAGA	111	NM_019906.1
		TGATGTGCCGAGGCTTTGT		
	TCF7L2	GTCCACCCACTCACACCTCT	100	NM_001191052.1
		TTCCTGTTTTGGGGTCTACG		
Fat transport	FATP-4	GACTTCTCCAGCCGTTTCCA	93	NM_001100706.1
		CACCTGGCTGTCAAAGTTGC		
	FABP-4	AACTGGGCGTGGAATTCGAT	147	NM_053365.1
		CCAGCTTGTCACCATCTCGT		
	CD36	GCAGCCTCCTTTCCACCTTT	176	NM_001109218.1
		TTGTCTGGGTTCTGGAGTGG		
	LPL	TGGTGGGAAATGATGTGGCC	188	NM_012598.2
		TGCATACTCAAAGTTAGGCCCA		
	ATGL	Bio-Rad probe qRnoCEP0023736	101	NM_001108509
Immune response	TNF	ACGTCGTAGCAAACCACCAA	164	XM_008772775.2
		GCAGCCTTGTCCCTTGAAGA		
	IL-6	ATGGATGCTTCCAAACTGGAT	139	NM_012589.2
		TGAATGACTCTGGCTTTGTCT		
	MCP1	AGCATCCACGTGCTGTCTC	78	NM_031530.1
		GATCATCTTGCCAGTGAATGAG		
		GCAGTTGTAGGAACCTGGTACA		
Housekeeping Genes	YWHAZ	GATGAAGCCATTGCTGAACTTG	117	XM_006241529.3
		GTCTCCTTGGGTATCCGATGTC		
	TBP	TGGGATTGTACCACAGCTCCA	132	XM_006227980.3
		CTCATGATGACTGCAGCAAACC		

Appendix 2 Interscapular brown adipose tissue mass, UCP1 protein and gene expression measurements

Interscapular gene expression measurements of genes of thermogenic, energy regulatory and fat transport pathways of females before and during pregnancy, when kept at either a cool temperature (20°C) or thermoneutrality (27°C), and fed a standard (S) or a high (H) fat and sucrose diet.

	Pregnancy time point (d/g)	**20S**	**20H**	**27S**	**27S**	**P value**
Interscapular BAT mass	0 10 19 P value	0.23 ± 0.01^{ab} 0.35 ± 0.02^{a} 0.42 ± 0.05^{b} *.0043*	0.36 ± 0.05^{c} 0.43 ± 0.04^{d} 0.58 ± 0.04^{cd} *0.0076*	0.28± 0.05 0.28± 0.02 0.33 ± 0.04 *N.S.*	0. 34±0.06 0.33 ± 0.02 0.43 ± 0.04 *N.S.*	*N.S.* *N.S.* *N.S.*
UCP1 Protein	0 10 19 P value	22.54±5.164^{a} 3.33 ±0.732^{a} 11.38± 3.84 *.0257*	32.96±7.744^{b} 18.05±6.55 21.2±6.769 *N.S.*	8.593± 3.155 8.448±2.87 9.185±3.554 *N.S.*	7.597±1.236^{b} 5.06 ±1.814 13.29± 5.345 *.N.S*	*0.001* *N.S.* *N.S.*
Genes						
Thermogenesis						
UCP1	0 10 19 P value	2.00± 0.29^{ab} 0.59 ± 0.14^{a} 0.45 ± 0.05^{b} *.0015*	1.60 ± 0.27^{cd} 0.37 ± 0.10^{c} 0.51 ± 0.09^{d} *0.0064*	1.04 ± 0.36 0.76 ± 0.15 0.44 ± 0.13 *N.S.*	1.13 ± 0.16^{e} 0.71 ± 0.17 0.44± 0.13^{e} *.0212*	*N.S.* *N.S.* *N.S.*
β3AR	0 10 19 P value	0.89 ± 0.06 0.62 ± 0.09 0.73 ± 0.08 *N.S.*	0.84 ± 0.06^{a} 0.46 ± 0.06^{ab} 0.65 ± 0.08^{b} *0.0055*	0.90 ± 0.15 0.67 ± 0.05 0.73 ± 0.13 *N.S.*	0.71 ± 0.10 0.64 ± 0.11 0.47 ± 0.06 *N.S.*	*N.S.* *N.S.* *N.S.*
SERCA2B	0 10 19 P value	0.49 ± 0.18 0.32 ± 0.17 0.32 ± 0.12 *N.S.*	0.58 ± 0.16^{a} 0.20 ± 0.16^{ab} 0.56 ± 0.17^{b} *0.0206*	0.41 ± 0.09 0.17 ± 0.07 0.48 ± 0.16 *N.S.*	0.43 ± 0.12 0.31 ± 0.14 0.28 ± 0.10 *N.S.*	*N.S.* *N.S.* *N.S.*

TRPV1	0 10 19 P value	0.58 ± 0.09[a] 1.73 ± 0.39[ab] 0.61 ± 0.05[b] *0.0048*	0.57 ± 0.06[c] 1.75 ± 0.26[cd] 0.72 ± 0.16[d] *0.0020*	0.75 ± 0.16 1.62 ± 0.54[e] 0.45 ± 0.05[e] *0.0047*	0.86 ± 0.18[f] 1.17 ± 0.13[g] 0.46 ± 0.06[fg] *0.0043*	*N.S.* *N.S.* *N.S.*
11βHSD	0 10 19 P value	0.41 ± 0.05[an] 0.61 ± 0.26[c] 0.73 ± 0.07[acr] *0.025*	0.30 ± 0.05[dj] 0.27 ± 0.05[fi] 0.92 ± 0.13[dfv] *<0.0001*	0.64 ± 0.13[bn] 0.50 ± 0.09[e] 2.80 ±0.23[ber] *0.0003*	0.64 ± 0.05[kj] 0.53 ± 0.05[gi] 3.11 ± 0.51[kgv] *0.0002*	*0.020* *0.005* *<0.001*
PPARɣ	0 10 19 P value	1.00 ± 0.07[ab] 0.67 ± 0.05[a] 0.61 ± 0.06[bf] *0.001*	1.07 ± 0.13[c] 0.85 ± 0.05[d] 0.60± 0.04[cdk] *0.0011*	0.80 ± 0.10 1.03 ± 0.07 1.09 ± 0.11[ef] *N.S*	0.84 ± 0.11 0.91 ± 0.19 0.83 ± 0.10[ek] *N.S*	*N.S.* *N.S.* *<0.0001*
PGC-1α	0 10 19 P value	1.14 ± 0.23[ab] 0.40 ± 0.06[a] 0.45 ± 0.09[b] *0.0453*	0.76± 0.15[cn] 0.61 ± 0.08[d] 0.31± 0.03[cdj] *0.0036*	0.44 ± 0.07[e] 0.31 ± 0.06 0.24 ± 0.01[e] *.0198*	0.37 ± 0.03[fn] 0.41 ± 0.11[k] 0.21 ± 0.03[fkj] *.0203*	*0.001* *N.S.* *0.01*
Leptin	0 10 19 P value	0.25 ± 0.11 0.41 ± 0.15 0.27 ± 0.06[d] *N.S.*	0.15 ± 0.03[b] 0.22 ± 0.06[c] 0.44 ± 0.16 *N.S.*	0.49 ± 0.15[a] 0.10 ± 0.21[a] 0.56 ± 0.08[d] *0.03*	0.25 ± 0.06[b] 0.91± 0.18[c] 0.53 ± 0.08 *N.S.*	*0.027* *<0.0001* *0.009*
Insulin sensitivity and energy sensing						
TCF7L2	0 10 19 P value	0.65 ± 0.04[ab] 1.24 ± 0.20[a] 1.62 ± 0.14[b] *0.0010*	0.70 ± 0.07[c] 1.14 ± 0.11[c] 1.53 ± 0.15[c] *0.0013*	0.70 ± 0.09[d] 0.95 ± 0.12 1.33 ± 0.19[d] *0.0204*	0.67 ± 0.11[e] 0.80 ± 0.13 2.80 ± 1.06[e] *0.0211*	*N.S.* *N.S.* *N.S.*
mTOR	0 10 19 P value	0.27 ± 0.03[a] 0.91 ± 0.06[a] 0.55 ± 0.04[a] *<0.0001*	0.28 ± 0.02[b] 1.00 ± 0.11[bc] 0.43 ± 0.03[c] *<0.0001*	0.26 ± 0.03[de] 1.08 ± 0.08[d] 0.43 ± 0.06[e] *<0.0001*	0.24 ± 0.03[fk] 0.85 ± 0.07[f] 0.34 ± 0.06[k] *0.0001*	*N.S.* *N.S.* *N.S.*

IRS1	0 10 19 P value	0.92 ± 0.14 1.00 ± 0.11 0.67 ± 0.05 *N.S.*	0.81 ± 0.04 0.86 ± 0.09 0.65 ± 0.05 *N.S.*	0.66 ± 0.14 0.75 ± 0.12 0.49 ± 0.07 *N.S.*	0.66 ± 0.06[a] 0.76 ± 0.04[b] 0.31 ± 0.05[ab] *<0.0001*	*N.S.* *N.S.* *0.001*
IRS2	0 10 19 P value	0.096±0.014[a] 0.069±0.019[b] 1.01 ± 0.16[ab] *<.0001*	0.052 ±0.004[c] 0.058 ±0.008[d] 0.98 ± 0.14[cd] *<0.0001*	0.124±0.020[e] 0.088±0.024[f] 1.24 ± 0.21[ef] *0.0001*	0.055± 0.012[g] 0.058± 0.006[k] 0.97 ± 0.23[gk] *0.0015*	*0.001* *N.S.* *N.S.*
Fat transport						
CD36	0 10 19 P value	0.98 ± 0.10 0.67 ± 0.09 0.85 ± 0.12[f] *N.S.*	0.92 ± 0.10 0.78 ± 0.10 1.00 ± 0.04[e] *N.S.*	0.83 ± 0.04[a] 0.84 ± 0.07[b] 1.16 ±0.06[abf] *0.0014*	0.80 ± 0.08[c] 0.89 ± 0.07[d] 1.12 ± 0.04[cde] *0.0121*	*N.S.* *N.S.* *<.0.0001*
ATGL	0 10 19 P value	1.40 ± 0.15[ab] 0.90 ± 0.14[a] 0.91 ± 0.05[bf] *0.0145*	1.14 ± 0.04 0.83 ± 0.14 0.90 ± 0.07 *N.S.*	1.28 ± 0.14[d] 1.15 ± 0.09 1.51 ± 0.12[cef] *N.S.*	0.85 ± 0.11[d] 1.07 ± 0.12 1.03 ± 0.12[e] *N.S.*	*0.020* *N.S.* *<0.0001*
LPL	0 10 19 P value	0.91 ± 0.08[a] 1.03 ± 0.04[b] 0.59 ± 0.04[ab] *<0.0003*	0.86 ± 0.07 0.89 ± 0.07 0.68 ± 0.05 *N.S.*	0.79 ± 0.07[c] 1.05 ± 0.10[cd] 0.53 ± 0.06[c] *0.0007*	0.64 ± 0.07 0.72 ± 0.07[d] 0.53 ± 0.07 *N.S.*	*N.S.* *0.016* *N.S.*
FATP4	0 10 19 P value	0.59 ± 0.04[ab] 0.92 ± 0.06[a] 0.85 ± 0.10[b] *0.0159*	0.56 ± 0.03 0.86 ± 0.05 0.87 ± 0.14 *N.S.*	0.62 ± 0.05[c] 1.00 ± 0.05[c] 1.32 ± 0.15[c] *0.0006*	0.59 ± 0.04[d] 0.89 ± 0.04[d] 1.17 ± 0.15[d] *0.0017*	*N.S.* *N.S.* *N.S.*

P values given are the statistically significant outcomes of comparisons (ANOVA or Kruskal-Wallis, indicated as 'ANOVA'). If data within one outcome carry the same superscripts they are statistically different (P<0.05).For all interscapular gene expression, unmated n=5-6, 10 d/g n=5-7, 19 d/g n=6-8.

Abbreviations: uncoupling protein 1 (UCP1), peroxisome proliferator-activated receptor gamma coactivator 1-alpha (PGC-1α), beta-3 adrenergic receptor (β*3AR*), ATPase sarcoplasmic/endoplasmic reticulum Ca2+ (*SERCA2B*), Transient receptor potential vanilloid 1 (*TRPV1*), hydroxysteroid 11 beta dehydrogenase (11*BHSD*), transcription factor 7 like 2 (*TCF7L2*), mammalian target or rapamycin

(*mTOR*), insulin receptor substrates 1 and 2 (*IRS1+2*), fatty acid translocase (*CD36*), adipose triglyceride lipase (*ATGL*), lipoprotein lipase (*LPL*), fatty acid transport protein 4 (*FATP4*). Peroxisome proliferator activated receptor gamma (PPARɣ), d/g: day of gestation.

Appendix 3 Plasma metabolites and hormones

Plasma metabolites hormones of females before and during pregnancy, when kept at either a cool temperature (20°C) or thermoneutrality (27°C), and fed a standard (S) or high (H) fat and sucrose diet.

Plasma measurement	Pregnancy time point (d/g)	20S	20H	27S	27H	*P value*
Glucose* (µg ml-1)	0	24 ± 4[ac]	28 ± 5	47 ± 6[c]	40 ± 4	*0.009*
	10	48 ± 9[ab]	38 ± 6	43 ± 9	35 ± 3	*N.S.*
	19	22 ± 2[b]	35 ± 9	28 ± 4	30 ± 4	*N.S.*
	P value	*0.0036*	*N.S.*	*N.S.*	*N.S.*	
Triglycerides (mg dl-1)	0	95 ± 14[a]	118 ± 19[c]	82 ± 17[e]	127 ± 28	*N.S.*
	10	106 ± 19[b]	107 ± 14[d]	130 ± 20	143 ± 27	*N.S.*
	19	245 ± 35[ab]	300 ± 36[cd]	320 ± 58[e]	227 ± 26	*N.S.*
	P value	*0.0031*	*0.002*	*<0.0001*	*0.038*	
NEFA* (mmol l-1)	0	0.17 ± 0.02	0.24 ± 0.05	0.31 ± 0.06	0.21 ± 0.03	*N.S.*
	10	0.15 ± 0.02	0.17 ± 0.02[a]	0.15 ± 0.01	0.20 ± 0.03	*N.S.*
	19	0.22 ± 0.03	0.33 ± 0.02[a]	0.24 ± 0.04	0.31 ± 0.04	*N.S.*
	P value	*N.S.*	*0.0099*	*N.S.*	*N.S.*	
Insulin (ng ml-1)	0	0.95 ± 0.12[a]	1.77 ± 0.21[a]	0.97 ± 0.14	1.67 ± 0.62	*0.008*
	10	1.24 ± 0.35	0.96 ± 0.10	1.17 ± 0.24	1.92 ± 0.23	*N.S.*
	19	1.24 ± 0.30	1.84 ± 0.45	3.58 ± 1.12	1.53 ± 0.46	*N.S.*
	P value	*N.S.*	*N.S.*	*N.S.*	*N.S.*	
Corticosterone (ng ml-1)	0	169 ± 52	106 ± 35	450 ± 171[b]	107 ± 23	*N.S.*
	10	68 ± 20	180 ± 100	32 ± 7[ab]	148 ± 94	*N.S.*
	19	111 ± 18	159 ± 25	242 ± 112[a]	178 ± 46	*N.S.*
	P value	*N.S.*	*N.S.*	*0.0099*	*N.S.*	
Leptin (ng ml-1)	0	3.2 ± 0.4[ab]	4.7 ± 0.6[c]	3.4 ± 0.8[de]	4.4 ± 0.2[fg]	*N.S.*
	10	5.5 ± 0.6[a]	7.1 ± 1.1	5.6 ± 0.7[d]	11.0 ± 2.1[f]	*N.S.*
	19	6.9 ± 0.7[b]	7.8 ± 1.2[c]	8.2 ± 1.7[e]	9.1 ± 1.6[g]	*N.S.*
	P value	*0.002*	*0.047*	*0.029*	*0.023*	

*****Due to stressful sacrifice procedure, changes in glucose or NEFA levels may be influenced by hypoxia and thus not reflect the metabolic/BAT status

Appendix 4 Inguinal adipose tissue mass and gene expression measurements

Inguinal adipose tissue fat mass and expression measurements of genes of thermogenic, energy regulatory, fat transport pathways and mammary cells markers of females before and during pregnancy, when kept at either a cool temperature (20°C) or thermoneutrality (27°C), and fed a standard (S) or a high (H) fat and sucrose diet.

	Pregnancy time point (d/g)	20S	20H	27S	27H	P value
Inguinal fat mass (g)	0 10 19 P value	0.71 ± 0.13^{abr} 2.70± 0.13^{a} 2.45 ± 0.12^{b} *0.0203*	1.24 ± 0.16^{cdr} 2.38 ± 0.18^{ct} 3.00 ± 0.30^{d} *0.0092*	0.79 ± 0.05^{efj} 2.52 ± 0.26^{e} 2.46 ± 0.20^{f} *0.0156*	1.45 ± 0.15^{knj} 3.87 ± 0.32^{kt} 2.87 ± 0.25^{n} *0.0254*	*<0.0001* *.03* *N.S.*
Genes						
Thermogenesis						
PPARɣ	0 10 19 P value	1.02 ± 0.15^{a} 0.78 ± 0.11 0.50 ± 0.07^{a} *0.0203*	0.71 ± 0.09^{b} 0.59 ± 0.13^{c} 0.29 ± 0.05^{bc} *0.0092*	0.84 ± 0.12^{d} 0.72 ± 0.04^{e} 0.46 ± 0.08^{de} *0.0156*	0.89 ± 0.16^{d} 0.76 ± 0.12^{e} 0.39 ± 0.04^{de} *0.0254*	*N.S.* *N.S.* *N.S.*
β3AR	0 10 19 P value	0.75 ± 0.14^{a} 0.30 ± 0.06^{a} N.D. *0.0203*	0.59 ± 0.09 0.42 ± 0.10 N.D. *N.S.*	0.91 ± 0.13 0.57 ± 0.10 N.D. *N.S.*	0.79 ± 0.13 0.63 ± 0.12 N.D. *N.S.*	*N.S.* *N.S.* ND
LEPTIN	0 10 19 P value	0.50 ± 0.16^{a} 0.11 ± 0.03^{ab} 0.26 ± 0.04^{b} *0.013*	0.31 ± 0.09 0.13 ± 0.02 0.20 ± 0.05 *N.S.*	0.47 ± 0.13 0.23 ± 0.05 0.21 ± 0.06 *N.S.*	0.20 ± 0.05 0.19 ± 0.03 0.25 ± 0.04 *N.S.*	*N.S.* *N.S.* *N.S.*
Insulin sensitivity and energy sensing						

IRS2	0	0.45 ± 0.04	0.47 ± 0.08^{b}	0.56 ± 0.03	0.55 ± 0.19^{e}	*N.S.*
	10	0.21 ± 0.03^{a}	0.32 ± 0.06^{c}	0.26 ± 0.04^{d}	0.17 ± 0.02^{ef}	*N.S.*
	19	1.26 ± 0.20^{a}	1.32 ± 0.16^{bc}	1.23 ± 0.21^{d}	1.07 ± 0.10^{f}	*N.S.*
	P value	*<0.0001*	*<0.0001*	*<0.0001*	*<0.0005*	
Fat transport						
FABP4	0	0.59 ± 0.20^{a}	0.37 ± 0.07	0.69 ± 0.22^{a}	0.38 ± 0.06	*N.S.*
	10	0.18 ± 0.04^{a}	0.18 ± 0.04	0.27 ± 0.05^{ab}	0.28 ± 0.05	*N.S.*
	19	0.29 ± 0.03	0.20 ± 0.03	0.30 ± 0.05^{b}	0.29 ± 0.04	*N.S.*
	P value	*.0354*	*N.S.*	*0.0156*	*N.S.*	
Mammary cells Biomarkers						
ELF5	0	0.43 ± 0.05^{ab}	0.37 ± 0.11^{cd}	0.39 ± 0.08^{e}	0.37 ± 0.11^{f}	*N.S.*
	10	1.29 ± 0.39^{a}	1.18 ± 0.28^{c}	1.11± 0.16^{e}	0.85 ± 0.10^{f}	*N.S.*
	19	1.79 ± 0.05^{b}	1.83 ± 0.22^{d}	1.68 ± 0.02^{e}	1.54 ± 0.14^{f}	*N.S.*
	P value	*.0008*	*.0008*	*<.0001*	*<.0001*	
WAP	0	0.0219±0.01^{a}	.0015±.0009^{b}	.0076±.0044^{d}	.0046±.0004^{f}	*N.S.*
	10	0.11 ± 0.02	0.08 ± 0.03^{c}	0.13 ± 0.055^{e}	0.03 ± 0.006^{k}	*N.S.*
	19	1.75 ± 0.42^{a}	1.15 ± 0.20^{bc}	1.72 ± 0.37^{de}	1.22 ± 0.25^{fk}	*N.S.*
	P value	*<.0001*	*<.0001*	*0<.0001*	*<.0001*	
OXTR	0	0.65 ± 0.16^{a}	0.57 ± 0.09	0.72 ± 0.17	0.72 ± 0.21	*N.S.*
	10	0.82 ± 0.03	0.61 ± 0.12	0.75 ± 0.12	0.44 ± 0.08	*N.S.*
	19	1.04 ± 0.03^{ab}	0.68 ± 0.01^{b}	0.79 ± 0.08	0.77 ± 0.08	*0.041*
	P value	*.0387*	*N.S.*	*N.S.*	*N.S.*	
STAT5A	0	0.61 ± 0.08^{a}	0.68 ± 0.17^{b}	0.97 ± 0.20^{d}	0.57 ± 0.15^{f}	*N.S.*
	10	1.06 ± 0.09^{a}	1.15 ± 0.16^{c}	1.08 ± 0.13^{e}	0.93 ± 0.08^{f}	*N.S.*
	19	1.61± 0.11^{a}	1.69 ± 0.14^{bc}	1.60 ± 0.18^{de}	1.50 ± 0.12^{f}	*N.S.*
	P value	*<.0001*	.0007	*0.0464*	*.0002*	

P values given are the statistically significant outcomes of comparisons. If data within one outcome carry the same superscripts they are statistically different (P<0.05). For all inguinal adipose tissue gene expression, unmated n=6, 10 d/g n=5-7, 19 d/g n=6-8.

Abbreviations: peroxisome proliferator activated receptor gamma (*PPARG*), beta-3 adrenergic receptor (β*3AR*), insulin receptor substrate 2 (*IRS2*), fatty acid binding protein 4 (*FABP4*), whey acidic protein (WAP), oxytocin receptor (OXTR), Signal transducer and activator of transcription 5A (STAT5A), E74 Like ETS transcription factor 5 (ELF5), Not detected (ND), d/g: day of gestation

Appendix 5 Omental adipose tissue mass and gene expression measurements

Omental adipose tissue mass and expression measurements of genes of thermogenic, energy regulatory, fat transport and immune response pathways of females before and during pregnancy, when kept at either a cool temperature (20°C) or thermoneutrality (27°C), and fed a standard (S) or a high (H) fat and sucrose diet.

	Pregnancy time point (d/g)	20S	20H	27S	27H	P value
Omental mass (g)	0 10 19 P value	0.166 ± 0.10[ab] 2.70.± 0.13[a] 2.80 ± 0.22[b] *N.S.*	2.04 ± 0.15[c] 2.38 ± 0.18[dr] 3.61 ± 0.30[cd] *N.S.*	1.49 ± 0.13[efh] 2.56 ± 0.26[en] 2.90 ± 0.21[f] *0.0113*	2.11 ± 0.24[kh] 3.78 ± 0.32[knr] 3.28± 0.57 *N.S*.	*0.006* *0.036, 0.01* *N.S.*
Genes						
Thermogenesis						
β3AR	0 10 19 P value	0.23 ± 0.12 0.78 ± 0.37 0.45 ± 0.11 *N.S.*	0.62 ± 0.22 1.46 ± 0.51 0.40 ± 0.15 *N.S.*	0.47 ± 0.14 1.37 ± 0.34[a] 0.32 ± 0.14[a] *0.0113*	0.99 ± 0.27 1.00 ± 0.29 0.33 ± 0.06 *N.S*.	*N.S.* *N.S.* *N.S.*
RYR2	0 10 19 P value	1.17 ± 0.38 0.83 ± 0.15 0.73 ± 0.18 *N.S.*	2.16 ± 0.46[a] 1.09 ± 0.20 0.61 ± 0.10[a] *0.0110*	1.92 ± 0.49[b] 1.09 ± 0.22 0.40 ± 0.09[b] *0.0027*	2.34 ± 0.56[d] 0.85 ± 0.19 0.50 ± 0.11[d] *0.0143*	*N.S.* *N.S.* *N.S.*
LEPTIN	0 10 19 P value	0.22 ± 0.15 0.56 ± 0.23 0.50 ± 0.13 *N.S.*	0.38 ± 0.14 0.62 ± 0.19 0.42 ± 0.13 *N.S.*	0.24 ± 0.16 0.60 ± 0.16 0.46 ± 0.21 *N.S.*	0.65 ± 0.13 0.95 ± 0.28 0.53 ± 0.19 *N.S.*	*N.S.* *N.S.* *N.S.*
TRPV1	0 10 19 P value	1.62 ± 1.10 2.25 ± 0.84 4.67 ± 0.85 *N.S.*	2.45 ± 1.08 2.29 ± 0.95 2.56 ± 0.56 *N.S.*	0.91 ± 0.25[a] 3.78 ± 0.58[a] 2.22 ± 0.68 *0.0064*	2.65 ± 0.89 3.17 ± 0.93 3.18 ± 0.85 *N.S.*	*N.S.* *N.S.* *N.S.*
VEGFA	0 10 19 P value	1.24 ± 0.61 0.84 ± 0.35 0.94 ± 0.20 *N.S.*	1.62 ± 0.63 1.10 ± 0.33 0.88 ± 0.19 *N.S.*	1.08 ± 0.22 1.91 ± 0.68 0.60 ± 0.18 *N.S.*	2.22 ± 0.59[a] 0.86 ± 0.23 0.61 ± 0.07[a] *0.0404*	*N.S.* *N.S.* *N.S.*

SERCA2B	0	0.23 ± 0.10	0.62 ± 0.21	0.68 ± 0.37	1.38 ± 0.45	*N.S.*
	10	0.28 ± 0.11	0.76 ± 0.31	0.62 ± 0.12	0.60 ± 0.29	*N.S.*
	19	0.51 ± 0.14	0.32 ± 0.10	0.30 ± 0.10	0.45 ± 0.17	*N.S.*
	P value	*N.S.*	*N.S.*	*N.S.*	*N.S.*	
Insulin sensitivity and energy sensing						
IRS1	0	0.38 ± 0.13	0.62 ± 0.24	0.68 ± 0.24	1.44 ± 0.56	*N.S.*
	10	0.67 ± 0.26	0.84 ± 0.25	0.99 ± 0.20	0.57 ± 0.16	*N.S.*
	19	0.76 ± 0.16	0.61 ± 0.15	0.52 ± 0.23	0.51 ± 0.10	*N.S.*
	P value	*N.S.*	*N.S.*	*N.S.*	*N.S.*	
IRS2	0	1.02 ± 0.23	0.56 ± 0.23	2.01 ± 0.40^{ab}	1.97 ± 0.61^{c}	*N.S.*
	10	0.91 ± 0.27	0.78 ± 0.17	0.78 ± 0.17^{a}	0.64 ± 0.15	*N.S.*
	19	0.73 ± 0.16	0.89 ± 0.14	0.63 ± 0.13^{b}	0.57 ± 0.10^{c}	*N.S.*
	P value	*N.S.*	*N.S.*	*0.0024*	*0.0401*	
Fat transport						
FATP4	0	0.23 ± 0.04	0.19 ± 0.03	0.23 ± 0.02	0.27 ± 0.02	*N.S.*
	10	0.35 ± 0.07^{a}	0.30 ± 0.05	0.75 ± 0.34^{c}	1.51 ± 0.87	*N.S.*
	19	0.15 ± 0.01^{a}	0.20 ± 0.03	0.17 ± 0.03^{c}	0.14 ± 0.02	*N.S.*
	P value	*0.0144*	*N.S.*	*0.0114*	*N.S.*	
FABP4	0	0.48 ± 0.30	1.35 ± 0.52	0.46 ± 0.16^{a}	1.01 ± 0.19	*N.S.*
	10	0.51 ± 0.20	1.38 ± 0.49	1.91 ± 0.20^{ab}	1.48 ± 0.42	*N.S.*
	19	1.18 ± 0.23	0.67 ± 0.23	0.62 ± 0.21^{b}	0.89 ± 0.26	*N.S.*
	P value	*N.S.*	*N.S.*	*<0.001*	*N.S.*	
Immune response						
TNF	0	1.26 ± 0.24	0.77 ± 0.25	1.11 ± 0.33	0.65 ± 0.20	*N.S.*
	10	0.90 ± 0.24	0.59 ± 0.17	0.42 ± 0.11	0.50 ± 0.22	*N.S.*
	19	0.44 ± 0.14	1.09 ± 0.31	0.76 ± 0.12	0.59 ± 0.19	*N.S.*
	P value	*.0468*	*N.S.*	*N.S.*	*N.S.*	
IL6	0	0.036 ± 0.013^{ab}	0.024 ± 0.006	0.019 ± 0.005	0.012 ± 0.002	*N.S.*
	10	0.010 ± 0.003^{a}	0.012 ± 0.003	0.010 ± 0.002	0.009 ± 0.002	*N.S.*
	19	0.012 ± 0.003^{b}	0.016 ± 0.004	0.014 ± 0.003	0.015 ± 0.006	*N.S.*
	P value	*0.0102*	*N.S.*	*N.S.*	*N.S.*	

MCP1	0	2.76 ± 0.92[a]	4.80 ± 1.04[ef]	2.93 ± 0.30[gh]	2.85 ± 0.70[i]	*N.S.*
	10	0.47 ± 0.06[ab]	0.57 ± 0.07[e]	0.59 ± 0.07[g]	0.43 ± 0.09[i]	*N.S.*
	19	1.12 ± 0.14[bkj]	0.66 ± 0.06[fk]	0.71 ± 0.09[hj]	0.51 ± 0.05	*0.01,.02*
	P value	*<0.0001*	*0.0002*	*0.0001*	*0.0026*	
NF_KB	0	1.67 ±0.298[ab]	1.09± 0.12[c]	1.82±0.39[de]	1.41 ±0.15[fg]	*N.S.*
	10	0.61±0.07[a]	0.41 ±.0.04[c]	0.43± 0.05[d]	0.40±0 .12[f]	*N.S.*
	19	0.35±0.04[b]	0.67 ±0.13	0.51± 0.08[e]	0.41± 0.08[g]	*N.S.*
	P value	*<.0001*	*.0126*	*.0003*	*.0006*	
EMR1	0	0.72 ± 0.16	0.72 ± 0.16[c]	0.61 ± 0.09	0.82 ± 0.15[abc]	*.029*
	10	0.79 ± 0.25	0.67 ± 0.17	0.85 ± 0.15	0.37 ± 0.10[a]	*N.S.*
	19	0.64 ± 0.06	0.79 ± 0.20	0.50 ± 0.14	0.40 ± 0.05[b]	*N.S.*
	P value	*N.S.*	*N.S.*	*N.S.*	*0.016*	

P values given are the statistically significant outcomes of comparisons. If data within one outcome carry the same superscripts they are statistically different (P<0.05; Analysis of variance (ANOVA) or Mann-Whitney according to the data distribution). For all omental AT gene expression, unmated n=5-6, 10 d/g n=5-7, 19 d/g n=6-8.

Abbreviations: beta-3 adrenergic receptor (β*3AR*); ryanodine receptor 2 (*RYR2*); vascular endothelial growth factor A (*VEGFA*); ATPase sarcoplasmic/endoplasmic reticulum Ca2+ (*SERCA2B*); insulin receptor substrates 1 and 2 (*IRS1+2*); fatty acid transport protein 4 (*FATP4*); fatty acid binding protein 4 (*FABP4*); tumour necrosis factor (*TNF*); interleukin 6 (*IL6*); interleukin 10 (*IL10*); monocyte attractant protein 1 (*MCP1*); Transient receptor potential vanilloid 1 (TRPV1); Nuclear *Factor Kappa B Subunit (NF_KB),* EGF-Like Module-Containing Mucin-Like Hormone Receptor-Like 1 *(EMR1)*

Appendix 6 List of Suppliers

ABgene	Abgene House, Blenheim Road, Epsom, KT19 9AP, UK. www.abgene.com
Abbot Nutrition	Granada, Spain. www.abbott.com
Alpha Diagnostic International	6203 Woodlake Center, San Antonio, TX 78244, USA. www.4adi.com
Alpha Laboratories Ltd	40 Parham Dr, Eastleigh, SO50 4NU, UK. www.alphalabs.co.uk
Ambion	850 Lincoln Centre Drive, Foster City, CA 94404, USA. www.ambion.com
Anglia Scientific	850 Lincoln Centre Drive, Foster City, CA, 94404, USA. www.appliedbiosystems.com
Applied Biosystems	Lingley House 120 Birchwood Boulevard, Warrington, Cheshire, WA3 7QH, Uk. www.appliedbiosystems.com
Bio-Rad Ltd.	Life Science Research, Education, Process Separations, Food Science, 2000 Alfred Nobel Drive, Hercules, California 94547, USA. www.bio-rad.com
Charles River Laboratories	www.criver.com
Dako	Cambridge House, St Thomas Place, Ely, Cambridgeshire, CB7 4EX, UK. www.dako.com
Envigo	www.envigo.com Madison, WI, US. www.envigo.com
Fisher Scientific UK Ltd	Bishop Meadow Road, Loughborough, LE11 5RG, UK. www.fishersci.co.uk
GraphPad Software	7825 Fay Avenue, Suite 230, La Jolla, CA, USA. www.graphpad.com

Hamamatsu Photonics (UK) Ltd	10 Tewin Rd, Welwyn Garden City, Hertfordshire, AL7 1BW, UK. www.hamamatsu.com
Improvision Ltd	Coventry, UK www.improvision.com
Leica Biosystems	Balliol Business Park West, Newcastle Upon Tyne, NE12 8EW, UK. www.leicabiosystems.com
Leica Microsystems	Larch House, Woodland Business Park, Breckland, Linford Woods, Milton Keynes, MK14 6FG, UK. www.leica-microsystems.com
Manor Farm Feeds	Green Lane, Owston, Oakham, Leicestershire LE15 8DH, UK. www.manorfarmfeeds.co.uk
Media Cybernetics	401 N Washington Street, Rockville, 20850, MD, USA. www.mediacy.com
Menzel-Gläser	Glasbearbeitungswerk GmbH & Co., Saarbrückener Str. 248, D-38116, Braunschweig, Germany. www.menzel.de
Merial Animal Health Ltd	Sandringham House, Harlow Business Park, Harlow, Essex, CM19 5QE, UK. http://merial.com/
Nikon UK Ltd	380 Richmond Rd, Kingston upon Thames, Surrey, KT2 5DB, UK. www.europe-nikon.com/en_GB/
Objective Imaging Ltd	Unit 1, Quy Court, Colliers Lane, Stow cum Quy, Cambridge, CB25 9AU, UK. http://www.objectiveimaging.com
Qiagen	Qiagen House, Fleming Way, Crawley, West Sussex, RH10 9NQ, UK. www.qiagen.com
QImaging, Surrey	19535 56th Avenue, Surrey, BC V3S 6K3, Canada. www.qimaging.com
Sakura Finetek	Flemingweg 10A, 2408 AV Alphen aan den Rijn, Netherlands. www.sakura.eu
Sigma-Aldrich Company	The Old Brickyard, New Road, Gillingham, Dorset, SP8 4XT, UK. www.sigma-aldrich.com

Simport Scientific	2588 Bernard-Pilon Street, Beloeil, QC J3G 4S5, Canada. www.simport.com
Millipore	Croxley Green Business Park, Watford, Hertfordshire, WD18 8YH, UK. www.emdmillipore.com
Nikon UK Ltd	380 Richmond Rd, Kingston upon Thames, Surrey, KT2 5DB, UK. www.europe-nikon.com/en_GB/
Objective Imaging Ltd	Unit 1, Quy Court, Colliers Lane, Stow cum Quy, Cambridge, CB25 9AU, UK. http://www.objectiveimaging.com
Partek Inc.	624 Trade Center Boulevard, St. Louis, Missouri 63005, USA. www.partek.com
Primer Design	Millbrook Technology Campus, Second Avenue, Southampton, Hampshire, SO15 0DJ, UK. www.primerdesign.co.uk
Qiagen	Qiagen House, Fleming Way, Crawley, West Sussex, RH10 9NQ, UK. www.qiagen.com
QImaging, Surrey	19535 56th Avenue, Surrey, BC V3S 6K3, Canada. www.qimaging.com
Raytek	26 Norton Park View, Sheffield, S8 8GS, UK. www.raytek.co.uk
Sakura Finetek	Flemingweg 10A, 2408 AV Alphen aan den Rijn, Netherlands. www.sakura.eu
Sarstedt	Sarstrabe 1, 51588 Nümbrecht, Germany. www.sarstedt.com
Scientific Laboratory Supplies	Orchard House, The Square, Hessle, East Riding of Yorkshire, HU13 0AE, UK. www.scientificlabs.co.uk
Sigma-Aldrich Company	The Old Brickyard, New Road, Gillingham, Dorset, SP8 4XT, UK. www.sigma-aldrich.com

Simport Scientific

2588 Bernard-Pilon Street, Beloeil, QC
J3G 4S5, Canada.
www.simport.com